NONLINEAR ADAPTIVE CONTROL IN THE DESIGN OF POWER SYSTEM STABILISERS

by

Miss Fangpo He, B.E., M.Eng.Sc.

A thesis submitted in fulfilment of the requirement for the degree of

Doctor of Philosophy

in the

Department of Electrical and Electronic Engineering

The University of Adelaide

November, 1991

To my parents

Contents

Abstract. viii

Statement of Originality. x

Acknowledgements. xi

List of Principal Symbols. xii

List of Abbreviations. xxv

List of Figures. xxvii

List of Tables. xxxv

1 Introduction. 1

1.1 The Basic Concept of Power System Stability. 1

1.2 The Effect of the Excitation Control System on Power System Stability. 3

1.3 The Role of Power System Stabilisers. 5

1.4 Shortcomings of the Conventional Power System Stabilisers. 7

1.5 Linear Adaptive Control in the Design of Power System Stabilisers. . . 8

1.6 Nonlinear Optimal Control in the Design of Power System Stabilisers. . 11

1.7 Nonlinear Adaptive Control in the Design of Power System Stabilisers. 13

1.8 Subject Coverage and Outline of the Thesis. 14

1.9 Original Contributions. 19

2 Power System Modelling. **22**

2.1 Introduction. 22

2.2 Simplified Nonlinear Models of the Synchronous Generator. 26

2.3 Nonlinear SMIB Power System Models for Simulation Studies. 38

2.3.1 The Development of the Complete System Models. 39

2.3.2 Comparisons of the Dynamic Performance of the Complete System Models. 46

2.4 Linearisation of the Nonlinear Power System Model. 53

2.4.1 Nonlinear Analytical Model of the Nonlinear Power System. . . 54

2.4.2 Linearised Analytical Model of the Nonlinear Power System. . . 57

2.4.3 Summary of the Models of the Power System. 61

2.5 Identification of Suitable Stabilising Signals for the Design of Power System Stabilisers. 63

2.6 Controllability and Observability. 67

2.7 Concluding Remarks. 72

3 SISO Linear Adaptive Power System Stabilisers. 75

3.1 Introduction. 75

3.2 SISO Linear Input-Output Power System Modelling. 77

3.2.1 SISO Linear Continuous-Time State-Space Power System Modelling. 79

3.2.2 SISO Linear Discrete-Time Input-Output Power System Modelling. 80

3.2.3 Linearised Nominal Model of the Power System. 82

3.3 SISO Linear Stochastic Optimal Control. 84

3.3.1 SISO Linear Stochastic Optimal d-Step-Ahead Predictor. 84

3.3.2 SISO Linear Stochastic Optimal Control Laws. 86

3.4 SISO Linear Stochastic Adaptive Generalised Minimum Variance Control. 92

3.4.1 Parameter Estimation Algorithms for the Linearised Nominal Model of the Power System. 93

3.4.2 SISO Linear Stochastic Adaptive Generalised Minimum Variance Control Algorithm. 95

3.5 A Linear Adaptive Weighted Minimum Variance Power System Stabiliser. 98

3.6 Evaluation of the Performance of the Linear Adaptive Weighted Minimum Variance Power System Stabiliser. 102

3.6.1 Verification and Identification of the Linearised Nominal Model of the Power System. 104

3.6.2 Evaluation of the Performance of the LAWMV-PSS for the CSM3.108

3.6.3 Studies on the Robustness of the LAWMV-PSS for the CSM1. . 116

3.7 Concluding Remarks. 128

4 SISO Nonlinear Optimal Power System Stabilisers. 130

4.1 Introduction. 130

4.2 SISO Nonlinear Input-Output Power System Modelling. 134

4.2.1 SISO Nonlinear Continuous-Time Input-Output Power System Modelling. 137

4.2.2 SISO Nonlinear Discrete-Time Input-Output Power System Modelling. 144

4.2.3 Nonlinear Nominal Model of the Power System and Its BIBO Stability. 151

4.3 SISO Nonlinear Stochastic Generalised Minimum Variance Control and Stability Analysis. 155

4.3.1 SISO Optimal One-Step-Ahead Predictor. 158

4.3.2 SISO Nonlinear Stochastic Generalised Minimum Variance Control Law. 160

4.4 A Nonlinear Optimal Weighted Minimum Variance Power System Stabiliser and Stability Analysis. 167

4.5 Evaluation of the Performance of the Nonlinear Optimal Weighted Minimum Variance Power System Stabiliser. 173

4.5.1 Verification of the Nonlinear Nominal Model of the Power System.175

4.5.2 Evaluation of the Performance of the NOWMV-PSS for the CSM3.180

4.5.3 Studies on the Robustness of the NOWMV-PSS for the CSM1. . 192

4.6 Concluding Remarks. 193

5 SISO Nonlinear Adaptive Power System Stabilisers. 198

5.1 Introduction. 198

5.2 Parameter Estimation Algorithms for the Nonlinear Nominal Model of the Power System and Convergence Analyses. 201

5.3 Nonlinear Adaptive Weighted Minimum Variance Power System Stabilisers and Convergence Analyses. 208

5.4 Evaluation of the Performance of the Nonlinear Adaptive Weighted Minimum Variance Power System Stabiliser. 217

5.4.1 Identification of the Nonlinear Nominal Model of the Power System. 218

5.4.2 Evaluation of the Performance of the NAWMV-PSS for the CSM3. 225

5.4.3 Studies on the Robustness of the NAWMV-PSS for the CSM1. . 228

5.5 Concluding Remarks. 235

6 Simplified SISO Nonlinear Adaptive Power System Stabilisers. 240

6.1 Introduction. 240

6.2 Analysis of Contributions of the Output Components of the Nonlinear Nominal Model to the System Dynamic and Steady-State Responses. . 243

6.3 Simplified Versions of the Nonlinear Adaptive Weighted Minimum Variance Power System Stabiliser. 247

6.4 SISO Bilinear Optimal and Adaptive Power System Stabilisers. 253

6.4.1 Bilinear Nominal Model of the Power System. 254

6.4.2 Bilinear Stochastic Generalised Minimum Variance Control. . . 255

6.4.3 A Bilinear Adaptive Weighted Minimum Variance Power System Stabiliser. 257

6.5 Evaluation of the Performance of the Bilinear Adaptive Weighted Minimum Variance Power System Stabiliser. 261

6.5.1 Verification and Identification of the Bilinear Nominal Model of the Power System. 262

6.5.2 Evaluation of the Performance of the BAWMV-PSS for the CSM3.265

6.5.3 Studies on the Robustness of the BAWMV-PSS for the CSM1. . 271

6.6 Concluding Remarks. 279

7 Conclusions and Recommendations for Future Research. 285

7.1 Conclusions. 285

7.2 Recommendations of Future Research. 291

A The Basic Model of a Single Machine Infinite Bus Power System. 294

A.1 Equations of the Synchronous Generator. 294

A.2 Equations of the Excitation System. 297

A.3 Equations of the Governor and Steam Turbine. 299

B Derivation of the Operational Functions $G_F(p)$ and $H_F(p)$ in Section 2.2. 303

C System Parameters. 305

D Derivation of the Linearised System State Matrix $\mathbf{A_0}$ in Subsection 2.4.2 and Section 2.5. 307

D.1 Derivation of $\mathbf{A_0}$ in Equation (2.116). 307

D.2 Derivation of $\mathbf{A_0}$ in Equation (2.126). 308

E Proofs of Theorems in Chapter 4. **310**

E.1 Proof of Theorem 4.3.1. 310

E.2 Proof of Theorem 4.4.2. 314

F Derivation of Algorithm 5.1. **318**

G Proofs of Theorems in Chapter 5. **320**

G.1 Proof of Theorem 5.2.1. 320

G.2 Proof of Theorem 5.2.2. 322

G.3 Proof of Theorem 5.3.1. 323

Bibliography. **329**

Abstract.

This thesis is concerned with the development of nonlinear adaptive power system stabilisers for single-machine infinite-bus power systems. Single-input single-output design methods are discussed. The studies of this thesis cover the areas of linear adaptive, nonlinear optimal, nonlinear adaptive, and bilinear adaptive control in the design of such stabilisers. Both theoretical analyses and simulation studies are presented for each area of study.

The modelling of the single-machine infinite-bus power system is discussed for the purposes of the analysis and design of the linear and nonlinear optimal/adaptive power system stabilisers, and the simulation studies for the evaluation of the stabilisers that result from the various control strategies. The weighted minimum variance control scheme is selected for the development of the various power system stabilisers for the sake of simplicity and consistency. A linear adaptive power system stabiliser is designed, and its performance is taken as a *reference* for the assessment of the nonlinear power system stabilisers. The validity of the reference is verified by comparison of its damping performance with that of a well-designed, robust, conventional power system stabiliser at various operating conditions.

A new nonlinear model which describes the relationship between the excitation control input and electrical torque output is derived from the mathematical description of the nonlinear power system of concern. The model is given in a regression equation form, linear in the parameters and in the control input, with additional feedback signals. The model is an accurate characterisation of the inherent nonlinearities of the power system, and provides a useful means for the development of a variety of nonlinear control laws for power system stabilisers.

New nonlinear optimal control laws (namely the generalised minimum variance control law and its special case, the weighted minimum variance control law) are developed from a general form of the cost function; the associated global closed-loop stability properties are established theoretically. A number of nonlinear adaptive control algorithms, in the sense of different tuning strategies, can be developed from proper selections of the weighting polynomials in the cost function.

New nonlinear adaptive weighted minimum variance control algorithms are derived, and the theoretical proofs of the convergence of these algorithms are given. This completes the

theoretical development of the nonlinear weighted minimum variance control scheme based on the new nonlinear model.

For practical implementations, simplifications of the nonlinear adaptive control algorithm are discussed. A new bilinear model that represents the simplest nonlinear relationship between the control input and output is derived. This model retains the inherent nonlinearities of the power system and requires a minimum set of measurable feedback signals. New simple bilinear optimal and adaptive control strategies for the design of power system stabilisers are studied. A new bilinear adaptive weighted minimum variance control algorithm is also developed.

Three new power system stabilisers based on the *same* (weighted minimum variance) control scheme but *different* (nonlinear optimal, nonlinear adaptive, and bilinear adaptive) control strategies are proposed. Systematic evaluations and comparisons of the performance of these power system stabilisers against the reference performance of the linear adaptive power system stabiliser are conducted through simulation studies. Conclusions of the advantages and disadvantages of the different control strategies, involving the areas of *linear* and *nonlinear* as well as *optimal* and *adaptive* control, in the design of power system stabilisers are drawn from the studies. The results of this work provide a basis for the development of a practical nonlinear adaptive power system stabiliser.

Statement of Originality.

This thesis contains no material which has been accepted for the award of any other degree or diploma in any University. To the best of the author's knowledge and belief, the thesis contains no material previously published or written by another person, except where due reference is made in the text.

The author consents to this thesis being made available for photocopying and loan if accepted for the award of the degree.

Fangpo He

Acknowledgements.

I wish to express my gratitude to my supervisor, Dr. M. J. Gibbard, for his guidance, inspiration and constructive criticism during the course of work for this thesis. Also, I would like to thank him for helping in the presentation of this thesis.

I sincerely thank the staff of the Department of Electrical and Electronic Engineering of the University of Adelaide and my colleagues for creating a stimulating and supportive environment for research and assistance.

I gratefully thank my parents for their encouragement, understanding and patience. Their constant love and support throughout the years are greatly appreciated.

I would like to acknowledge the award of the University of Adelaide Postgraduate Research Scholarship for the financial support to the research.

List of Principal Symbols.

Symbol	Description	Defined in Section
$\mathbf{A}(\mathbf{X}(t))$	nonlinear continuous-time system state matrix	4.2.1
$\mathbf{A_0}$	linear continuous-time system state matrix	2.4.2
$\tilde{\mathbf{A}}_\mathbf{0}$	linear discrete-time system state matrix	2.6
$a_1 \sim a_2$	parameters of the NNM	4.2.2
$A(q^{-1})$	polynomial of the LNM	3.2.3
$A_1 \sim A_6$	coefficients of synchronous generator models	2.2
$A^*(q^{-1})$	polynomial of the desired closed-loop poles	3.3.2
$\bar{A}(p)$	polynomial of p in SISO continuous-time nonlinear model	4.2.1
$\mathbf{b}_{u0}$	linear continuous-time system input vector	2.4.2
$\mathbf{b}_{w0}$	linear continuous-time system noise vector	2.4.2
$\tilde{\mathbf{b}}_{u0}$	linear discrete-time system input vector	3.2.2
$\mathbf{B}$	nonlinear continuous-time system input matrix	2.3.1
$\mathbf{B_0}$	linear continuous-time system input matrix	2.4.2
$\mathbf{B_r}(\mathbf{b}_{\bar{u}})$	nonlinear continuous-time system input matrix (vector)	4.2.1
$\tilde{\mathbf{B}}_\mathbf{0}(\tilde{\mathbf{b}}_\mathbf{0})$	linear discrete-time system input matrix (vector)	2.6
$b_1 \sim b_2$	parameters of the NNM	4.2.2
$\bar{b}_0 \sim \bar{b}_2$	parameters of SISO discrete-time nonlinear model	4.2.2
$B(q^{-1})$	polynomial of the LNM	3.2.3
$\bar{B}(p)$	polynomial of p in SISO continuous-time nonlinear model	4.2.1
$\mathbf{c}(\mathbf{X}(t))$	nonlinear continuous-time system output vector	4.2.1
$\mathbf{C_0}(\mathbf{c_0})$	linear continuous-time system output matrix (vector)	2.6,3.2.1

$\tilde{\mathbf{C}}_0(\tilde{\mathbf{c}}_0)$	linear discrete-time system output matrix (vector)	2.6
$c_1 \sim c_2$	parameters of the NNM	4.2.2
$\tilde{c}_1 \sim \tilde{c}_2$	parameters of the BNM	6.4.1
C	estimator parameter	3.4.2
$C(q^{-1})$	polynomial of the LNM	3.2.3
C_y	maximum decreasing rate of the output	6.4.3
$C_\varepsilon(q^{-1})$	linear filter polynomial	4.3
$\bar{C}(p)$	polynomial of p in SISO continuous-time nonlinear model	4.2.1
$\mathcal{C}$	linear time-invariant continuous-time system controllability matrix	2.6
$d(t)$	system measurable deterministic disturbance	4.2.2
d_1	parameter of the NNM	4.2.2
$\bar{d}(t)$	theoretical value of $d(t)$	4.2.1
D	generator rotor damping coefficient	App. A
D_d	damping coefficient of the CPSS	3.6.2
$\bar{D}(p)$	polynomial of p in SISO continuous-time nonlinear model	4.2.1
$e(k), \tilde{e}(k)$	prediction errors	3.4.2,5.2
e_1	parameter of the NNM	4.2.2
$e_{\bar{K}}$	parameter of the BNM	6.4.1
$E_{FD}(t)$	exciter output voltage	App. A
$E'_q(t)$	generator quadrature-axis transient stator EMF	2.2
E'_{q0}	steady-state value of $E'_q(t)$	2.4.2
$E''_d(t)$	generator direct-axis subtransient stator EMF	2.2
$E''_q(t)$	generator quadrature-axis subtransient stator EMF	2.2

$\bar{E}(p)$	polynomial of p in SISO continuous-time nonlinear model	4.2.1
$f(k)$	nonlinear function of the NNM	4.3
$f_y(k), \bar{f}_y(k)$	piece-wise functions of the BAWMV-PSS	6.4.3
$F(q^{-1})$	identity polynomial of optimal predictor	3.3.1
F_{HP}	high pressure (HP) turbine power fraction	App. A
F_{IP}	intermediate pressure (IP) turbine power fraction	App. A
F_{LP}	low pressure (LP) turbine power fraction	App. A
$g(k)$	nonlinear function of the NNM	4.3.2
$G(q^{-1})$	identity polynomial of optimal predictor	3.3.1
$G_d(p)$	operational function of the synchronous generator	2.2
$G_F(p)$	operational function of the synchronous generator	2.2
$G_q(p)$	operational function of the synchronous generator	2.2
$\overline{G}_F(p)$	operational function of the synchronous generator	2.2
h	sampling period	3.2.2
H	generator inertia constant	App. A
$H_d(p)$	operational function of the synchronous generator	2.2
$H_F(p)$	operational function of the synchronous generator	2.2
$\overline{H}_F(p)$	operational function of the synchronous generator	2.2
$\bar{H}(q^{-1})$	pulse-transfer operator	3.2.2
$\tilde{H}(q^{-1}, k)$	closed-loop system matrix	4.3.2
$\tilde{H}_0(z)$	system transfer function	2.6
$I_d(t)$	generator direct-axis stator current	App. A
$I_D(t)$	generator direct-axis damper winding current	App. A
$I_F(t)$	generator field current	App. A

$I_q(t)$	generator quadrature-axis stator current	App. A
$I_Q(t)$	generator quadrature-axis damper winding current	App. A
$I_t(t)$	generator terminal current	App. A
$J(k)$	cost function	3.3.2,4.3.2
$k_1 \sim k_4$	coefficients of SISO continuous-time nonlinear model	4.2.1
K_0	estimator parameter	3.4.2
K_1	maximum absolute value of $E_{FD}(t)$	4.2.1
K_2	maximum absolute value of $P_{GV}(t)$	4.2.1
K_3	maximum absolute value of $E'_q(t)$	4.2.1
K_4	maximum absolute value of $\omega_s(t)$	4.2.1
K_A	voltage regulator gain	App. A
K_E	exciter constant related to self-excited field	App. A
K_F	excitation control system stabiliser gain	App. A
K_G	speed-governing system gain	App. A
K_m	gain coefficient of the CPSS	3.6.2
$\bar{K}_1 \sim \bar{K}_6$	coefficients of the LAM and the SLAM	2.4.2
$L(q^{-1})$	linear optimal controller polynomial	3.3.2
L_d	generator direct-axis synchronous inductance	App. A
L_D	generator direct-axis damper winding inductance	App. A
L_e	transmission line inductance	App. A
L_F	generator field winding inductance	App. A
L_{md}	generator direct-axis mutual inductance	App. A
L_{mq}	generator quadrature-axis mutual inductance	App. A
L_q	generator quadrature-axis synchronous inductance	App. A

L_Q	generator quadrature-axis damper winding inductance	App. A
L_d'	generator direct-axis transient inductance	2.2
L_d''	generator direct-axis subtransient inductance	2.2
L_q''	generator quadrature-axis subtransient inductance	2.2
$m_1 \sim m_8$	parameters of SISO continuous-time nonlinear model	4.2.1
$M(q^{-1})$	linear optimal controller polynomial	3.3.2
Nf_1	saturation function of nonlinear power system	2.3.1
Nf_2	saturation function of nonlinear power system	2.3.1
Nf_3	saturation function of nonlinear power system	2.3.1
$\mathcal{O}$	linear time-invariant continuous-time system observability matrix	2.6
p	differential operator denoted as $\frac{d}{dt}$	2.2
$\tilde{p}_{ij}$	participation factor	2.5
$P(k)$	estimator covariance matrix	3.4.1
$P(q^{-1})$	linear optimal controller polynomial	3.3.2
P_{dn}	lower limit on rate of change of power imposed by control valve rate limit	App. A
$P_e(t)$	generator electrical power	App A
$P_{GV}(t)$	power at gate or valve outlet	App. A
$P_{HP}(t)$	high pressure turbine power component	App. A
$P_{IP}(t)$	intermediate pressure turbine power component	App. A
$P_{LP}(t)$	low pressure turbine power component	App. A
$P_m(t)$	mechanical power	App. A
P_{max}, P_{min}	maximum and minimum power limits imposed by valve or gate travel	App. A

$P_{ref}(t)$	reference power of the generator	App. A
P_t	active power at generator terminal	2.2
P_{up}	upper limit on rate of change of power imposed by control valve rate limit	App. A
$P_\Sigma(t)$	summing power to the power rate control	App. A
$\overline{P}_{GV}(t)$	power before limits imposed by valve or gate travel	App. A
$\overline{P}_\Sigma(t)$	power after the limits on rate of change of power imposed by control valve rate limits	App. A
$\bar{P}(q^{-1})$	costing polynomial	3.3.2
$\tilde{P}$	participation matrix	2.5
$\bar{q}_0$	leading coefficient of $\bar{Q}(q^{-1})$	3.3.2
Q_t	reactive power at generator terminal	2.2
$\bar{Q}(q^{-1})$	costing polynomial	3.3.2
$\mathbf{R}(t)$	set point input vector	4.2.1
r	generator armature resistance (stator winding resistance)	App. A
r_D	generator direct-axis damper winding resistance	App. A
r_F	generator field winding resistance (rotor resistance)	App. A
r_Q	generator quadrature-axis damper winding resistance	App. A
R_e	transmission line resistance	App. A
$\bar{R}(q^{-1})$	costing polynomial	3.3.2
S_E	exciter saturation function	App. A
t_k	sampling instant	4.2.2
$T_d(\cdot)$	damping torque	1.2,3.6.2
$T_e(t)$	generator electrical torque	App. A

$T_m(t)$	generator mechanical torque	App. A
$T_s(\cdot)$	synchronising torque	1.2
$T_e^0(k\|k-1)$	optimal prediction of $T_e(k)$	4.5.1
$\mathbf{U_r}(t)$	nonlinear continuous-time system input vector	2.3.1
$\mathbf{U_{r0}}$	initial value of $\mathbf{U_r}(t)$	2.4.2
$u(t_k)$	control input	3.2.3
u_{max}, u_{min}	maximum and minimum values of $u(k)$	3.5
$u_r(t)$	input to the AVR	2.4.2
$u^0(k)$	unbounded control input	3.5
$u^*(k)$	final form of the optimal control	3.3.2
$\bar{u}(t)$	theoretical value of $u(t)$	3.2.1
$\bar{u}_{max}$	upper bound for $\|\bar{u}(t_k)\|$	4.2.2
$v(t_k+h)$	error due to discretisation and approximation in SISO discrete-time nonlinear model	4.2.2
$\bar{v}(t_k+h)$	error due to discretisation in SISO discrete-time nonlinear model	4.2.2
$V_d(t)$	generator direct-axis stator voltage	App. A
$V_F(t)$	generator filed voltage	App. A
$V_{ref}(t)$	voltage regulator reference voltage	App. A
$V_R(t)$	voltage regulator output	App. A
V_{Rmax}, V_{Rmin}	maximum and minimum values of $V_R(t)$	App. A
$V_q(t)$	generator quadrature-axis stator voltage	App. A
$V_t(t)$	generator terminal voltage	App. A
V_{t0}	steady-state value of $V_t(t)$	2.4.2

$V_{t\,max}$	upper bound for $\lvert\bar{y}_F(t)\rvert$	4.2.1
V_∞	infinite bus voltage	App. A
$V_\Sigma(t)$	summing voltage to the voltage regulator	App. A
$\bar{V}_{max}$	upper bound for $\left\lvert\bar{d}(t_k)\right\rvert$	4.2.2
$w(q^{-1})$	closed-loop system polynomial	3.3.2
$w(t)$	mechanical torque disturbance	2.4.2
$w(t_k+h)$	total error due to discretisation, approximation, measurements, etc., in SISO discrete-time nonlinear model	4.2.2
$w_1(t)\sim w_8(t)$	measurement, actuator, and computer round-off errors in SISO discrete-time nonlinear model	4.2.2
w_{u0}, w_{y0}	leading coefficients of $W_u(q^{-1})$ and $W_y(q^{-1})$	4.3.2
$\tilde{w}(q^{-1},k)$	closed-loop system polynomial	4.3.2
$W_C(\cdot,\cdot)$	linear time-varying continuous-time system controllability Gramian	2.6
$W_O(\cdot,\cdot)$	linear time-varying continuous-time system observability Gramian	2.6
$W_r(q^{-1})$	costing polynomial	4.3.2
$W_u(q^{-1})$	costing polynomial	4.3.2
$W_y(q^{-1})$	costing polynomial	4.3.2
$\mathbf{X}(t)$	nonlinear continuous-time system state vector	2.3.1
$\mathbf{X_0}$	initial value of $\mathbf{X}(t)$	2.4.2
X_d	generator direct-axis synchronous reactance	2.2
X_e	transmission line reactance	2.2
X_q	generator quadrature-axis synchronous reactance	2.2

X'_d	generator direct-axis transient reactance	2.2
X''_d	generator direct-axis subtransient reactance	2.2
X''_q	generator quadrature-axis subtransient reactance	2.2
$\bar{\mathbf{Y}}(t)$	nonlinear continuous-time system output vector	2.6
$\bar{\mathbf{Y}}_\mathbf{0}$	initial value of $\bar{\mathbf{Y}}(t)$	2.6
$y(t_k)$	output variable	3.2.3
$y_B(k)$	output component of $y^0(k \mid k-1)$ of the NNM	6.2
$y_C(k)$	output component of $y^0(k \mid k-1)$ of the NNM	6.2
$y_D(k)$	output component of $y^0(k \mid k-1)$ of the NNM	6.2
$y_E(k)$	output component of $y^0(k \mid k-1)$ of the NNM	6.2
$y_F(t_k)$	additional output feedback signal in SISO nonlinear models	4.2.2
y_o	lower bound of the output variable	6.4.3
$y^0(k+d \mid k)$	d-step-ahead optimal prediction of $y(k+d)$	3.3.1
$y^*(k)$	desired output trajectory	3.3.2
$\bar{y}(t)$	theoretical value of $y(t)$	3.2.1
$\bar{y}_F(t)$	theoretical value of $y_F(t)$	4.2.1
$\bar{y}_{max}$	upper bound for $\lvert\bar{y}(t)\rvert$	4.2.1
$\bar{y}^*(t)$	system output set point	4.2.1
$\tilde{y}(k)$	modified output variable of the NNM	5.2
$\hat{y}(k)$	adaptive prediction of $y(k)$	3.5
$\hat{\tilde{y}}(k)$	adaptive prediction of $\tilde{y}(k)$	5.2
$\mathbf{Z}(t)$	nonlinear continuous-time system auxiliary variable vector	2.3.1
$\mathbf{Z_0}$	initial value of $\mathbf{Z}(t)$	2.4.2

$z_1(t_k) \sim z_4(t_k)$	additional feedback signals in SISO nonlinear models	4.2.2
$\bar{z}_1(t) \sim \bar{z}_4(t)$	theoretical values of $z_1(t_k) \sim z_4(t_k)$	4.2.1
$\bar{z}_{2\,max}$	upper bound for $\lvert\bar{z}_2(t)\rvert$	4.2.1
$\bar{z}_{3\,max}$	upper bound for $\lvert\bar{z}_3(t)\rvert$	4.2.1
$\alpha(q^{-1})$	optimal predictor polynomial	3.3.1
$\beta(q^{-1})$	optimal predictor polynomial	3.3.1
β_0	leading coefficient of $\beta(q^{-1})$	3.3.2
$\beta_0(k)$	time variable in the nonlinear optimal control law	4.3.2
$\beta_{0max}, \beta_{0min}$	maximum and minimum values of $\beta_0(k)$	4.3.2,4.4
$\tilde{\beta}_0(k)$	nonlinear function in the nonlinear optimal control law	4.3.2
$\delta(t)$	generator rotor angle	App. A
δ_0	steady-state value of $\delta(t)$	2.4.2
Δ	incremental symbol	2.4.2
$\Delta_1 \sim \Delta_8$	upper bounds for $\lvert w_1(t_k)\rvert \sim \lvert w_8(t_k)\rvert$	4.2.2
Δ_w	upper bound for $\lvert w(t_k)\rvert$	4.2.2
Δ_δ	minimum positive value of $\delta(k)$	5.3
τ_1, τ_2	speed deviation feedback filter time constants	App. A
τ_A	voltage regulator time constant	App. A
τ_{CO}	crossover time constant in turbine	App. A
τ_{CH}	steam chest time constant in turbine	App. A
$\tau_{d1} \sim \tau_{d7}$	generator direct-axis time constants	2.2
τ_D	generator direct-axis damper leakage time constant	2.2
τ_e	transmission line time constant	2.2
τ_E	exciter time constant	App. A

τ_F	excitation control system stabiliser time constant	App. A
τ_G	speed-governing system time constant	App. A
$\tau_m, \tau_m^{'}$	time constants in SISO nonlinear models	4.2.1
τ_R	terminal voltage transducer time constant	App. A
τ_{RH}	reheat time constant in turbine	App. A
τ_p, τ_w	time constants of the CPSS washout filter	3.6.2
$\tau_{pss1} \sim \tau_{pss4}$	time constants of the CPSS	3.6.2
τ_{q1}, τ_{q2}	generator quadrature-axis time constants	2.2
$\tau_d^{'}$	generator direct-axis transient short-circuit time constant	2.2
$\tau_{d0}^{'}$	generator direct-axis transient open-circuit time constant	2.2
$\tau_d^{''}$	generator direct-axis subtransient short-circuit time constant	2.2
$\tau_{d0}^{''}$	generator direct-axis subtransient open-circuit time constant	2.2
$\tau_q^{''}$	generator quadrature-axis subtransient short-circuit time constant	2.2
$\tau_{q0}^{''}$	generator quadrature-axis subtransient open-circuit time constant	2.2
$\epsilon(k), \bar{\epsilon}(k)$	uncorrelated noises	3.2.3
$\epsilon_{t_k}, \bar{\epsilon}_{t_k}$	residuals of the linearised prediction $\bar{z}_1(t_k + h)$	4.2.2
ϵ_{u^*}	upper bound for steady-state $\lvert u^*(k)\rvert$	3.3.2
$\epsilon_{\tilde{w}}$	sufficiently small value associated with $\Theta_{\tilde{w}}(k)$	4.3.2
$\varepsilon(k)$	white noise	3.3.1
$\varepsilon_\varphi(k)$	uncorrelated noise	3.4.2
$\eta.(\cdot,\cdot,\cdot)$	third-order residual of discretisation	4.2.2

$\theta_{\tilde{w}i}(k)$	the i-th element of $\Theta_{\tilde{w}}(k)$	4.3.2
Θ_0	parameter vector	3.4.2
$\Theta_{\tilde{w}}(k)$	coefficient vector of $\tilde{w}(z^{-1},k)$	4.3.2
$\hat{\Theta}(k)$	estimate of Θ_0	3.4.2
λ	weighting coefficient	3.3.2
λ_i	the i-th eigenvalue	2.5
$\Lambda_d(t)$	generator direct-axis stator flux linkage	App. A
$\Lambda_D(t)$	generator direct-axis damper winding flux linkage	App. A
$\Lambda_F(t)$	generator field winding flux linkage	App. A
$\Lambda_q(t)$	generator quadrature-axis stator flux linkage	App. A
$\Lambda_Q(t)$	generator quadrature-axis damper winding flux linkage	App. A
$\Lambda''_d(t)$	generator direct-axis subtransient stator flux linkage	2.2
$\Lambda''_q(t)$	generator quadrature-axis subtransient stator flux linkage	2.2
μ	forgetting factor	3.4.1
$\mu(k)$	time-varying forgetting factor	3.4.1
μ_{min}	minimum value of $\mu(k)$	3.4.2
$\mu_.(\cdot,\cdot)$	second-order residual of discretisation	4.2.2
$\sigma(k)$	switching function of the estimator	5.2
$\sigma_w^2, \sigma_\varepsilon^2$	values of noise covariances	4.3.1,3.3.1
Σ_0	constant associated with $\mu(k)$	3.4.1
$\Xi(\cdot,\cdot,\cdot)$	nonlinear function of the power system	2.3.1
$\Upsilon(\cdot,\cdot)$	output function of the power system	2.6
$\Upsilon_{\mathbf{X_0}}$	Jacobian matrix of $\Upsilon(\cdot,\cdot)$	2.6
$\Upsilon_{\mathbf{Z_0}}$	Jacobian matrix of $\Upsilon(\cdot,\cdot)$	2.6

$\mathbf{\Phi}(\cdot,\cdot,\cdot)$	state function of the power system	2.3.1
$\mathbf{\Phi_X}$	state matrix of the power system	2.3.1
$\mathbf{\Phi_{X_0}}$	Jacobian matrix of $\mathbf{\Phi}(\cdot,\cdot,\cdot)$	2.4.2
$\mathbf{\Phi_Z}$	auxiliary variable matrix of the power system	2.3.1
$\mathbf{\Phi_{Z_0}}$	Jacobian matrix of $\mathbf{\Phi}(\cdot,\cdot,\cdot)$	2.4.2
$\phi(k), \tilde{\phi}(k)$	regression vectors	3.4.1,5.2
$\varphi(k)$	auxiliary variable	3.4.2
$\varphi_t(\cdot,\cdot)$	linear time-varying continuous-time system state transition matrix	2.6
$\varphi^*(k)$	optimal prediction of $\varphi(k)$	3.4.2
$\hat{\varphi}(k)$	adaptive prediction of $\varphi(k)$	3.4.2
$\mathbf{\Psi}(\cdot,\cdot)$	nonlinear function of the power system	2.3.1
$\mathbf{\Psi_{X_0}}$	Jacobian matrix of $\mathbf{\Psi}(\cdot,\cdot)$	2.4.2
$\mathbf{\Psi_{Z_0}}$	Jacobian matrix of $\mathbf{\Psi}(\cdot,\cdot)$	2.4.2
$\psi_1 \sim \psi_5$	elements of $\mathbf{\Psi}(\cdot,\cdot)$	2.3.1
$\chi(k)$	nonlinear function in the nonlinear optimal control law	4.3.2
$\omega(t)$	generator rotor speed	App. A
ω_0	generator synchronous (nominal) speed	App. A
ω_B	base speed in per unit transformation	App. A
$\omega_s(t)$	generator speed deviation	App. A

List of Abbreviations.

Abbreviation	Description	Defined in Section
ARMAX	AutoRegressive Moving-Average with auXiliary input	3.2
AVR	Automatic Voltage Regulator	1.2
BAWMV-PSS	Bilinear Adaptive Weighted Minimum Variance Power System Stabiliser	6.4.3
BDA	Backward Difference Approximation	4.3.2
BIBO	Bounded-Input Bounded-Output	4.2
BNM	Bilinear Nominal Model	6.4.1
CPSS	Conventional Power System Stabiliser	3.6.2
CSM	Complete System Model	2.1
DARMA	Deterministic AutoRegressive Moving-Average	3.2
FDA	Forward Difference Approximation	4.3.2
LAM	Linearised Analytical Model	2.4.2
LAWMV-PSS	Linear Adaptive Weighted Minimum Variance Power System Stabiliser	3.5
LNM	Linearised Nominal Model	3.2.3
MIMO	Multi-Input Multi-Output	1.5
NAM	Nonlinear Analytical Model	2.4.1
NARMAX	Nonlinear AutoRegressive Moving-Average with auXiliary input	4.3
NAWMV-PSS	Nonlinear Adaptive Weighted Minimum Variance Power System Stabiliser	5.3
NDARMA	Nonlinear Deterministic AutoRegressive Moving- Average	4.3

NNM	Nonlinear Nominal Model	4.2.3
NOWMV-PSS	Nonlinear Optimal Weighted Minimum Variance Power System Stabiliser	4.4
PRBS	Pseudo Random Binary Sequence	3.6.1
SGM	Simplified Generator Model	2.1
SIMO	Single-Input Multi-Output	2.5
SISO	Single-Input Single-Output	1.5
SLAM	Simplified Linearised Analytical Model	2.4.2
SMA	Selective Model Analysis	2.5
SMIB	Single Machine Infinite Bus	2.1
SVI-NAWMV-PSS	Simplified Version I of the Nonlinear Adaptive Weighted Minimum Variance Power System Stabiliser	6.3
SVII-NAWMV-PSS	Simplified Version II of the Nonlinear Adaptive Weighted Minimum Variance Power System Stabiliser	6.3

List of Figures

2.1 A single machine infinite bus power system. 24

2.2 A synchronous generator and steam turbine generating unit. 24

2.3 Comparison of the performance of the complete system models: speed response for Case 1. 51

2.4 Comparison of the performance of the complete system models: speed response for Case 2. 51

2.5 Comparison of the performance of the complete system models: speed response for Case 3. 52

2.6 Comparison of the performance of the complete system models: speed response for Case 4. 52

3.1 Control structure of the SMIB power system with the LAWMV-PSS. . 102

3.2 Structure of the verification and identification of the LNM. 105

3.3 Verification and identification of the LNM: estimated parameters of the LNM for Case 1. 109

3.4 Verification and identification of the LNM: electrical torque deviation response for Case 1. 109

3.5 Evaluation of the performance of the LAWMV-PSS: electrical torque response for Study 1. 117

3.6 Evaluation of the performance of the LAWMV-PSS: electrical torque response for Study 2. 117

3.7 Evaluation of the performance of the LAWMV-PSS: electrical torque response for Study 3. 118

3.8 Evaluation of the performance of the LAWMV-PSS: electrical torque response for Study 4. 118

3.9 Evaluation of the performance of the LAWMV-PSS: electrical torque response for Study 5. 119

3.10 Evaluation of the performance of the LAWMV-PSS: field voltage response for Study 5. 119

3.11 Evaluation of the performance of the LAWMV-PSS: electrical torque response for Study 6. 120

3.12 Evaluation of the performance of the LAWMV-PSS: electrical torque response for Study 7. 120

3.13 Evaluation of the performance of the LAWMV-PSS: estimated parameters of the LNM for Study 7. 121

3.14 Evaluation of the performance of the LAWMV-PSS: electrical torque response for Study 8. 121

3.15 Evaluation of the performance of the LAWMV-PSS: electrical torque response for Study 9. 122

3.16 Evaluation of the performance of the LAWMV-PSS: electrical torque response for Study 10. 122

3.17 Evaluation of the performance of the LAWMV-PSS: electrical torque response for Study 11. 123

3.18 Studies on the robustness of the LAWMV-PSS: electrical power response for Study 12. 126

3.19 Studies on the robustness of the LAWMV-PSS: electrical power response for Study 13. 126

3.20 Studies on the robustness of the LAWMV-PSS: electrical power response for Study 14. 127

3.21 Studies on the robustness of the LAWMV-PSS: electrical power response for Study 15. 127

4.1 SISO nonlinear continuous-time state-space modelling of the SMIB power system. 139

4.2 SISO nonlinear continuous-time input-output modelling of the SMIB power system. 142

4.3 SISO nonlinear discrete-time input-output modelling of the SMIB power system. 152

4.4 Control structure of the SMIB power system with the NOWMV-PSS. . 173

4.5 Structure of the verification of the NNM. 176

4.6 Verification of the NNM: electrical torque response for Case 1. 181

4.7 Verification of the NNM: error in electrical torque for Case 1. 181

4.8 Verification of the NNM: electrical torque response for Case 3. 182

4.9 Verification of the NNM: electrical torque response for Case 4. 182

4.10 Evaluation of the performance of the NOWMV-PSS: electrical torque response for Study 1. 186

4.11 Evaluation of the performance of the NOWMV-PSS: electrical torque response for Study 2. 186

4.12 Evaluation of the performance of the NOWMV-PSS: electrical torque response for Study 3. 187

4.13 Evaluation of the performance of the NOWMV-PSS: electrical torque response for Study 4. 187

4.14 Evaluation of the performance of the NOWMV-PSS: electrical torque response for Study 5. 188

4.15 Evaluation of the performance of the NOWMV-PSS: field voltage response for Study 5. 188

4.16 Evaluation of the performance of the NOWMV-PSS: electrical torque response for Study 6. 189

4.17 Evaluation of the performance of the NOWMV-PSS: electrical torque response for Study 7. 189

4.18 Evaluation of the performance of the NOWMV-PSS: electrical torque response for Study 8. 190

4.19 Evaluation of the performance of the NOWMV-PSS: electrical torque response for Study 9. 190

4.20 Evaluation of the performance of the NOWMV-PSS: electrical torque response for Study 10. 191

4.21 Evaluation of the performance of the NOWMV-PSS: electrical torque response for Study 11. 191

4.22 Studies on the robustness of the NOWMV-PSS: electrical power response for Study 12. 194

4.23 Studies on the robustness of the NOWMV-PSS: electrical power response for Study 13. 194

4.24 Studies on the robustness of the NOWMV-PSS: electrical power response for Study 14. 195

4.25 Studies on the robustness of the NOWMV-PSS: electrical power response for Study 15. 195

5.1 Control structure of the SMIB power system with the NAWMV-PSS. . 216

5.2 Structure of the identification of the NNM. 219

5.3 Identification of the NNM: electrical torque response for Case 1. 222

5.4 Identification of the NNM: error in electrical torque for Case 1. 222

5.5 Identification of the NNM: estimated parameters of the LNM for Case 1. 223

5.6 Identification of the NNM: estimated parameters of the NNM for Case 1. 223

5.7 Identification of the NNM: error in electrical torque for Case 2. 224

5.8 Evaluation of the performance of the NAWMV-PSS: electrical torque response for Study 1. 229

5.9 Evaluation of the performance of the NAWMV-PSS: electrical torque response for Study 3. 229

5.10 Evaluation of the performance of the NAWMV-PSS: electrical torque response for Study 4. 230

5.11 Evaluation of the performance of the NAWMV-PSS: electrical torque response for Study 5. 230

5.12 Evaluation of the performance of the NAWMV-PSS: field voltage response for Study 5. 231

5.13 Evaluation of the performance of the NAWMV-PSS: electrical torque response for Study 6. 231

5.14 Evaluation of the performance of the NAWMV-PSS: electrical torque response for Study 7. 232

5.15 Evaluation of the performance of the NAWMV-PSS: estimated parameters of the NNM for Study 7. 232

5.16 Evaluation of the performance of the NAWMV-PSS: electrical torque response for Study 8. 233

5.17 Evaluation of the performance of the NAWMV-PSS: electrical torque response for Study 11. 233

5.18 Studies on the robustness of the NAWMV-PSS: electrical power response for Study 13. 236

5.19 Studies on the robustness of the NAWMV-PSS: electrical power response for Study 14. 236

5.20 Studies on the robustness of the NAWMV-PSS: electrical power response for Study 15. 237

6.1 Decomposition of the output prediction of the NNM. 246

6.2 Decomposition of the output prediction of the NNM: electrical torque prediction and its components for Case 1. 248

6.3 Decomposition of the output prediction of the NNM: electrical torque prediction and its components for Case 2. 248

6.4 Evaluation of the performance of the simplified NAWMV-PSS: electrical torque response for Study 1. 252

6.5 Evaluation of the performance of the simplified NAWMV-PSS: electrical torque response for Study 5. 252

6.6 Control structure of the SMIB power system with the BAWMV-PSS. . 260

6.7 Structure of the verification and identification of the BNM. 263

6.8 Verification and identification of the BNM: electrical torque response for Case 1. 266

6.9 Verification and identification of the BNM: error in electrical torque for Case 1. 266

6.10 Verification and identification of the BNM: estimated parameters of the BNM for Case 1. 267

6.11 Evaluation of the performance of the BAWMV-PSS: electrical torque response for Study 1. 272

6.12 Evaluation of the performance of the BAWMV-PSS: electrical torque response for Study 2. 272

6.13 Evaluation of the performance of the BAWMV-PSS: electrical torque response for Study 3. 273

6.14 Estimated parameter $\hat{a}_2(k)$ of the NNM and the BNM for Studies 1-2. . 273

6.15 Evaluation of the performance of the BAWMV-PSS: electrical torque response for Study 4. 274

6.16 Evaluation of the performance of the BAWMV-PSS: electrical torque response for Study 5. 274

6.17 Evaluation of the performance of the BAWMV-PSS: electrical torque response for Study 6. 275

6.18 Evaluation of the performance of the BAWMV-PSS: electrical torque response for Study 7. 275

6.19 The effect of the function $f_y(k)$ in the BAWMV-PSS: electrical torque response for Study 7. 276

6.20 The effect of the function $f_y(k)$ in the BAWMV-PSS: control input for Study 7. 276

6.21 Evaluation of the performance of the BAWMV-PSS: electrical torque response for Study 8. 277

6.22 Evaluation of the performance of the BAWMV-PSS: electrical torque response for Study 9. 277

6.23 Evaluation of the performance of the BAWMV-PSS: electrical torque response for Study 10. 278

6.24 Evaluation of the performance of the BAWMV-PSS: electrical torque response for Study 11. 278

6.25 Studies on the robustness of the BAWMV-PSS: electrical power response for Study 12. 280

6.26 Studies on the robustness of the BAWMV-PSS: electrical power response for Study 13. 280

6.27 Studies on the robustness of the BAWMV-PSS: electrical power response for Study 14. 281

6.28 Studies on the robustness of the BAWMV-PSS: electrical power response for Study 15. 281

A.1 IEEE Type 1 excitation system representation. 297

A.2 General model of a governor/valve system for a steam turbine. 299

A.3 Linear model of a tandem-compound single-reheat turbine. 301

A.4 Linear model of a nonreheat turbine. 302

List of Tables

2.1 The models of the synchronous generator and the SMIB power system. 62

2.2 System parameters at the lagging and leading operating conditions. . . 66

2.3 System eigenvalues and participation factors at the lagging and leading operating conditions. 67

3.1 Estimated parameters of the LNM for Cases 1-3. 107

3.2 Identified zeros of the polynomials of the LNM for Cases 1-3. 107

3.3 Variations in the system operating point of the CSM3 for Studies 1-3 and 8-11. 114

4.1 SISO nonlinear optimal control laws with their selections of weighting polynomials. 168

4.2 Parameters of the NNM at the lagging and leading operating points. . . 177

5.1 Estimated parameters of the LNM for Case 1. 221

5.2 Estimated parameters of the NNM for Case 1. 224

6.1 Estimated parameters of the BNM for Case 1. 267

Chapter 1

Introduction.

1.1 The Basic Concept of Power System Stability.

Problems associated with power system stability emerged in the 30's [1], and have formed the basis for many areas of study since that time. As the complexity of modern power systems increases, improving the stability and dynamic performance of the system has become increasingly desirable, and has attracted the attention of control engineers [2].

Power systems rely on synchronous generators for the generation of electrical power. A necessary condition for the transmission and exchange of electrical energy is that all generators in a system rotate in synchronism. The concept of power system stability relates to the *ability* of the generators in the system to maintain synchronism and the *tendency* to return to and remain at their steady-state operating points following system disturbances.

A heuristic non-mathematical definition of power system stability can be given as follows [3]:

> **Power System Stability.** If the oscillatory response of a power system during the transient period following a disturbance is damped, and the

system settles in a finite time to a (new) steady operating condition at constant frequency, then the system is said to be *stable*. If the system is not stable according to this definition, then it is considered *unstable*.

Due to the nonlinear nature of the power system, and to describe its wide range of behaviour, power system stability is further classified into three categories: *steady-state stability* due to minute disturbances, *dynamic stability* due to small disturbances, and *transient stability* due to large disturbances [4,5,2,6]. [1]

Steady-State Stability, Power System. *Steady-state stability* refers to the stability of a power system subject to minute and gradual changes in the operating conditions. The system is described by algebraic equations with phasor representations.

The studies in this category are concerned with the system *steady-state stability limit*, which is the maximum power that can be transmitted in the steady state without the loss of synchronism. The minute disturbances that are applied to the system cannot cause the loss of synchronism unless the system is operated at, or very near to, its steady-state stability limit.

Dynamic Stability, Power System. *Dynamic stability* refers to the stability of a power system subject to small and "sudden" perturbations. The system can be described by linear differential equations which are obtained by linearising the system nonlinear differential equations about a certain steady-state operating point.

Typical perturbations under this category may be small, randomly occurring changes in load or small alterations in reference settings. It is assumed that the system under study is stable at the initial operating condition. If the system is *dynamically stable*, it

[1] It should be pointed out that there is *no* universally accepted classification of power system stability [2]. For example, in some different classifications, only steady-state stability (or dynamic stability) and transient stability are categorised.

is expected that after a temporary small disturbance the system will return to its initial state, while for a permanent small disturbance the system will acquire a new operating state after a transient period [3]. In both cases the synchronism of the system should not be lost. The size of *small* disturbances may be measured by the criterion that the perturbed system can be stabilised in an approximately linear region [3].

> **Transient Stability, Power System.** *Transient stability* refers to the stability of a power system subject to severe disturbances for which the linearised model of the system is invalid. The system must be described by nonlinear differential equations.

The severe disturbances which cause transient stability problems may typically be large changes in load, three-phase faults or transmission line switching. It is usually assumed that the system under study is stable before a large disturbance happens. If the system is *transiently stable*, the system oscillations resulting from large disturbances are damped. However, transient stability of the system depends very much on the initial operating condition of the system and the nature (i.e., the type, magnitude, duration, and location, etc.) of the large disturbances that are applied to the system [3], as well as on the post-fault system configuration.

For successful operation and control of power systems, the latter two categories of stability of the system must be carefully considered.

1.2 The Effect of the Excitation Control System on Power System Stability.

In the analysis of power system stability, considerable attention has been given in the literature to the *excitation control system*, which is one of the basic components in a generating unit (see, e.g., Fig. A.1 of Appendix A). By the use of an *Automatic Voltage Regulator* (**AVR**) with machine terminal voltage feedback, the *primary functions* of an excitation control system are

- to maintain the desired constant voltage at the synchronous generator terminal within a specified error limit;
- to continuously adjust the generator excitation level in response to changes in reference voltage.

A high-gain AVR was recommended for reducing the steady-state error of the system output. It was, then, realised by early investigators that the steady-state stability limit of the system could be increased when a high-gain AVR was used [7]. Analyses based on several different stability criteria also pointed out that the increase of the steady-state stability limit was restricted by the general characteristics of the system, such as time lags and gain levels [7]-[18].

The study of the excitation control is further complicated by a conflict in control requirements in the time period immediately following a transient. For different stability control problems, the requirements on the excitation control system may be significantly different. In transient stability studies, the time period of interest during a transient is the first few cycles of rotor oscillations, with the first swing being of primary importance. During the first swing, the generator is suddenly subjected to a large change in its output power, causing its rotor to accelerate (or decelerate) at a rate large enough to threaten the loss of synchronism. To prevent the loss of synchronism, a very fast and high-ceiling voltage control action from the excitation control system is needed to reduce the amplitude of the first swing and to help the generator to maintain its synchronism. From this point of view, a fast excitation system with a high-gain AVR is beneficial to the control of the system transient stability. In dynamic stability studies, however, a high-gain excitation control system introduces a negative damping effect to the rotor oscillations. This can be analysed by using the *small signal linearised system model* (D.2)-(D.7) [2] given in Section D.2 of Appendix D, with constant reference signals [8,19]. For a system *without* the AVR regulation, the damping torque

[2]The parameters K_i $(i = 1, 2, \cdots, 6)$ in the model are defined in (2.107)-(2.108), (2.119)-(2.120), and (2.109)-(2.110), respectively.

component of the electrical torque at frequency ω is given by

$$\Delta T_d(\omega) = \frac{\bar{K}_2 \bar{K}_3^2 \bar{K}_4 \tau'_{d0} \omega}{1 + \bar{K}_3^2 \tau'^2_{d0} \omega^2} \Delta\delta(\omega). \tag{1.1}$$

Since the parameters $\bar{K}_2$, $\bar{K}_3$, and $\bar{K}_4$ are all positive, the damping torque given by (1.1) is positive too. However, for a system *with* the AVR in service, the damping torque component of the electrical torque is described approximately as

$$\Delta T_d(\omega) \approx \frac{\bar{K}_2 \bar{K}_5 K_A \left(\tau'_{d0} + \frac{\tau_A}{\bar{K}_3}\right) \omega}{2V_{t0} \left\{ \left[\left(\frac{1}{\bar{K}_3} + \frac{\bar{K}_6 K_A}{2V_{t0}} \right) - \tau'_{d0} \tau_A \omega^2 \right]^2 + \left(\tau'_{d0} + \frac{\tau_A}{\bar{K}_3} \right)^2 \omega^2 \right\}} \Delta\delta(\omega), \tag{1.2}$$

where $\Delta T_d(\omega)$ has the same sign as the parameter $\bar{K}_5$. At low frequencies, the synchronising torque component of the electrical torque is given approximately by

$$\Delta T_s(\omega) \approx \left[\bar{K}_1 - \frac{\bar{K}_2 \bar{K}_5}{\bar{K}_6} \right] \Delta\delta(\omega). \tag{1.3}$$

At some operating conditions the parameter $\bar{K}_5$ can be negative (see, e.g., Table 2.2 of Section 2.5). In these cases the damping torque (1.2) becomes negative, while the synchronising torque (1.3) is augmented (since $\bar{K}_1$ and $\bar{K}_6$ are positive). Therefore, whereas the AVR regulation improves the synchronising torques on the generators in the system at low frequencies of rotor oscillations, it reduces the inherent damping of the system at operating conditions where $\bar{K}_5$ is negative.

The above analysis indicates that the excitation control system has the potential to introduce negative damping into the system dynamics. This phenomenon has been observed by many researchers (e.g., [19]-[29]) and has been reported widely in the literature.

1.3 The Role of Power System Stabilisers.

Based on the fact that the *negative* damping effect is caused by the closed-loop excitation control of generator terminal voltage, it is reasonable to expect that a *positive* damping effect may be introduced into the system by using a *supplementary damping signal* through the same control loop. The network used to generate this signal has

been known as a *power system stabiliser* network. By the use of the supplementary damping signal, not only can the negative damping effect of the AVR regulation be cancelled, but the positive damping effect of the system can also be increased so as to allow the system to operate even beyond the steady-state stability limit. This is the basic idea behind the design of power system stabilisers. The role of power system stabilisers is to improve the damping performance of the system and to extend the steady-state stability limit of the system via modulation of the generator excitation.

By means of the power system stabiliser, a component of torque in phase with speed is introduced onto the shaft of the generator. This component of torque is a *pure damping torque.* If the system characteristic between the reference voltage input and the shaft speed output is described by a transfer function $GEP(s)$ [29], the supplementary damping signal generated by the power system stabiliser is then aimed to compensate for the phase and gain characteristics of $GEP(s)$ by giving, ideally, that

$$PSS(s) = \frac{K_{PSS}}{GEP(s)}, \tag{1.4}$$

where K_{PSS} represents the desired damping contribution from the stabiliser. A practical realisation of the transfer function $PSS(s)$ (1.4) is to use analogue controllers to achieve the desired adjustments in phase and gain over the frequency range of concern. A washout circuit is usually added into the final form of the stabiliser to eliminate the steady-state offset in the stabilising signal.

Design issues involved in the use of various tuning techniques and input (or stabilising) signals for power system stabilisers have been studied extensively in the literature under classical control theory. For example, a detailed analysis of the damping and synchronising torques of synchronous generators with speed as a stabilising signal was given in [19]. A comparative study on the proper selection of transfer functions for a number of stabilising signals, namely speed, frequency, and power, was described in [30,29]. Other input signals, such as the accelerating power [31]-[33], for power system stabilisers have also been studied. Practical aspects associated with the implementation of the designed power system stabilisers have been discussed in the literature (e.g., [32,30]). Studies reported by researchers in this field have shown that improved

damping performance is achievable with properly tuned power system stabilisers in the frequency range of concern.

1.4 Shortcomings of the Conventional Power System Stabilisers.

Power system stabilisers designed using classical control theory can be called conventional power system stabilisers. For design purposes, *linearised fixed-parameter* models of the nonlinear power system are derived from the linearisation of the system about a given operating point. Such models are valid, in theory, only at the chosen operating point. If the system operating point changes or the system configuration alters, the basis for the design of linearised fixed-parameter power system stabilisers is violated. This implies that a conventional power system stabiliser, based on a linearised fixed-parameter model, cannot track the variations in the system operating conditions over a wide range.

A conventional power system stabiliser is operated through the system transfer function $GEP(s)$. Frequency analyses shown in [29] for the design of the transfer function $PSS(s)$ of the power system stabiliser indicate that the characteristics of $GEP(s)$ vary with different operating conditions. [3] The gain of $GEP(s)$ increases with the generator loading and the a.c. transmission system strength. Also, the phase lag of $GEP(s)$ increases as the a.c. transmission system becomes stronger [4]. Since the parameters of the stabiliser are constant, the stabiliser gain fixed for the strong system conditions can not be as high as desired by the weak system conditions, and the damping performance under these conditions will deteriorate [29]. Therefore, a compromise has to be made in the selection of the stabiliser gain in order to give satisfactory performance for different operating conditions.

[3] This statement is made for systems having a relatively low AVR gain. Higher AVR gain may improve the characteristics of the system transfer function [34].

[4] The term *stronger* or *weaker* refers here to the strength of the a.c. transmission system [30].

Furthermore, power systems are nondeterministic. Changes in the system configuration, disturbances from load demands, and occurrences of unpredicted faults happen randomly. A conventional power system stabiliser, designed in a deterministic environment, has no means of coping with the stochastic nature of the system.

The above shortcomings associated with the conventional power system stabilisers indicate that in order to enhance the stability and damping performance of a time-varying nonlinear power system over a wide range of operating conditions, a power system stabiliser *must* be able to identify the current system operating condition and to adapt to the system changes on-line. A particularly useful approach to realise this requirement is the use of adaptive control strategies for the design of power system stabilisers.

1.5 Linear Adaptive Control in the Design of Power System Stabilisers.

Adaptive control has been a topic of research for more than a quarter of a century. An *adaptive control system* can be defined as a control system within which automatic means are used to change the control system parameters in a way intended to improve the performance of the closed-loop system [35]. The goal of adaptive control is to make the system under control less sensitive to parameter variations and unmodelled dynamics. As the system dynamics change, adaptive control systems attempt to sense the changes and to make on-line adjustments to control parameters and/or control strategies. Different *philosophies* are used in making on-line adjustments. The *approaches* taken to implement each philosophy vary, as in other aspects of control system design. Surveys of various approaches to adaptive control are given in [36]-[39].

The adaptive control approach that is considered in this thesis for the design of power system stabilisers is the *self-tuning adaptive control approach.* In this approach, *parameter estimation algorithms* are used to identify the system parameters on-line, and these parameter estimates are then incorporated into the *control scheme* as if the

estimated parameters were the true parameters. The *controller* that implements the self-tuning adaptive control scheme is called the *self-tuning adaptive controller.* Issues of general interest regarding the self-tuning adaptive control approach include global stability properties [40], persistency of excitation requirements [41], and convergence properties [42].

In this thesis, the self-tuning adaptive control schemes that are based on *linear* finite-dimensional discrete-time models are called *linear adaptive control schemes.* Correspondingly, those that are based on *nonlinear* finite-dimensional discrete-time models are called *nonlinear adaptive control schemes.* These definitions are necessary in order to distinguish the adaptive *linear* and *nonlinear* control methodologies to be presented in this thesis.

Much effort has been devoted in recent years to the application of *linear* adaptive control theory to the stabilisation of power systems. In References [43] and [44], summaries of the approaches and developments of adaptive power system control are presented. The emphasis in most approaches has been placed on *adaptive generator excitation control* [45]-[67], which is based on *Single-Input Single-Output* **(SISO)** models of the power systems. Such SISO adaptive controllers are used as either power system stabilisers (i.e., the adaptive controller operates as a conventional power system stabiliser to provide an auxiliary damping signal to the ordinary AVR control loop) or excitation controllers (i.e., the adaptive controller combines the functions of the AVR and the power system stabiliser). Research interest has also been shown in the *adaptive generator control via both governor and exciter controls* [68]-[74], where the adaptive controllers are based on *Multi-Input Multi-Output* **(MIMO)** models of the power systems. Moreover, the power systems under study have been extended from single machine systems [45,46,47,48,49,50,51,52,68,54,69,57,70,58,71,72,59,62,63,73,67,74] to multi-machine systems [53,55,56,60,61,62,64,65,66], and research has also been carried out in both simulation studies [45,47,49,52,53,54,55,69,56,57,58,60,61,62,64,73,65,66,74] and laboratory experiments [46,48,50,51,68,70,71,72,59,63,67]. In the studies of those *linear adaptive power system stabilisers* (both the SISO [49,50,51,53,54,56,58,59,63,64, 65,66] and the MIMO devices [70,73,74]), the dynamic and transient performance of the power systems has been shown to be improved over the conventional power system

stabilisers (which may not have been properly designed in some instances). Linear adaptive power system stabilisers (or controllers) are currently being implemented in laboratories (e.g., [70,59,67]). This represents the **state-of-the-art** in terms of the design and implementation of adaptive power system stabilisers (or controllers).

An important feature of a linear adaptive power system stabiliser is that it identifies the power system dynamics continuously by operating the parameter estimation algorithm on-line. On the basis of this up-to-date model of the system, it is then possible to 'find' suitable stabiliser parameters so that the control action can be tuned to damp the oscillations that may arise from disturbances. From this point of view, a linear adaptive power system stabiliser is actually a *time-varying linear* controller which is able to cope with the system nonlinearities by adjusting the estimated parameters on-line.

Linear adaptive power system stabilisers, when used to stabilise *nonlinear* power systems, are based on *linearised models* of the power systems. The reason for adopting linearised models for the development of adaptive power system stabilisers is for the purpose of parameter estimation and for the development of control algorithms. Since theories associated with linear adaptive estimation/prediction/control are well developed, the use of linear adaptive control strategies for the design of power system stabilisers may be relatively straightforward. However, because of the use of linearised models, the parameters of the linear adaptive power system stabilisers *have to* change in order to *track* the changes in operating conditions of the nonlinear power systems. Before the parameters converge to new values, the linearised models may not accurately represent the actual systems. Consequently, the control actions that are generated by unconverged estimates may not give the optimal control effects.

The underlying problem may be handled by the formulation of some kind of *nonlinear control strategy* that exploits the nonlinear structure of the power system. Since a power system is a nonlinear system, improvements in the control (or stabilisation) of the system may be obtained by incorporating the nonlinearities of the system into the control law. This is the *motivation* of the work of this thesis. The idea of introducing nonlinear control schemes for the control of nonlinear dynamic systems has been rec-

ommended by many researchers in different fields of studies [44,75]. In recent years, nonlinear control theory, such as the differential geometric theory [76] and the direct feedback linearisation theory [77], has been employed in the design of power system controllers. The research reported in [78]-[87] represents the **state-of-the-art** in term of the development of nonlinear controllers for power systems.

1.6 Nonlinear Optimal Control in the Design of Power System Stabilisers.

The differential and algebraic equations describing the generating unit and the external system of a power system possess nonlinearities which often have *known* forms. As the modelling accuracy increases, nonlinearities associated with the power system of concern can be modelled in analytical forms [3,88,6,89]. If the nonlinearities of the system are incorporated into a control law, then the control law will have the advantage of *not* requiring the controller parameters to change when the operating point of the power system changes. From this point of view, a fixed-parameter *nonlinear optimal* power system stabiliser will be able to stabilise the nonlinear power system over a wide range of operating conditions in which the controller parameters are constant. The control action of such a stabiliser is optimal at the new operating point immediately, and the resulting system transition from one operating point to another is also optimal. These are the anticipated advantages of a nonlinear optimal power system stabiliser over a linear adaptive power system stabiliser.

Optimal control strategies have been considered in the literature for the stabilisation of power systems [90]-[106]. At an early stage in the design of power system stabilisers, many studies on the utilisation of *linear optimal* control strategies were carried out in order to achieve an optimum tuning of the stabiliser parameters [90,92,93,94,95,97,99,101,104,105]. Most of the results are based on the assumption that an explicit deterministic mathematical model of the system is available. The system model was then linearised around a chosen operating point with the system parameters assumed constant. By numerous off-line simulation studies, suitable weighting

factors involved in the control law could thus be found. However, since a linear optimal power system stabiliser is still based on a *linearised fixed-parameter* model of the nonlinear power system, the optimal control action for *one* operating point may *not* be optimal for *another*. Therefore, a linear optimal power system stabiliser may have the same deficiencies as a conventional power system stabiliser in tracking a wide range of variations of the system operating point.

A nonlinear optimal power system stabiliser, however, can overcome the above problem by utilising a *nonlinear model* that *inherently* represents the nonlinearities of the power system. Subject to the provision of a valid nonlinear model, the control action of a *nonlinear* optimal power system stabiliser will be globally optimal, unlike a *linear* optimal power system stabiliser. This is an important consideration behind the study of nonlinear optimal power system stabilisers.

A number of problems associated with a nonlinear optimal power system stabiliser can be anticipated:

- Power systems are not only nonlinear but also time-varying. The system parameters and configuration are changing randomly. Therefore, the parameters of the nonlinear model that is used for the calculation of the nonlinear optimal control law are *time-varying* in nature. With *fixed parameters*, the nonlinear optimal power system stabiliser is not able to track the changes in the system parameters and/or the system configuration.

- Since a power system is a complex nonlinear system, the derivation of a feasible nonlinear optimal control law from the mathematical description of the power system inevitably involves certain assumptions. If the conditions in the assumptions are violated, the control action generated by the nonlinear optimal power system stabiliser is not optimal.

These problems are due to the inability of the nonlinear optimal controller to adapt to changes in the system. It is then reasonable to suggest that the nonlinear *optimal* control strategies should be replaced by the corresponding nonlinear *adaptive* control strategies.

1.7 Nonlinear Adaptive Control in the Design of Power System Stabilisers.

The development of nonlinear adaptive control algorithms requires

- formulation of a nonlinear model of the system;
- implementation of on-line parameter estimation algorithms;
- synthesis of nonlinear control methodologies.

A survey of approaches to adaptive control of nonlinear dynamic systems in a wide range of fields is given in [75]. It has been pointed out that [75]:

> *researchers have to focus their interest in the direction of special nonlinear methods and problems which are not formal extensions of linear ones.*

This feature of nonlinear adaptive control explains the reason why there is less research activity in this area than in the area of linear adaptive control. The development of nonlinear adaptive control algorithms for nonlinear dynamic systems is, then, one of the *recent trends* in both adaptive control theory and adaptive control applications [44]. In the field of power system control, an investigation on the design of an adaptive excitation controller with a nonlinear control approach for a single-machine infinite-bus power system is reported in [86].

If a nonlinear model developed for the design of a nonlinear adaptive control algorithm is derived in a regression form, linear in the parameters, then the parameter estimation algorithms that are developed for linear models can be utilised for the identification of the parameters of the nonlinear model. Moreover, if the nonlinear model is linear in the control input, then a nonlinear optimal control law that is based on the nonlinear model is most likely to be solved explicitly. With the availability of a suitable nonlinear model and a solvable nonlinear optimal control law, the development of a

nonlinear adaptive control algorithm from a nonlinear optimal control law is straightforward. This forms the general guideline for the design of a nonlinear adaptive power system stabiliser.

A nonlinear adaptive power system stabiliser is expected to exhibit the following important features that distinguish it from the corresponding nonlinear optimal and linear adaptive power system stabilisers:

- If there is no change in the power system parameters or configuration, the nonlinear adaptive power system stabiliser will behave in the same way as the nonlinear optimal power system stabiliser. Thus it will inherently track the variations in the system operating point without changing its parameters.
- Upon the occurrence of a change in the power system parameters or configuration, the nonlinear adaptive power system stabiliser will behave in the same way as the linear adaptive power system stabiliser by adjusting its parameters on-line.
- When any assumption that is used in the derivation of the nonlinear optimal control law is violated, the nonlinear adaptive power system stabiliser will adapt to the new environment by identifying new parameters and generating an appropriate control action.

It is anticipated that the combination of *nonlinear* models with *adaptive* control schemes will provide better stabilisation of the *time-varying* and *nonlinear* power systems than more conventional approaches.

1.8 Subject Coverage and Outline of the Thesis.

This thesis is concerned with the development of nonlinear adaptive power system stabilisers for single-machine infinite-bus models of power systems. The studies of this thesis will cover the areas of *linear adaptive*, *nonlinear optimal*, *nonlinear adaptive*, and *bilinear adaptive* control in the design of such stabilisers. Both theoretical analyses and

simulation studies will be presented for each area of study. SISO design methods will be considered. The aims of this study are

- to *explore* the possibility of using nonlinear adaptive control strategies in the stabilisation of power systems;
- to *establish* the nonlinear optimal/adaptive control theory relevant to the design;
- to *investigate* the effectiveness of nonlinear adaptive power system stabilisers in improving the system damping performance over a wide range of operating conditions.

For these purposes, a *consistent* control scheme will be used for the development of the power system stabilisers in the above-mentioned areas. With this arrangement, the comparisons of the performance of the different stabilisers will then provide a meaningful basis for assessing their relative benefits and deficiencies. The conclusions drawn from these studies will therefore provide a general guideline for future research and the development of practical nonlinear adaptive power system stabilisers.

This thesis consists of seven chapters. The outline of the thesis is as follows.

Chapter 2 is concerned with the *modelling* of the single-machine infinite-bus power system for the analysis and design of the linear and nonlinear optimal/adaptive power system stabilisers, and simulation studies for the evaluation of the stabilisers that result from the various control strategies.

- In Sections 2.2 and 2.3 *three* complete models of the nonlinear single-machine infinite-bus power system, including the generator, the excitation system, the governor, the steam turbine, and the transmission system, are developed from the basic model described in Appendix A. Decisions with regard to the selection of the models, used for the analysis and design of power system stabilisers and for the evaluation of the stabilisers which are to be designed, are made with the aid of the model-matching studies presented in Subsection 2.3.2. Nonlinear and

linearised analytical models [5] of the power system are derived in Section 2.4 for the development of the power system stabilisers to be undertaken in Chapters 3 to 6. The models developed in this chapter are summarised in Subsection 2.4.3.

- In Section 2.5 the selection of a suitable stabilising signal for the power system stabilisers that will be designed in this thesis is discussed using participation factor analyses [107].

- In Section 2.6 the concepts of controllability and observability associated with the models developed in this chapter are briefly introduced, and the aspects of the system realisation and input-output properties are discussed. This facilitates the development of the linear adaptive power system stabiliser to be designed in Chapter 3.

In Chapter 3 the design of *SISO linear adaptive power system stabilisers* is discussed:

- In Section 3.2 a linearised nominal model [6] is derived from the simplified linearised analytical model given in Subsection 2.4.2 for the development of linear optimal and adaptive control laws.

- In Section 3.3 linear stochastic optimal control laws are developed from a general form of the cost function. Aspects of the use of different linear stochastic optimal control schemes for the design of linear adaptive power system stabilisers are discussed. The weighted minimum variance control scheme is selected as the control scheme for the development of the corresponding nonlinear optimal/adaptive power system stabilisers in Chapters 4 to 6.

- In Sections 3.4 and 3.5 the linear stochastic adaptive weighted minimum variance control algorithm is developed from the generalised minimum variance control algorithm, and a linear adaptive weighted minimum variance power system stabiliser is proposed.

[5] See Section 2.4 for the definition of an "analytical model" used in this thesis.

[6] See Section 3.2 for the definition of a "nominal model" used in this thesis.

- In Section 3.6 a series of simulation studies is defined to form a systematic method for comparing the performance of the various stabilisers that will be designed in this thesis. The performance of the proposed linear adaptive power system stabiliser is then assessed by comparison with a robust conventional power system stabiliser (designed in Subsection 3.6.2), and is taken as the *reference* for the evaluation of the performance of the nonlinear optimal/adaptive power system stabilisers in Chapters 4 to 6.

Chapters 2 to 3 provide the basis upon which the studies of the nonlinear optimal/adaptive power system stabilisers are presented in later chapters.

In Chapter 4 the design of *SISO nonlinear optimal power system stabilisers* is discussed:

- In Section 4.2 a nonlinear nominal model is derived from the nonlinear analytical model given in Subsection 2.4.1. This model describes the nonlinear relationship between the control input and the electrical torque (or power) output of the generator, and is used for the development of the nonlinear optimal and adaptive control laws.

- In Section 4.3 a SISO nonlinear stochastic generalised minimum variance control law is developed and its closed-loop stability conditions are established (Section E.1 of Appendix E).

- In Section 4.4 a nonlinear weighted minimum variance control law and the sufficient condition for its global closed-loop system stability (Section E.2 of Appendix E) are described. A nonlinear optimal power system stabiliser which is based on the nonlinear weighted minimum variance control scheme is then proposed.

- In Section 4.5 the performance of the proposed nonlinear optimal power system stabiliser is evaluated by comparison with the performance of the linear adaptive power system stabiliser proposed in Chapter 3. The effectiveness of the nonlinear control strategy in the design of power system stabilisers is investigated.

Chapter 4 establishes a valid basis for the further development of the nonlinear adaptive power system stabilisers in Chapters 5 and 6.

In Chapter 5 the design of *SISO nonlinear adaptive power system stabilisers* is discussed:

- In Section 5.2 parameter estimation algorithms for the nonlinear nominal model are proposed and convergence analyses are given (Sections G.1 and G.2 of Appendix G).
- In Section 5.3 nonlinear adaptive weighted minimum variance control algorithms are derived and theoretical proofs of the convergence are presented (Section G.3 of Appendix G). A nonlinear adaptive weighted minimum variance power system stabiliser is proposed.
- In Section 5.4 the evaluation of the performance of the proposed nonlinear adaptive power system stabiliser is conducted through simulation studies. The performance of the nonlinear *adaptive* (Chapter 5) control strategy is compared with that of the nonlinear *optimal* (Chapter 4) control strategy. The improvement in the system damping performance associated with the *nonlinear* adaptive (Chapter 5) control strategy over that with the *linear* adaptive (Chapter 3) control strategy is demonstrated.

Chapter 5 provides an *ideal* design of a nonlinear adaptive power system stabiliser.

In Chapter 6 the simplification of the ideal nonlinear adaptive power system stabiliser proposed in Chapter 5 is discussed, and the design of a *SISO bilinear adaptive power system stabiliser* is presented:

- In Section 6.2 the predicted output of the nonlinear nominal model is decomposed, and the dominant components in the system dynamic and steady-state responses are extracted. Simplified versions of the nonlinear adaptive power system stabiliser proposed in Chapter 5 are then developed in Section 6.3.

- In Subsection 6.4.1 a bilinear nominal model which gives the simplest nonlinear relationship between the control input and the electrical torque (or power) output is derived. Bilinear optimal and adaptive control strategies are discussed in Subsections 6.4.2 and 6.4.3. A bilinear adaptive weighted minimum variance power system stabiliser is then proposed.

- In Section 6.5 the assessment of the performance of the bilinear adaptive power system stabiliser is conducted through comparisons with the linear and nonlinear adaptive power system stabilisers proposed in Chapters 3 and 5, respectively. The validity of the bilinear adaptive power system stabiliser for the development of a real-time nonlinear adaptive power system stabiliser is verified.

Chapter 6 provides a basis for the future development of a practical nonlinear adaptive power system stabiliser.

In Chapter 7 general conclusions regarding the development of the new nonlinear optimal/adaptive control strategies for the design of power system stabilisers are drawn. The features of each power system stabiliser developed in this thesis are highlighted. From these conclusions and the experience obtained through this research, a number of recommendations are made for future research.

1.9 Original Contributions.

To the author's knowledge, the development of the *nonlinear optimal* control (Chapter 4), the *nonlinear adaptive* control (Chapter 5), and the *bilinear adaptive* control (Chapter 6) strategies in the design of power system stabilisers, presented in this thesis, are **original**. The **original contributions** are listed in Sections 4.1, 5.1, and 6.1, and are *highlighted* as follows:

1. *Two new* models, namely the nonlinear nominal model and the bilinear nominal model, novel in the sense that they *inherently* represent the nonlinear relationship between the control input and the electrical torque (or power) output, are derived

in Chapters 4 and 6 from the mathematical descriptions of the nonlinear power system outlined in Chapter 2. These models are linear in the parameters and in the control input. The establishment of these models provides a useful means for the development of a variety of nonlinear control laws for the design of power system stabilisers.

2. *Two new* nonlinear optimal control laws (namely the generalised minimum variance control law and its special case, the weighted minimum variance control law) are developed from a general form of the cost function in Chapter 4. The associated *global closed-loop stability properties* are established theoretically. A number of nonlinear adaptive control algorithms, in the sense of different tuning strategies, can be developed from proper selections of the weighting polynomials in the cost function.

3. *Two new* nonlinear adaptive weighted minimum variance control algorithms are derived in Chapter 5 and the theoretical *proofs of the convergence* of these algorithms are given. This completes the theoretical development of the nonlinear weighted minimum variance control scheme based on the nonlinear nominal model.

4. Simplifications necessary for the practical implementation of the nonlinear adaptive control algorithms are discussed in Chapter 6. *New* simple bilinear optimal and adaptive control strategies in the design of power system stabilisers are studied. A *new* bilinear adaptive weighted minimum variance control strategy, incorporating a novel protection function that prevents ineffective control actions when large transients of the power system occur, is developed.

5. *Three new* power system stabilisers based on the *same* (weighted minimum variance) control scheme but *different* (nonlinear optimal, nonlinear adaptive, and bilinear adaptive) control strategies are proposed and evaluated in Chapters 4, 5, and 6.

Systematic evaluations and comparisons of the performance of the power system stabilisers designed in Chapters 4 to 6, against an identical reference (established by

a valid linear adaptive power system stabiliser proposed in Chapter 3), are conducted through simulation studies. Conclusions are drawn regarding the benefits and deficiencies of the different control strategies, including *linear* and *nonlinear* as well as *optimal* and *adaptive* control, in the design of power system stabilisers. Of the power system stabilisers studied in this thesis, the *bilinear adaptive power system stabiliser* is the most significant one because it maintains excellent dynamic and transient performance while using a minimum number of feedback signals which are measurable in a practical situation.

Apart from the above original contributions, this thesis makes several *extensions* to previous work (shown in the literature) on aspects of *power system modelling* and the design of *linear adaptive power system stabilisers.* These extensions are listed in Sections 2.1 and 3.1, respectively.

Chapter 2

Power System Modelling.

2.1 Introduction.

In this chapter the modelling of the synchronous generator and power system for simulation studies involving the linear and nonlinear adaptive control of generating units is discussed.

In an electric power network, each individual generating unit is a nonlinear multivariable system. The characteristics of a power system vary with the system loading conditions imposed on the nonlinear generating unit. On the one hand, to analyse the dynamic performance of such a system, it is necessary to know, in detail, the system configuration and to provide an adequate mathematical description of the system under study. On the other hand, due to the difficulties associated with the field testing and the real-time implementation in laboratories, a practical and effective method for evaluating the system dynamic performance is through simulation studies of the system. This emphasis on simulation also requires an adequate representation of the system. The provision of suitable *models* of power systems is, therefore, an important feature in the investigation of system performance and the development of controllers.

Numerous mathematical models of generating units and power systems have been discussed in the literature [108]-[120]. The representations of components in a power

system have become increasingly detailed and accurate in order to meet the needs of modern technologies in system operation and control [88]. Because power systems differ considerably in practice, it is impossible to devise a universal model that will satisfy all systems. It is, therefore, necessary to specify the *components* in the power system under study and to make clear the *purposes* for which the model of the power system is used.

In this chapter mathematical models of a power system consisting of a *synchronous generator* driven by a *steam turbine* for use in *dynamic performance analyses* and *simulation studies* are discussed. Attention will be paid to a single machine power system connected to a very large power network through two parallel transmission lines, as shown in Fig. 2.1. Such a system is usually called a *Single Machine Infinite Bus* **(SMIB)** power system. Although a SMIB power system representation may not be appropriate to a practical power system, this type of model

- is simple for the purpose of assessing control strategies;
- is sufficient to establish basic control effects as well as feasibilities;
- provides useful insight and understanding of the system dynamic behaviour.

In the literature the SMIB power system representations have been widely utilised for steady-state analysis (e.g., [7,8,121]), the design of power system stabilisers (e.g., [19,29,54]), and so on. The concepts developed by using the SMIB models have been extended to multi-machine power system analyses (e.g., [53,55,122,34]).

A functional block diagram of a synchronous generator and steam turbine generating unit is illustrated in Fig. 2.2. Four basic components, which are important to power system dynamic studies, are considered for the system modelling. They are the steam turbine, which converts thermal energy to mechanical power; the governor, which controls the flow of steam to the turbine; the generator, in which the mechanical to electrical energy conversion takes place; and the exciter and voltage regulator, which control the terminal voltage output. In Appendix A detailed mathematical models of the components shown in Fig. 2.2 are described.

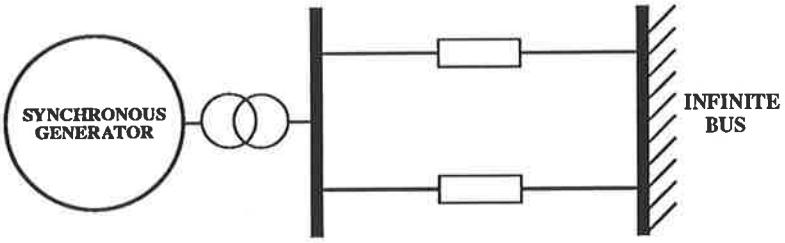

Figure 2.1: A single machine infinite bus power system.

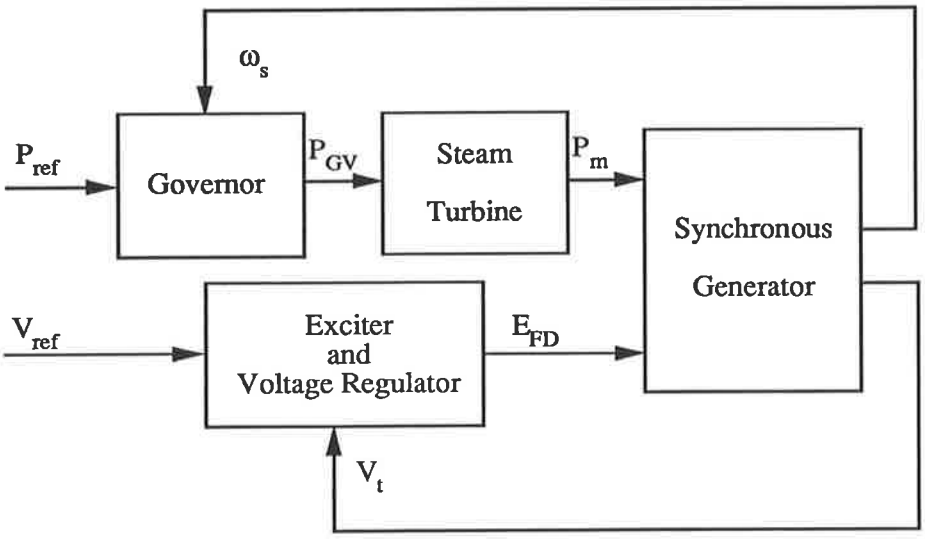

Figure 2.2: A synchronous generator and steam turbine generating unit.

The organisation of this chapter is as follows. Three simplified synchronous generator models, developed from the basic model of the synchronous generator given in Section A.1 of Appendix A, are introduced in Section 2.2. The resulting nonlinear models of the SMIB power system for simulation studies are presented in Section 2.3. In Section 2.4 *analytical models* [1] of the nonlinear power system for the development of linear and nonlinear optimal/adaptive power system stabilisers are described. In Section 2.5 the selection of suitable stabilising signals for the design of power system stabilisers is discussed. Finally, for the purpose of establishing theoretical foundations for the modelling analysis of the linear adaptive power system stabiliser, concepts of controllability and observability related to the models developed in this chapter are briefly discussed in Section 2.6.

The previous work described in the literature is extended in this chapter in the following aspects:

1. A systematical derivation of simplified models of the synchronous generator from the basic machine equations is given in Section 2.2. This procedure differs from those described in the literature, and provides insight into the mathematical description of the generator/tie-line system.

2. The three nonlinear SMIB power system representations are presented and compared in Section 2.3. The effect of increasing the value of the rotor damping coefficient in the machine equation of motion in order to compensate for the omission of damper windings is demonstrated. This work establishes a sound foundation for using a low-order nonlinear model to design a system controller which in practice controls a higher-order system.

3. Nonlinear and linearised analytical models of the power system are proposed in Section 2.4. These models provide mathematical bases for the implementation of the linear and nonlinear optimal/adaptive power system stabilisers in Sections 3.2 and 4.2.

[1] **The definition of an "analytical model" will be given in Section 2.4.**

4. The preferred choice of the electrical torque as the stabilising signal for the design of power system stabilisers is discussed in Section 2.5 through the analysis of participation factors of the system. This knowledge will be used to construct the linear and nonlinear optimal/adaptive power system stabilisers which are discussed in Chapters 3 to 6.

Two types of SMIB power system models will be developed in this chapter, namely,

SGM (*Simplified Generator Model*): this model represents only the synchronous generator and the tie-line; representations of the excitation system, the governor, and the steam turbine are excluded (see Section 2.2).

CSM (*Complete System Model*): this model gives a 'complete' system description which contains not only the synchronous generator and the tie-line, but also the components omitted from the SGM type (see Section 2.3).

2.2 Simplified Nonlinear Models of the Synchronous Generator.

In this section:

- three simplified nonlinear models of the synchronous generator are systematically derived from the basic machine equations given in Section A.1 of Appendix A;
- the selection of appropriate models for the simulation studies and for the development of adaptive power system stabilisers is discussed.

In a power system, the system dynamic behaviour is determined mainly by the characteristics of the synchronous generator, its loading condition (P_t, Q_t, V_t), and the external network parameters. A basic representation of a synchronous generator connected to an infinite bus through a double-circuit transmission line is given by

(A.1)-(A.12) of Appendix A. This model includes seven first-order nonlinear differential equations and a set of simultaneous nonlinear algebraic equations. In addition to these, other equations describing the excitation system, the governor, and the steam turbine must be included in the system mathematical model. Thus a complete mathematical description of a power system may be complex, and *simplifications* are often made in modelling the system.

A variety of models of the synchronous generator have been discussed in the literature [117,118]. In extensive analyses and comparisons based on system performance, the effect of the various degrees of approximation commonly used in the simplification procedure has been examined in detail [117,123]. Such studies provide guidelines upon which the three simplified nonlinear models of the synchronous generator will be selected. In contrast to the previous work in the literature, the simplified generator models described in this section are a result of adopting a different sequence of approximations, forming a systematic way of developing the simplified models of the generator and the transmission system. The three simplified generator models are listed in order of decreasing complexity. This is achieved by making a number of simplifying assumptions which are introduced sequentially, as described below.

Step 1:

Eliminate the damper winding variables $I_D(t), I_Q(t), \Lambda_D(t)$, and $\Lambda_Q(t)$ and the field current $I_F(t)$ from the basic synchronous machine equations (A.1)-(A.2) of Appendix A. The flux linkage equations and the voltage equations of this machine model are rearranged as

$$\begin{bmatrix} \Lambda_d(t) \\ \Lambda_q(t) \\ \Lambda_F(t) \end{bmatrix} = \begin{bmatrix} G_d(p) & 0 \\ 0 & G_q(p) \\ G_F(p) & 0 \end{bmatrix} \begin{bmatrix} I_d(t) \\ I_q(t) \end{bmatrix} + \begin{bmatrix} H_d(p) \\ 0 \\ H_F(p) \end{bmatrix} \frac{L_{md}}{r_F} V_F(t) \qquad (2.1)$$

and

$$\begin{bmatrix} V_d(t) \\ V_q(t) \end{bmatrix} = - \begin{bmatrix} r & 0 \\ 0 & r \end{bmatrix} \begin{bmatrix} I_d(t) \\ I_q(t) \end{bmatrix} - \frac{1}{\omega_0} \begin{bmatrix} \dot{\Lambda}_d(t) \\ \dot{\Lambda}_q(t) \end{bmatrix} - \begin{bmatrix} \omega(t)\Lambda_q(t) \\ -\omega(t)\Lambda_d(t) \end{bmatrix}. \qquad (2.2)$$

The operational functions in (2.1) are of the form

$$
\begin{aligned}
G_d(p) &= \frac{1+p(\tau_{d4}+\tau_{d5})+p^2\tau_{d4}\tau_{d6}}{1+p(\tau_{d1}+\tau_{d2})+p^2\tau_{d1}\tau_{d3}}L_d, \\
G_q(p) &= \frac{1+p\tau_{q2}}{1+p\tau_{q1}}L_q, \\
G_F(p) &= \frac{1+p\tau_{d7}}{1+p(\tau_{d1}+\tau_{d2})+p^2\tau_{d1}\tau_{d3}}L_{md},
\end{aligned}
$$

and

$$
\begin{aligned}
H_d(p) &= \frac{1+p\tau_{d7}}{1+p(\tau_{d1}+\tau_{d2})+p^2\tau_{d1}\tau_{d3}}, \\
H_F(p) &= \frac{1+p\tau_{d3}}{1+p(\tau_{d1}+\tau_{d2})+p^2\tau_{d1}\tau_{d3}}\frac{L_F}{L_{md}},
\end{aligned}
$$

where p is the differential operator denoted as $\frac{d}{dt}$. [2] Similar expressions for $G_d(p), G_q(p)$, and $H_d(p)$ can be found in the literature, e.g., in [117,125], while the expressions for $G_F(p)$ and $H_F(p)$ are derived in Appendix B. The time constants in the above equations are defined as

$$\tau_{d1} \triangleq \frac{L_F}{\omega_0 r_F}, \tag{2.3}$$

$$\tau_{d2} \triangleq \frac{L_D}{\omega_0 r_D}, \tag{2.4}$$

$$\tau_{d3} \triangleq \frac{1}{\omega_0 r_D}\left(L_D - \frac{L_{md}^2}{L_F}\right), \tag{2.5}$$

$$\tau_{d4} \triangleq \frac{1}{\omega_0 r_F}\left(L_F - \frac{L_{md}^2}{L_d}\right),$$

$$\tau_{d5} \triangleq \frac{1}{\omega_0 r_D}\left(L_D - \frac{L_{md}^2}{L_d}\right),$$

$$\tau_{d6} \triangleq \frac{1}{\omega_0 r_D}\left[L_D - \frac{L_{md}^2(L_d+L_F)-2L_{md}^3}{L_d L_F - L_{md}^2}\right],$$

$$\tau_{d7} \triangleq \frac{1}{\omega_0 r_D}\left(L_D - L_{md}\right), \tag{2.6}$$

[2] Precise definitions of the symbols p and $\frac{1}{p}$ are given as [124]

$$py(t) \triangleq \frac{dy(t)}{dt}, \qquad p^2y(t) \triangleq \frac{d^2y(t)}{dt^2}, \qquad \ldots,$$

and

$$p^{-1}y(t) \triangleq \frac{1}{p}y(t) \triangleq \int_0^t y(t)dt + y_0$$

where y_0 represents the initial value of the integral.

$$\tau_{q1} \triangleq \frac{L_Q}{\omega_0 r_Q},$$
$$\tau_{q2} \triangleq \frac{1}{\omega_0 r_Q}\left(L_Q - \frac{L_{mq}^2}{L_q}\right),$$

where the inductances and resistances are given in their per unit values.

Step 2:

Consider that, in per unit, $r_D \gg r_F$ while L_D and L_F are of similar magnitude [3]. It is assumed that

Assumption 2.2.1

$$\tau_{d1} + \tau_{d2} \approx \tau_{d1} + \tau_{d3}, \tag{2.7}$$

$$\tau_{d4} + \tau_{d5} \approx \tau_{d4} + \tau_{d6}. \tag{2.8}$$

The operational functions in (2.1) are then simplified to read

$$G_d(p) \approx \frac{(1+p\tau_d^{'})(1+p\tau_d^{''})}{(1+p\tau_{d0}^{'})(1+p\tau_{d0}^{''})}L_d, \tag{2.9}$$
$$G_q(p) = \frac{1+p\tau_q^{''}}{1+p\tau_{q0}^{''}}L_q, \tag{2.10}$$
$$G_F(p) \approx \frac{1+p\tau_D}{(1+p\tau_{d0}^{'})(1+p\tau_{d0}^{''})}L_{md}, \tag{2.11}$$
$$H_d(p) \approx \frac{1+p\tau_D}{(1+p\tau_{d0}^{'})(1+p\tau_{d0}^{''})}, \tag{2.12}$$
$$H_F(p) \approx \frac{1}{1+p\tau_{d0}^{'}}\frac{L_F}{L_{md}}, \tag{2.13}$$

where the d, q-axis subtransient and transient time constants as well as the d-axis damper leakage time constant are defined as [117,3]

$$\tau_{d0}^{'} \triangleq \tau_{d1}, \quad \tau_{d0}^{''} \triangleq \tau_{d3}, \quad \tau_d^{'} \triangleq \tau_{d4},$$
$$\tau_d^{''} \triangleq \tau_{d6}, \quad \tau_D \triangleq \tau_{d7}, \quad \tau_{q0}^{''} \triangleq \tau_{q1},$$
$$\tau_q^{''} \triangleq \tau_{q2}.$$

Step 3:

Introduce the per unit d, q-axis subtransient and transient inductances [3]

$$L_d^{'} \triangleq \frac{\tau_d^{'}}{\tau_{d0}^{'}} L_d, \quad L_d^{''} \triangleq \frac{\tau_d^{''}}{\tau_{d0}^{''}} L_d^{'}, \quad L_q^{''} \triangleq \frac{\tau_q^{''}}{\tau_{q0}^{''}} L_q,$$

and the relationship between per unit stator EMF's and rotor quantities [3]

$$E_{FD}(t) \triangleq \frac{L_{md}}{r_F} V_F(t), \qquad E_q^{'}(t) \triangleq \frac{L_{md}}{L_F} \Lambda_F(t).$$

Equation (2.1) is rewritten as

$$\begin{bmatrix} \Lambda_d(t) \\ \Lambda_q(t) \\ E_q^{'}(t) \end{bmatrix} = \begin{bmatrix} G_d(p) & 0 \\ 0 & G_q(p) \\ \overline{G}_F(p) & 0 \end{bmatrix} \begin{bmatrix} I_d(t) \\ I_q(t) \end{bmatrix} + \begin{bmatrix} H_d(p) \\ 0 \\ \overline{H}_F(p) \end{bmatrix} E_{FD}(t) \tag{2.14}$$

where $G_d(p), G_q(p)$, and $H_d(p)$ are described by (2.9), (2.10), and (2.12) respectively; $\overline{G}_F(p)$ and $\overline{H}_F(p)$ are related to $G_F(p)$ (2.11) and $H_F(p)$ (2.13) through

$$\overline{G}_F(p) = \frac{L_{md}}{L_F} G_F(p),$$

$$\overline{H}_F(p) = \frac{L_{md}}{L_F} H_F(p).$$

The operational functions in (2.14), when expanded into partial fractions, become

$$G_d(p) = \frac{A_1}{1 + p\tau_{d0}^{'}} + \frac{A_2}{1 + p\tau_{d0}^{''}} + L_d^{''}, \tag{2.15}$$

$$G_q(p) = \frac{L_q - L_q^{''}}{1 + p\tau_{q0}^{''}} + L_q^{''},$$

$$\overline{G}_F(p) = \frac{A_5}{1 + p\tau_{d0}^{'}} + \frac{A_6}{1 + p\tau_{d0}^{''}}, \tag{2.16}$$

$$H_d(p) = \frac{A_3}{1 + p\tau_{d0}^{'}} + \frac{A_4}{1 + p\tau_{d0}^{''}}, \tag{2.17}$$

$$\overline{H}_F(p) = \frac{1}{1 + p\tau_{d0}^{'}}, \tag{2.18}$$

where the constants $A_i (i = 1, 2, ..., 6)$ are

$$A_1 = \left(L_d - L_d^{'}\right) \frac{\tau_{d0}^{'} - \tau_d^{''}}{\tau_{d0}^{'} - \tau_{d0}^{''}}, \tag{2.19}$$

$$A_2 = \left(L_d - L_d^{''}\right) - \left(L_d - L_d^{'}\right) \frac{\tau_{d0}^{'} - \tau_d^{''}}{\tau_{d0}^{'} - \tau_{d0}^{''}}, \tag{2.20}$$

$$A_3 = \frac{\tau_{d0}^{'} - \tau_D}{\tau_{d0}^{'} - \tau_{d0}^{''}}, \tag{2.21}$$

$$A_4 = 1 - \frac{\tau_{d0}^{'} - \tau_D}{\tau_{d0}^{'} - \tau_{d0}^{''}}, \tag{2.22}$$

$$A_5 = \left(L_d - L_d^{'}\right) \frac{\tau_{d0}^{'} - \tau_D}{\tau_{d0}^{'} - \tau_{d0}^{''}}, \tag{2.23}$$

$$A_6 = \left(L_d - L_d^{'}\right) \frac{\tau_D - \tau_{d0}^{''}}{\tau_{d0}^{'} - \tau_{d0}^{''}}. \tag{2.24}$$

Step 4:

Note that usually $\tau_{d0}^{'} \gg \tau_d^{''}$, $\tau_{d0}^{'} \gg \tau_{d0}^{''}$, and $\tau_{d0}^{'} \gg \tau_D$ while $\tau_d^{''}$, $\tau_{d0}^{''}$, and τ_D are of the same order [117]. It is further assumed that

Assumption 2.2.2

$$\tau_{d0}^{'} - \tau_d^{''} \approx \tau_{d0}^{'} - \tau_{d0}^{''}, \tag{2.25}$$

$$\tau_{d0}^{'} - \tau_D \approx \tau_{d0}^{'} - \tau_{d0}^{''}. \tag{2.26}$$

The parameters $A_i (i = 1, 2, ..., 6)$ in (2.19)-(2.24) are then simplified to read

$$A_1 \approx L_d - L_d^{'}, \quad A_2 \approx L_d^{'} - L_d^{''}, \quad A_3 \approx 1,$$
$$A_4 \approx 0, \quad A_5 \approx L_d - L_d^{'}, \quad A_6 \approx 0,$$

so that the subtransient components in the operational functions $\overline{G}_F(p)$ (2.16) and $H_d(p)$ (2.17) are eliminated. $\overline{G}_F(p)$ is now the transient component of $G_d(p)$ (2.15), while $\overline{H}_F(p)$ (2.18) and $H_d(p)$ become identical.

Step 5:

Define the per unit subtransient stator flux linkages as [3]

$$\Lambda_d^{''}(t) \triangleq \Lambda_d(t) - L_d^{''} I_d(t), \tag{2.27}$$

$$\Lambda_q^{''}(t) \triangleq \Lambda_q(t) - L_q^{''} I_q(t), \tag{2.28}$$

from which the per unit d, q-axis voltages behind the subtransient reactances are introduced [3]

$$E_d''(t) \triangleq -\omega(t)\Lambda_q''(t), \tag{2.29}$$

$$E_q''(t) \triangleq \omega(t)\Lambda_d''(t). \tag{2.30}$$

Hence, five first-order differential equations that represent the machine electro-magnetic relationship are re-formed from (2.14) and (2.2), so that

$$\tau_{d0}'\dot{E}_q'(t) = \left(L_d - L_d'\right) I_d(t) + E_{FD}(t) - E_q'(t), \tag{2.31}$$

$$\tau_{d0}''\dot{\Lambda}_d''(t) = \left(L_d' - L_d''\right) I_d(t) + E_q'(t) + \tau_{d0}''\dot{E}_q'(t) - \Lambda_d''(t), \tag{2.32}$$

$$\tau_{q0}''\dot{\Lambda}_q''(t) = \left(L_q - L_q''\right) I_q(t) - \Lambda_q''(t), \tag{2.33}$$

$$\frac{1}{\omega_0}\dot{\Lambda}_d(t) = -rI_d(t) - \omega(t)\Lambda_q''(t) - L_q''\omega(t)I_q(t) - V_d(t), \tag{2.34}$$

$$\frac{1}{\omega_0}\dot{\Lambda}_q(t) = -rI_q(t) + \omega(t)\Lambda_d''(t) + L_d''\omega(t)I_d(t) - V_q(t). \tag{2.35}$$

Substituting for $\Lambda_d(t)$ and $\Lambda_q(t)$ from (2.27) and (2.28) into the electrical torque equation (A.6) of Appendix A yields

$$T_e(t) = \Lambda_d''(t)I_q(t) - \Lambda_q''(t)I_d(t) + \left(L_d'' - L_q''\right) I_d(t)I_q(t). \tag{2.36}$$

Remark 2.2.1 *From Step 1 to Step 5, only two numerical approximations (eqns. (2.7)-(2.8) and (2.25)-(2.26)) are introduced. The errors due to Assumptions 2.2.1 and 2.2.2 are not significant [117].*

Step 6:

Note that under stable dynamic conditions the transformer voltage terms ($\frac{1}{\omega_0}\dot{\Lambda}_d(t)$ and $\frac{1}{\omega_0}\dot{\Lambda}_q(t)$) in the machine stator voltage equations (2.34) and (2.35) are numerically small compared to the speed voltage terms in these equations [118,123,3]. Furthermore, the time constant $\tau_e \triangleq \frac{L_e}{\omega_0 R_e}$ associated with transmission line dynamics is usually small compared to those of the machine [126]. Two major assumptions are therefore introduced.

Assumption 2.2.3 *In the stator voltage equations (2.34) and (2.35)*

$$\frac{1}{\omega_0}\dot{\Lambda}_d(t) \approx 0, \qquad \frac{1}{\omega_0}\dot{\Lambda}_q(t) \approx 0.$$

Assumption 2.2.4 *The transmission line dynamics can be neglected.*

Application of these two assumptions to (2.34)-(2.35) and (A.9)-(A.10) of Appendix A results in

$$V_d(t) = -rI_d(t) - \omega(t)\Lambda_q''(t) - L_q''\omega(t)I_q(t), \tag{2.37}$$

$$V_q(t) = -rI_q(t) + \omega(t)\Lambda_d''(t) + L_d''\omega(t)I_d(t), \tag{2.38}$$

and

$$V_d(t) = -V_\infty \sin\delta(t) + R_eI_d(t) + L_e\omega(t)I_q(t), \tag{2.39}$$

$$V_q(t) = V_\infty \cos\delta(t) + R_eI_q(t) - L_e\omega(t)I_d(t). \tag{2.40}$$

A simplified model, called the *Simplified Generator Model 1* **(SGM1)**, is obtained by combining the third-order electro-magnetic characteristics (eqns. (2.31)-(2.33) and (2.36)-(2.38)) with the second-order shaft dynamics (eqns. (A.3)-(A.5) of Appendix A), together with the transmission line characteristics (eqns. (2.39)-(2.40), (A.8) and (A.11)-(A.12) of Appendix A). The order of the synchronous generator model is now reduced from seven to five, while the two inherent nonlinearities, the product nonlinearity and the trigonometric nonlinearity, associated with the basic machine representation (A.1)-(A.12), are still retained.

Step 7:

In this thesis the design of stable, relatively well-damped shaft dynamics is of concern. Under such conditions, the shaft speed $\omega(t)$ (in rad/s) deviates, typically, from the synchronous speed ω_0 (in rad/s) by less than 2%. Assume, therefore, that

Assumption 2.2.5 *In the machine voltage equations, in per unit,*

$$\omega(t) \approx 1. \tag{2.41}$$

The per unit machine and transmission line reactances are thus numerically equal to the corresponding per unit values of the inductances, so that these parameters become independent of frequency. Also, the machine electrical torque $T_e(t)$ and mechanical torque $T_m(t)$ are numerically equal to the machine electrical power $P_e(t)$ and mechanical power $P_m(t)$, respectively. Furthermore, the subtransient stator flux linkages $\Lambda_d''(t)$ and $\Lambda_q''(t)$ can be replaced by the commonly-used subtransient voltages $E_d''(t)$ and $E_q''(t)$, according to their definitions in (2.29) and (2.30). Consequently, the equations of the SGM1 reduce to

$$\tau_{d0}'\dot{E}_q'(t) = \left(X_d - X_d'\right) I_d(t) + E_{FD}(t) - E_q'(t), \tag{2.42}$$

$$\tau_{d0}''\dot{E}_q''(t) = \left(X_d' - X_d''\right) I_d(t) + E_q'(t) + \tau_{d0}''\dot{E}_q'(t) - E_q''(t), \tag{2.43}$$

$$\tau_{q0}''\dot{E}_d''(t) = -\left(X_q - X_q''\right) I_q(t) - E_d''(t), \tag{2.44}$$

$$V_d(t) = -rI_d(t) + E_d''(t) - X_q''I_q(t), \tag{2.45}$$

$$V_q(t) = -rI_q(t) + E_q''(t) + X_d''I_d(t), \tag{2.46}$$

and

$$T_e(t) = E_d''(t)I_d(t) + E_q''(t)I_q(t) + \left(X_d'' - X_q''\right) I_d(t)I_q(t), \tag{2.47}$$

$$T_m(t) = P_m(t), \tag{2.48}$$

$$V_d(t) = -V_\infty \sin\delta(t) + R_eI_d(t) + X_eI_q(t), \tag{2.49}$$

$$V_q(t) = V_\infty \cos\delta(t) + R_eI_q(t) - X_eI_d(t). \tag{2.50}$$

The model described by equations (2.42)-(2.50), (A.3)-(A.4), (A.8), and (A.11)-(A.12) is called the *Simplified Generator Model 2* **(SGM2)**. Although the SGM2 is of the same order as the SGM1, some product nonlinearities in the equations of the SGM1 become linear expressions in the SGM2 as a result of applying Assumption 2.2.5 (e.g., the $L_e\omega(t)I_q(t)$ product in (2.39) becomes a linear expression $X_eI_q(t)$ in (2.49)). However, as $\omega(t)$ usually deviates from its nominal value by less than 2%, the elimination of some machine nonlinearities caused by the introduction of Assumption 2.2.5 into the machine representation may be considered insignificant [3]. Note that in the machine equation of motion (A.4), $\omega(t)$ is retained as a state variable; Assumption 2.2.5 is used only to simplify certain terms in the relevant machine equations.

Remark 2.2.2 *A version similar to the SGM2 is called the* E'' *model in [3] in which the two numerical assumptions (Assumptions 2.2.1 and 2.2.2) are not involved. Likewise, the SGM2 is also called machine representation 4 in [117] in which a further assumption,* $X_d'' = X_q''$*, is sometimes included.*

Step 8:

Consider the case in which the effect of the damper windings on the transient response is small enough to be negligible or may be compensated for by increasing the value of the rotor damping coefficient D in the machine swing equation (A.4) [3]. Another assumption, as given below, can be introduced.

Assumption 2.2.6 *The machine amortisseur effects are neglected.*

This assumption is equivalent to assuming that in (2.43) and (2.44)

$$\tau_{d0}'' \approx 0, \qquad \tau_{q0}'' \approx 0.$$

Accordingly, the machine equations (2.43)-(2.47) become the simple algebraic equations

$$V_d(t) = -rI_d(t) - X_q I_q(t), \tag{2.51}$$

$$V_q(t) = -rI_q(t) + X_d' I_d(t) + E_q'(t), \tag{2.52}$$

$$T_e(t) = E_q'(t) I_q(t) + \left(X_d' - X_q\right) I_d(t) I_q(t), \tag{2.53}$$

while the other equations ((2.42), (2.48)-(2.50), (A.3)-(A.4), (A.8), and (A.11)-(A.12)) of the SGM2 stay unmodified. As a result of Assumption 2.2.6, the order of the generator model is reduced from five to three, so the simplification can be viewed as significant. However, the main nonlinearities inherent in the original machine characteristics are still retained. On the other hand, since increasing the value of the rotor damping coefficient D can compensate for the omission of damper windings [3], the error due to Assumption 2.2.6 can be minimised. This simplification will be illustrated in Subsection 2.3.2.

Remark 2.2.3 *From this step, a simplified generator model (represented by (2.51)-(2.53) and equations (2.42), (2.48)-(2.50), (A.3)-(A.4), (A.8), and (A.11)-(A.12) of the SGM2) is obtained. The same expression as for this simplified generator model can be obtained directly by eliminating $I_D(t)$ and $I_Q(t)$ in the basic machine equations (A.1)-(A.2) (resulting in the $\mathbf{E}'_\mathbf{q}$ model in [3]) and then applying Assumptions 2.2.3-2.2.5. In [117] this generator model is referred to as machine representation 2.*

Step 9:

Note that the voltage drops across the resistances of both the generator stator windings and the transmission lines are normally small compared to those across the reactances. Finally, it is assumed that

Assumption 2.2.7 *The generator stator winding resistance and the transmission line resistance can be neglected.*

The machine stator and line voltage equations (2.51)-(2.52) and (2.49)-(2.50) are then represented by

$$V_d(t) = -X_q I_q(t), \tag{2.54}$$

$$V_q(t) = X'_d I_d(t) + E'_q(t), \tag{2.55}$$

and

$$V_d(t) = -V_\infty \sin\delta(t) + X_e I_q(t), \tag{2.56}$$

$$V_q(t) = V_\infty \cos\delta(t) - X_e I_d(t). \tag{2.57}$$

These equations ((2.54)-(2.57)), together with (2.42), (2.48), (2.53), (A.3)-(A.4), (A.8), and (A.11)-(A.12), form a model which is called the *Simplified Generator Model 3* **(SGM3)**.

In the studies of this thesis, the SGM1 is used as the *benchmark model of the synchronous generator/tie-line system* for the analysis of the system dynamic behaviour. This is because the SGM1 most closely represents the basic model of the synchronous generator given by (A.1)-(A.12) as explained in the following. Recall that the SGM1

results from neglecting the time-derivative terms in (2.34)-(2.35) and (A.9)-(A.10) and including Assumptions 2.2.1 and 2.2.2. In [117] it is stated that neglecting the time-derivative terms of d, q-axis stator flux linkages in the machine voltage equations (2.34) and (2.35) may lead to a less stable system response than that observed in tests on an actual system under severe fault conditions; nevertheless the errors are still not significant [118,3]. It is also pointed out in [123] that neglecting the time-derivative terms in the differential equations (A.9) and (A.10) of the transmission system is generally justified on the basis of reducing computational effort. The justification for adopting the SGM1 as the benchmark instead of using the basic seventh-order generator model (A.1)-(A.12) is based on the trade-off between the use of a more accurate model and the computational burden that is involved. It is also based on the fact that the studies in this thesis are concerned with the investigation and comparison of system performance of the **same model** with different control methodologies. Therefore, inaccuracies introduced by using the SGM1 as the benchmark model for the synchronous generator/tie-line system will not significantly affect the analysis and design of system controllers, nor the evaluation of system dynamic behaviour.

A distinct feature of the SGM1 is that it retains the shaft speed as a time-varying quantity in the machine voltage equations and in the power and torque equations. Consequently, time-varying parameters of the form $L\omega(t)$ in the generator and the transmission line equations are retained in this model. The SGM1 also includes all the product nonlinearities in the model equations. Omitting some of the product nonlinearities in Assumption 2.2.5 results in the SGM2. The influence of adopting Assumption 2.2.5 on machine modelling is investigated in Subsection 2.3.2 by comparing the system performance of the SGM1 and the SGM2 at various operating conditions (see Remark 2.3.2(i)).

The SGM3 is characterised by the simplicity of its equations. In this thesis it is an important machine model for the analysis and design of power system stabilisers. The use of this model is based on the following considerations:

(1) Modern control strategies rely on the mathematical description of the system for the development of control laws. When such control strategies are considered in

the design of power system stabilisers, it is necessary to employ a simple model of the synchronous generator in order to avoid the complexities involved with a high-order representation [123]. This argument has been supported by the previous work on the linear optimal control [90,91,92,94,97,98,99,101], nonlinear optimal control [127]-[132], and linear adaptive control [45,47,58,73] of power systems. It will be further supported by the studies of the nonlinear optimal and adaptive power system stabilisers to be presented in this thesis. The use of a simple model will be justified in Chapters 4 and 5 in which issues such as closed-loop system stability of the nonlinear optimal control laws and convergence analysis of the nonlinear adaptive control algorithms are considered.

(2) The system time response of the SGM3 closely matches that of the benchmark (SGM1) by appropriately adjusting the rotor damping coefficient D in the machine equation of motion (see Subsection 2.3.2).

For the above reasons, the SGM3 is used for the assessment and comparison of the controller performance. However, with a final form of the controller design, the performance is evaluated with the SGM1 to ensure its validity (see Subsections 3.6.3, 4.5.3, 5.4.3, and 6.5.3). It is also important to point out that, though simple, the SGM3 retains the basic nonlinear characteristics associated with the basic machine equations.

2.3 Nonlinear SMIB Power System Models for Simulation Studies.

In this section:

- three nonlinear SMIB power system models are presented; each model combines one of the simplified generator/tie-line models described in Section 2.2 with those of the excitation system, the governor, and the steam turbine as described in Appendix A;

- comparisons of system dynamic performance of the three nonlinear SMIB power system models are given;
- the effect of increasing the value of the rotor damping coefficient D as compensation for the omission of damper windings is demonstrated;
- the power system models used for the analysis and design of power system stabilisers and for the evaluation of the designed stabilisers are introduced.

The layout of this section is as follows. Mathematical descriptions of the three nonlinear SMIB power system models are given in Subsection 2.3.1. Simulation studies of the system time response are conducted in Subsection 2.3.2, where conclusions on the choice of models are drawn from comparisons of the dynamic performance of the three models.

2.3.1 The Development of the Complete System Models.

In choosing adequate representations of the excitation system, the governor, and the steam turbine to form a complete mathematical description of the SMIB power system, it is desirable to select appropriately simple models of these components to represent the limiting nonlinearities and the associated dynamic performance. There is little benefit in introducing detailed models for these components if some significant simplifications of the generator/tie-line models are also implemented. For this reason, simplifications in modelling the excitation system, the governor, and the steam turbine have been made in Assumptions A.2.1-A.2.3 and A.3.1-A.3.2 of Appendix A to match the simplified generator/tie-line models proposed in Section 2.2.

The use of the simplified models for these components is based also on the consideration that the comparison of system dynamic performance will be conducted in this thesis with the **same models** of these components. This approach is similar to that expressed in Section 2.2 in which the use of simplified generator/tie-line models is justified.

In the following, three nonlinear SMIB power system representations which correspond, seriatim, to the three simplified generator/tie-line models defined in Section 2.2, and which include the additional components, are developed. To provide a compact mathematical description of the resulting three complete system models, a general form of a *nonlinear, continuous-time, expanded state-space representation* is defined as

$$\begin{bmatrix} \dot{\mathbf{X}}(t) \\ \mathbf{0} \\ \mathbf{0} \end{bmatrix} = \begin{bmatrix} \mathbf{\Phi}(\mathbf{X}(t), \mathbf{Z}(t), \mathbf{U_r}(t)) \\ \mathbf{\Psi}(\mathbf{X}(t), \mathbf{Z}(t)) \\ \mathbf{\Xi}(\mathbf{X}(t), \mathbf{Z}(t), \mathbf{U_r}(t)) \end{bmatrix}. \tag{2.58}$$

Here, $\mathbf{X}(t)$ is the system state vector, $\mathbf{Z}(t)$ is the system auxiliary (algebraic) variable vector, and $\mathbf{U_r}(t)$ is the system input vector. The dimensions and/or the definitions of $\mathbf{X}(t)$ and $\mathbf{Z}(t)$ vary with the different generator/tie-line models, while the definition of $\mathbf{U_r}(t)$ is common to all three system models, i.e.,

$$\mathbf{U_r}(t) \triangleq \begin{bmatrix} P_{ref}(t) & V_{ref}(t) \end{bmatrix}^T \tag{2.59}$$

where the superscript T denotes transpose. In general, the function $\mathbf{\Phi}(\mathbf{X}(t), \mathbf{Z}(t), \mathbf{U_r}(t))$ in (2.58) is a linear function of $\mathbf{X}(t)$, $\mathbf{Z}(t)$, and $\mathbf{U_r}(t)$, expressed as

$$\mathbf{\Phi}(\mathbf{X}(t), \mathbf{Z}(t), \mathbf{U_r}(t)) = \mathbf{\Phi_X}\mathbf{X}(t) + \mathbf{\Phi_Z}\mathbf{Z}(t) + \mathbf{B}\mathbf{U_r}(t) \tag{2.60}$$

where $\mathbf{\Phi_X}$, $\mathbf{\Phi_Z}$, and $\mathbf{B}$ are all constant matrices. The functions $\mathbf{\Psi}(\mathbf{X}(t), \mathbf{Z}(t))$ and $\mathbf{\Xi}(\mathbf{X}(t), \mathbf{Z}(t), \mathbf{U_r}(t))$ in (2.58) are vector-valued, nonlinear, algebraic functions that describe the nonlinear characteristics of the system. The product nonlinearities and the trigonometric nonlinearities inherent in the synchronous generator and the tie-line are formulated in $\mathbf{\Psi}(\mathbf{X}(t), \mathbf{Z}(t))$, while the nonlinearities caused by limiting in the excitation system and the governor are expressed in $\mathbf{\Xi}(\mathbf{X}(t), \mathbf{Z}(t), \mathbf{U_r}(t))$. The latter has the same structure for the three complete system models, i.e.,

$$\mathbf{\Xi}(\mathbf{X}(t), \mathbf{Z}(t), \mathbf{U_r}(t)) = \begin{bmatrix} E_{FD}(t) - Nf_1 \\ \overline{P}_{\Sigma}(t) - Nf_2 \\ P_{GV}(t) - Nf_3 \end{bmatrix} \tag{2.61}$$

where Nf_1, Nf_2, and Nf_3 are the saturation functions given in the right-hand side of (A.14), (A.16), and (A.18) of Appendix A. Therefore, for each of the nonlinear power

system representations addressed below, only $\mathbf{\Phi_X}$, $\mathbf{\Phi_Z}$, $\mathbf{B}$, and $\mathbf{\Psi}(\mathbf{X}(t), \mathbf{Z}(t))$, together with $\mathbf{X}(t)$ and $\mathbf{Z}(t)$, need to be specified.

Based on the general form of the state representation (2.58), three nonlinear system models are defined as follows:

Complete System Model 1 (CSM1): the synchronous generator and the tie-line are described by the SGM1; the models for the excitation system, the governor, and the steam turbine are given by (A.13)-(A.24) of Appendix A.

In the CSM1 the state vector $\mathbf{X}(t)$ and the auxiliary variable vector $\mathbf{Z}(t)$ are defined as

$$\mathbf{X}(t) = \left[\begin{array}{ccccccccc} \delta(t) & \omega_s(t) & E'_q(t) & \Lambda''_d(t) & \Lambda''_q(t) & V_R(t) & \overline{P}_{GV}(t) & P_{HP}(t) & P_{IP}(t) & P_{LP}(t) \end{array} \right]^{\mathrm{T}} \tag{2.62}$$

and

$$\mathbf{Z}(t) = \left[\begin{array}{ccccccc} I_d(t) & I_q(t) & T_e(t) & V_t(t) & T_m(t) & E_{FD}(t) & \overline{P}_{\Sigma}(t) & P_{GV}(t) \end{array} \right]^{\mathrm{T}}. \tag{2.63}$$

The matrices $\mathbf{\Phi_X}$, $\mathbf{\Phi_Z}$, and $\mathbf{B}$ in (2.60) are given by

$$\mathbf{\Phi_X} = \begin{bmatrix} 0 & \omega_0 & 0 & 0 & 0 & 0 & 0 & 0 & 0 & 0 \\ 0 & -\frac{D}{2H} & 0 & 0 & 0 & 0 & 0 & 0 & 0 & 0 \\ 0 & 0 & -\frac{1}{\tau'_{d0}} & 0 & 0 & 0 & 0 & 0 & 0 & 0 \\ 0 & 0 & \frac{1}{\tau''_{d0}} - \frac{1}{\tau'_{d0}} & -\frac{1}{\tau''_{d0}} & 0 & 0 & 0 & 0 & 0 & 0 \\ 0 & 0 & 0 & 0 & -\frac{1}{\tau''_{q0}} & 0 & 0 & 0 & 0 & 0 \\ 0 & 0 & 0 & 0 & 0 & -\frac{1}{\tau_A} & 0 & 0 & 0 & 0 \\ 0 & 0 & 0 & 0 & 0 & 0 & 0 & 0 & 0 & 0 \\ 0 & 0 & 0 & 0 & 0 & 0 & 0 & -\frac{1}{\tau_{CH}} & 0 & 0 \\ 0 & 0 & 0 & 0 & 0 & 0 & 0 & \frac{1}{\tau_{RH}} & -\frac{1}{\tau_{RH}} & 0 \\ 0 & 0 & 0 & 0 & 0 & 0 & 0 & 0 & \frac{1}{\tau_{CO}} & -\frac{1}{\tau_{CO}} \end{bmatrix}, \tag{2.64}$$

$$\mathbf{\Phi_Z} = \begin{bmatrix} 0 & 0 & 0 & 0 & 0 & 0 & 0 & 0 \\ 0 & 0 & -\frac{1}{2H} & 0 & \frac{1}{2H} & 0 & 0 & 0 \\ \frac{L_d - L_d^{'}}{\tau_{d0}^{'}} & 0 & 0 & 0 & 0 & \frac{1}{\tau_{d0}^{'}} & 0 & 0 \\ \frac{L_d^{'} - L_d^{''}}{\tau_{d0}^{''}} + \frac{L_d - L_d^{'}}{\tau_{d0}^{'}} & 0 & 0 & 0 & 0 & \frac{1}{\tau_{d0}^{'}} & 0 & 0 \\ 0 & \frac{L_q - L_q^{''}}{\tau_{q0}^{''}} & 0 & 0 & 0 & 0 & 0 & 0 \\ 0 & 0 & 0 & -\frac{K_A}{\tau_A} & 0 & 0 & 0 & 0 \\ 0 & 0 & 0 & 0 & 0 & 0 & 1 & 0 \\ 0 & 0 & 0 & 0 & 0 & 0 & 0 & \frac{1}{\tau_{CH}} \\ 0 & 0 & 0 & 0 & 0 & 0 & 0 & 0 \\ 0 & 0 & 0 & 0 & 0 & 0 & 0 & 0 \end{bmatrix}, \tag{2.65}$$

and

$$\mathbf{B} = \begin{bmatrix} 0 & 0 & 0 & 0 & 0 & 0 & 0 & 0 & 0 & 0 \\ 0 & 0 & 0 & 0 & 0 & \frac{K_A}{\tau_A} & 0 & 0 & 0 & 0 \end{bmatrix}^{\mathrm{T}}. \tag{2.66}$$

The nonlinear algebraic function $\mathbf{\Psi}(\mathbf{X}(t), \mathbf{Z}(t))$ is derived by equating (2.37) with (2.39) and (2.38) with (2.40), and substituting (2.37) and (2.38) into (A.10). This results in

$$\mathbf{\Psi}(\mathbf{X}(t), \mathbf{Z}(t)) = \begin{bmatrix} \psi_1 & \psi_2 & \psi_3 & \psi_4 & \psi_5 \end{bmatrix}^T \tag{2.67}$$

with

$$\begin{aligned}
\psi_1 &= (r + R_e)\left(-\omega(t)\Lambda_q^{''}(t) + V_\infty \sin\delta(t)\right) \\
&\quad - \left(L_e\omega(t) + L_q^{''}\omega(t)\right)\left(\omega(t)\Lambda_d^{''}(t) - V_\infty \cos\delta(t)\right) - cI_d(t), && (2.68)\\
\psi_2 &= (r + R_e)\left(\omega(t)\Lambda_d^{''}(t) - V_\infty \cos\delta(t)\right) \\
&\quad + \left(L_e\omega(t) + L_d^{''}\omega(t)\right)\left(-\omega(t)\Lambda_q^{''}(t) + V_\infty \sin\delta(t)\right) - cI_q(t), && (2.69)\\
\psi_3 &= \Lambda_d^{''}(t)I_q(t) - \Lambda_q^{''}(t)I_d(t) + \left(L_d^{''} - L_q^{''}\right)I_d(t)I_q(t) - T_e(t), && (2.70)\\
\psi_4 &= \omega(t)^2\left[\Lambda_q^{''}(t)^2 + \Lambda_d^{''}(t)^2 + 2\left(L_d^{''}\Lambda_d^{''}(t)I_d(t) + L_q^{''}\Lambda_q^{''}(t)I_q(t)\right)\right] \\
&\quad + \left(r^2 + L_d^{''^2}\omega(t)^2\right)I_d(t)^2 + \left(r^2 + L_q^{''^2}\omega(t)^2\right)I_q(t)^2 \\
&\quad - 2r\omega(t)T_e(t) - V_i(t)^2, && (2.71)\\
\psi_5 &= F_{HP}P_{HP}(t) + F_{IP}P_{IP}(t) + F_{LP}P_{LP}(t) - \omega(t)T_m(t), && (2.72)
\end{aligned}$$

where

$$\omega(t) = \omega_s(t) + 1 \tag{2.73}$$

and

$$c = (r + R_e)^2 + \left(L_e\omega(t) + L_d^{''}\omega(t)\right)\left(L_e\omega(t) + L_q^{''}\omega(t)\right). \tag{2.74}$$

In this thesis the CSM1 is referred to as the *benchmark model of the complete system* in which the associated generator/tie-line model (SGM1) most closely represents the basic synchronous generator/tie-line system described by (A.1)-(A.12).

Complete System Model 2 (CSM2): the synchronous generator and the tie-line are described by the SGM2; the models for the excitation system, the governor, and the steam turbine are given by (A.13)-(A.24) of Appendix A.

This representation is the consequence of applying Assumption 2.2.5 to the CSM1. The state vector $\mathbf{X}(t)$ and the auxiliary variable vector $\mathbf{Z}(t)$ in the CSM2 are defined as

$$\mathbf{X}(t) = \left[\begin{array}{cccccccccc} \delta(t) & \omega_s(t) & E'_q(t) & E''_q(t) & E''_d(t) & V_R(t) & \overline{P}_{GV}(t) & P_{HP}(t) & P_{IP}(t) & P_{LP}(t) \end{array} \right]^{\mathrm{T}} \tag{2.75}$$

and

$$\mathbf{Z}(t) = \left[\begin{array}{cccccc} I_d(t) & I_q(t) & T_e(t) & V_t(t) & E_{FD}(t) & \overline{P}_{\Sigma}(t) & P_{GV}(t) \end{array} \right]^{\mathrm{T}} \tag{2.76}$$

in which the dimension of $\mathbf{Z}(t)$ is reduced by one compared to its definition in (2.63) for the CSM1. The matrix $\mathbf{B}$ in the CSM2 is identical with that of the CSM1 (eqn. (2.66)), while the other two matrices, $\mathbf{\Phi_X}$ and $\mathbf{\Phi_Z}$, are described by

$$\mathbf{\Phi_X} = \begin{bmatrix} 0 & \omega_0 & 0 & 0 & 0 & 0 & 0 & 0 & 0 & 0 \\ 0 & -\frac{D}{2H} & 0 & 0 & 0 & 0 & 0 & \frac{F_{HP}}{2H} & \frac{F_{IP}}{2H} & \frac{F_{LP}}{2H} \\ 0 & 0 & -\frac{1}{\tau'_{d0}} & 0 & 0 & 0 & 0 & 0 & 0 & 0 \\ 0 & 0 & \frac{1}{\tau''_{d0}} - \frac{1}{\tau'_{d0}} & -\frac{1}{\tau''_{d0}} & 0 & 0 & 0 & 0 & 0 & 0 \\ 0 & 0 & 0 & 0 & -\frac{1}{\tau''_{q0}} & 0 & 0 & 0 & 0 & 0 \\ 0 & 0 & 0 & 0 & 0 & -\frac{1}{\tau_A} & 0 & 0 & 0 & 0 \\ 0 & 0 & 0 & 0 & 0 & 0 & 0 & 0 & 0 & 0 \\ 0 & 0 & 0 & 0 & 0 & 0 & 0 & -\frac{1}{\tau_{CH}} & 0 & 0 \\ 0 & 0 & 0 & 0 & 0 & 0 & 0 & \frac{1}{\tau_{RH}} & -\frac{1}{\tau_{RH}} & 0 \\ 0 & 0 & 0 & 0 & 0 & 0 & 0 & 0 & \frac{1}{\tau_{CO}} & -\frac{1}{\tau_{CO}} \end{bmatrix} \tag{2.77}$$

and

$$\mathbf{\Phi_Z} = \begin{bmatrix} 0 & 0 & 0 & 0 & 0 & 0 & 0 \\ 0 & 0 & -\frac{1}{2H} & 0 & 0 & 0 & 0 \\ \frac{X_d - X_d^{'}}{\tau_{d0}^{'}} & 0 & 0 & 0 & \frac{1}{\tau_{d0}^{'}} & 0 & 0 \\ \frac{X_d^{'} - X_d^{''}}{\tau_{d0}^{''}} + \frac{X_d - X_d^{'}}{\tau_{d0}^{'}} & 0 & 0 & 0 & \frac{1}{\tau_{d0}^{'}} & 0 & 0 \\ 0 & -\frac{X_q - X_q^{''}}{\tau_{q0}^{''}} & 0 & 0 & 0 & 0 & 0 \\ 0 & 0 & 0 & -\frac{K_A}{\tau_A} & 0 & 0 & 0 \\ 0 & 0 & 0 & 0 & 0 & 1 & 0 \\ 0 & 0 & 0 & 0 & 0 & 0 & \frac{1}{\tau_{CH}} \\ 0 & 0 & 0 & 0 & 0 & 0 & 0 \\ 0 & 0 & 0 & 0 & 0 & 0 & 0 \end{bmatrix}. \tag{2.78}$$

The nonlinear algebraic function $\mathbf{\Psi}(\mathbf{X}(t), \mathbf{Z}(t))$ of the CSM2 is simplified by substituting $\omega(t) \approx 1$ into (2.67), resulting in

$$\mathbf{\Psi}(\mathbf{X}(t), \mathbf{Z}(t)) = \begin{bmatrix} \psi_1 & \psi_2 & \psi_3 & \psi_4 \end{bmatrix}^T \tag{2.79}$$

with

$$\begin{aligned} \psi_1 &= (r + R_e)\left(E_d^{''}(t) + V_\infty \sin\delta(t)\right) \\ &\quad - \left(X_e + X_q^{''}\right)\left(E_q^{''}(t) - V_\infty \cos\delta(t)\right) - cI_d(t), \qquad (2.80) \\ \psi_2 &= (r + R_e)\left(E_q^{''}(t) - V_\infty \cos\delta(t)\right) \\ &\quad + \left(X_e + X_d^{''}\right)\left(E_d^{''}(t) + V_\infty \sin\delta(t)\right) - cI_q(t), \qquad (2.81) \\ \psi_3 &= I_d(t)E_d^{''}(t) + I_q(t)E_q^{''}(t) + \left(X_d^{''} - X_q^{''}\right) I_d(t)I_q(t) - T_e(t), \qquad (2.82) \\ \psi_4 &= E_d^{''}(t)^2 + E_q^{''}(t)^2 + 2\left(X_d^{''}E_q^{''}(t)I_d(t) - X_q^{''}E_d^{''}(t)I_q(t)\right) \\ &\quad + \left(r^2 + X_d^{''2}\right) I_d(t)^2 + \left(r^2 + X_q^{''2}\right) I_q(t)^2 - 2rT_e(t) - V_t(t)^2, \qquad (2.83) \end{aligned}$$

where c given by (2.74) becomes a constant

$$c = (r + R_e)^2 + \left(X_e + X_d^{''}\right)\left(X_e + X_q^{''}\right). \tag{2.84}$$

Complete System Model 3 (CSM3): the synchronous generator and the tie-line are described by the SGM3; the models for the excitation system, the governor, and the steam turbine are given by (A.13)-(A.24) of Appendix A.

This combination yields the simplest system model used in this thesis. The four elements ($\mathbf{\Phi_X}$, $\mathbf{\Phi_Z}$, $\mathbf{B}$, and $\mathbf{\Psi}(\mathbf{X}(t), \mathbf{Z}(t))$) defining the system state expres-

sion (2.58) are expressed as

$$\mathbf{\Phi_X} = \begin{bmatrix} 0 & \omega_0 & 0 & 0 & 0 & 0 & 0 & 0 \\ 0 & -\frac{D}{2H} & 0 & 0 & 0 & \frac{F_{HP}}{2H} & \frac{F_{IP}}{2H} & \frac{F_{LP}}{2H} \\ 0 & 0 & -\frac{1}{\tau'_{d0}} & 0 & 0 & 0 & 0 & 0 \\ 0 & 0 & 0 & -\frac{1}{\tau_A} & 0 & 0 & 0 & 0 \\ 0 & 0 & 0 & 0 & 0 & 0 & 0 & 0 \\ 0 & 0 & 0 & 0 & 0 & -\frac{1}{\tau_{CH}} & 0 & 0 \\ 0 & 0 & 0 & 0 & 0 & \frac{1}{\tau_{RH}} & -\frac{1}{\tau_{RH}} & 0 \\ 0 & 0 & 0 & 0 & 0 & 0 & \frac{1}{\tau_{CO}} & -\frac{1}{\tau_{CO}} \end{bmatrix}, \tag{2.85}$$

$$\mathbf{\Phi_Z} = \begin{bmatrix} 0 & 0 & 0 & 0 & 0 & 0 & 0 \\ 0 & 0 & -\frac{1}{2H} & 0 & 0 & 0 & 0 \\ \frac{X_d - X'_d}{\tau'_{d0}} & 0 & 0 & 0 & \frac{1}{\tau'_{d0}} & 0 & 0 \\ 0 & 0 & 0 & -\frac{K_A}{\tau_A} & 0 & 0 & 0 \\ 0 & 0 & 0 & 0 & 0 & 1 & 0 \\ 0 & 0 & 0 & 0 & 0 & 0 & \frac{1}{\tau_{CH}} \\ 0 & 0 & 0 & 0 & 0 & 0 & 0 \\ 0 & 0 & 0 & 0 & 0 & 0 & 0 \end{bmatrix}, \tag{2.86}$$

$$\mathbf{B} = \begin{bmatrix} 0 & 0 & 0 & 0 & 0 & 0 & 0 & 0 \\ 0 & 0 & 0 & \frac{K_A}{\tau_A} & 0 & 0 & 0 & 0 \end{bmatrix}^{\mathrm{T}}, \tag{2.87}$$

and

$$\mathbf{\Psi}(\mathbf{X}(t), \mathbf{Z}(t)) = \begin{bmatrix} V_\infty \cos\delta(t) - E'_q(t) - \left(X_e + X'_d\right) I_d(t) \\ V_\infty \sin\delta(t) - (X_e + X_q)\, I_q(t) \\ I_q(t) E'_q(t) + \left(X'_d - X_q\right) I_d(t) I_q(t) - T_e(t) \\ E'_q(t)^2 + 2X'_d E'_q(t) I_d(t) + X'^2_d I_d(t)^2 + X_q^2 I_q(t)^2 - V_t(t)^2 \end{bmatrix}. \tag{2.88}$$

In the CSM3 the dimension of the state vector $\mathbf{X}(t)$ is reduced by two due to the elimination of the subtransient states $E''_d(t)$ and $E''_q(t)$ from (2.75)

$$\mathbf{X}(t) = \begin{bmatrix} \delta(t) & \omega_s(t) & E'_q(t) & V_R(t) & \overline{P}_{GV}(t) & P_{HP}(t) & P_{IP}(t) & P_{LP}(t) \end{bmatrix}^T. \tag{2.89}$$

The auxiliary variable vector $\mathbf{Z}(t)$ is the same as in (2.76) for the CSM2.

Remark 2.3.1 *In the three complete system models given in this subsection, the system equations are formulated with reheating. However, as indicated in Remark A.3.1,*

the system equations with nonreheating can be easily obtained by the proper selection of the values of the parameters associated with the model of the steam turbine and reheater.

2.3.2 Comparisons of the Dynamic Performance of the Complete System Models.

In order to select the power system models for controller analysis and design and for the evaluation of the designed controllers, a set of simulation studies is conducted for the various operating conditions in which the three complete system models derived from Subsection 2.3.1 are subjected to the same disturbances.

Aims and structure of the simulation studies.

The dynamic performance of the CSM1 is taken as the benchmark performance which is verified by the comparison of the system time response with that obtained from the established software package, ADSTAB [133]. [3] The dynamic behaviour of the CSM2 and the CSM3 is then compared with the result obtained from the benchmark. The aims of this study are

- to establish the degradation in system performance associated with the various system models;
- to demonstrate the effect of increasing the value of the rotor damping coefficient D as compensation for the omission of damper windings in the CSM3.

[3] For the simulation studies in this thesis, the software package SIMNON [134,135,136] is used. The software written by the author of this thesis for the simulation studies in SIMNON has been verified by comparing the results with those obtained from the ADSTAB package. The ADSTAB package is a multi-machine transient stability program that has been designed for research use in the University of Adelaide [133]. The accuracy of the models and algorithms used in ADSTAB has been verified against the results obtained by tests on actual power systems (e.g., a series of tests at Northfleet in the U.K. [137]).

For the purpose of simulation studies *in this thesis*, **identical** models and parameters of the nonreheat turbine, the governor, and the excitation system are used. The parameters and limits of the system models are listed in Appendix C.

Two system operating conditions with two distinct disturbances have been selected for the simulation studies:

Case 1: The generator is operating at $P_t = 0.6$ pu and $Q_t = 0.3$ pu, and is subjected to a step change of 0.05 pu increase in reference power.

Case 2: The generator is operating at $P_t = 0.6$ pu and $Q_t = -0.1$ pu, and is subjected to a step change of 0.05 pu decrease in reference power.

Case 3: The generator is operating at $P_t = 0.6$ pu and $Q_t = 0.3$ pu, and is subjected to a symmetrical three-phase fault [4] on the receiving end busbars. The fault is cleared in 100 ms, and the system returns to its pre-fault operating condition.

Case 4: The generator is operating at $P_t = 0.6$ pu and $Q_t = -0.1$ pu, and is subjected to a symmetrical three-phase fault at the machine terminal. The line is switched out [5] after the fault duration of 100 ms, and a new steady-state operating point is established.

The simulation studies are conducted in two steps:

Step 1: Compare the system performance of the three power system models with the same value of the rotor damping coefficient ($D = 0.1$ pu) to establish the degradation in system performance.

Step 2: Compare the system performance of the CSM3 ($D = 4.0$ pu) with that of the CSM1 ($D = 0.1$ pu) to demonstrate the effect of increasing the value of the rotor

[4] Although the majority of the faults occurring in practice on a power system are asymmetrical between the phases and the phase(s) to ground, the symmetrical fault is important because it is more severe and easier to analyze [125].

[5] In the simulation studies *of this thesis*, the values of R_e and X_e are doubled to represent the event of a transmission line switching-out.

damping coefficient D as compensation for the omission of damper windings in the CSM3.

Simulation results which take account of the above steps are plotted for the four cases in Figs. 2.3-2.6.

Analysis of the simulation results.

Step 1: The simulation studies in the first step involve the comparison of damping performance of the three complete system models with the same value of $D = 0.1$ pu. This value of D is given *a priori*. Figures 2.3 and 2.4 show the transient speed deviations in Cases 1 and 2. It is seen that under normal operating conditions the performance of the CSM2 (dashed line) agrees closely with that of the CSM1 (solid line). However, since there are no damper windings in the CSM3, the speed response of the CSM3 (dotted line) differs significantly from the result of the CSM1. The same conclusions can be derived from the simulation result of Case 3, shown in Fig. 2.5. It is seen that with the occurrence of the remote fault, the CSM2 still provides satisfactory agreement with the CSM1, whereas the CSM3 exhibits instability. In Case 4, appreciable errors in phase between the responses of the CSM1 and the CSM2 are found, as shown in Fig. 2.6. Nevertheless the amplitudes of the speed deviation of the CSM2 are almost the same as those of the CSM1. It is noted that, in this simulation study, the response of the CSM3 is unstable and is unacceptable.

Remark 2.3.2 *The above simulation studies reveal that*

(i) The CSM2 is a good approximation of the CSM1 at the chosen operating conditions. This justifies Assumption 2.2.5 and indicates that the nonlinearities in system parameters and in machine stator voltage equations can be neglected.

(ii) The CSM3 with the given value of D cannot be used to represent the benchmark model (CSM1) directly. To achieve good agreement between the performance of the two models, the damping of the CSM3 has to be increased.

The approach of using the CSM3 to approximately represent the benchmark model is important because of the simplicity of the CSM3 for the analysis and design of system controllers. Since the subtransient effects which are omitted in the representation of the CSM3 are normally very short, it is possible to compensate for the omission of damper windings in the CSM3 by adjusting the rotor damping coefficient D to a higher value. This simplification has been proposed in Section 2.2 (when Assumption 2.2.6 was introduced).

Step 2: The simulation studies in the second step involve the demonstration of the above-mentioned simplification. The value of the rotor damping coefficient D is adjusted to make the response of the CSM3 agree *as closely as possible* with that of the CSM1. For the various operating conditions, the value of $D = 4.0$ pu is found to be the optimal value. D is therefore increased from 0.1 pu (the given value) to 4.0 pu in the equations of the CSM3. The performance of the CSM3 ($D = 4.0$ pu) (dot-dashed line) is compared with that of the CSM1. It is observed from Figs. 2.3-2.5 that significant improvements in overall model matching are achieved in these three simulation cases. In Case 4, referring to Fig. 2.6, the CSM3 ($D = 4.0$ pu) shows stronger damping than the CSM1.

Remark 2.3.3 *The comparison of system performance of the CSM3 ($D = 4.0$ pu) and the CSM1 in Case 4 indicates a possibility that a controller particularly designed for the CSM3 ($D = 4.0$ pu) may not be able to damp the oscillations associated with the CSM1 satisfactorily. This initiates the discussion of the validation of the designed power system stabilisers in Subsections 3.6.3, 4.5.3, 5.4.3, and 6.5.3.*

Remark 2.3.4 *The comments made in Remarks 2.3.2 and 2.3.3 are valid when the system operating point varies (e.g., $P_t = 0.75$ pu, $P_t = 0.4$ pu, etc.).*

Robustness studies.

The validations of the designed power system stabilisers are regarded to be the *robustness studies* in this thesis. As far as the system modelling is concerned, robustness

studies in power system control are required when an approximate model is used as a basis for controller analysis and design. For the purpose of this thesis, there are two major concerns in employing the approximate model (CSM3 with $D = 4.0$ pu) for representing the benchmark (CSM1):

- Unmodelled dynamics — caused by ignoring the damper windings (i.e., omitting the subtransient states $E''_d(t)$ and $E''_q(t)$) (see Assumption 2.2.6), and/or by assuming a constant rotor speed in some terms of the synchronous generator equations (see Assumption 2.2.5);
- Modelling simplifications — for example, by assuming zero values for some system parameters (see Assumption 2.2.7), and/or by increasing the given value of D to a higher value.

It will therefore be necessary to verify the various power system stabilisers using the benchmark model (CSM1) to confirm that the simplified model (CSM3 with $D = 4.0$ pu) is suitable for their design.

Conclusions.

In view of the simulation results shown in Figs. 2.3-2.6, it is proposed that:

1. The CSM3 ($D = 4.0$ pu) be taken to be the *approximate power system model* for the purpose of the analysis and design of power system stabilisers in Chapters 3 to 6.
2. The CSM1 ($D = 0.1$ pu) be taken to be the *accurate power system model* for validating the designed power system stabilisers in Subsections 3.6.3, 4.5.3, 5.4.3, and 6.5.3.

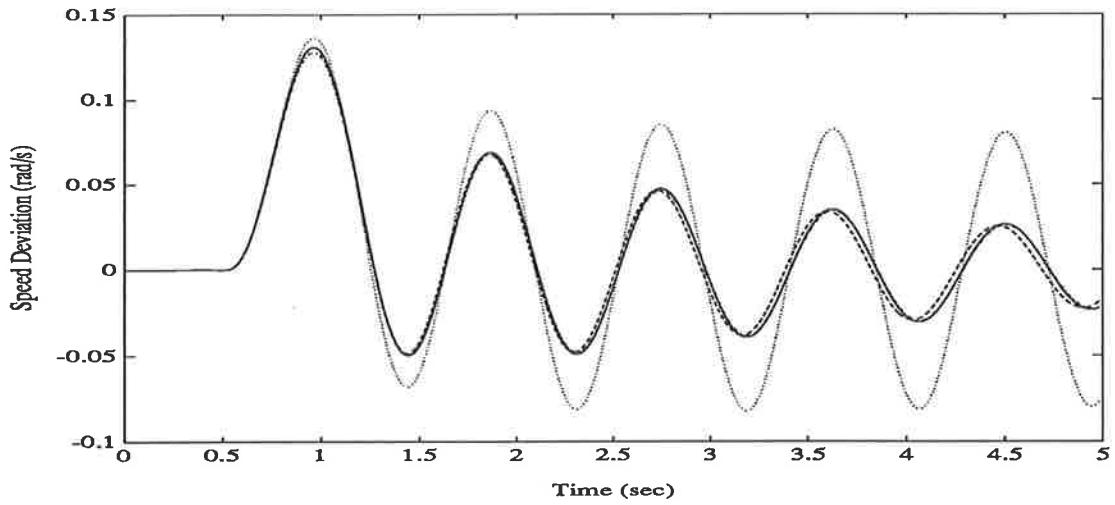

Figure 2.3: Speed response for Case 1 ($P_t = 0.6$ pu, $Q_t = 0.3$ pu; 0.05 pu increase in reference power). CSM1 ($D = 0.1$ pu) - solid line, CSM2 ($D = 0.1$ pu) - dashed line, CSM3 ($D = 0.1$ pu) - dotted line, CSM3 ($D = 4.0$ pu) - dot-dashed line.

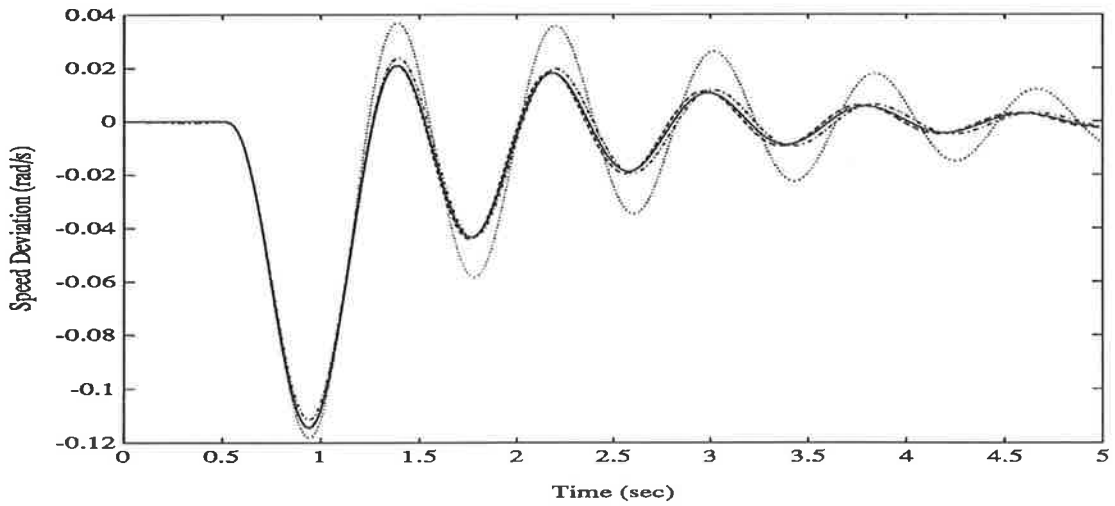

Figure 2.4: Speed response for Case 2 ($P_t = 0.6$ pu, $Q_t = -0.1$ pu; 0.05 pu decrease in reference power). CSM1 ($D = 0.1$ pu) - solid line, CSM2 ($D = 0.1$ pu) - dashed line, CSM3 ($D = 0.1$ pu) - dotted line, CSM3 ($D = 4.0$ pu) - dot-dashed line.

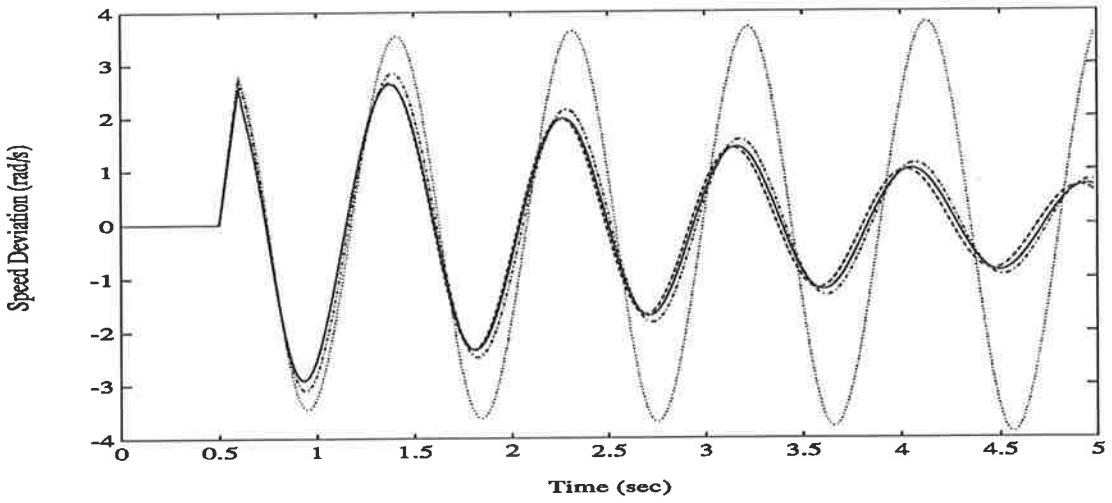

Figure 2.5: Speed response for Case 3 ($P_t = 0.6$ pu, $Q_t = 0.3$ pu; 100 ms short-circuit on the receiving end busbars). CSM1 ($D = 0.1$ pu) - solid line, CSM2 ($D = 0.1$ pu) - dashed line, CSM3 ($D = 0.1$ pu) - dotted line, CSM3 ($D = 4.0$ pu) - dot-dashed line.

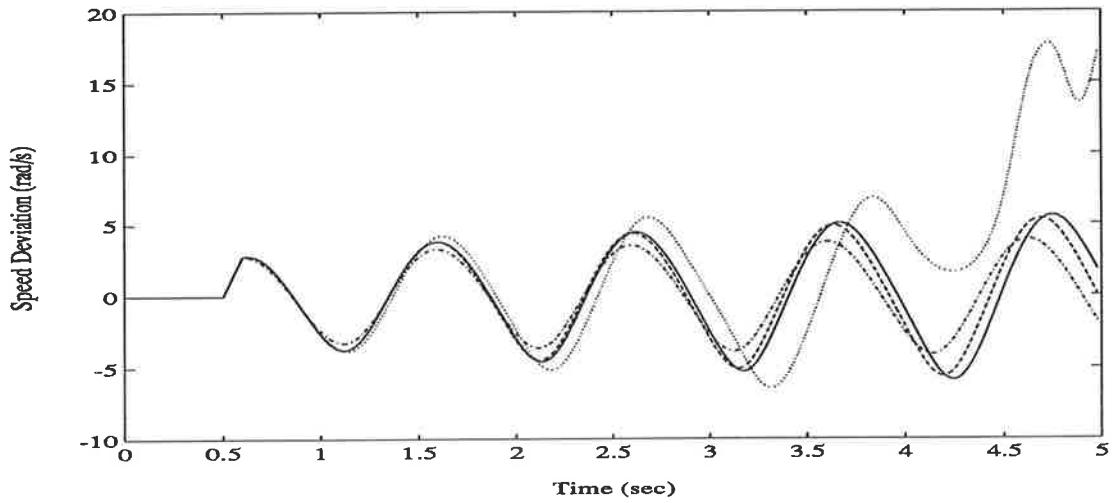

Figure 2.6: Speed response for Case 4 ($P_t = 0.6$ pu, $Q_t = -0.1$ pu; 100 ms short-circuit at the machine terminal). CSM1 ($D = 0.1$ pu) - solid line, CSM2 ($D = 0.1$ pu) - dashed line, CSM3 ($D = 0.1$ pu) - dotted line, CSM3 ($D = 4.0$ pu) - dot-dashed line.

2.4 Linearisation of the Nonlinear Power System Model.

In this section:

- the nonlinear power system model (CSM3) proposed in Subsection 2.3.1 is linearised;
- **analytical models** [6] of the nonlinear power system for the development of the linear and nonlinear adaptive power system stabilisers are introduced;
- the models derived in Sections 2.2 to 2.4 are summarised.

The nonlinearities associated with a power system can be divided into two categories: *inherent nonlinearities* and *intentional nonlinearities* [138]. In general terms, an inherent nonlinearity is defined as an *inseparable* characteristic of the laws governing the operation of the system to be controlled, while an intentional nonlinearity is considered to be *deliberately* introduced into the design of the system by control engineers. For a power system, the inherent nonlinearities of the system are mainly characterised by the product nonlinearities and the trigonometric nonlinearities which are contained in the term $\Psi(\mathbf{X}(t), \mathbf{Z}(t))$ (e.g., (2.88)) in (2.58). On the other hand, the intentional nonlinearities of the system include the amplitude and rate limits that are given by the term $\Xi(\mathbf{X}(t), \mathbf{Z}(t), \mathbf{U}_r(t))$ (e.g., (2.61)) in (2.58). The intentional nonlinearities which are introduced by the power system control components (such as the exciter and the governor) are usually determined from a trade-off between technical and economic considerations.

Analytical models of the power system are derived from the following two steps:

[6] In this thesis, an **analytical model** is defined for the purpose of simplifying the analysis. It is used for developing the *nominal model* of the system. The definition of a "nominal model" will be given in Section 3.2.

(1) eliminate the intentional nonlinearities by assuming that the perturbations that are injected into the nonlinear system are *mild* enough so that limiting of the system variables does not occur (see Assumption 2.4.1);

(2) eliminate the inherent nonlinearities by linearising the system equations about one or more steady-state operating points (see Assumption 2.4.2).

Following (1) a nonlinear analytical model results, in which the inherent nonlinearities of the power system are still retained. Following (2) the nonlinear power system model is completely linearised, and a linearised analytical model is obtained.

Most methods for the design of power system controllers in the literature are based on linearised models of power systems. Linearisation of the nonlinear power system about a steady-state operating point provides information on the small-perturbation dynamic behaviour of the system at the specified operating point. Since low-frequency, lightly-damped rotor oscillations dominate the system transient response, the CSM3 introduced in Subsection 2.3.1 is used in this section for the derivation of the analytical models upon which the development of control strategies is based.

The layout of this section is as follows. In Subsection 2.4.1 a nonlinear analytical model is derived from the nonlinear power system model (CSM3). A linearised analytical model is then developed from the nonlinear analytical model in Subsection 2.4.2. These analytical models are prepared for the development of the linear and nonlinear adaptive power system stabilisers discussed later in Sections 3.2 and 4.2 respectively. The models proposed in this chapter are finally summarised in Subsection 2.4.3.

2.4.1 Nonlinear Analytical Model of the Nonlinear Power System.

Consider the situations where the perturbations injected into the nonlinear power system are *mild* enough that limiting of the system variables does not occur. Under these circumstances, the intentional nonlinearities of the system can be ignored by assuming that

Assumption 2.4.1 *Under transient conditions, the nonlinear power system under study is operating within the limiting actions described by the functions Nf_1, Nf_2, and Nf_3 in (A.14), (A.16), and (A.18).*

On removing the limits, the nonlinear function $\mathbf{\Xi}(\mathbf{X}(t), \mathbf{Z}(t), \mathbf{U_r}(t))$ in (2.61) becomes a linear expression

$$\mathbf{\Xi}(\mathbf{X}(t), \mathbf{Z}(t), \mathbf{U_r}(t)) = \begin{bmatrix} E_{FD}(t) - V_R(t) \\ \overline{P}_{\Sigma}(t) - \frac{P_{ref}(t) - K_G\omega_s(t) - P_{GV}(t)}{\tau_G} \\ P_{GV}(t) - \overline{P}_{GV}(t) \end{bmatrix}$$

which can be incorporated into the expressions for $\mathbf{\Phi}(\mathbf{X}(t), \mathbf{Z}(t), \mathbf{U_r}(t))$ and $\mathbf{\Psi}(\mathbf{X}(t), \mathbf{Z}(t))$ in (2.58). Hence, the mathematical description of the CSM3 can be rewritten as

$$\begin{bmatrix} \dot{\mathbf{X}}(t) \\ \mathbf{0} \end{bmatrix} = \begin{bmatrix} \mathbf{\Phi}(\mathbf{X}(t), \mathbf{Z}(t), \mathbf{U_r}(t)) \\ \mathbf{\Psi}(\mathbf{X}(t), \mathbf{Z}(t)) \end{bmatrix} \tag{2.90}$$

where

$$\mathbf{X}(t) = \begin{bmatrix} \delta(t) & \omega_s(t) & E'_q(t) & E_{FD}(t) & P_{GV}(t) & P_{HP}(t) & P_{IP}(t) & P_{LP}(t) \end{bmatrix}^T, \tag{2.91}$$

$$\mathbf{Z}(t) = \begin{bmatrix} I_d(t) & T_e(t) & V_t(t) \end{bmatrix}^T, \tag{2.92}$$

and

$$\mathbf{\Phi}(\mathbf{X}(t), \mathbf{Z}(t), \mathbf{U_r}(t)) = \mathbf{\Phi_X}\mathbf{X}(t) + \mathbf{\Phi_Z}\mathbf{Z}(t) + \mathbf{B}\mathbf{U_r}(t) \tag{2.93}$$

(as expressed in (2.60)). The elements $\mathbf{\Phi_X}$, $\mathbf{\Phi_Z}$, $\mathbf{B}$, and $\mathbf{\Psi}(\mathbf{X}(t), \mathbf{Z}(t))$ in (2.90) are written as

$$\mathbf{\Phi_X} = \begin{bmatrix} 0 & \omega_0 & 0 & 0 & 0 & 0 & 0 & 0 \\ 0 & -\frac{D}{2H} & 0 & 0 & 0 & \frac{F_{HP}}{2H} & \frac{F_{IP}}{2H} & \frac{F_{LP}}{2H} \\ 0 & 0 & -\frac{1}{\tau_{d0}} & \frac{1}{\tau_{d0}} & 0 & 0 & 0 & 0 \\ 0 & 0 & 0 & -\frac{1}{\tau_A} & 0 & 0 & 0 & 0 \\ 0 & -\frac{K_G}{\tau_G} & 0 & 0 & -\frac{1}{\tau_G} & 0 & 0 & 0 \\ 0 & 0 & 0 & 0 & \frac{1}{\tau_{CH}} & -\frac{1}{\tau_{CH}} & 0 & 0 \\ 0 & 0 & 0 & 0 & 0 & \frac{1}{\tau_{RH}} & -\frac{1}{\tau_{RH}} & 0 \\ 0 & 0 & 0 & 0 & 0 & 0 & \frac{1}{\tau_{CO}} & -\frac{1}{\tau_{CO}} \end{bmatrix}, \tag{2.94}$$

$$\mathbf{\Phi_Z} = \begin{bmatrix} 0 & 0 & 0 \\ 0 & -\frac{1}{2H} & 0 \\ \frac{X_d - X_d'}{\tau_{do}'} & 0 & 0 \\ 0 & 0 & -\frac{K_A}{\tau_A} \\ 0 & 0 & 0 \\ 0 & 0 & 0 \\ 0 & 0 & 0 \\ 0 & 0 & 0 \end{bmatrix}, \tag{2.95}$$

$$\mathbf{B} = \begin{bmatrix} 0 & 0 & 0 & 0 & \frac{1}{\tau_G} & 0 & 0 & 0 \\ 0 & 0 & 0 & \frac{K_A}{\tau_A} & 0 & 0 & 0 & 0 \end{bmatrix}^{\mathrm{T}}, \tag{2.96}$$

and

$$\mathbf{\Psi}(\mathbf{X}(t), \mathbf{Z}(t)) =$$

$$\begin{bmatrix} V_\infty \cos\delta(t) - E_q'(t) - \left(X_e + X_d'\right) I_d(t) \\ \frac{X_d' - X_q}{(X_e+X_q)(X_e+X_d')} \frac{V_\infty^2}{2} \sin 2\delta(t) + \frac{V_\infty}{X_e+X_d'} E_q'(t) \sin\delta(t) - T_e(t) \\ \frac{X_d'^2 V_\infty^2}{(X_e+X_d')^2} \cos^2\delta(t) + \frac{X_q^2 V_\infty^2}{(X_e+X_q)^2} \sin^2\delta(t) + \frac{2X_d' X_e V_\infty}{(X_e+X_d')^2} E_q'(t) \cos\delta(t) + \frac{X_e^2}{(X_e+X_d')^2} E_q'(t)^2 - V_t(t)^2 \end{bmatrix}, \tag{2.97}$$

in which the expressions for $I_d(t)$ and $I_q(t)$ in (2.88) have been substituted into the expressions for $T_e(t)$ and $V_t(t)$ in (2.97).

Equations (2.90)-(2.97) form a model which is called the *Nonlinear Analytical Model* **(NAM)** of the nonlinear power system (CSM3) for the development of the nonlinear optimal and adaptive power system stabilisers to be discussed in Section 4.2. It is important to note that although the intentional nonlinearities of the CSM3 have been eliminated in (2.90)-(2.97), the inherent nonlinearities of the system are still retained by the term $\mathbf{\Psi}(\mathbf{X}(t), \mathbf{Z}(t))$ in (2.97).

Remark 2.4.1 *The NAM is* identical *with the CSM3 provided that the external disturbances that are applied to the system are mild enough that the system state variables vary within the range of linear operation of the limiting nonlinearities.*

2.4.2 Linearised Analytical Model of the Nonlinear Power System.

Consider the case where the nonlinear system (2.90)-(2.97) is operating with small deviations about an arbitrary steady-state operating point $(\mathbf{X_0}, \mathbf{Z_0}, \mathbf{U_{r0}})$, i.e.,

$$\mathbf{X}(t) = \mathbf{X_0} + \Delta\mathbf{X}(t), \tag{2.98}$$

$$\mathbf{Z}(t) = \mathbf{Z_0} + \Delta\mathbf{Z}(t), \tag{2.99}$$

$$\mathbf{U_r}(t) = \mathbf{U_{r0}} + \Delta\mathbf{U_r}(t). \tag{2.100}$$

It is assumed that

Assumption 2.4.2 *The new state* $(\mathbf{X_0} + \Delta\mathbf{X}(t), \mathbf{Z_0} + \Delta\mathbf{Z}(t), \mathbf{U_{r0}} + \Delta\mathbf{U_r}(t))$ *of the system (2.90)-(2.97) is a small perturbation from the steady-state* $(\mathbf{X_0}, \mathbf{Z_0}, \mathbf{U_{r0}})$.

The dynamic behaviour of the nonlinear system (2.90)-(2.97) can then be examined by linearising the system equations around the steady-state operating point $(\mathbf{X_0}, \mathbf{Z_0}, \mathbf{U_{r0}})$. The linearisation technique is briefly discussed as follows:

By the substitution of (2.98)-(2.100) into (2.90) and the use of a *Taylor's series approximation* [139] that neglects the terms of second-order and above, a linearised model of the nonlinear system (2.90)-(2.97) is derived

$$\begin{bmatrix} \Delta\dot{\mathbf{X}}(t) \\ \mathbf{0} \end{bmatrix} = \begin{bmatrix} \mathbf{\Phi_{X_0}} & \mathbf{\Phi_{Z_0}} \\ \mathbf{\Psi_{X_0}} & \mathbf{\Psi_{Z_0}} \end{bmatrix} \begin{bmatrix} \Delta\mathbf{X}(t) \\ \Delta\mathbf{Z}(t) \end{bmatrix} + \begin{bmatrix} \mathbf{B_0} \\ \mathbf{0} \end{bmatrix} \Delta\mathbf{U_r}(t) \tag{2.101}$$

where, according to Taylor's expansion theorem,

$$\mathbf{\Phi_{X_0}} \triangleq \left.\frac{\partial\mathbf{\Phi}(\mathbf{X}(t), \mathbf{Z}(t), \mathbf{U_r}(t))}{\partial\mathbf{X}(t)}\right|_{(\mathbf{X_0}, \mathbf{Z_0}, \mathbf{U_{r0}})},$$

$$\mathbf{\Phi_{Z_0}} \triangleq \left.\frac{\partial\mathbf{\Phi}(\mathbf{X}(t), \mathbf{Z}(t), \mathbf{U_r}(t))}{\partial\mathbf{Z}(t)}\right|_{(\mathbf{X_0}, \mathbf{Z_0}, \mathbf{U_{r0}})},$$

$$\mathbf{B_0} \triangleq \left.\frac{\partial\mathbf{\Phi}(\mathbf{X}(t), \mathbf{Z}(t), \mathbf{U_r}(t))}{\partial\mathbf{U_r}(t)}\right|_{(\mathbf{X_0}, \mathbf{Z_0}, \mathbf{U_{r0}})}$$

are the Jacobian matrices of $\mathbf{\Phi}(\mathbf{X}(t), \mathbf{Z}(t), \mathbf{U_r}(t))$. Since $\mathbf{\Phi_X}$, $\mathbf{\Phi_Z}$, and $\mathbf{B}$ in (2.93) are all constant matrices independent of the system operating point $(\mathbf{X_0}, \mathbf{Z_0}, \mathbf{U_{r0}})$, one obtains

$$\mathbf{\Phi}_{\mathbf{X_0}} = \mathbf{\Phi_X}, \quad \text{(eqn. (2.94))}; \tag{2.102}$$

$$\mathbf{\Phi}_{\mathbf{Z_0}} = \mathbf{\Phi_Z}, \quad \text{(eqn. (2.95))}; \tag{2.103}$$

$$\mathbf{B_0} = \mathbf{B}, \quad \text{(eqn. (2.96))}. \tag{2.104}$$

The nonlinear function $\mathbf{\Psi}(\mathbf{X}(t), \mathbf{Z}(t))$ in (2.90) does not depend explicitly on $\mathbf{U_{r0}}$, and is therefore linearised around $(\mathbf{X_0}, \mathbf{Z_0})$, resulting in

$$\mathbf{\Psi}(\mathbf{X_0} + \Delta\mathbf{X}(t), \mathbf{Z_0} + \Delta\mathbf{Z}(t)) \approx \mathbf{\Psi}(\mathbf{X_0}, \mathbf{Z_0}) + \mathbf{\Psi}_{\mathbf{X_0}}\Delta\mathbf{X}(t) + \mathbf{\Psi}_{\mathbf{Z_0}}\Delta\mathbf{Z}(t)$$

where

$$\mathbf{\Psi}_{\mathbf{X_0}} \triangleq \left.\frac{\partial\mathbf{\Psi}(\mathbf{X}(t), \mathbf{Z}(t))}{\partial\mathbf{X}(t)}\right|_{(\mathbf{X_0}, \mathbf{Z_0})},$$

$$\mathbf{\Psi}_{\mathbf{Z_0}} \triangleq \left.\frac{\partial\mathbf{\Psi}(\mathbf{X}(t), \mathbf{Z}(t))}{\partial\mathbf{Z}(t)}\right|_{(\mathbf{X_0}, \mathbf{Z_0})}$$

are the Jacobian matrices of $\mathbf{\Psi}(\mathbf{X}(t), \mathbf{Z}(t))$ and

$$\mathbf{\Psi}(\mathbf{X_0}, \mathbf{Z_0}) = 0$$

due to (2.90). The matrices $\mathbf{\Psi}_{\mathbf{X_0}}$ and $\mathbf{\Psi}_{\mathbf{Z_0}}$, according to the above definitions, are functions of the operating point $(\mathbf{X_0}, \mathbf{Z_0})$, given by

$$\mathbf{\Psi}_{\mathbf{X_0}} = \begin{bmatrix} -V_\infty \sin\delta_0 & 0 & -1 & 0 & 0 & 0 & 0 & 0 \\ \bar{K}_1 & 0 & \bar{K}_2 & 0 & 0 & 0 & 0 & 0 \\ \bar{K}_5 & 0 & \bar{K}_6 & 0 & 0 & 0 & 0 & 0 \end{bmatrix} \tag{2.105}$$

and

$$\mathbf{\Psi}_{\mathbf{Z_0}} = \begin{bmatrix} -\left(X_e + X_d'\right) & 0 & 0 \\ 0 & -1 & 0 \\ 0 & 0 & -2V_{t0} \end{bmatrix}, \tag{2.106}$$

where [7]

$$\bar{K}_1 = \frac{X_d' - X_q}{(X_e + X_q)\left(X_e + X_d'\right)} V_\infty^2 \cos 2\delta_0 + \frac{1}{X_e + X_d'} V_\infty E_{q0}' \cos\delta_0, \tag{2.107}$$

[7] It should be pointed out that $\bar{K}_i$ $(i = 1, 2, 5, 6)$ defined in this thesis are related to K_i $(i = 1, 2, 5, 6)$ commonly named in the literature (e.g. in [19]) through the relationships: $\bar{K}_i = K_i$ for $(i = 1, 2)$ and $\bar{K}_i = 2V_{t0}K_i$ for $(i = 5, 6)$.

$$\bar{K}_2 = \frac{1}{Xe + X_d^{'}} V_\infty \sin\delta_0, \tag{2.108}$$

$$\bar{K}_5 = \frac{X_e^2\left(X_q^2 - X_d^2\right) + 2X_e\left(X_q^2 X_d^{'} - X_d^{'2} X_q\right)}{\left(X_e + X_q\right)^2\left(X_e + X_d^{'}\right)^2} V_\infty^2 \sin 2\delta_0$$
$$- \frac{2X_e X_d^{'}}{\left(X_e + X_d^{'}\right)^2} V_\infty E_{q0}^{'} \sin\delta_0, \tag{2.109}$$

$$\bar{K}_6 = \frac{2X_e X_d^{'}}{\left(X_e + X_d^{'}\right)^2} V_\infty \cos\delta_0 + \frac{2X_e^2}{\left(X_e + X_d^{'}\right)^2} E_{q0}^{'}. \tag{2.110}$$

It may be seen that the matrix $\mathbf{\Psi_{Z_0}}$ in (2.106) is non-singular. From (2.101) one has

$$\Delta\mathbf{Z}(t) = -\mathbf{\Psi_{Z_0}}^{-1}\mathbf{\Psi_{X_0}}\Delta\mathbf{X}(t). \tag{2.111}$$

A standard linear state equation is finally formed from (2.101) and (2.111) by elementary matrix reduction, resulting in

$$\Delta\dot{\mathbf{X}}(t) = \mathbf{A_0}\Delta\mathbf{X}(t) + \mathbf{B_0}\Delta\mathbf{U_r} \tag{2.112}$$

where

$$\mathbf{A_0} \triangleq \mathbf{\Phi_{X_0}} - \mathbf{\Phi_{Z_0}}\mathbf{\Psi_{Z_0}}^{-1}\mathbf{\Psi_{X_0}} \tag{2.113}$$

and $\mathbf{B_0}$ is given by (2.104).

The model formed from equations (2.112)-(2.113) is called the *Linearised Analytical Model* **(LAM)** of the nonlinear power system (CSM3) for the development of the linear adaptive power system stabiliser to be discussed in Section 3.2. The inherent nonlinearities that are retained in the NAM are linearised after Assumption 2.4.2, resulting in a completely linearised version of the nonlinear power system model. According to Poincaré's theorem [140], the linearised model (2.112)-(2.113) is valid for small perturbations about the steady-state condition specified by $(\mathbf{X_0}, \mathbf{Z_0}, \mathbf{U_{r0}})$. The elements of the matrix $\mathbf{A_0}$ depend upon the values of $(\mathbf{X_0}, \mathbf{Z_0}, \mathbf{U_{r0}})$ and the system parameters, e.g., R_e and X_e. For a specific dynamic study at a specified operating point, $\mathbf{A_0}$ is a constant matrix. Generally speaking, $\mathbf{A_0}$ may be considered to be a time-varying state-functional matrix having *piece-wise constant* [141] elements that are functions of the system operating point. Therefore, the system (2.112)-(2.113) is *linear, piece-wise, time-varying* in nature. It should be pointed out that the assumption, that the elements of $\mathbf{A_0}$ are piece-wise constant, provides only the information on the dynamic

behaviour of the system *around* each operating point as perturbations on the system variables tend to zero. It does not describe the transient behaviour of the system *between* operating points.

When small signal excitation control of power systems is under consideration, a simplified version of the LAM can be employed assuming that the system is stable. It is based on the following assumption.

Assumption 2.4.3 *The effective time constants associated with the AVR-excitation system loop and the governor-steam turbine loop are so widely different that the interactions between these two control loops can be considered as disturbances on each other [47].*

Under this assumption, for excitation control studies, the deviation of the mechanical torque input to the synchronous generator can be viewed as a disturbance that is added to the system. The governor and the steam turbine are excluded from the system model, and the power system is simply treated as being controlled by the excitation voltage input, with injected mechanical torque disturbance.

By the elimination of the dynamic models of the governor and the steam turbine from the equations of the LAM, the system state equation (2.112) is rewritten as

$$\Delta\dot{\mathbf{X}}(t) = \mathbf{A_0}\Delta\mathbf{X}(t) + \mathbf{b}_{u0}\Delta u_r(t) + \mathbf{b}_{w0}\Delta w(t) \tag{2.114}$$

where

$$\Delta\mathbf{X}(t) = \left[\begin{array}{cccc} \Delta\delta(t) & \Delta\omega_s(t) & \Delta E'_q(t) & \Delta E_{FD}(t) \end{array}\right]^T \tag{2.115}$$

and $\Delta u_r(t)$ and $\Delta w(t)$ are the system voltage reference input, $\Delta V_{ref}(t)$, and mechanical torque disturbance, $\Delta T_m(t)$, respectively. The matrices in (2.114) are given (see Section D.1 of Appendix D) by

$$\mathbf{A_0} = \left[\begin{array}{cccc} 0 & \omega_0 & 0 & 0 \\ -\frac{K_1}{2H} & -\frac{D}{2H} & -\frac{K_2}{2H} & 0 \\ -\frac{K_4}{\tau'_{d0}} & 0 & -\frac{1}{\tau'_{d0}K_3} & \frac{1}{\tau'_{d0}} \\ -\frac{K_A K_5}{2\tau_A V_{t0}} & 0 & -\frac{K_A K_6}{2\tau_A V_{t0}} & -\frac{1}{\tau_A} \end{array}\right], \tag{2.116}$$

$$\mathbf{b}_{u0} = \begin{bmatrix} 0 & 0 & 0 & \frac{K_A}{\tau_A} \end{bmatrix}^T, \tag{2.117}$$

$$\mathbf{b}_{w0} = \begin{bmatrix} 0 & \frac{1}{2H} & 0 & 0 \end{bmatrix}^T, \tag{2.118}$$

where [8]

$$\bar{K}_3 = \frac{X_e + X'_d}{X_e + X_d}, \tag{2.119}$$

$$\bar{K}_4 = \frac{X_d - X'_d}{X_e + X'_d} V_\infty \sin \delta_0. \tag{2.120}$$

This *Simplified Linearised Analytical Model* **(SLAM)**, without the governor and the steam turbine, will be used in Section 2.5, when the selection of stabilising signals for the design of power system stabilisers is discussed. It is also used in Section 3.2 for the modelling of the power system under linear adaptive excitation control.

2.4.3 Summary of the Models of the Power System.

The various models of the synchronous generator/tie-line and the complete power system proposed in this chapter are summarised in Table 2.1. Of these models, SLAM, NAM, CSM3, and CSM1 are used in the studies of this thesis for the following purposes:

- SLAM — for the discussion of selection of stabilising signals, and for the design of the *linear* adaptive power system stabiliser;
- NAM — for the design of the *nonlinear* optimal and adaptive power system stabilisers;
- CSM3 ($D = 4.0$ pu) — for simulation studies for evaluating the performance of the designed power system stabilisers;
- CSM1 ($D = 0.1$ pu) — for studies of the robustness of these controllers.

[8] As noted earlier, $\bar{K}_i$ $(i = 3, 4)$ defined in this thesis are related to K_i $(i = 3, 4)$ commonly used in the literature through the relationship: $\bar{K}_i = K_i$ $(i = 3, 4)$.

Name	Explanation	Section	Equations
SGM1	simplified generator model 1	2.2	(2.31)-(2.33), (2.36)-(2.40), (A.3)-(A.5), (A.8), (A.11)-(A.12)
SGM2	simplified generator model 2	2.2	(2.42)-(2.50), (A.3)-(A.4), (A.8), (A.11)-(A.12)
SGM3	simplified generator model 3	2.2	(2.42), (2.48), (2.53)-(2.57), (A.3)-(A.4), (A.8), (A.11)-(A.12)
CSM1	complete system model 1	2.3.1	(2.58)-(2.74)
CSM2	complete system model 2	2.3.1	(2.58)-(2.61), (2.66), (2.75)-(2.84)
CSM3	complete system model 3	2.3.1	(2.58)-(2.61), (2.76), (2.85)-(2.89)
NAM	nonlinear analytical model	2.4.1	(2.90)-(2.97)
LAM	linearised analytical model	2.4.2	(2.102)-(2.104), (2.105)-(2.110), (2.112)-(2.113)
SLAM	simplified linearised analytical model	2.4.2	(2.114)-(2.120), (2.107)-(2.110)

Table 2.1: The models of the synchronous generator and the SMIB power system.

2.5 Identification of Suitable Stabilising Signals for the Design of Power System Stabilisers.

In this section:

- the concepts associated with participation factors are highlighted;
- the selection of suitable stabilising signals for improving the damping behaviour of rotor oscillations is discussed;
- a conclusion regarding the choice of the electrical torque as the stabilising signal for the design of power system stabilisers is drawn from the discussion.

It is clear from the literature that the most commonly-used techniques in designing power system stabilisers, from the original analogue lead-lag compensators to recent digital self-tuning controllers, are SISO linear control strategies. The power systems are reduced to SISO linear systems for which the control strategies are derived. A simple state-space realisation of such a SISO linearised system representation has been given by the SLAM in Subsection 2.4.2.

The feedback signals for power system stabilisers are usually chosen from a variety of available (measurable) system output signals. Utilising alternative input signals, frequency response analysis has been employed for the design of power system stabilisers [29]. In this section the selection of the suitable feedback signals for damping system oscillations is based on the analysis of *participation factors* of the system matrix $\mathbf{A_0}$. Such an approach is based on [142].

The concept of participation factors was proposed by Pérez-Arriaga in 1981 [107] as a means of providing a quantitative description of the participation of each state variable in system oscillatory modes. A direct application of participation factors to the so-called *Selective Modal Analysis* (**SMA**), a physically motivated framework for understanding and simplifying complex models of linear time-invariant systems, has been extensively discussed in [143]-[149]. Successful applications of this technique

for choosing significant states for developing a reduced-order model of a large-scale power system have been investigated in [146,147]. The concept has been applied to the design of power system stabilisers with the use of eigenvalue sensitivities and the SMA techniques [150], and to the analyses of power system oscillatory instability [151] and small-signal stability [152]. As an extension of the applications, a novel approach based on participation factors for the selection of a suitable set of feedback signals for a *Single-Input Multi-Output* **(SIMO)** excitation controller was introduced in [142]. In this section, the same approach as that in [142] is used to investigate the participation of each state in the system oscillatory modes. Here, emphasis will be placed on the damping effects introduced by the stabilisers using signals such as the speed deviation and the electrical torque.

The basic concepts associated with participation factors are highlighted as follows. Consider a *linear time-invariant* dynamic system of the form

$$\dot{X}(t) = AX(t) \tag{2.121}$$

with $A = \{a_{ij}\}$ being an $n \times n$ system matrix that is assumed, for the sake of simplicity, to have distinct eigenvalues λ_i $(i = 1, 2, ..., n)$ [107]. The dynamic behaviour of the system (2.121) can be described by the association between groups of state variables and groups of natural modes of the system matrix A. This association is precisely defined in [107] by means of the participation matrix $\tilde{P} = \{\tilde{p}_{ij}\}$ with elements

$$\tilde{p}_{ij} \triangleq \tilde{l}_{ij}\tilde{r}_{ij} \left(= \frac{\partial \lambda_i}{\partial a_{jj}}\right) \tag{2.122}$$

where $\tilde{r}_{ij}$ $(\tilde{l}_{ij})$ is the j-th element of the i-th right (left) eigenvector $\tilde{r}_i$ $(\tilde{l}_i)$ associated with the i-th eigenvalue (λ_i) of A. The elements $\tilde{p}_{ij}$ of $\tilde{P}$ are termed participation factors of the system and are dimensionless [146,142]. The time response of the system (2.121) with the initial condition $X(0)$ can be expressed as

$$X(t) = \sum_{i=1}^{n} \tilde{l}_i{}^T X(0) e^{\lambda_i t} \tilde{r}_i \tag{2.123}$$

where the right eigenvector, $\tilde{r}_i$, describes the activity of each state variable in the i-th mode while the left eigenvector, $\tilde{l}_i$, gives the state constitution of the mode. Assume $X(0) = e_j$, where e_j represents the j-th unit vector (i.e., the j-th element of e_j is 1,

all others in e_j are 0). The time response of the j-th state variable in (2.123) then becomes

$$x_j(t) = \sum_{i=1}^{n} \tilde{l}_{ij}\tilde{r}_{ij}e^{\lambda_i t} = \sum_{i=1}^{n} \tilde{p}_{ij}e^{\lambda_i t}. \tag{2.124}$$

This solution shows that $\tilde{r}_{ij}$ describes the activity of x_j in the i-th mode and $\tilde{l}_{ij}$ weights the contribution of this activity to the mode. Thus $\tilde{p}_{ij}$, according to its definition in (2.124) (or (2.122)), gives the *net participation* of the j-th state variable in the i-th mode.

The property of participation factors thus provides a means for determining the participation of the state variables in the oscillatory mode of concern. To apply this methodology to the SLAM given in Subsection 2.4.2, a set of measurable signals

$$\Delta\mathbf{X}(t) = \begin{bmatrix} \Delta\omega_s(t) & \Delta T_e(t) & \Delta V_t(t) & \Delta E_{FD}(t) \end{bmatrix}^T \tag{2.125}$$

is used which replaces the set of state variables in (2.115) [92,142]. With this new set of state variables, the system matrix $\mathbf{A_0}$ in the SLAM is rewritten (see Section D.2 of Appendix D) as

$$\mathbf{A_0} = \begin{bmatrix} -\frac{D}{2H} & -\frac{1}{2H} & 0 & 0 \\ \bar{K}_1\omega_0 & \frac{K_2}{\tau'_{d0}K_3}\frac{K_5-K_3K_4K_6}{K_1K_6-K_2K_5} & -\frac{2V_{t0}K_2}{\tau'_{d0}K_3}\frac{K_1-K_2K_3K_4}{K_1K_6-K_2K_5} & \frac{K_2}{\tau'_{d0}} \\ \frac{K_5}{2V_{t0}}\omega_0 & \frac{K_6}{2V_{t0}\tau'_{d0}K_3}\frac{K_5-K_3K_4K_6}{K_1K_6-K_2K_5} & -\frac{K_6}{\tau'_{d0}K_3}\frac{K_1-K_2K_3K_4}{K_1K_6-K_2K_5} & \frac{K_6}{2V_{t0}\tau'_{d0}} \\ 0 & 0 & -\frac{K_A}{\tau_A} & -\frac{1}{\tau_A} \end{bmatrix}. \tag{2.126}$$

The decision on choosing suitable stabilising signals can then be made by analysing the participation factors of the system matrix $\mathbf{A_0}$ in the above equation.

Given a system operating point $(\mathbf{X_0}, \mathbf{Z_0}, \mathbf{U_{r0}})$, the elements of $\mathbf{A_0}$ are constant. The eigenvalues of $\mathbf{A_0}$ in (2.126) describe the dynamic behaviour of the system free response at the specified operating point, whereas the participation factors of $\mathbf{A_0}$ measure the contributions of the system variables (2.125) to each mode that forms the system free response. Since the role of power system stabilisers is to improve system damping performance, and hence to extend the system dynamic stability boundary, the specified operating point $(\mathbf{X_0}, \mathbf{Z_0}, \mathbf{U_{r0}})$ is chosen to be close to the edge of the system steady-state stability region. This facilitates the observation of the participation of the system variables in the lightly-damped oscillatory modes.

Two operating points are selected as study conditions:

- a full-load lagging operating condition with $P_t = 0.8$ pu, $Q_t = 0.3$ pu, and $V_t = 1.0$ pu;
- a full-load leading operating condition with $P_t = 0.75$ pu, $Q_t = -0.1$ pu, and $V_t = 1.0$ pu.

At each operating point the system response to a small disturbance is highly oscillatory and barely stable. The system parameters $\bar{K}_i$ $(i = 1, 2, ..., 6)$ associated with the equations of the SLAM are calculated in each study condition and their values are listed in Table 2.2. The system eigenvalues and the corresponding absolute values of the participation factors (indicated in the columns associated with each state variable) at these two operating conditions are shown in Table 2.3.

	$\bar{K}_1$	$\bar{K}_2$	$\bar{K}_3$	$\bar{K}_4$	$\bar{K}_5$	$\bar{K}_6$
lagging	1.0752	1.1807	0.3090	1.8798	-0.0595	0.8098
leading	1.2518	1.4762	0.3090	2.3500	-0.0896	0.5605

Table 2.2: System parameters at the lagging ($P_t = 0.8$ pu, $Q_t = 0.3$ pu, $V_t = 1.0$ pu) and leading ($P_t = 0.75$ pu, $Q_t = -0.1$ pu, $V_t = 1.0$ pu) operating conditions.

As expected, for the lightly-damped rotor oscillatory mode ($-0.1602 \pm j7.0083$ and/or $-0.0750 \pm j7.4619$), signals $\Delta\omega_s(t)$ and $\Delta T_e(t)$ have much greater participation factors than the other states. The voltage signals, $\Delta V_t(t)$ and $\Delta E_{FD}(t)$, show very small participation in this mode. Hence, for successful damping of rotor oscillations, one of the two signals, $\Delta\omega_s(t)$ and $\Delta T_e(t)$, should be chosen as the stabilising signal.

Frequency analyses shown in [29] indicate that power system stabilisers utilising the electrical torque (or power) signal as the input can be designed with a characteristic that is less sensitive to high frequency noise and torsional interaction. This property is

operating conditions	participation factors → eigenvalues ↓		$\tilde{P}$			
			$\Delta\omega_s(t)$	$\Delta T_e(t)$	$\Delta V_t(t)$	$\Delta E'_q(t)$
lagging	$\lambda_{1,2}$	$-0.1602 \pm j7.0083$	0.4800	0.4573	0.0514	0.0290
	$\lambda_{3,4}$	$-5.4232 \pm j7.1957$	0.0247	0.0476	0.5542	0.5784
leading	$\lambda_{1,2}$	$-0.0750 \pm j7.4619$	0.4782	0.4578	0.0789	0.0467
	$\lambda_{3,4}$	$-5.5085 \pm j5.6886$	0.0481	0.0736	0.5945	0.6455

Table 2.3: System eigenvalues and participation factors at the lagging ($P_t = 0.8$ pu, $Q_t = 0.3$ pu, $V_t = 1.0$ pu) and leading ($P_t = 0.75$ pu, $Q_t = -0.1$ pu, $V_t = 1.0$ pu) operating conditions.

superior to that associated with the use of the speed signal. The damping performance associated with the use of the electrical torque (or power) input can be equivalent to that with speed input but more robust [29]. In practice, the electrical torque (or power) signal is easily measured or synthesised, while the location, on the shaft of a turbo-generator, of a speed transducer requires special attention [30]. For these reasons, the electrical torque (or power) is chosen as the stabilising signal for the design of the power system stabilisers to be discussed in the following chapters.

2.6 Controllability and Observability.

In this section:

- concepts of the controllability and observability of the models developed in Sub-sections 2.3.1 and 2.4.2 are briefly introduced;
- aspects of the system realisation [9] and input-output properties are discussed.

[9] See, e.g., [153] p.53.

Controllability and observability of a system are often the key concepts leading to successful system identification and control. These concepts are also important to the explanation of the system realisation and to the determination of the external properties of the system models. The conclusions drawn from the discussion of this section will be used for the modelling analysis of the linear adaptive power system stabiliser to be discussed in Section 3.2.

For the discussion of the system observability, the system output equation is required. Such an equation depends on the selection of output variables in the models presented in the previous sections. In general, the nonlinear output equation of the power system can be written as

$$\bar{\mathbf{Y}}(t) = \boldsymbol{\Upsilon}(\mathbf{X}(t), \mathbf{Z}(t)) \tag{2.127}$$

where $\bar{\mathbf{Y}}(t)$ is the system output vector, and $\boldsymbol{\Upsilon}(\mathbf{X}(t), \mathbf{Z}(t))$ is a nonlinear function. For example, for the CSM3 given in Subsection 2.3.1, with the chosen system output variables

$$\bar{\mathbf{Y}}(t) = \begin{bmatrix} T_e(t) & V_t(t) \end{bmatrix}^T,$$

the nonlinear function $\boldsymbol{\Upsilon}(\mathbf{X}(t), \mathbf{Z}(t))$ can be derived, on the basis of (2.88), as

$$\boldsymbol{\Upsilon}(\mathbf{X}(t), \mathbf{Z}(t)) = \begin{bmatrix} I_q(t)E'_q(t) + \left(X'_d - X_q\right) I_d(t)I_q(t) \\ \sqrt{E'_q(t)^2 + 2X'_d E'_q(t)I_d(t) + X'^2_d I_d(t)^2 + X_q^2 I_q(t)^2} \end{bmatrix}.$$

Equation (2.127) combined with the general form of the system state equation (2.58) gives a *complete state-space description* of the nonlinear SMIB power system. It is seen that the system described by (2.58) and (2.127) is functionally dependent (via functions $\boldsymbol{\Phi}(\mathbf{X}(t), \mathbf{Z}(t), \mathbf{U_r}(t))$, $\boldsymbol{\Psi}(\mathbf{X}(t), \mathbf{Z}(t))$, $\boldsymbol{\Xi}(\mathbf{X}(t), \mathbf{Z}(t), \mathbf{U_r}(t))$, and $\boldsymbol{\Upsilon}(\mathbf{X}(t), \mathbf{Z}(t))$) on the values of the state vector $\mathbf{X}(t)$, the auxiliary variable vector $\mathbf{Z}(t)$, and the input vector $\mathbf{U_r}(t)$. Moreover, the system parameters, such as R_e and X_e, may change according to changes in system configurations. This indicates that the system parameters (or structures) are also implicitly dependent on time t. Therefore, a power system formulated by (2.58) and (2.127) is classified as a *nonlinear time-varying system.*

Standard results concerning the controllability and observability of linear time-invariant systems have been well documented (see, e.g., [153]). However, to handle

nonlinear time-varying systems, new tools of differential geometry and topology are needed. Basic concepts of these techniques have been given in [154]. A detailed description of the principles can be found in [155].

One may wish to investigate the controllability and observability of the system (2.58) and (2.127) using the above techniques. Difficulties arise as the system is high-order with complicated nonlinearities. For *sufficiently small* alterations of the inputs $\mathbf{U_r}$, the response of a nonlinear system is very close to that of its linearised model [139]. The concepts of controllability and observability of the nonlinear system may then be presented for its equivalent linearised version in terms of the same concepts. Under these conditions, the problems of controllability and observability of the *time-varying nonlinear* system (2.58) and (2.127) may be considered as the problems of controllability and observability of the corresponding *time-varying linear* system.

Consider the linearised time-varying system state equation (2.112) given by the LAM in Subsection 2.4.2. To derive an equivalent expression for the linearised time-varying system output equation, the same procedure as shown in Subsection 2.4.2 is followed:

i) Linearise the nonlinear function $\boldsymbol{\Upsilon}(\mathbf{X}(t), \mathbf{Z}(t))$ in (2.127) about the system operating point $(\mathbf{X_0}, \mathbf{Z_0}, \mathbf{U_{r0}})$. This yields

$$\boldsymbol{\Upsilon}(\mathbf{X_0} + \Delta\mathbf{X}(t), \mathbf{Z_0} + \Delta\mathbf{Z}(t)) \approx \boldsymbol{\Upsilon}(\mathbf{X_0}, \mathbf{Z_0}) + \boldsymbol{\Upsilon}_{\mathbf{X_0}}\Delta\mathbf{X}(t) + \boldsymbol{\Upsilon}_{\mathbf{Z_0}}\Delta\mathbf{Z}(t)$$

where

$$\boldsymbol{\Upsilon}_{\mathbf{X_0}} \triangleq \left.\frac{\partial\boldsymbol{\Upsilon}(\mathbf{X}(t), \mathbf{Z}(t))}{\partial\mathbf{X}(t)}\right|_{(\mathbf{X_0}, \mathbf{Z_0})},$$
$$\boldsymbol{\Upsilon}_{\mathbf{Z_0}} \triangleq \left.\frac{\partial\boldsymbol{\Upsilon}(\mathbf{X}(t), \mathbf{Z}(t))}{\partial\mathbf{Z}(t)}\right|_{(\mathbf{X_0}, \mathbf{Z_0})}$$

are the Jacobian matrices of $\boldsymbol{\Upsilon}(\mathbf{X}(t), \mathbf{Z}(t))$. The linearised system output equation is then expressed as

$$\Delta\bar{\mathbf{Y}}(t) = \boldsymbol{\Upsilon}_{\mathbf{X_0}}\Delta\mathbf{X}(t) + \boldsymbol{\Upsilon}_{\mathbf{Z_0}}\Delta\mathbf{Z}(t) \tag{2.128}$$

where

$$\Delta\bar{\mathbf{Y}}(t) = \bar{\mathbf{Y}}(t) - \bar{\mathbf{Y}}_{\mathbf{0}}$$

and, due to (2.127),

$$\bar{\mathbf{Y}}_0 - \boldsymbol{\Upsilon}(\mathbf{X}_0, \mathbf{Z}_0) = 0.$$

ii) Substitute for $\Delta\mathbf{Z}(t)$ from (2.111) into (2.128). A standard linearised system output equation is obtained

$$\Delta\bar{\mathbf{Y}}(t) = \mathbf{C}_0\Delta\mathbf{X}(t) \tag{2.129}$$

where

$$\mathbf{C}_0 \triangleq \boldsymbol{\Upsilon}_{\mathbf{X}_0} - \boldsymbol{\Upsilon}_{\mathbf{Z}_0}\boldsymbol{\Psi}_{\mathbf{Z}_0}{}^{-1}\boldsymbol{\Psi}_{\mathbf{X}_0}. \tag{2.130}$$

In a similar manner as for $\mathbf{A}_0$ in (2.113), $\mathbf{C}_0$ in (2.130) may be explained as a time-varying state-functional matrix that depends on the system operating point $(\mathbf{X}_0, \mathbf{Z}_0, \mathbf{U}_{r0})$ as well as the system parameters.

Hence, a complete linearised version of the nonlinear time-varying system (2.58) and (2.127) is formulated by (2.112) (with (2.113)) and (2.129) (with (2.130)). It is linear, time-varying in nature.

The general notions of controllability and observability of linear time-varying systems over the time interval $[t_0, t_1]$ are given in [156] (by Definitions 23.6 and 23.4 respectively). If it is assumed that each matrix in the system (2.112) and (2.129) has *piece-wise continuous* [10] elements over $[0, \infty)$, then the system (2.112) and (2.129) is controllable on $[t_0, t_1]$ if and only if the *controllability Gramian*

$$W_C(t_0, t_1) = \int_{t_0}^{t_1} \varphi_t(t_1, \tau)\,\mathbf{B}_0(\tau)\mathbf{B}_0{}^*(\tau)\varphi_t{}^*(t_1, \tau)\,d\tau \tag{2.131}$$

is positive definite (see Theorem 23.5 in [156]); and the system (2.112) and (2.129) is observable on $[t_0, t_1]$ if and only if the *observability Gramian*

$$W_O(t_0, t_1) = \int_{t_0}^{t_1} \varphi_t{}^*(\tau, t_0)\,\mathbf{C}_0{}^*(\tau)\mathbf{C}_0(\tau)\varphi_t(\tau, t_0)\,d\tau \tag{2.132}$$

satisfies the same condition (see Theorem 23.2 in [156]). The asterisk $*$ denotes the complex conjugate transpose, and $\varphi_t(t, t_0)$ is the *state transition matrix*. In theory, for a given state matrix $\mathbf{A}_0$, $\varphi_t(t, t_0)$ is known (according to Definition 11.2 in [156]).

[10] See Definition 10.5 in [156].

Therefore, given the matrices $\mathbf{A_0}$, $\mathbf{B_0}$, and $\mathbf{C_0}$, the calculation of the system Gramian matrices (2.131) and (2.132) is (at least theoretically) possible.

At a specific steady-state operating condition, the matrices $\mathbf{A_0}$ and $\mathbf{C_0}$ may be considered to be constant so that the system (2.112) and (2.129) becomes *linear time-invariant.* The basic controllability condition (2.131) and observability condition (2.132) that apply to the linear time-varying systems then reduce respectively to the familiar *linear time-invariant* condition that the system *controllability matrix*

$$\mathcal{C} = \begin{bmatrix} \mathbf{B_0} & \mathbf{A_0 B_0} & \dots & \mathbf{A_0}^{n-1}\mathbf{B_0} \end{bmatrix} \tag{2.133}$$

has full rank n (see [153] Subsection 9.2.1), and likewise the system *observability matrix*

$$\mathcal{O} = \begin{bmatrix} \mathbf{C_0} \\ \mathbf{C_0 A_0} \\ \vdots \\ \mathbf{C_0 A_0}^{n-1} \end{bmatrix} \tag{2.134}$$

has full rank n (see [153] Subsection 9.2.2), where n denotes the order of the system.

For the analysis of computer-controlled real-time systems, it may become necessary to use a discrete-time equivalent of the continuous-time system (2.112) and (2.129). By taking the z-transform, a zero-order-hold sampling of the linear system $\{\mathbf{A_0}, \mathbf{B_0}, \mathbf{C_0}\}$ given by (2.112) (with (2.113)) and (2.129) (with (2.130)) may be described by $\left\{\tilde{\mathbf{A}}_\mathbf{0}, \tilde{\mathbf{B}}_\mathbf{0}, \tilde{\mathbf{C}}_\mathbf{0}\right\}$ in the z-domain. It is well known that in *linear time-invariant* cases the controllability condition (assuming that $\tilde{\mathbf{A}}_\mathbf{0}$ is invertible) and the observability condition of the discrete-time system are of the *same* form as the conditions (2.133) and (2.134) respectively. However, since the z-transform is a nonlinear transformation and the resulting discrete-time system depends on the sampling period (e.g., see eqns. (3.4) and (3.5) of [141]), the discrete-time system $\left\{\tilde{\mathbf{A}}_\mathbf{0}, \tilde{\mathbf{B}}_\mathbf{0}, \tilde{\mathbf{C}}_\mathbf{0}\right\}$ may become *uncontrollable* or *unobservable* even if the corresponding continuous-time system $\{\mathbf{A_0}, \mathbf{B_0}, \mathbf{C_0}\}$ is controllable or observable [141].

As far as a *SISO linear time-invariant discrete-time* system $\left\{\tilde{\mathbf{A}}_\mathbf{0}, \tilde{\mathbf{b}}_\mathbf{0}, \tilde{\mathbf{c}}_\mathbf{0}\right\}$ is concerned, the following properties related to the controllability and observability of the system are important [153,157].

(1) The state-space system $\left\{\tilde{\mathbf{A}}_0, \tilde{\mathbf{b}}_0, \tilde{\mathbf{c}}_0\right\}$ is a *minimal realisation* [11] if and only if the system is controllable and observable.

(2) The system transfer function

$$\tilde{H}_0(z) \triangleq \tilde{\mathbf{c}}_0 \left[z\mathbf{I} - \tilde{\mathbf{A}}_0\right]^{-1} \tilde{\mathbf{b}}_0 \tag{2.135}$$

is *irreducible* (or *coprime*) if and only if the system $\left\{\tilde{\mathbf{A}}_0, \tilde{\mathbf{b}}_0, \tilde{\mathbf{c}}_0\right\}$ is a minimal realisation.

These properties establish some theoretical foundations for the modelling analysis of the SISO linear adaptive power system stabiliser to be discussed in Section 3.2.

2.7 Concluding Remarks.

In this chapter the modelling of the SMIB power system for studies in this thesis is discussed. This facilitates the analysis and design of the linear and nonlinear optimal/adaptive power system stabilisers, and the simulation studies for the evaluation of the controlled system.

In Section 2.2 three simplified synchronous generator/tie-line models (SGM1, SGM2, and SGM3) are developed from the basic equations of the synchronous generator/tie-line given in Appendix A. These three models are presented in order of decreasing complexity. Combination of these three models with *identical* models of the excitation system, the governor, and the steam turbine results in three complete system models (CSM1, CSM2, and CSM3) in Section 2.3. The modelling accuracy of the three complete system models is degraded in comparison with the system described by the basic model given by Appendix A. The acceptance of the degradation is justified on the basis that these complete system models are used for comparisons of system performance with *different* control strategies. It is based also on the need to reduce the computational burden. The significant decrease in modelling accuracy associated with the

[11] See, e.g., [157] p.19.

simplest power system model (CSM3 with $D = 0.1$ pu) is compensated for by increasing the rotor damping coefficient D to a higher value (4.0 pu). Satisfactory agreement in system performance of the CSM3 ($D = 4.0$ pu) and the CSM1 ($D = 0.1$ pu) is then achieved. Selections of the CSM1 ($D = 0.1$ pu) as the benchmark model for the SMIB power system under study and of the CSM3 ($D = 4.0$ pu) for controller analysis and design are finalised.

Nonlinear and linearised analytical models (NAM, LAM, and SLAM) of the power system are developed from the CSM3 in Section 2.4. The application of these analytical models is in the design of linear and nonlinear optimal/adaptive power system stabilisers to be discussed in the following chapters. The nonlinearities associated with the power system are classified as two categories: the inherent nonlinearities and the intentional nonlinearities. Elimination of the system intentional nonlinearities results in the NAM in which the inherent nonlinearities of the system are still retained. The NAM represents the CSM3 *accurately* within the range of linear operation of the limiting nonlinearities; it thus can be used to derive a nonlinear *nominal model* [12] (see Section 4.2) for the design of nonlinear optimal and adaptive power system stabilisers. Linearisation of the NAM about a steady-state operating point results in the LAM with its state matrix being linear, piece-wise, time-varying in nature. The LAM is a *valid* representation of the NAM in a neighbourhood of the steady-state operating point of concern. Further simplification of the LAM yields the SLAM which is used for the derivation of a linearised nominal model (see Section 3.2) for the design of linear adaptive power system stabilisers.

In Section 2.5 suitable stabilising signals for improving the system damping performance are chosen among the measurable state variables. From the analysis of participation factors of the system state matrix as well as the consideration of practical measurements, the electrical torque (or power) is selected as the feedback signal for the stabilisation of the power system via excitation control. This knowledge will be utilised for the design of power system stabilisers using different control strategies.

In Section 2.6 the concepts of controllability and observability associated with the

[12]The definition of a "nominal model" will be given in Section 4.2.

models developed in this chapter are discussed. For the purpose of providing a theoretical basis for the modelling analysis of the linear adaptive power system stabiliser in Section 3.2, consideration is finally given to a SISO linear time-invariant discrete-time model. The state-space and input-output properties established for this model will be used in Section 3.2.

The extensions in this chapter to the previous work described in the literature have been listed in Section 2.1.

Chapter 3

SISO Linear Adaptive Power System Stabilisers.

3.1 Introduction.

In this chapter the design of *SISO linear adaptive* power system stabilisers is discussed. This forms the basis for the comparisons of system damping performance of the linear adaptive and nonlinear optimal/adaptive control strategies to be conducted in Chapters 4, 5, and 6, respectively.

In the literature, the so-called conventional power system stabilisers are based on time-invariant linearised models of the nonlinear power system. Such models are obtained from linearisation of the nonlinear power system about a chosen operating condition and, subsequently, are valid only at the chosen operating condition. The design of conventional power system stabilisers utilises classical control theory which gives the required damping performance when the system is operating at the chosen condition. If the system operating point and/or the system configuration vary widely, the parameters of the linearised models change. However, with fixed parameters, the conventional power system stabilisers are unable to respond satisfactorily over the wide range of system operating conditions. If not designed properly, the system damping performance may deteriorate significantly.

Linear optimal control theory was introduced into the design of power system stabilisers (e.g., [92,99,104]). Because a linear optimal power system stabiliser is still based on a linearised time-invariant model of the nonlinear system, its damping performance also degrades when the system operating condition changes from that at which the optimal stabiliser is designed. There is, consequently, considerable interest in the application of adaptive control theory for the design of power system stabilisers.

A key feature that distinguishes a linear adaptive power system stabiliser from a conventional (or linear optimal) power system stabiliser is that, theoretically, the linear adaptive power system stabiliser can track the changes in the system operating condition by changing its parameters on-line. In doing so, a *time-varying linear* controller is able to control the *nonlinear* system over a wide range of operating conditions.

Potential applications of the linear adaptive control theory to the design of power system stabilisers have been explored in recent years. Considerable interest has been shown in introducing a variety of linear adaptive control strategies into the design of power system stabilisers, with the objectives of extending the operational margins of the system stability and improving the system dynamic performance. It has been shown, from simulation studies [49,53,54,56,58,64,65,66,74] and/or from laboratory experiments [50,51,70,59,63], that well-tuned linear adaptive power system stabilisers can provide substantial improvement in performance at various operating conditions.

In this chapter an evaluation of a linear adaptive power system stabiliser applied to the SMIB power system given in Subsection 2.3.1 is conducted. The evaluation involves the establishment of a linearised nominal mode for the design of the linear adaptive power system stabiliser, the selection of the parameter estimation algorithm suitable for the identification of the SMIB power system, the design of the linear adaptive control law, and the assessment of the system damping performance of the resulting stabiliser.

The organisation of this chapter is as follows. In Section 3.2 a linearised nominal model is derived from the SLAM given in Subsection 2.4.2. Linear stochastic optimal control of the linearised nominal model is discussed in Section 3.3. The linear stochastic adaptive generalised minimum variance control algorithm is developed in Section 3.4.

In Section 3.5 a linear adaptive weighted minimum variance power system stabiliser is proposed. The damping performance of the proposed stabiliser is assessed through simulation studies in Section 3.6.

The previous work described in the literature is extended in this chapter in the following aspects:

1. The linearised nominal model used for the development of the linear adaptive power system stabiliser is developed *directly* from the mathematical model of the SMIB power system described by the SLAM. The derivation procedure provides insight into the model.

2. The commonly-used linear optimal control strategies for the development of linear adaptive control laws are derived and discussed under a general form of the cost function.

3. A linear adaptive weighted minimum variance power system stabiliser is proposed for the SMIB power system described by the models given in Subsection 2.3.1. The performance of the proposed stabiliser is evaluated at various system operating conditions through a set of simulation studies and its effectiveness is demonstrated by comparison with the performance of a well-designed conventional power system stabiliser.

It should be pointed out that the theory for linear adaptive estimation/prediction/control of SISO systems has been well documented. For this reason, proofs of lemmas and theorems, as well as convergence analyses of algorithms used in this chapter are omitted.

3.2 SISO Linear Input-Output Power System Modelling.

In this section:

- a SISO linear discrete-time input-output model of the power system is derived from the SLAM given in Subsection 2.4.2;
- a *linearised* **nominal model** [1] in a regression form is then developed; this model is used for the design of the linear adaptive power system stabiliser;

The choice of a linearised nominal model for the design of a linear adaptive power system stabiliser is the first step towards the successful control of the system dynamics. In the area of adaptive control, an appropriately chosen model for the estimator can greatly simplify the parameter estimation procedure and facilitate the design of the prediction and control algorithms for the system.

The significance of utilising linear adaptive control strategies for the design of power system stabilisers is that for small dynamics the nonlinear power system can be modelled approximately by a *time-varying linearised* form. Such a form can be called a *linear dynamic equivalent model* [61] of the nonlinear power system. In this thesis, it is termed a *linearised nominal model* for which linear adaptive control laws are to be designed.

The structure of a linearised nominal model for the nonlinear power system can be *proposed* in a "black-box" form, in which a model with fixed order and fixed delay-time but unknown parameters is *assumed* at first. The data collected from a detailed simulation of the nonlinear power system (or from real-time field testing) is then fed into the assumed model in order to modify the proposed model structure and to identify the unknown parameters (if required) [158]-[165]. This procedure is based on the concept of the *external equivalent* [61] of the system. In the literature, the structure of a linearised nominal model for the design of linear adaptive power system stabilisers (or controllers) has been assumed as either a *Deterministic AutoRegressive Moving-Average* (**DARMA**) *model* [45,49,50,68,53,69,56,58,59,62,63,64,65] or an *AutoRegressive Moving-Average model with auXiliary input* (**ARMAX**) [46,47,48,52,54,55,57,70, 71,72,60,61,67,74]. [2]

[1] In this thesis, a **nominal model** is defined as a model for which control laws are directly designed.

[2] The definitions of a DARMA model and an ARMAX model in linear forms are given in [157].

Alternatively, the structure of a linearised nominal model can be *derived* from a reduced-order nonlinear model of the SMIB power system through linearisation and discretisation. Theoretically, the validity of the derived model relies heavily on the techniques that are employed in the linearisation and discretisation and/or the assumptions that are introduced into the derivation of the model. Since a derived linearised nominal model is based on a simplified nonlinear model of the power system, its validity needs to be confirmed through *external equivalent* studies as well. Nevertheless, a *derived* model provides insight into the system and, hence, confidence in using such a model for design purposes.

Due to the time-varying nature of the model parameters, the order of a linearised nominal model can often be lower than that of the actual nonlinear system. It is required that such a model represent the dominant dynamics of the system and omit the less significant dynamics of the system. The consequence of this requirement is to simplify the design of the system controllers. Since the model is derived in a linear form, linear adaptive control strategies that have been well documented can be applied directly to the model.

In this section the linearised nominal model of the SMIB power system is *derived* from the SLAM proposed in Subsection 2.4.2. The layout of the remainder of this section is as follows. A SISO linear continuous-time state-space model of the nonlinear power system is given in Subsection 3.2.1. The subsequent discrete-time state-space and input-output models are derived in Subsection 3.2.2. The final form of the linearised nominal model for the design of the linear adaptive power system stabiliser is determined in Subsection 3.2.3.

3.2.1 SISO Linear Continuous-Time State-Space Power System Modelling.

As far as small signal excitation control of the power system is concerned, the nonlinear SMIB power system can be described by the SLAM (2.114) derived in Subsection 2.4.2

with the linearised output equation (2.129) given in Section 2.6, i.e.,

$$\Delta\dot{\mathbf{X}}(t) = \mathbf{A_0}\Delta\mathbf{X}(t) + \mathbf{b}_{u0}\Delta u_r(t) + \mathbf{b}_{w0}\Delta w(t), \tag{3.1}$$

$$\Delta\bar{y}(t) = \mathbf{c_0}\Delta\mathbf{X}(t), \tag{3.2}$$

where $\Delta u_r(t)$ is the input to the summing junction of the AVR-excitation system, and is expressed as

$$\Delta u_r(t) = \Delta V_{ref}(t) + \Delta\bar{u}(t) \tag{3.3}$$

with $\Delta\bar{u}(t)$ being the control signal generated by the linear adaptive power system stabiliser which is to be designed; $\Delta w(t)$ is the deviation of the machine mechanical torque, $\Delta T_m(t)$, which has been considered as the system disturbance (see Subsection 2.4.2). The matrix $\mathbf{A_0}$ and the vector $\mathbf{c_0}$ are defined by (2.113) and (2.130), respectively. With the selection of the state variables, $\Delta\mathbf{X}(t)$, being the set of measurable variables given by (2.125), $\mathbf{A_0}$ is derived in (2.126). The vectors $\mathbf{b}_{u0}$ and $\mathbf{b}_{w0}$ in (3.1) are written as

$$\mathbf{b}_{u0} = \begin{bmatrix} 0 & 0 & 0 & \frac{K_A}{\tau_A} \end{bmatrix}^T \tag{3.4}$$

and

$$\mathbf{b}_{w0} = \begin{bmatrix} \frac{1}{2H} & 0 & 0 & 0 \end{bmatrix}^T. \tag{3.5}$$

The expression for the vector $\mathbf{c_0}$ in (3.2) depends on the selection of the system output variable, $\Delta\bar{y}(t)$. Choosing $\Delta\bar{y}(t)$ to be the electrical torque deviation, $\Delta T_e(t)$, [3] $\mathbf{c_0}$ is then given by

$$\mathbf{c_0} = \begin{bmatrix} 0 & 1 & 0 & 0 \end{bmatrix}. \tag{3.6}$$

3.2.2 SISO Linear Discrete-Time Input-Output Power System Modelling.

For the sake of simplicity, the disturbance term $\Delta w(t)$ from (3.1) is omitted for the time being. It is assumed that for small disturbances about an operating point, $\mathbf{A_0}$ in

[3] The reason of using $\Delta T_e(t)$ as the stabilising signal has been explained in Section 2.5.

(3.1) is a constant matrix. The so-called *zero-order-hold equivalent* [141] of the linear continuous-time state-space representation (3.1)-(3.6) is then described by

$$\Delta \mathbf{X}(kh+h) = \tilde{\mathbf{A}}_0 \Delta \mathbf{X}(kh) + \tilde{\mathbf{b}}_{u0} \Delta u_r(kh), \tag{3.7}$$

$$\Delta \bar{y}(kh) = \mathbf{c}_0 \Delta \mathbf{X}(kh), \tag{3.8}$$

where

$$\tilde{\mathbf{A}}_0 = e^{\mathbf{A}_0 h}, \tag{3.9}$$

$$\tilde{\mathbf{b}}_{u0} = \int_0^h e^{\mathbf{A}_0 \tau} d\tau \, \mathbf{b}_{u0}; \tag{3.10}$$

h is the constant sampling period and $k \in [0, 1, 2, \cdots)$. An input-output representation of the discrete-time state-space model (3.7)-(3.10) in the backward-shift operator form is obtained by eliminating the state variables using purely algebraic manipulations to give

$$\Delta \bar{y}(kh) = \mathbf{c}_0 \left(I - q^{-1} \tilde{\mathbf{A}}_0\right)^{-1} q^{-1} \tilde{\mathbf{b}}_{u0} \Delta u_r(kh) \tag{3.11}$$

where

$$q^{-1}\Delta \bar{y}(kh) \triangleq \Delta \bar{y}(kh-h), \qquad \text{for } k \geq 1; \qquad\qquad q^{-1}\Delta y(0) \triangleq 0,$$

and so on. It is assumed that

Assumption 3.2.1 *In the model (3.1)-(3.6) the system matrix* $\mathbf{A}_0$ *is nonsingular.*

Assumption 3.2.2 *The input signal* $\Delta V_{ref}(t)$ *is zero except in the cases in which* $V_{ref}(t)$ *has step changes.*

Subject to Assumptions 3.2.1-3.2.2, the SISO linear discrete-time input-output model (3.11) can be rewritten as

$$\Delta \bar{y}(kh) = \mathbf{c}_0 \left(I - q^{-1} e^{\mathbf{A}_0 h}\right)^{-1} q^{-1} \mathbf{A}_0{}^{-1} \left(e^{\mathbf{A}_0 h} - I\right) \mathbf{b}_{u0} \Delta \bar{u}(kh), \tag{3.12}$$

which utilises the result

$$\tilde{\mathbf{b}}_{u0} = \mathbf{A}_0{}^{-1} \left(e^{\mathbf{A}_0 h} - I\right) \mathbf{b}_{u0}.$$

The *pulse-transfer operator* [141] of the model (3.12) is defined as

$$\bar{H}(q^{-1}) \triangleq \mathbf{c}_0 \left(I - q^{-1} e^{\mathbf{A}_0 h}\right)^{-1} q^{-1} \mathbf{A}_0{}^{-1} \left(e^{\mathbf{A}_0 h} - I\right) \mathbf{b}_{u0} \triangleq \frac{\bar{B}(q^{-1})}{\bar{A}(q^{-1})}. \tag{3.13}$$

The model (3.12) can then be expressed as

$$\Delta\bar{y}(kh) = \bar{H}(q^{-1})\Delta\bar{u}(kh). \tag{3.14}$$

For convenience of notation, the sampling period h is omitted. The model (3.14) is then written as

$$\bar{A}(q^{-1})\Delta\bar{y}(k) = \bar{B}(q^{-1})\Delta\bar{u}(k) \tag{3.15}$$

where the polynomial $\bar{A}(q^{-1})$ is of fourth-order and the polynomial $\bar{B}(q^{-1})$ is of third-order.

For a given operating point of the nonlinear system, the state-space model (3.7)-(3.10) and the input-output model (3.15) are time-invariant and linear. According to the conclusions drawn in Section 2.6, the order of the input-output model (3.15) is equal to the order of the state-space model (3.7)-(3.10) *if and only if* the model (3.7)-(3.10) is completely controllable and observable. In this case, the given system operating point that determines a minimal realization of the state-space model (3.7)-(3.10) will result in an irreducible pulse-transfer operator $\bar{H}(q^{-1})$ (3.13), and therefore unique coefficients of the polynomials $\bar{A}(q^{-1})$ and $\bar{B}(q^{-1})$ in (3.15). However, as the operating condition of the nonlinear system varies widely, the controllability and observability of the model (3.7)-(3.10) over a wide range of operating conditions is not guaranteed, nor is the uniqueness of the coefficients of the polynomials $\bar{A}(q^{-1})$ and $\bar{B}(q^{-1})$. Consequently, it may happen in theory that multiple sets of values of the polynomial coefficients in (3.15) represent an identical operating point at which the controllability and observability of the model (3.7)-(3.10) are not satisfied.

3.2.3 Linearised Nominal Model of the Power System.

From a practical point of view, one allows for measurement errors, actuator errors, and in some instances computer round-off errors in (3.15) by assuming that

Assumption 3.2.3 *For the model (3.15), the measured or computed values of the input and output variables, $u(k)$ and $y(k)$, satisfy that*

$$\sup_{0\leq k<\infty} |\Delta y(k) - \Delta\bar{y}(k)| \leq \Delta_1,$$

$$\sup_{0\leq k<\infty} |\Delta u(k) - \Delta\bar{u}(k)| \leq \Delta_2,$$

where Δ_i $(i = 1, 2)$ *are fixed known values.*

Taking the omitted disturbance term $\Delta w(t)$ and the errors introduced by Assumption 3.2.3 into account, one adds a noise term $\bar{C}(q^{-1})\,\bar{\epsilon}(k)$ in (3.15), resulting in

$$\bar{A}(q^{-1})\Delta y(k) = \bar{B}(q^{-1})\Delta u(k) + \bar{C}(q^{-1})\bar{\epsilon}(k) \tag{3.16}$$

where $\bar{C}(q^{-1})$ is an unknown polynomial and $\{\bar{\epsilon}(k)\}$ is uncorrelated with $\{\Delta y(k)\}$ and $\{\Delta u(k)\}$.

For the system operating points at which zero-pole cancellations in $\bar{H}(q^{-1})$ (3.13) take place, the order of the model (3.16) is higher than it should be. In the context of the adaptive estimation and prediction, an overparametric model may result in a low convergence rate of the estimated parameters and, subsequently, a poor prediction of the system output. To avoid it, the polynomials $\bar{A}(q^{-1})$ and $\bar{B}(q^{-1})$ in (3.16) may need to be replaced by the corresponding lower-order ones. Consequently, a general form of the *Linearised Nominal Model* **(LNM)** of the SLAM is described by

$$A(q^{-1})\Delta y(k) = q^{-1}B(q^{-1})\Delta u(k) + C(q^{-1})\epsilon(k) \tag{3.17}$$

where $A(q^{-1})$ is of third-order

$$A(q^{-1}) = 1 + a_1 q^{-1} + a_2 q^{-2} + a_3 q^{-3}; \tag{3.18}$$

$B(q^{-1})$ is of second-order

$$B(q^{-1}) = b_0 + b_1 q^{-1} + b_2 q^{-2}. \tag{3.19}$$

The roots of the polynomial $C(z)$ are restricted to lie within the unit circle of the z-domain. The noise $\{\epsilon(k)\}$ is an uncorrelated random sequence of zero mean and is unmeasurable. The order of $C(q^{-1})$ is to be specified. For the sake of simplicity, $C(q^{-1}) = 1$ can be taken [46,48,54,55,57,70,71,72,60,67,74]. Note that the coefficients of the polynomials in (3.17) are *time-varying* in nature, in accordance with the changes in system operating conditions. The LNM given by (3.17)-(3.19) will be used for the design of the linear adaptive power system stabiliser in the following sections of this chapter.

3.3 SISO Linear Stochastic Optimal Control.

In this section:

- the SISO linear stochastic optimal control laws which lead to the corresponding linear stochastic adaptive control laws are derived from a general form of the cost function;
- features of the different linear stochastic optimal control strategies are described;
- aspects of utilising the different optimal control strategies for the development of linear adaptive power system stabilisers are discussed.

The establishment of the LNM (3.17)-(3.19) in Section 3.2 provides a basis for the design of linear adaptive power system stabilisers. As the LNM is given in an ARMAX form, for a given control performance index in a stochastic environment linear stochastic optimal control laws can be derived for the LNM. The derivation and discussion of the linear stochastic optimal control strategies conducted in this section will establish a foundation for the development of the subsequent linear stochastic adaptive control strategies in Sections 3.4 and 3.5.

The layout of this section is as follows. In Subsection 3.3.1 a linear stochastic optimal d-step-ahead predictor is given. The linear stochastic optimal control laws are derived and discussed in Subsection 3.3.2.

3.3.1 SISO Linear Stochastic Optimal d-Step-Ahead Predictor.

Consider, in general terms, a *SISO linear finite-dimensional time-invariant discrete-time* model given by

$$A(q^{-1})y(k) = q^{-d}B(q^{-1})u(k) + C(q^{-1})\varepsilon(k) \tag{3.20}$$

where $y(k) \in \mathcal{R}$ is the output; $u(k) \in \mathcal{R}$ is the control input; $\varepsilon(k)$ is a white noise satisfying

$$E\{\varepsilon(k) \mid \mathcal{F}_{k-1}\} = 0, \qquad E\left\{\varepsilon(k)^2 \mid \mathcal{F}_{k-1}\right\} = \sigma_\varepsilon^2, \qquad \text{for } k \geq 1; \tag{3.21}$$

d is the system pure time delay; $A(q^{-1})$, $B(q^{-1})$, and $C(q^{-1})$ are polynomials of order n, m, and l, respectively, and are given by

$$A(q^{-1}) = 1 + a_1 q^{-1} + \ldots + a_n q^{-n}, \tag{3.22}$$

$$B(q^{-1}) = b_0 + b_1 q^{-1} + \ldots + b_m q^{-m}, \qquad (b_0 \neq 0), \tag{3.23}$$

$$C(q^{-1}) = 1 + c_1 q^{-1} + \ldots + c_l q^{-l}. \tag{3.24}$$

The roots of $C(z)$ are strictly inside the unit circle of the z-domain.

For the model (3.20)-(3.24) having d-step pure time delay, the optimal d-step-ahead prediction, $y^0(k+d \mid k)$, of $y(k+d)$ is given by

Lemma 3.3.1 *The optimal prediction of the output of the model (3.20)-(3.24) at time $(k+d)$ can be expressed in the following predictor form*

$$C(q^{-1})y^0(k+d \mid k) = \alpha(q^{-1})y(k) + \beta(q^{-1})u(k) \tag{3.25}$$

where

$$y^0(k+d \mid k) \triangleq E\{y(k+d) \mid \mathcal{F}_k\} = y(k+d) - F(q^{-1})\varepsilon(k+d), \tag{3.26}$$

$$\alpha(q^{-1}) \triangleq G(q^{-1}), \tag{3.27}$$

$$\beta(q^{-1}) \triangleq F(q^{-1})B(q^{-1}) \tag{3.28}$$

with $\beta_0 = b_0 \neq 0$. $F(q^{-1})$ and $G(q^{-1})$ are the unique polynomials of order $(d-1)$ and $(n-1)$, respectively, satisfying

$$C(q^{-1}) = F(q^{-1})A(q^{-1}) + q^{-d}G(q^{-1}), \qquad (f_0 = 1). \tag{3.29}$$

3.3.2 SISO Linear Stochastic Optimal Control Laws.

The linear stochastic optimal control performance index leading to the linear stochastic adaptive control schemes is of the following form

$$J(k+d) \triangleq E\left\{\left[\bar{P}(q^{-1})y(k+d) - \bar{R}(q^{-1})y^*(k+d)\right]^2 + \left[\bar{Q}(q^{-1})u(k)\right]^2\right\} \tag{3.30}$$

where $y^*(k+d)$ is the desired output trajectory which the system should follow and $\bar{P}(q^{-1})$, $\bar{R}(q^{-1})$, and $\bar{Q}(q^{-1})$ are the preselected weighting polynomials which are used to penalise excessive control actions and to deal with nonminimum phase problems. The leading coefficient of $\bar{P}(q^{-1})$, $\bar{p}_0$, is taken as 1.

The optimal control law which minimises (3.30) sets

$$\bar{P}(q^{-1})y^0(k+d \mid k) - \bar{R}(q^{-1})y^*(k+d) + \frac{\bar{Q}(q^{-1})\bar{q}_0}{\beta_0}u(k) = 0 \tag{3.31}$$

which utilises the definition of $y^0(k+d \mid k)$ in (3.26), the optimal d-step-ahead predictor (3.25), as well as the numerical characteristics of $\varepsilon(k)$ in (3.21). The consequent linear optimal control law as well as its closed-loop characteristics is then given by

Theorem 3.3.1 *For the model (3.20)-(3.24) having the optimal predictor (3.25)-(3.29),*

(a) the optimal control law minimising the cost function (3.30) has the form [4]

$$L(q^{-1})u^*(k) = M(q^{-1})y^*(k+d) - P(q^{-1})y(k) \tag{3.32}$$

where $L(q^{-1})$, $M(q^{-1})$, and $P(q^{-1})$ are defined as

$$L(q^{-1}) \triangleq \bar{P}(q^{-1})\beta(q^{-1}) + \frac{\bar{Q}(q^{-1})\bar{q}_0}{\beta_0}C(q^{-1}), \tag{3.33}$$

$$M(q^{-1}) \triangleq \bar{R}(q^{-1})C(q^{-1}), \tag{3.34}$$

$$P(q^{-1}) \triangleq \bar{P}(q^{-1})\alpha(q^{-1}); \tag{3.35}$$

[4]Note that in this thesis the *final* form of the *optimal control* input is symbolised by $u^*(k)$.

(b) the closed-loop system is given by

$$w(q^{-1})\begin{bmatrix} y(k+d) \\ u^*(k) \end{bmatrix} = \begin{bmatrix} B(q^{-1})\bar{R}(q^{-1}) & L(q^{-1}) \\ A(q^{-1})\bar{R}(q^{-1}) & -q^{-d}P(q^{-1}) \end{bmatrix}\begin{bmatrix} y^*(k+d) \\ \varepsilon(k+d) \end{bmatrix} \tag{3.36}$$

where

$$w(q^{-1}) \triangleq \bar{P}(q^{-1})B(q^{-1}) + \frac{\bar{Q}(q^{-1})\bar{q}_0}{\beta_0}A(q^{-1}); \tag{3.37}$$

(c) the resulting closed-loop system (3.36)-(3.37) is bounded-input bounded-output stable provided that

$$w(z^{-1}) \triangleq \bar{P}(z^{-1})B(z^{-1}) + \frac{\bar{Q}(z^{-1})\bar{q}_0}{\beta_0}A(z^{-1}) \neq 0, \quad \textit{for all } |z^{-1}| \leq 1.$$

Discussions of different linear stochastic optimal control schemes.

The cost function (3.30) describes the following important cases, each resulting in a linear optimal control scheme:

(1) Select $\bar{P}(q^{-1}) = \bar{R}(q^{-1}) = 1$ and $\bar{Q}(q^{-1}) = 0$. A *minimum variance* controller is formed from (3.32)

$$\beta(q^{-1})u^*(k) = C(q^{-1})y^*(k+d) - \alpha(q^{-1})y(k). \tag{3.38}$$

The resulting closed-loop system poles are given by

$$B(z^{-1}) = 0.$$

The features of a minimum variance controller are:

- the controller can only be used when the system is minimum phase;
- with a small value of the leading coefficient of the polynomial $\beta(q^{-1})$, an excessive control effort may be called for.

(2) Select $\bar{P}(q^{-1}) = \bar{R}(q^{-1}) = 1$ and $\bar{Q}(q^{-1}) = \lambda^{\frac{1}{2}}$ (where $\lambda > 0$). A *weighted minimum variance* controller is formed from (3.32)

$$\left[\beta(q^{-1}) + \frac{\lambda}{\beta_0}C(q^{-1})\right]u^*(k) = C(q^{-1})y^*(k+d) - \alpha(q^{-1})y(k). \tag{3.39}$$

The resulting closed-loop system poles are given by

$$B(q^{-1}) + \frac{\lambda}{\beta_0} A(q^{-1}) = 0.$$

The features of a weighted minimum variance controller are:

- by including a weighting coefficient λ into the construction of the control law, the controller can be used to stabilise a nonminimum phase system;
- with a suitable choice of the value of λ, excessive control actions can be penalised without losing the optimal control effect;
- the controller will, in general, produce a steady-state tracking error unless the control action converges to zero in the steady state.

(3) Select $\bar{P}(q^{-1}) = \bar{R}(q^{-1}) = 1$ and $\bar{Q}(q^{-1}) = \lambda^{\frac{1}{2}}(1 - q^{-1})$. An *integrated minimum variance* controller is formed from (3.32)

$$\left[\beta(q^{-1}) + \frac{\lambda}{\beta_0}\left(1 - q^{-1}\right) C(q^{-1})\right] u^*(k) = C(q^{-1}) y^*(k+d) - \alpha(q^{-1}) y(k). \quad (3.40)$$

The resulting closed-loop system poles are given by

$$B(q^{-1}) + \frac{\lambda}{\beta_0}\left(1 - q^{-1}\right) A(q^{-1}) = 0.$$

The features of an integrated minimum variance controller are:

- the controller can be used for a nonminimum phase system;
- zero steady-state tracking error is guaranteed by the introduction of a pure integrator into the control loop;
- the effect of "integral wind-up" may result if saturation in the input and/or the output signals occurs.

(4) Solve $\bar{P}(q^{-1})$ and $\bar{Q}(q^{-1})$ from

$$w(q^{-1}) = \bar{P}(q^{-1}) B(q^{-1}) + \frac{\bar{Q}(q^{-1})\bar{q}_0}{\beta_0} A(q^{-1}) = A^*(q^{-1}) \quad (3.41)$$

where $A^*(q^{-1})$ defines the prespecified locations of the desired closed-loop poles. Let $M(q^{-1}) = q^{-d} P(q^{-1})$ (i.e., choose $\bar{R}(q^{-1})$ such that

$\bar{R}(q^{-1})C(q^{-1}) = q^{-d}\bar{P}(q^{-1})\alpha(q^{-1}))$. A *pole assignment* controller is formed from (3.32)

$$L(q^{-1})u^*(k) = P(q^{-1})\left[y^*(k) - y(k)\right].$$

The resulting closed-loop system poles are given by

$$A^*(q^{-1}) = 0.$$

The features of a pole assignment controller are:

- the choice of $A^*(q^{-1})$ is random provided that a unique solution of $\bar{P}(q^{-1})$ and $\bar{Q}(q^{-1})$ can be found from (3.41), i.e., $A(q^{-1})$ and $B(q^{-1})$ are *relatively prime*;
- a poor choice of $A^*(q^{-1})$ may lead to an unstable $L(q^{-1})$, thus an unstable controller.

Remark 3.3.1 *The linear optimal control schemes given by (3.38), (3.39), and (3.40) can be summarised under the name of* generalised minimum variance control *[166,167].*

Utilisation of the linear stochastic optimal control schemes for the development of linear adaptive power system stabilisers.

The linear optimal control laws given above provide the bases for the development of the corresponding linear adaptive control algorithms. To choose an appropriate optimal control scheme for the design of a linear adaptive power system stabiliser, the following basic requirements are essential:

(1) the control scheme should be able to stabilise a nonminimum phase system;

(2) the control action generated by the control law should not saturate during the system dynamics following a disturbance;

(3) the design of the control law should not rely heavily on the *a priori* knowledge of the system;

(4) the computation of the control action should not affect the practicality of the control algorithm;

(5) the resulting controller should be able to be tuned by one parameter in the control law, to achieve the best trade-off between the system performance and the control effort.

Based on the above requirements, the following are considerations which need to be taken into account when applying the different linear optimal control schemes to the design of linear adaptive power system stabilisers [49,43,44]:

- The minimum variance control scheme is not suitable for the adaptive excitation control of power systems because
  - the resulting closed-loop system will be unstable if the system is nonminimum phase;
  - an excessively large control action will cause the exciter to reach its ceiling level with the result that poor damping performance of the system occurs.
- The integrated minimum variance control scheme may not be suitable for the adaptive excitation control of power systems because
  - during large excursions of the system variables, saturation of the input and/or the output signals occurs. The integrator output will then build up to a large value which leads to poor control system performance or even instability.
- The pole assignment control scheme may not be suitable for the adaptive excitation control of power systems because
  - it may be difficult to choose the closed-loop system poles which are appropriate for a wide range of system operating conditions;
  - the computation burden in calculating the control action may become excessive, since at each iteration two identity equations ((3.29) and (3.41)) are required to be solved;

– a poor choice of $A^*(q^{-1})$ may lead to an unstable control action and, thus, poor damping performance.

It can be seen from the above discussion that the weighted minimum variance control scheme meets the basic requirements (1)-(5) and is simple to be implemented in practice. Since a high-gain AVR is usually used in the excitation control system, for stable system responses the control action $u^*(k)$ from (3.39) will converge to a very small value in the steady state, as expressed by

$$\lim_{k\to\infty} |u^*(k)| \leq \epsilon_{u^*} \tag{3.42}$$

where ϵ_{u^*} is a small constant which is dependent of the value of the gain of the AVR. It should be emphasised here that an important advantage of utilising the weighted minimum variance control scheme for the development of the linear adaptive power system stabiliser is that, due to its simplicity, it can be extended into a *nonlinear* control case. This advantage will facilitate the comparisons of system performance of the linear adaptive and nonlinear optimal/adaptive control strategies to be conducted in the following chapters.

Remark 3.3.2 *The features of the adaptive excitation control of power systems associated with the use of the* optimal linear quadratic control *scheme and the* model reference control *scheme are described in [49,43], however they are not included in this thesis.*

Remark 3.3.3 *Modified versions of the pole assignment control law, called the* pole-shifting *control law [49,50] and the* self-searching pole-shifting *control law [53,54,55, 56,70], have been proposed and implemented in the literature. However, due to the complexity in computation, these control laws may not be easily extended into a nonlinear control case and, therefore, are considered to be unsuitable for the purposes of this thesis.*

3.4 SISO Linear Stochastic Adaptive Generalised Minimum Variance Control.

In this section:

- aspects of the selection of the parameter estimation algorithm for the identification of the LNM are discussed;
- the SISO linear stochastic adaptive generalised minimum variance control algorithm is described.

The derivation of the linear stochastic optimal control laws discussed in Section 3.3 provides a basis for the development of the linear adaptive control laws for the LNM. Since the parameters of the LNM are *time-varying* and, in general, are *unknown* in nature, a properly selected parameter estimation algorithm is incorporated into the control law (3.32) to identify the *model* or the *controller* parameters on-line. The control law is then updated using the estimated parameters as if they were the true ones. Such a design scheme is based on the so-called *certainty equivalence principle* [37]. If the estimated parameters are the controller parameters, the resulting adaptive control algorithm forms a *direct* self-tuning adaptive controller. However, if the estimated parameters are the model parameters, intermediate control design calculations are needed at each iteration step in order to obtain the controller parameters. The resulting adaptive control algorithm is then called an *indirect* self-tuning adaptive controller.

The layout of this section is as follows. In Subsection 3.4.1 the selection of parameter estimation algorithms for on-line model identification of power systems is briefly discussed and the basic algorithm used for the simulation studies *of this thesis* is finalised. In Subsection 3.4.2 a *direct* SISO linear stochastic adaptive generalised minimum variance control algorithm is described.

3.4.1 Parameter Estimation Algorithms for the Linearised Nominal Model of the Power System.

In an adaptive control scheme, the parameter estimation algorithm plays an important part in the successful control of system dynamics. Standard parameter estimation algorithms, such as

- projection method;
- least squares method;
- instrumental variable method;
- extended least squares method; etc.,

have been well documented in the literature (e.g., [168,157,169,170]). The applications of these algorithms to a variety of fields of studies have been widely reported. One of the most popular methods, the *recursive least squares* algorithm, has been accepted as a suitable *standard* algorithm for the parameter estimation in power system studies. Several modified versions of this standard algorithm have been proposed and implemented for the identification of power systems either through simulation studies [57,61] or laboratory experiments [71,72,67].

For identifying a steady-state power system at a fixed operating point, the unknown parameters of the LNM are time-invariant. The standard recursive least squares algorithm can then be used without modifications. However, as indicated in Section 3.2, the parameters of the LNM are time-varying due to the changes in system operating conditions. This nature of the parameters of the LNM requires that the estimation algorithm possess the ability to track the parameters. The standard recursive least squares algorithm does not track the changes in the parameters well. This is because after the initial convergence of the estimated parameters, the covariance matrix $P(k)$ in the algorithm becomes very small and the estimator is close to a 'switching-off' condition. To improve the tracking ability of the algorithm, several modifications have been proposed [45,47,57,71]. Among them, the application of an exponential forgetting

factor, μ, with a constant value of less than one has received considerable attention [45,57,71,72,61,64,67]. The best value of μ depends upon the system operating condition. For small variations from the system steady-state operating point, the value of μ should be close to unity, but for large excursions in the system operating condition, the value of μ should be less than one. Since the covariance matrix $P(k)$ is constantly scaled by μ, the phenomenon whereby the matrix $P(k)$ 'blowing-up' occurs if μ is chosen relatively small while the system is operating at a steady-state point for a long time. When this happens, the estimator becomes very sensitive to any disturbances or numerical errors in computation. A small disturbance or numerical error will cause bursting in the estimated parameters [171,54].

To overcome this problem, a time-varying forgetting factor, $\mu(k)$, has been proposed instead [171]. The proposed structure of $\mu(k)$ is a function of the error, $e(k)$, between the system output variable and its prediction, i.e.,

$$\mu(k) = 1 - \frac{e(k)^2}{1 + \phi(k-d)^T P(k-d-1)\phi(k-d)} \frac{1}{\Sigma_0}.$$

For steady-state operation, the error $e(k)$ is close or equal to zero. The value of $\mu(k)$ is then close or equal to unity, preventing the matrix $P(k)$ from 'blowing-up'. For small disturbances, $\mu(k)$ decreases as $e(k)$ increases. This improves the parameter tracking ability of the estimator and prevents the estimator from 'switching-off'. The occurrence of large disturbances causes $\mu(k)$ to decrease significantly, resulting in fast parameter tracking.

The above approach (or other similar versions of this method, e.g., [60]) has been employed in several applications of adaptive control to power systems in the literature. Its performance in tracking parameter changes over a wide range of system operating conditions has been verified through simulation studies [53,54,56,58,60,65,74] and experimental results [70]. This approach is adopted to form a *basic* parameter estimation algorithm for the design of the linear adaptive power system stabiliser in this chapter and the nonlinear adaptive power system stabilisers in Chapters 5 and 6. The detailed forms of the estimators will be given in Subsection 3.4.2 and Sections 3.5 and 5.2, along with the relevant control laws.

3.4.2 SISO Linear Stochastic Adaptive Generalised Minimum Variance Control Algorithm.

The design of an adaptive control law involves the combination of a parameter estimation algorithm with an optimal control law. This combination results in the controller possessing the ability to adapt to variations in operating conditions of the nonlinear power system.

Combining the linear optimal control law (3.32) with the recursive least squares algorithm with the time-varying forgetting factor selected in Subsection 3.4.1, one obtains the basic structure of a linear adaptive power system stabiliser. To derive a *direct* adaptive generalised minimum variance control algorithm from (3.32), an auxiliary variable $\varphi(k+d)$ and its optimal prediction $\varphi^*(k+d \mid k)$ are introduced as

$$\varphi(k+d) \triangleq \bar{P}(q^{-1})y(k+d) - \bar{R}(q^{-1})y^*(k+d) + \frac{\bar{Q}(q^{-1})\bar{q}_0}{\beta_0}u(k) \tag{3.43}$$

and

$$\varphi^*(k+d \mid k) \triangleq \bar{P}(q^{-1})y^0(k+d \mid k) - \bar{R}(q^{-1})y^*(k+d) + \frac{\bar{Q}(q^{-1})\bar{q}_0}{\beta_0}u(k). \tag{3.44}$$

Due to (3.26), it follows from (3.43) and (3.44) that

$$\varphi^*(k+d \mid k) = \varphi(k+d) - \varepsilon_\varphi(k+d) \tag{3.45}$$

where

$$\varepsilon_\varphi(k+d) \triangleq \bar{P}(q^{-1})F(q^{-1})\varepsilon(k+d); \tag{3.46}$$

$\{\varepsilon_\varphi(k+d)\}$ is uncorrelated with $\{y(k)\}$ and $\{u(k)\}$. According to (3.26), (3.25), and (3.31), an equivalent form of the model (3.20)-(3.24) can be derived from (3.43)-(3.46):

$$\begin{aligned} \varphi(k+d) &= P(q^{-1})y(k) + L(q^{-1})u(k) - M(q^{-1})y^*(k+d) + \varepsilon_\varphi(k+d) \\ &\triangleq \phi(k)^T\Theta_0 + \varepsilon_\varphi(k+d) \end{aligned} \tag{3.47}$$

where $P(q^{-1})$, $L(q^{-1})$, and $M(q^{-1})$ are given by (3.35), (3.33), and (3.34), respectively, and

$$\phi(k)^T \triangleq \left[\begin{array}{cccccccccc} y(k) & y(k-1) & \cdots & u(k) & u(k-1) & \cdots & -y^*(k+d) & -y^*(k+d-1) & \cdots \end{array}\right]; \tag{3.48}$$

$$\Theta_0^T \triangleq \begin{bmatrix} p_0 & p_1 & \cdots & l_0 & l_1 & \cdots & m_0 & m_1 & \cdots \end{bmatrix}. \tag{3.49}$$

The *optimal control* law given by (3.32) is then written concisely as

$$\phi(k)^T \Theta_0 = 0$$

with $u(k)$ in (3.48) denoted by $u^*(t)$.

Using the certainty equivalence principle, the *d-step-ahead adaptive prediction*, $\hat{\varphi}(k+d)$, of $\varphi(k+d)$ in (3.47) can then be defined as

$$\hat{\varphi}(k+d) \triangleq \phi(k)^T \hat{\Theta}(k)$$

where

$$\hat{\Theta}(k)^T \triangleq \begin{bmatrix} \hat{p}_0(k) & \hat{p}_1(k) & \cdots & \hat{l}_0(k) & \hat{l}_1(k) & \cdots & \hat{m}_0(k) & \hat{m}_1(k) & \cdots \end{bmatrix}. \tag{3.50}$$

$\hat{\Theta}(k)$ is the estimate of Θ_0 (3.49). Hence, the *adaptive control* $u(k)$ is chosen such that

$$\phi(k)^T \hat{\Theta}(k) = 0. \tag{3.51}$$

The linear estimate $\hat{\Theta}(k)$ of Θ_0 is obtained at each iteration step by using the selected recursive least squares algorithm with the time-varying forgetting factor. At the sampling instant k, the vector of the parameter estimates previously available is $\hat{\Theta}(k-1)$. A new estimate $\hat{\Theta}(k)$ of the parameters can be generated by the following algorithm. Note that as the algorithm is given in a direct form, the control input $u(k)$ is solved directly by using the estimated controller parameters in $\hat{\Theta}(k)$ (3.50).

Algorithm 3.1 [direct SISO linear stochastic adaptive generalised minimum variance control algorithm.]

Estimate:

$$\hat{\Theta}(k) = \hat{\Theta}(k-1) + P(k-d)\phi(k-d)\left[\varphi(k) - \phi(k-d)^T \hat{\Theta}(k-1)\right];$$

Covariance:

$$P(k-d) = \left[P(k-d-1) - \frac{P(k-d-1)\phi(k-d)\phi(k-d)^T P(k-d-1)}{\mu(k-1) + \phi(k-d)^T P(k-d-1)\phi(k-d)}\right]\frac{1}{\mu(k-1)};$$

Auxiliary Variable:

$$\varphi(k) = \bar{P}(q^{-1})y(k) - \bar{R}(q^{-1})y^*(k) + \frac{\bar{Q}(q^{-1})\bar{q}_0}{\beta_0}u(k-d);$$

Prediction:

$$\hat{\varphi}(k) = \phi(k-d)^T\hat{\Theta}(k-d);$$

Error:

$$e(k) = \varphi(k) - \hat{\varphi}(k);$$

Forgetting Factor:

$$\mu_0(k) = 1 - \frac{e(k)^2}{1 + \phi(k-d)^T P(k-d-1)\phi(k-d)}\frac{1}{\Sigma_0},$$

$$\bar{\mu}(k) = \begin{cases} \mu_0(k) & \text{if } \mu_0(k) \geq \mu_{min} > 0 \\ \mu_{min} & \text{otherwise} \end{cases},$$

$$\mu(k) = \begin{cases} \bar{\mu}(k) & \text{if } \dfrac{\text{trace}[P(k-d)]}{\bar{\mu}(k)} < C \\ 1 & \text{otherwise} \end{cases};$$

Control Law:

$$\phi(k)^T\hat{\Theta}(k) = 0;$$

where $k \geq d$, $P(-1) = K_0 I$ $(0 < K_0 < C)$, and $\mu(d-1) = 1$. $\bar{P}(q^{-1})$, $\bar{R}(q^{-1})$, and $\bar{Q}(q^{-1})$ are preselected weighting polynomials. Σ_0, μ_{min}, and C are preselected positive constants. $\hat{\Theta}(k)$ and $\phi(k)$ are defined by (3.50) and (3.48), respectively. $\hat{\Theta}(0)$ is given.

$\nabla\ \nabla\ \nabla$

Remark 3.4.1 *In Algorithm 3.1, it is required that*

(i) $\hat{l}_0(k)$ *be non-zero for all* k. *If this assumption is violated in practice, it is then necessary to introduce boundaries in the estimate in order to prevent* $\hat{l}_0(k)$ *from being zero.*

(ii) the value of β_0 *be known.*

Remark 3.4.2 *The introduction of* μ_{min} *and* C *in the algorithm is to guarantee the convergence of the estimates [172,173].*

Algorithm 3.1 will be used in Section 3.5 for the development of the desired linear adaptive power system stabiliser.

3.5 A Linear Adaptive Weighted Minimum Variance Power System Stabiliser.

In this section:

- the SISO linear stochastic adaptive weighted minimum variance control algorithm is developed from Algorithm 3.1 given in Subsection 3.4.2;
- a linear adaptive weighted minimum variance power system stabiliser is proposed.
- the control structure of the SMIB power system equipped with the proposed linear adaptive power system stabiliser is given.

Algorithm 3.1 proposed in Subsection 3.4.2 can be used for the implementation of the three important linear adaptive controllers as discussed in Subsection 3.3.2 (see Remark 3.3.1). Based on the discussions of the features associated with each control law in Subsection 3.3.2, the weighted minimum variance control law is adopted for the development of the linear adaptive power system stabiliser. As indicated previously, the advantage of using this control law is that it facilitates the development of a corresponding nonlinear control law and the comparison of system performance of the *linear* and *nonlinear* adaptive control strategies.

With the selections of $\bar{P}(q^{-1}) = \bar{R}(q^{-1}) = 1$ and $\bar{Q}(q^{-1}) = \lambda^{\frac{1}{2}}$, Algorithm 3.1 immediately results in a *direct* SISO linear adaptive weighted minimum variance controller. Furthermore, it is assumed that $C(q^{-1}) = 1$ in the LNM (3.17)-(3.19) in which the time delay $d = 1$. From (3.33)-(3.35), it follows that the estimated *controller* parameters of the polynomials $\hat{L}(k, q^{-1})$, $\hat{P}(k, q^{-1})$, and $\hat{M}(k, q^{-1})$ in Algorithm 3.1 can be constructed *directly* by the estimated *model* parameters of the polynomials $\hat{A}(k, q^{-1})$

and $\hat{B}(k, q^{-1})$ of the LNM, i.e.,

$$\hat{L}(k, q^{-1}) = \hat{B}(k, q^{-1}) + \frac{\lambda}{\hat{b}_0(k)},$$

$$\hat{P}(k, q^{-1}) = [1 - \hat{A}(k, q^{-1})]q,$$

and

$$\hat{M}(k, q^{-1}) = 1.$$

The incremental notations for the input and output signals of the LNM are used, and the control law (3.51) can then be reconstructed *directly* by the estimated parameters of the LNM, i.e.,

$$\phi(k)^T \hat{\Theta}(k) + \frac{\lambda}{\hat{b}_0(k)} \Delta u(k) = 0 \tag{3.52}$$

where

$$\hat{\Theta}(k)^T \triangleq \left[\begin{array}{cccccc} \hat{a}_1(k) & \hat{a}_2(k) & \hat{a}_3(k) & \hat{b}_0(k) & \hat{b}_1(k) & \hat{b}_2(k) \end{array} \right], \tag{3.53}$$

$$\phi(k)^T \triangleq \left[\begin{array}{cccccc} -\Delta y(k) & -\Delta y(k-1) & -\Delta y(k-2) & \Delta u(k) & \Delta u(k-1) & \Delta u(k-2) \end{array} \right]. \tag{3.54}$$

Hence, an *indirect* SISO linear adaptive weighted minimum variance control law for the LNM can be developed from Algorithm 3.1, and is given by Algorithms 3.2(A) and 3.2(B) for the parameter estimation and the calculation of the control input, respectively.

Algorithm 3.2(A) [indirect SISO linear stochastic adaptive weighted minimum variance control algorithm — parameter estimation.]

Estimate:

$$\hat{\Theta}(k) = \hat{\Theta}(k-1) + P(k-1)\phi(k-1)\left[\Delta y(k) - \Delta \hat{y}(k)\right];$$

Covariance:

$$P(k-1) = \left[P(k-2) - \frac{P(k-2)\phi(k-1)\phi(k-1)^T P(k-2)}{\mu(k-1) + \phi(k-1)^T P(k-2)\phi(k-1)}\right] \frac{1}{\mu(k-1)};$$

Prediction:

$$\Delta \hat{y}(k) = \phi(k-1)^T \hat{\Theta}(k-1);$$

Error:

$$e(k) = \Delta y(k) - \Delta \hat{y}(k);$$

Forgetting Factor:

$$\mu_0(k) = 1 - \frac{e(k)^2}{1 + \phi(k-1)^T P(k-2)\phi(k-1)} \frac{1}{\Sigma_0},$$

$$\bar{\mu}(k) = \begin{cases} \mu_0(k) & \text{if } \mu_0(k) \geq \mu_{min} > 0 \\ \mu_{min} & \text{otherwise} \end{cases},$$

$$\mu(k) = \begin{cases} \bar{\mu}(k) & \text{if } \dfrac{\text{trace}[P(k-1)]}{\bar{\mu}(k)} < C \\ 1 & \text{otherwise} \end{cases};$$

where $k \geq 1$, $P(-1) = K_0 I$ $(0 < K_0 < C)$, and $\mu(0) = 1$. Σ_0, μ_{min}, and C are preselected positive constants. $\hat{\Theta}(k)$ and $\phi(k)$ are defined by (3.53) and (3.54), respectively. $\hat{\Theta}(0)$ is given.

$\nabla \nabla \nabla$

In practice, the control signal $\Delta u(k)$ in (3.52) is bounded by physical limits. The control law (3.52) is then modified to form the desired *Linear Adaptive Weighted Minimum Variance Power System Stabiliser* (**LAWMV-PSS**) which is described as

Algorithm 3.2(B) [indirect SISO linear stochastic adaptive weighted minimum variance control algorithm — control law.]

$$u^0(k) = \frac{\hat{b}_0(k)}{\hat{b}_0(k)^2 + \lambda} \left\{ \left[\hat{A}(k, q^{-1}) - 1 \right] q \Delta y(k) - \left[\hat{B}(k, q^{-1}) - \hat{b}_0(k) \right] \Delta u(k) \right\}, \quad (3.55)$$

$$\Delta u(k) = \begin{cases} u_{max} & \text{if } u^0(k) \geq u_{max} \\ u^0(k) & \text{if } u_{min} < u^0(k) < u_{max} \\ u_{min} & \text{if } u^0(k) \leq u_{min} \end{cases}; \quad (3.56)$$

where λ is the weighting coefficient, u_{max} and u_{min} are known constants, and the estimated parameters are provided by Algorithm 3.2(A).

$\nabla \nabla \nabla$

Clearly, the calculation of the control action of the LAWMV-PSS is a two-step procedure:

- the recursive least squares algorithm with the time-varying forgetting factor (Algorithm 3.2(A)) provides the estimated parameters of the LNM;
- the control law (3.55)-(3.56) (Algorithm 3.2(B)) generates the control signal by the use of the estimates of the LNM.

Remark 3.5.1 *The advantage of using an indirect form of the control algorithm (Algorithms 3.2(A)-(B)) is that the requirements in Remark 3.4.1(i)-(ii) need not be involved. Also, since the control law (3.55)-(3.56) is constructed by the estimated parameters of the LNM, intermediate calculations of the controller parameters are not needed.*

The system to be stabilised is a SMIB power system, the models of which have been derived in Subsection 2.3.1. The control structure of the system equipped with the proposed LAWMV-PSS is illustrated in Fig. 3.1. The stabilising signal, $\Delta y(k)$, is the deviation of the machine electrical power, $\Delta P_e(k)$ (or torque, $\Delta T_e(k)$). The performance of the LAWMV-PSS will be evaluated in Section 3.6.

Remark 3.5.2 *It should be pointed out that the output trajectory $y^*(k)$ in Fig. 3.1 can be provided by feeding back the output variable $y(k)$ through a low-pass filter. The frequency of the low-pass filter should be designed such that any rotor oscillations can be attenuated while the maximum rate of the loading due to the mechanical system can be followed. However, for the sake of simplicity, $y^*(k)$ is set, artificially, to be the reference power ($P_{ref}(k)$) in the simulation studies of this chapter. The same approach will be utilised in Chapters 4 to 6.*

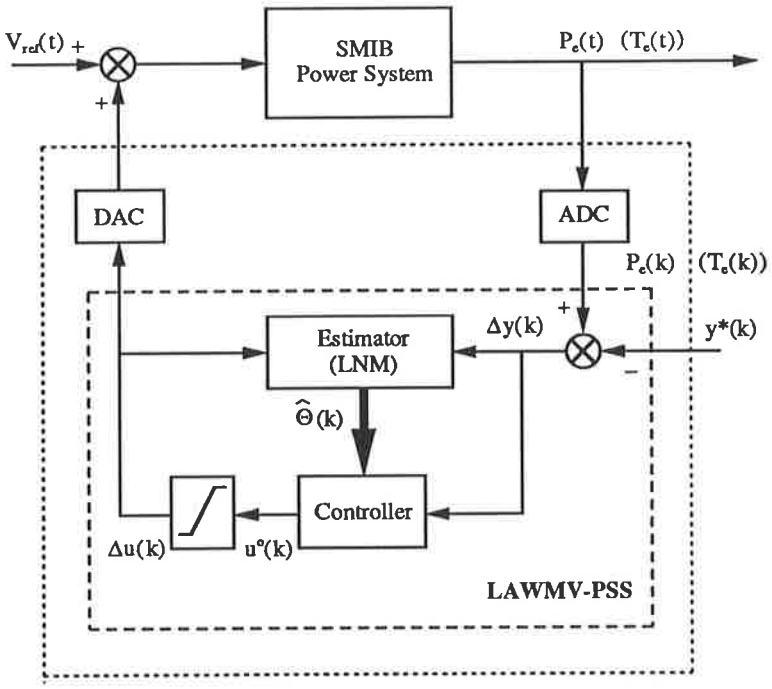

Figure 3.1: Control structure of the SMIB power system with the LAWMV-PSS.

3.6 Evaluation of the Performance of the Linear Adaptive Weighted Minimum Variance Power System Stabiliser.

In this section:

- the validity of the LNM derived in Subsection 3.2.3 to represent the nonlinear power system (CSM3) is verified through *external equivalent* studies;
- the performance of the LAWMV-PSS proposed in Section 3.5 is evaluated through simulation studies;
- the robustness of the LAWMV-PSS is tested with unmodelled dynamics and modelling errors.

The LAWMV-PSS proposed in Section 3.5 is implemented via excitation control of the SMIB power system modelled in Subsection 2.3.1. The steam turbine of the power system is controlled by the conventional speed-governor as described in Appendix A.

A sampling period of 20 ms is chosen for the simulation studies of this chapter as well as the following chapters. This period has been used in laboratory experiments in the literature and found to be satisfactory [68,71,67].

The *procedure* for the simulation studies in this section is as follows:

- The LAWMV-PSS is *initially* designed for the CSM3 ($D = 4.0$ pu), the performance of which has been verified, in Subsection 2.3.2, to give the satisfactory agreement with that of the higher-order, more accurate model of the actual power system (CSM1 with $D = 0.1$ pu). A series of simulation studies will be conducted for the CSM3 equipped with the LAWMV-PSS to evaluate the performance of the LAWMV-PSS.
- The effectiveness of the LAWMV-PSS will be *further* tested through robustness studies. The major issues of concern in this type of study have been explained in Subsection 2.3.2. The simulation studies will involve the replacement of the CSM3 by the CSM1, and will include different situations in which the LAWMV-PSS is subjected to unmodelled dynamics and modelling errors. These studies will confirm the validity of the proposed LAWMV-PSS.

Note that this *procedure* will be *followed* by the simulation studies in Chapters 4 to 6 for the evaluation of the nonlinear optimal and adaptive power system stabilisers which will be designed later.

To fulfill the above *procedure*, three **Stages** of simulation studies are conducted:

Stage 1: Verification and identification of the LNM — to examine the performance of the estimated LNM in tracking and predicting the dynamics of the nonlinear power system (CSM3) at different system operating points with different system configurations.

Stage 2: Evaluation of the performance of the LAWMV-PSS — to compare the dynamic and transient behaviour of the LAWMV-PSS with that of a well-designed conventional power system stabiliser at different operating conditions and under fault conditions.

Stage 3: Studies on the robustness of the LAWMV-PSS — to test the performance of the LAWMV-PSS when the CSM3 is replaced by the CSM1.

The implementation of the above three **Stages** will be discussed in the following Subsections 3.6.1, 3.6.2, and 3.6.3, respectively. The parameters and limits associated with the SMIB power system and the LAWMV-PSS are listed in Appendix C. The simulation results obtained from this section will be used as a *reference* for the comparisons of system performance of the linear and nonlinear control approaches in Chapters 4 and 6.

3.6.1 Verification and Identification of the Linearised Nominal Model of the Power System.

In this subsection the validity of using the estimated LNM to represent the nonlinear power system (CSM3 with $D = 4.0$ pu) is verified through simulation studies at different system operating points with different system configurations. The output signal is the machine electrical torque deviation, $\Delta T_e(k)$. This subsection is the implementation of **Stage 1**.

Aims and structure of the simulation studies.

The nonlinear power system (CSM3 with $D = 4.0$ pu) is operating at a specified steady-state operating point. An *external Pseudo Random Binary Sequence* **(PRBS)** signal is used as the control signal $u(k)$ which is injected into the summing junction of the input of the AVR to excite the dynamics of the nonlinear power system. The PRBS signal as well as the sampled output signal ($\Delta T_e(k)$) from the CSM3 is fed into

the estimator, the model of which is the LNM. At each sampling instant, the estimator generates the estimated parameters ($\hat{\Theta}(k)$) and the predicted output ($\Delta\hat{T}_e(k)$) by the implementation of the recursive least squares algorithm with the time-varying forgetting factor (Algorithm 3.2(A)). The configuration of this study is given by Fig. 3.2 [5]. The aims of this study are

- to confirm that the estimated LNM is an adequate representation of the CSM3;
- to examine the convergence of the estimated parameters;
- to verify the output tracking ability of the estimated LNM at different system operating conditions.

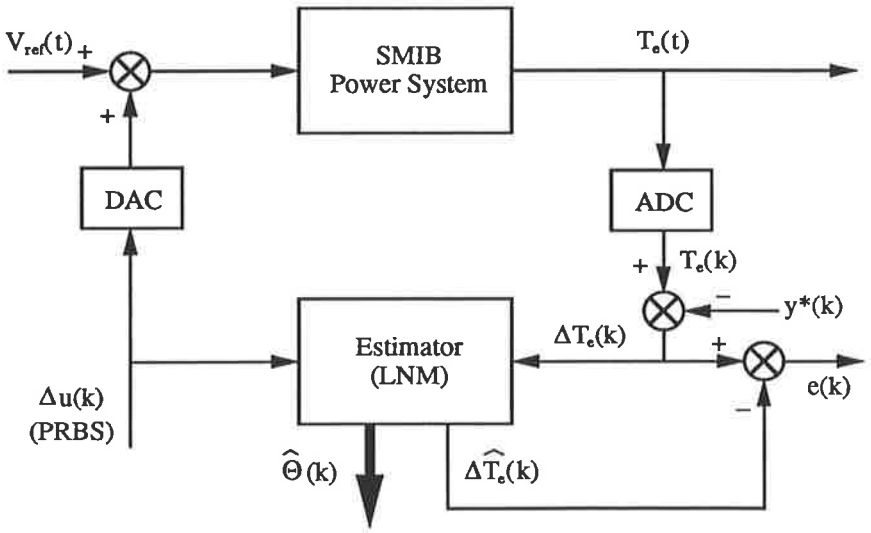

Figure 3.2: Structure of the verification and identification of the LNM.

The PRBS signal is generated by a seventh-order shift register. The step length and clock period of this signal are chosen to be 100 ms, and its amplitude 0.002 pu, causing about 2% perturbation about the specified operating point.

A variety of system operating points have been tested. Two of them are selected as examples:

[5] See Remark 3.5.2 for the explanation of the signal $y^*(k)$ in Fig. 3.2.

- Lagging Operating Point: $P_t = 0.6$ pu, $Q_t = 0.3$ pu, $V_t = 1.0$ pu;
- Leading Operating Point: $P_t = 0.4$ pu, $Q_t = -0.1$ pu, $V_t = 1.0$ pu.

Three simulation studies at the above two operating points are constructed as follows:

Case 1: The system is operating at the lagging operating point with the *original* system parameters (as listed in Appendix C).

Case 2: The system is operating at the leading operating point with the *original* system parameters.

Case 3: The system is operating at the lagging operating point with the *original* system parameters *except* that the value of the transmission line reactance, X_e, is doubled; this represents a change in the system configuration.

The simulation results associated with these three cases are given by Figs. 3.3-3.4 and Tables 3.1-3.2. The estimator parameters are: $K_0 = 10^4$, $C = 10^5$, $\mu_{min} = 0.2$, and $\Sigma_0 = 0.8$. The initial value of the estimate, $\hat{\Theta}(0)$, is set to zero.

Analysis of the simulation results.

The estimated parameters of the LNM in Case 1 are plotted in Fig. 3.3. It is seen that all estimates converge satisfactorily. The responses of the electrical torque deviation of the generator and its prediction of the estimated LNM in this case are superimposed in Fig. 3.4, from which it is seen that the estimated LNM describes the dynamic characteristics of the machine electrical torque deviation around this operating condition. These conclusions about the convergence of the estimated model parameters and the output tracking ability of the LNM in Case 1 are also applicable entirely to Cases 2 and 3 the graphs of which are, therefore, omitted.

Notice that Cases 1 and 2 represent the situation in which the power system works at *different* operating points with the *same* system configuration, while Cases 1 and 3 represent the situation in which the power system works at the *same* operating point

but with *different* system configurations. To demonstrate the ability of the LNM to identify the power system in different system operating environments, two tables of simulation results are given by Tables 3.1-3.2. Table 3.1 shows the converged values of the estimates of the LNM for the three simulation cases, while Table 3.2 lists the identified zeros of the polynomials of the LNM for each case. It is seen that if the system operating point and/or the system configuration change, the estimated parameters of the LNM change, resulting in the changes of the identified zeros of the polynomials of the LNM. It is then evident that the estimated LNM can adapt to the changes in the system operating environment by giving different sets of estimates as well as polynomial zeros in its *linear* representation.

	$\hat{a}_1$	$\hat{a}_2$	$\hat{a}_3$	$\hat{b}_0$	$\hat{b}_1$	$\hat{b}_2$
Case 1	-1.2623	-0.2932	0.5975	0.0424	0.0472	-0.0245
Case 2	-1.2540	-0.2677	0.5730	0.0462	0.0568	-0.0189
Case 3	-1.2921	-0.2840	0.6037	0.0315	0.0371	-0.0259

Table 3.1: Estimated parameters of the LNM for Cases 1-3.

		zero 1	**zero 2**	**zero 3**
Case 1	$\hat{A}(q^{-1})$	-0.6423	0.9523+j0.1527	0.9523-j0.1527
	$\hat{B}(q^{-1})$	0.3860	-1.4995	
Case 2	$\hat{A}(q^{-1})$	-0.6275	0.9408+j0.1673	0.9408-j0.1673
	$\hat{B}(q^{-1})$	0.2720	-1.5019	
Case 3	$\hat{A}(q^{-1})$	-0.6377	0.9649+j0.1248	0.9649-j0.1248
	$\hat{B}(q^{-1})$	0.4921	-1.6720	

Table 3.2: Identified zeros of the polynomials of the LNM for Cases 1-3.

Conclusions.

From the above studies, it is concluded that:

1. The estimated LNM is a good representation of the CSM3 at different operating conditions.

2. The estimated LNM possesses the ability to track and predict the dynamics of the CSM3 in different system operating environments.

3.6.2 Evaluation of the Performance of the LAWMV-PSS for the CSM3.

In this subsection the evaluation of the performance of the LAWMV-PSS is conducted for the CSM3 ($D = 4.0$ pu) through a series of simulation studies. The performance of the CSM3 *without* a power system stabiliser is taken as the performance of the **original system**, and the performance of the CSM3 equipped with the LAWMV-PSS will be compared with that of the CSM3 equipped with a conventional power system stabiliser. This subsection is the implementation of **Stage 2**.

The design of a conventional power system stabiliser.

To provide a basis for the evaluation of the performance of the LAWMV-PSS, a conventional power system stabiliser is designed for the CSM3 at a chosen operating point. The basic principle for the design of a conventional power system stabiliser is to provide an additional electrical damping torque that is in phase with the shaft speed deviation of the generator, i.e., $\Delta T_d = D_d \Delta\omega$, where ΔT_d is the desired damping torque and D_d is the damping coefficient. A variety of design methods are available in the literature, and a robust design method proposed in [122,34] is used in this thesis to construct the desired characteristic of the conventional power system stabiliser for the CSM3. The

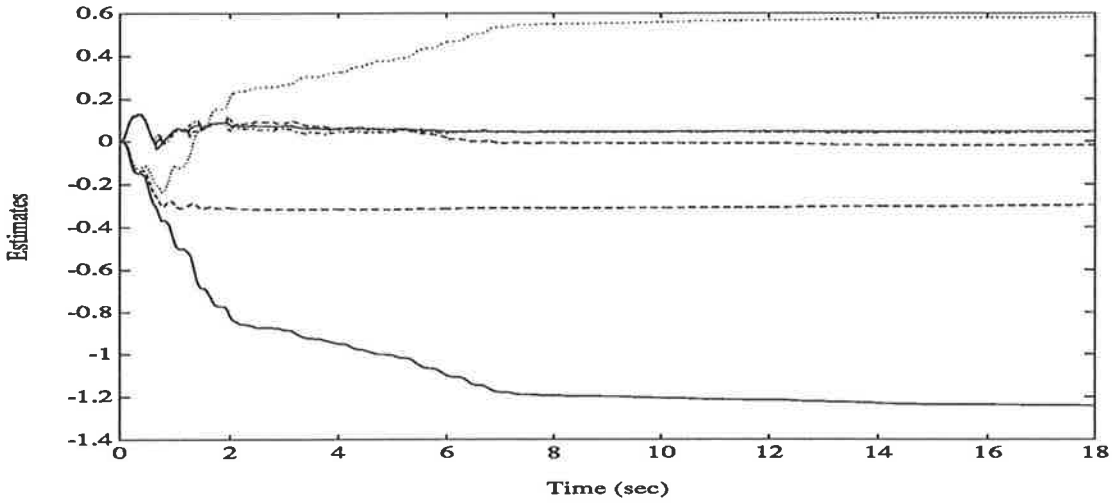

Figure 3.3: Estimated parameters of the LNM for Case 1 (lagging operating point with original system parameters).

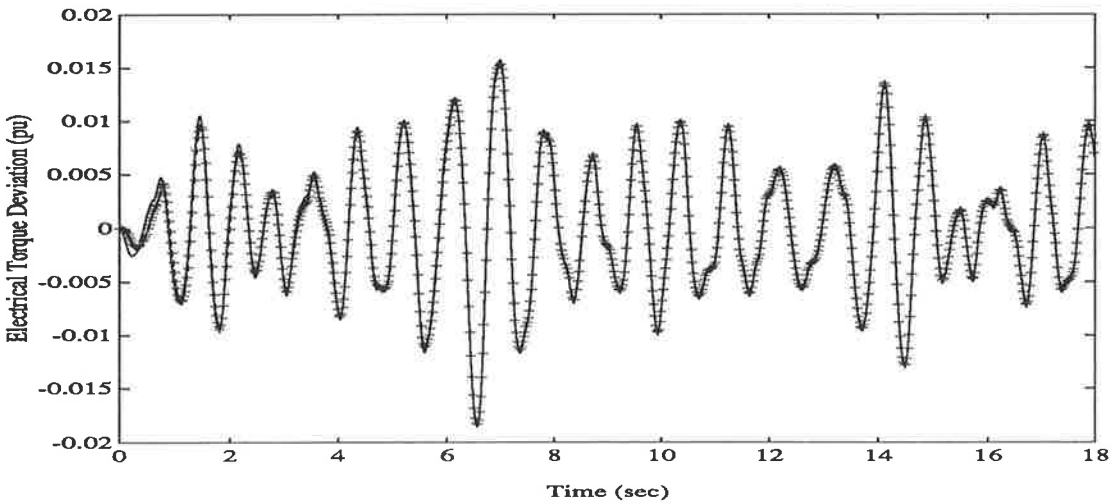

Figure 3.4: Electrical torque deviation response for Case 1 (lagging operating point with original system parameters). CSM3 - solid line, LNM - line marked by '+'.

stabiliser with speed input takes the form

$$PSS_{\omega}(s) = D_d \frac{\tau_{\omega} s}{1 + \tau_{\omega} s} \frac{1}{K_m} \frac{(1 + s\tau_{pss1})(1 + s\tau_{pss2})}{(1 + s\tau_{pss3})(1 + s\tau_{pss4})}. \tag{3.57}$$

A washout stage has been included in (3.57) to eliminate the steady-state offset in the stabilising signal. The term $\frac{1}{K_m} \frac{(1 + s\tau_{pss1})(1 + s\tau_{pss2})}{(1 + s\tau_{pss3})(1 + s\tau_{pss4})}$ accounts for the so-called PVr characteristic of the generator [122,34]. Since the electrical torque (or power) has been chosen as the stabilising signal in this thesis, an ideal stabiliser for the electrical torque (or power) input is derived from (3.57), given by

$$PSS_{p}(s) = -D_d \frac{\tau_{p} s}{1 + \tau_{p} s} \frac{1}{2Hs} \frac{1}{K_m} \frac{(1 + s\tau_{pss1})(1 + s\tau_{pss2})}{(1 + s\tau_{pss3})(1 + s\tau_{pss4})}. \tag{3.58}$$

Equation (3.58) forms the transfer function of the desired *Conventional Power System Stabiliser* **(CPSS)**. For a chosen steady-state operating point of the CSM3: $P_t = 0.6$ pu, $Q_t = 0.3$ pu, and $V_t = 1.0$ pu, the fixed parameters of the CPSS in (3.58) are listed in Appendix C. The performance of the LAWMV-PSS will be compared with that of the CPSS designed with $D_d = 20$ pu.

Remark 3.6.1 *A higher value of D_d (say, $D_d = 30$ or 40 pu) may give better damping effects in small dynamics, but may present worse performance during large transients (e.g., three-phase faults). Therefore, a value of 20 pu is used as a compromise in the design of the CPSS in this thesis.*

Aims and structure of the simulation studies.

The control structure of the CSM3 equipped with the LAWMV-PSS is described by Fig. 3.1. Alternatively, replacing the dotted-line box in Fig. 3.1 by the transfer function (3.58), one obtains the control structure of the CSM3 with the use of the designed CPSS. Also, removing the dotted-line box in Fig. 3.1 results in the control structure of the **original system**. In this subsection each simulation study will be conducted for the *three* control structures of the CSM3 to evaluate the system performance under the different control schemes. The electrical torque deviation is used as the stabilising signal. The aims of this study are

- to demonstrate that the CPSS is properly designed;
- to confirm that the proposed LAWMV-PSS is superior to the CPSS ($D_d = 20$ pu) at various system operating conditions;
- to establish a reference for the comparisons of the performance of the linear and nonlinear optimal/adaptive control approaches in Subsections 4.5.2 and 6.5.2.

Five **Groups** of simulation studies are conducted to evaluate the damping performance of the LAWMV-PSS at various system operating conditions:

Group 1: *Dynamic Response* — the performance of the LAWMV-PSS is assessed by simulating the changes in the system operating point. Three simulation studies are given:

Study 1: The generator is operating at $P_t = 0.6$ pu and $Q_t = 0.3$ pu, and is subjected to periodic variations in reference power (column 2 of Table 3.3).

Study 2: The generator is operating at $P_t = 0.6$ pu and $Q_t = -0.1$ pu, and is subjected to periodic variations in reference power (column 2 of Table 3.3).

Study 3: The generator is operating at $P_t = 0.6$ pu and $Q_t = 0.3$ pu, and is subjected to periodic variations in reactive power between lagging and leading power factors (column 3 of Table 3.3). [6]

Group 2: *Transient Response* — the performance of the LAWMV-PSS is assessed by simulating three-phase faults on the receiving end busbars or at the machine terminal. Three simulation studies are given:

Study 4: The generator is operating at $P_t = 0.65$ pu and $Q_t = 0.3$ pu, and is subjected to a three-phase fault on the receiving end busbars. The fault is cleared in 100 ms and the system returns to its pre-fault operating condition.

Study 5: The generator is operating at $P_t = 0.55$ pu and $Q_t = -0.1$ pu, and is subjected to a three-phase fault of 100 ms duration at the machine terminal.

[6] The periodic variations in reactive power (Q_t) are simulated by varying the value of the infinite bus voltage (V_∞) accordingly.

The line is switched out after the fault, and a new operating condition is established.

Study 6: The generator is operating at $P_t = 0.65$ pu and $Q_t = 0.3$ pu, and is subjected to two successive three-phase faults on the receiving end busbars, each of duration 100 ms. The first fault is cleared by returning the system to its pre-fault operating condition. The second fault is cleared by opening both ends of the line, and the system returns to its pre-fault output power with the value of the transmission line reactance doubled.

Group 3: *Response to the Changes in the System Configuration* — the performance of the LAWMV-PSS is assessed by simulating the changes in the transmission line system. One simulation study is given:

Study 7: The generator is operating at $P_t = 0.55$ pu and $Q_t = 0.3$ pu, and is subjected to two successive changes in the transmission line system: one transmission line is opened, causing the value of the transmission line reactance to be doubled; the opened line is then reclosed and the value of the transmission line reactance returns to its initial value.

Group 4: *Response to External Disturbances* — the performance of the LAWMV-PSS is assessed by simulating the variations in reference voltage. Two simulation studies are given:

Study 8: The generator is operating at $P_t = 0.6$ pu and $Q_t = 0.3$ pu, and is subjected to periodic disturbances in reference voltage (column 4 of Table 3.3).

Study 9: The generator is operating at $P_t = 0.6$ pu and $Q_t = -0.1$ pu, and is subjected to periodic disturbances in reference voltage (column 4 of Table 3.3).

Group 5: *Response to Unstable System Oscillations* — the performance of the LAWMV-PSS is assessed by simulating large excursions in the system operating point which is beyond the stability region of the original system. Two simulation studies are given:

Study 10: The generator is operating at $P_t = 0.6$ pu and $Q_t = 0.3$ pu, and is subjected to large periodic excursions in reference power (column 5 of Table 3.3).

Study 11: The generator is operating at $P_t = 0.6$ pu and $Q_t = -0.1$ pu, and is subjected to large periodic excursions in reference power (column 5 of Table 3.3).

The simulation results of **Studies 1-11** are plotted in Figs. 3.5-3.17. In each study, three dynamic responses — of the original system, the CSM3 with the CPSS, and the CSM3 with the LAWMV-PSS — are shown. Identical controller output limits, $u_{min} = -0.05$ pu and $u_{max} = 0.05$ pu, are used in the CPSS and the LAWMV-PSS. The same limits will be used to construct the nonlinear power system stabilisers to be designed in Chapters 4 to 6. The weighting coefficient λ of the LAWMV-PSS is adjusted to be 0.4. Note that **Studies 1-11** form *a series of* **evaluation studies** to be conducted in Chapters 4 to 6 to evaluate and compare the system damping performance associated with different control approaches. For the sake of simplicity, in the sequel the titles of these simulation studies will be quoted directly without repeating the detailed explanations.

Remark 3.6.2 *To avoid radical variations in the estimated parameters of the LAWMV-PSS, a fixed-length freezing time period can be applied to the estimator to suspend the estimation of the parameters for a short period of time following the onset of a fault. Such a technique has been widely used for simulation studies in the literature [50,57,71,72,60,61,67], and is adopted in this thesis for simulation purposes. A length of 120 ms (1.2 times the usual fault duration) freezing time period is arranged in the simulation software upon the occurrence of a fault. Practically, switch logic can be used to turn the estimator off automatically. The switch logic can be operated by the detection of a sudden terminal voltage drop greater than a certain amount, say* 30%, *of its ordinary level [60]. It can also be operated by using other practical techniques [57,71,72,61,67].*

Time (sec) (from-to)	**Studies 1-2** P_t (pu)	**Study 3** Q_t (pu)	**Studies 8-9** V_t (pu)	**Studies 10-11** P_t (pu)
0 — 0.5	0.60	0.30	1.00	0.60
0.5 — 10.5	0.65	-0.1	1.02	0.90
10.5 — 20.5	0.55	0.30	0.98	0.30
20.5 — 30.5	0.65	-0.1	1.02	0.90
30.5 — 40.0	0.60	0.30	1.00	0.60

Table 3.3: Variations in the system operating point of the CSM3 for Studies 1-3 and 8-11.

Analysis of the simulation results.

Group 1: From Study 1 to Study 3, the *dynamic performance* of the LAWMV-PSS is examined by simulating the periodic changes in the system operating point at the lagging and leading power factors. The simulation results are shown in Figs. 3.5-3.7. It is seen that in dynamic situations, both the LAWMV-PSS and the CPSS can provide an adequate damping torque to the oscillations of the original system. The CPSS works well for small changes in the system operaing point. Though the difference in system performance associated with the CPSS and the LAWMV-PSS is not significant, the LAWMV-PSS shows a faster output tracking ability than the CPSS.

Group 2: From Study 4 to Study 6, the *transient performance* of the LAWMV-PSS is examined by simulating the three-phase faults in the transmission line system. The simulation results are plotted in Figs. 3.8-3.11. It is seen from Fig. 3.8 that with the occurrence of a remote fault followed by a recovery of the pre-fault operating condition, the CPSS can stabilise the system after a few swings. However, when the fault is severe (as shown in Fig. 3.9) and/or when the fault is followed by a change in the system configuration (as shown in Fig. 3.9 after the fault and in Fig. 3.11 after the second fault), the original system tends to be unstable and the CPSS barely damps the system oscillations. Under these circumstances, the LAWMV-PSS provides stronger

damping than the CPSS to retrieve the system from the unstable state. It is evident that the transient behaviour of the LAWMV-PSS is more effective than that of the CPSS.

Remark 3.6.3 *Figure 3.10 illustrates the field voltage $E_{FD}(t)$ response for the test in Study 5. The conclusions regarding the field voltage responses of the different power system stabilisers support those made for the torque responses. Further to this, the field voltage response of the LAWMV-PSS shows that the LAWMV-PSS can provide a control action with appropriate amplitude and phase, resulting in the stronger damping of the rotor oscillations as revealed by the responses.*

Group 3: In Study 7, the *ability* of the LAWMV-PSS to track the changes in the system parameters and configuration is examined. With one transmission line switching out and in, the parameters of the power system become time-varying, causing the changes in the parameters associated with the models of the LAWMV-PSS and the CPSS. With fixed parameters, the CPSS can not adapt to the system changes on-line. Consequently, as shown in Fig. 3.12, the damping performance of the CPSS is worse than that of the LAWMV-PSS, the parameters of which (plotted in Fig. 3.13) are self-adjusted on-line.

Group 4: From Study 8 and Study 9, the *ability* of the LAWMV-PSS to overcome the external disturbances of the system is examined. The simulation results are given in Figs. 3.14-3.15. In these two cases, the LAWMV-PSS provides better damping than the CPSS. An advantage associated with the LAWMV-PSS is that it reflects the effects of the external disturbances through the inclusion of a noise term in the estimated LNM, thus it gives a fast control action to the external disturbances.

Group 5: From Study 10 and Study 11, the *ability* of the LAWMV-PSS to extend the system stability region is examined. Figures 3.16-3.17 show the simulation results. It is seen that with the large excursions in the system operating point, the original system responses to the step changes towards 0.9 pu power are unstable both at lagging and leading power factors. The CPSS can stabilise the system unstable oscillations in the lagging operating condition, as shown in Fig. 3.16. However, it fails to do so in

the leading operating condition, as shown in Fig. 3.17 during 10.5-20.5 seconds. The LAWMV-PSS can successfully damp the system unstable oscillations in both cases. There is no doubt that the LAWMV-PSS can extend the system stability region beyond the capacity of the CPSS. Nevertheless, it is demonstrated that although the CPSS is designed for a chosen operating point, it can implement the stabilising task over a certain range of operating conditions.

Conclusions.

From the analysis of the simulation results in this subsection, it is concluded that:

1. The CPSS is well designed, and possesses robust characteristics to be able to work when the system operating conditions change.

2. The CPSS (D_d = 20 pu) and the LAWMV-PSS are comparable for the small and less severe disturbances covered by Studies 1-3 and 8-9. As indicated in Remark 3.6.1, higher values of D_d (e.g., 30 pu) can be used in practice, which may give improved damping performance for small and less severe disturbances.

3. The LAWMV-PSS is more effective than the CPSS in improving the system damping performance and extending the system stability region in different operating environments following major disturbances and for large increase in transmission line reactance. This can be seen by comparing the settling times of the relevant output response curves. With the use of the LAWMV-PSS, the settling time is greatly reduced.

3.6.3 Studies on the Robustness of the LAWMV-PSS for the CSM1.

In this subsection the robustness of the LAWMV-PSS is tested with unmodelled dynamics and modelling errors. This subsection is the implementation of **Stage 3.**

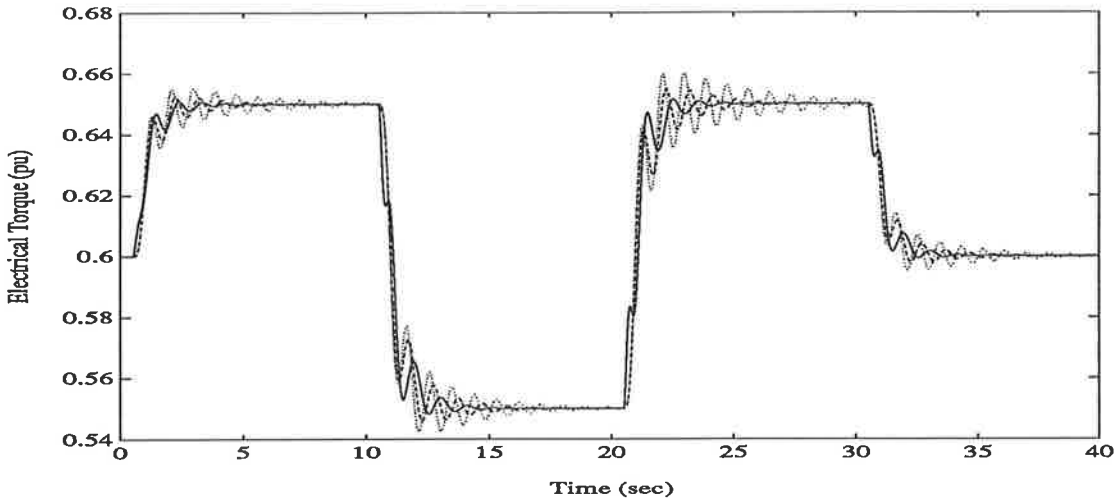

Figure 3.5: Electrical torque response for Study 1 ($P_t = 0.6$ pu, $Q_t = 0.3$ pu; periodic variations in reference power). CSM3 with the LAWMV-PSS - solid line, CSM3 with the CPSS - dashed line, CSM3 only - dotted line.

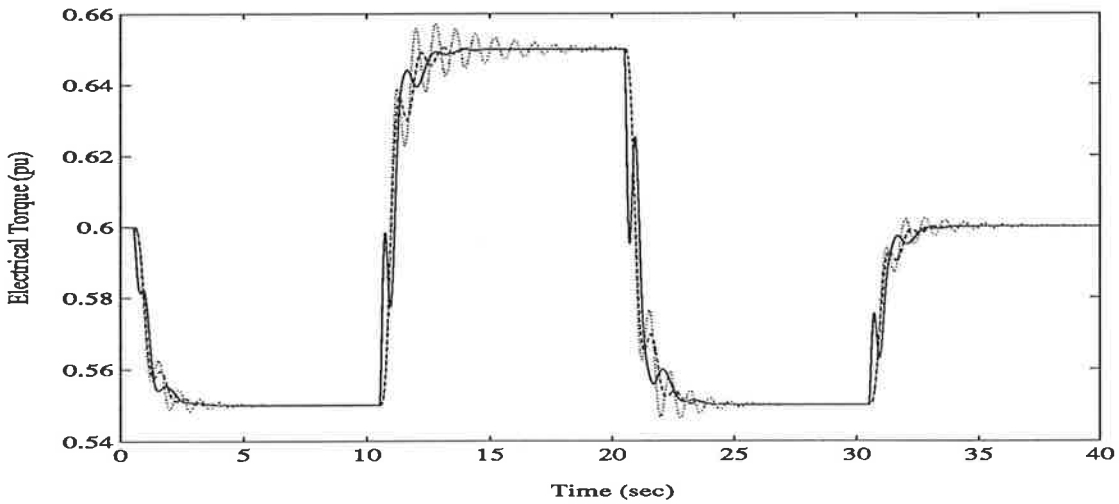

Figure 3.6: Electrical torque response for Study 2 ($P_t = 0.6$ pu, $Q_t = -0.1$ pu; periodic variations in reference power). CSM3 with the LAWMV-PSS - solid line, CSM3 with the CPSS - dashed line, CSM3 only - dotted line.

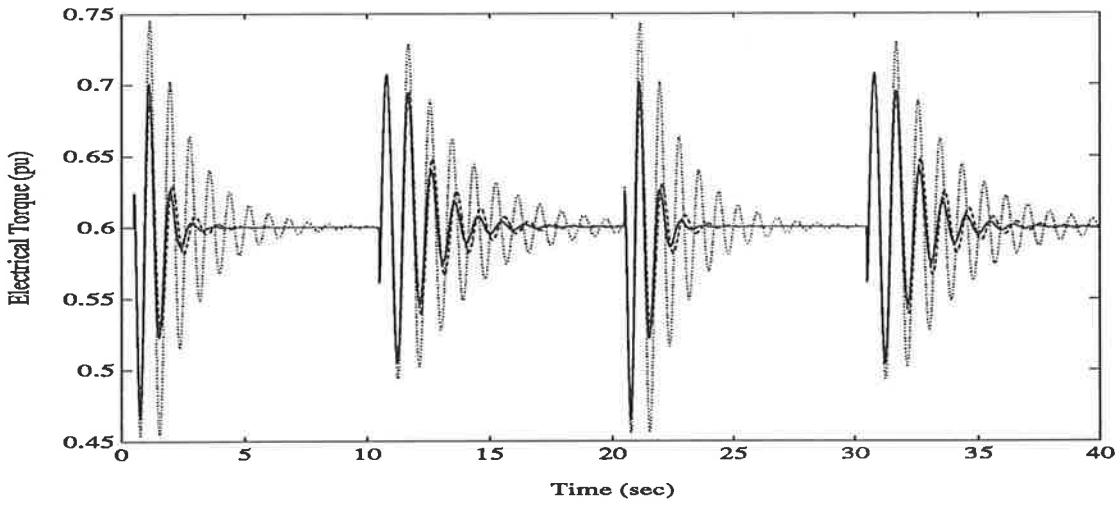

Figure 3.7: Electrical torque response for Study 3 ($P_t = 0.6$ pu, $Q_t = 0.3$ pu; periodic variations in reactive power between lagging and leading operating conditions). CSM3 with the LAWMV-PSS - solid line, CSM3 with the CPSS - dashed line, CSM3 only - dotted line.

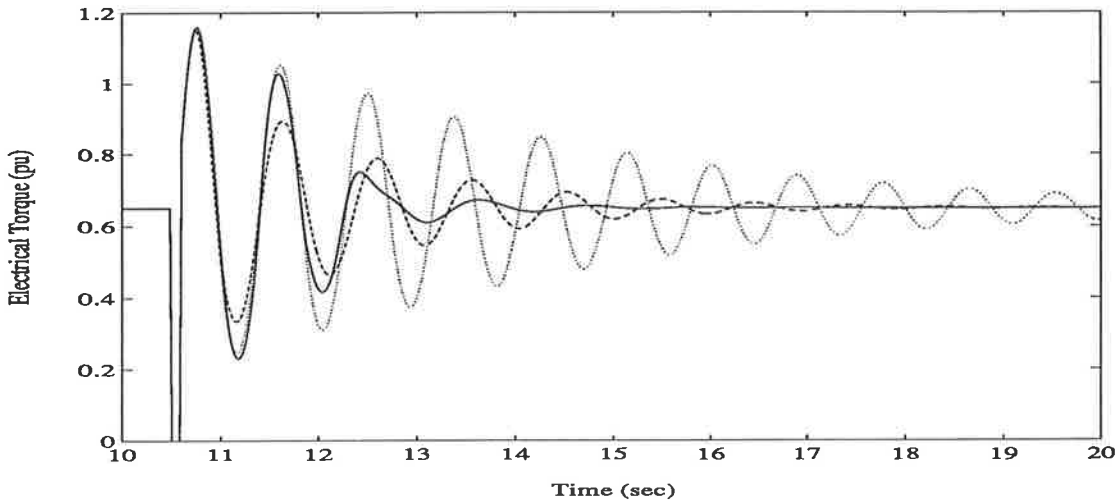

Figure 3.8: Electrical torque response for Study 4 ($P_t = 0.65$ pu, $Q_t = 0.3$ pu; 100 ms short-circuit on the receiving end busbars). CSM3 with the LAWMV-PSS - solid line, CSM3 with the CPSS - dashed line, CSM3 only - dotted line.

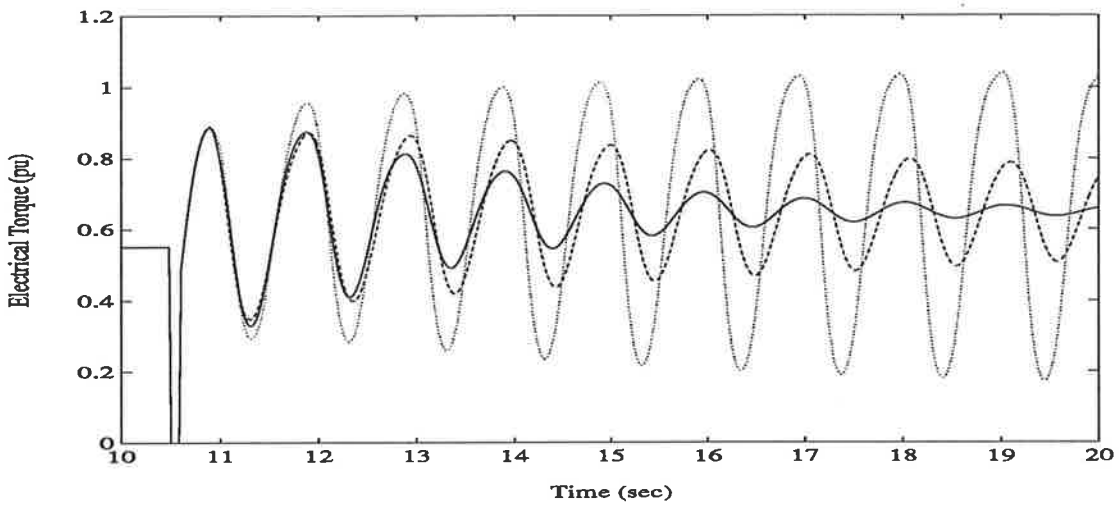

Figure 3.9: Electrical torque response for Study 5 ($P_t = 0.55$ pu, $Q_t = -0.1$ pu; 100 ms short-circuit at the machine terminal). CSM3 with the LAWMV-PSS - solid line, CSM3 with the CPSS - dashed line, CSM3 only - dotted line.

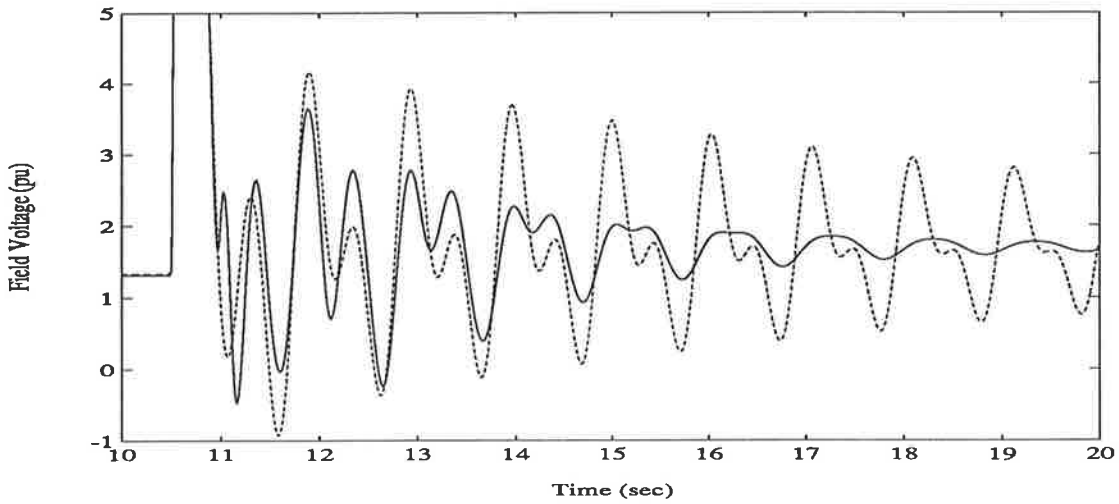

Figure 3.10: Field voltage response for Study 5 ($P_t = 0.55$ pu, $Q_t = -0.1$ pu; 100 ms short-circuit at the machine terminal). CSM3 with the LAWMV-PSS - solid line, CSM3 with the CPSS - dashed line.

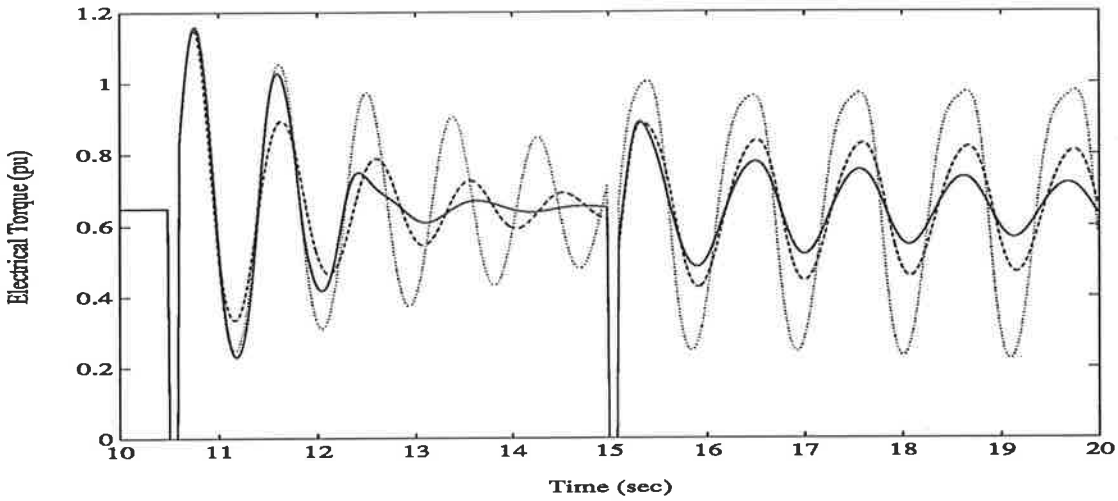

Figure 3.11: Electrical torque response for Study 6 ($P_t = 0.65$ pu, $Q_t = 0.3$ pu; two successive faults of 100 ms duration on the receiving end busbars). CSM3 with the LAWMV-PSS - solid line, CSM3 with the CPSS - dashed line, CSM3 only - dotted line.

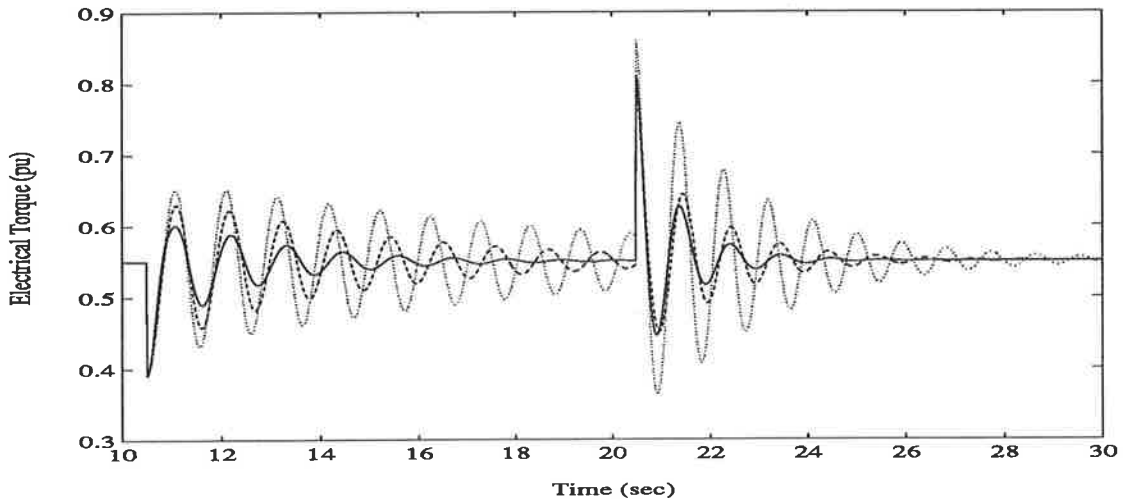

Figure 3.12: Electrical torque response for Study 7 ($P_t = 0.55$ pu, $Q_t = 0.3$ pu; one transmission line is opened and then reclosed). CSM3 with the LAWMV-PSS - solid line, CSM3 with the CPSS - dashed line, CSM3 only - dotted line.

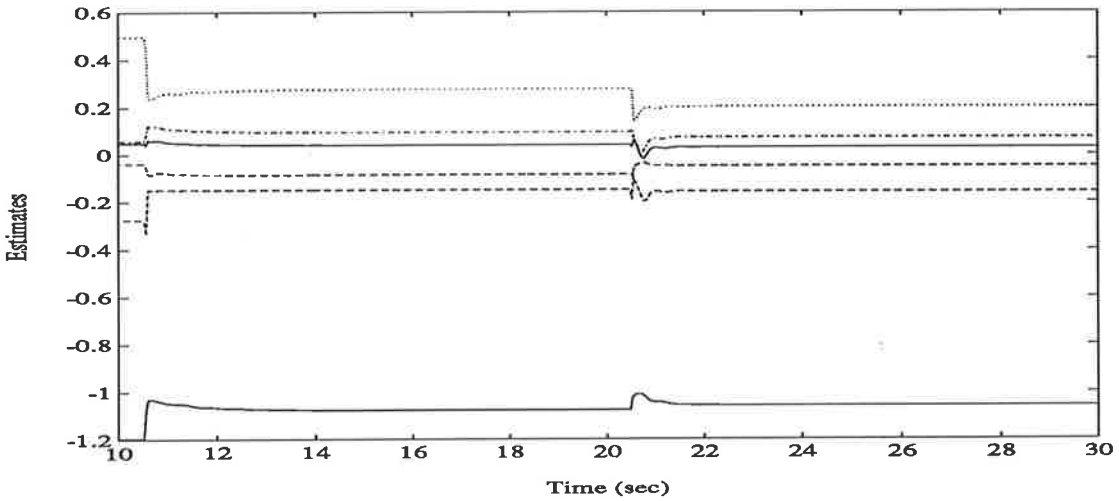

Figure 3.13: Estimated parameters of the LNM for Study 7 ($P_t = 0.55$ pu, $Q_t = 0.3$ pu; one transmission line is opened and then reclosed).

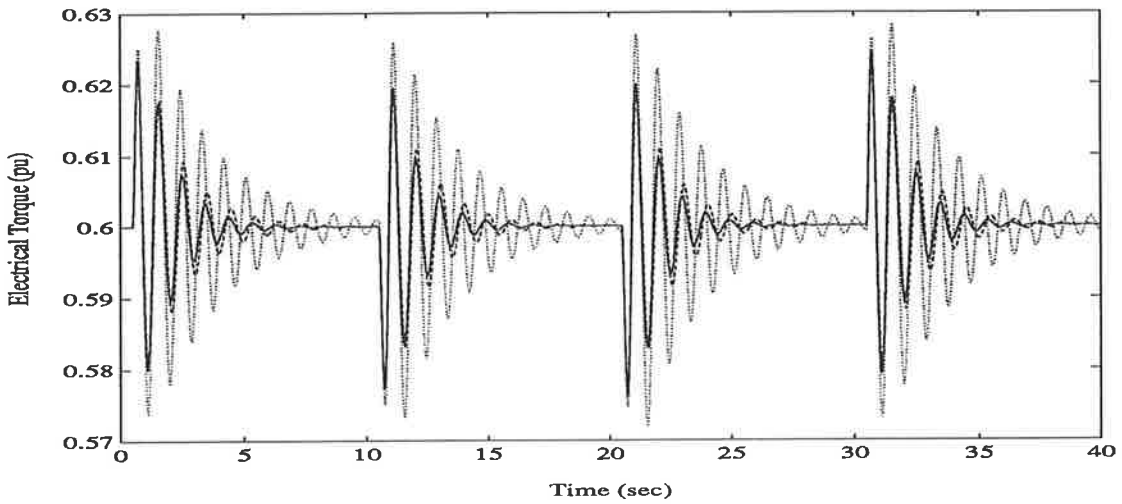

Figure 3.14: Electrical torque response for Study 8 ($P_t = 0.6$ pu, $Q_t = 0.3$ pu; periodic disturbances in reference voltage). CSM3 with the LAWMV-PSS - solid line, CSM3 with the CPSS - dashed line, CSM3 only - dotted line.

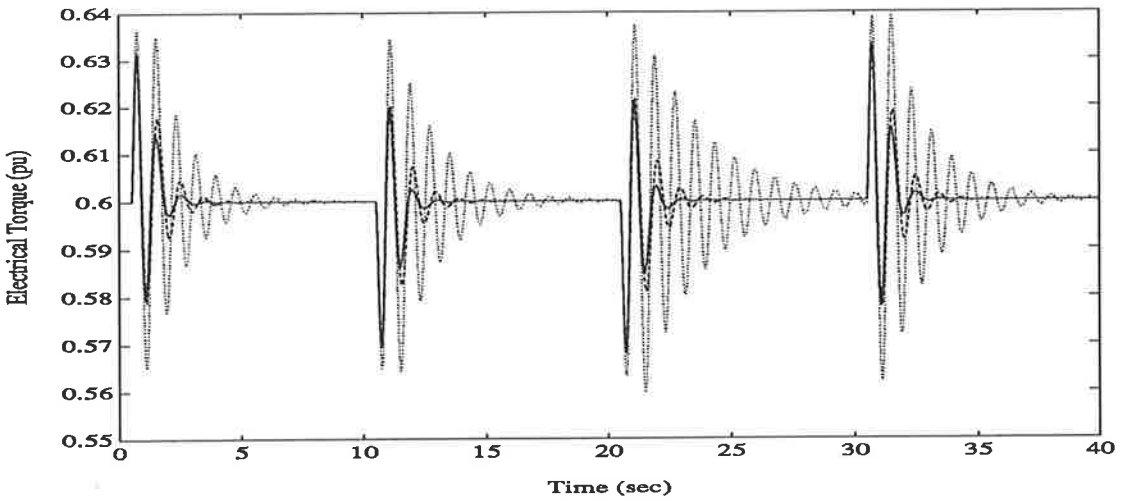

Figure 3.15: Electrical torque response for Study 9 ($P_t = 0.6$ pu, $Q_t = -0.1$ pu; periodic disturbances in reference voltage). CSM3 with the LAWMV-PSS - solid line, CSM3 with the CPSS - dashed line, CSM3 only - dotted line.

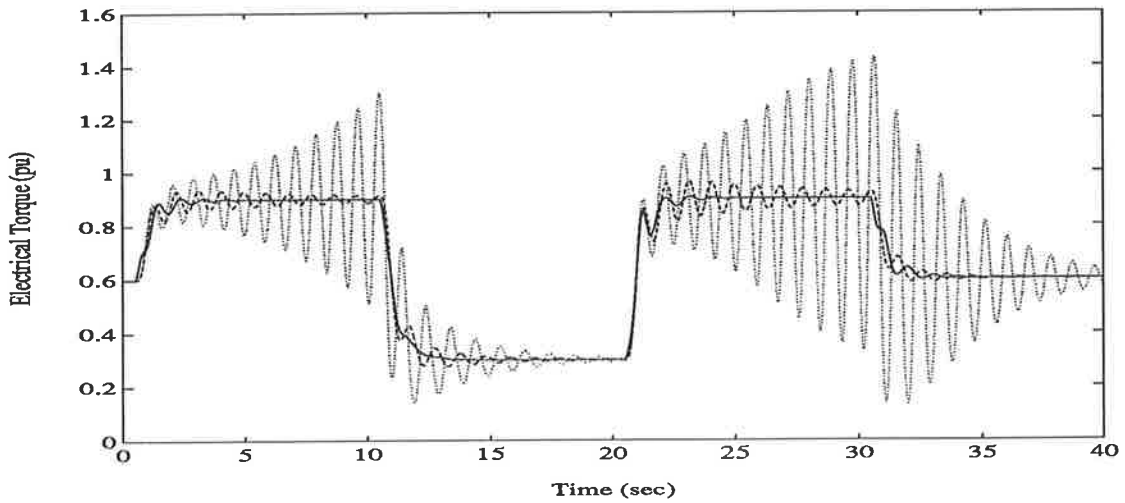

Figure 3.16: Electrical torque response for Study 10 ($P_t = 0.6$ pu, $Q_t = 0.3$ pu; large periodic excursions in reference power). CSM3 with the LAWMV-PSS - solid line, CSM3 with the CPSS - dashed line, CSM3 only - dotted line.

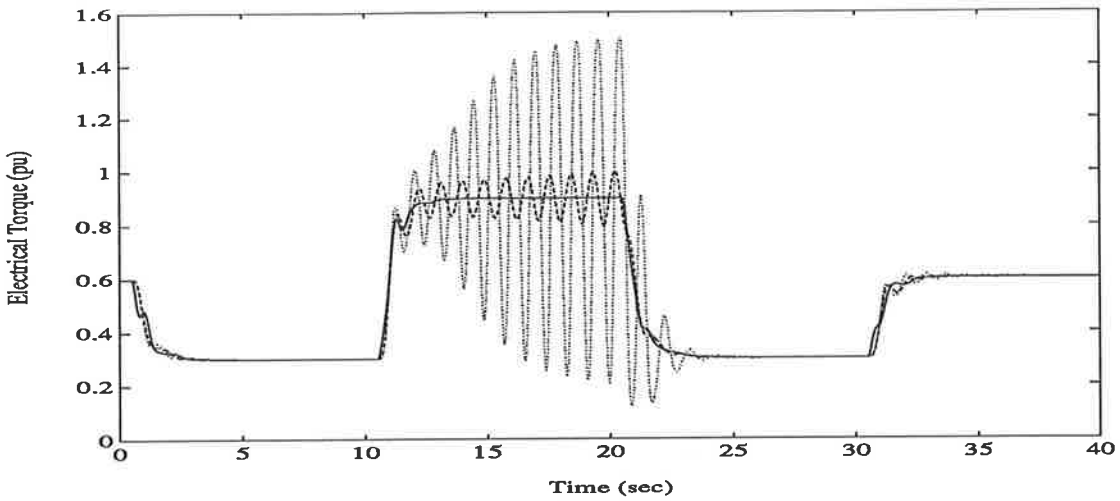

Figure 3.17: Electrical torque response for Study 11 ($P_t = 0.6$ pu, $Q_t = -0.1$ pu; large periodic excursions in reference power). CSM3 with the LAWMV-PSS - solid line, CSM3 with the CPSS - dashed line, CSM3 only - dotted line.

Aims and structure of the simulation studies.

The CSM3 ($D = 4.0$ pu) is replaced by the CSM1 ($D = 0.1$ pu) in the *three* control structures of the power system arranged in **Stage 2**. The performance of the LAWMV-PSS is further evaluated with a higher-order, more accurate model of the power system. Higher-order dynamics are therefore present. Since the assumption of $\omega(t) \approx 1$ pu is not included in the modelling of the CSM1, the stabilising signal is taken to be the electrical power deviation. The aims of this study are

- to confirm the performance of the LAWMV-PSS for the actual power system represented by the more accurate model (CSM1);
- to establish a reference for the comparisons of the performance of the linear and nonlinear control approaches with unmodelled dynamics and modelling errors in Subsections 4.5.3 and 6.5.3.

A variety of simulation studies have been conducted for the above purposes. It is found that the conclusions drawn from the simulation studies of **Stage 2** are applicable to the simulation studies of this **Stage**. Brief examples are given in the following two **Groups** of studies to illustrate the dynamic and transient behaviour of the SMIB power system (CSM1) with the LAWMV-PSS:

Group 1: *Dynamic Response* — the performance of the LAWMV-PSS is assessed by simulating the step variations in the system operating point. Two simulation studies are given:

Study 12: The generator is operating at $P_t = 0.6$ pu and $Q_t = 0.3$ pu, and is subjected to a step change of 0.1 pu increase in reference power.

Study 13: The generator is operating at $P_t = 0.6$ pu and $Q_t = -0.1$ pu, and is subjected to a step change of 0.1 pu increase in reference power.

Group 2: *Transient Response* — the performance of the LAWMV-PSS is assessed by simulating three-phase faults in the transmission line system. Two simulation studies are given:

Study 14: The generator is operating at $P_t = 0.6$ pu and $Q_t = 0.3$ pu, and is subjected to a three-phase fault on the receiving end busbars. The fault is cleared in 100 ms and the system returns to its pre-fault operating condition.

Study 15: The generator is operating at $P_t = 0.6$ pu and $Q_t = -0.1$ pu, and is subjected to a three-phase fault of 100 ms duration at the machine terminal. The line is switched out after the fault, and a new operating point is established.

The simulation results of **Studies 12-15** are given by Figs. 3.18-3.21, each showing three responses associated with the original system (CSM1), the CSM1 with the CPSS, and the CSM1 with the LAWMV-PSS. Note that **Studies 12-15** form *a series of* **robustness studies** to be conducted in Chapters 4 to 6 to evaluate and compare the system damping performance associated with different control approaches. Again, in the sequel the titles of these simulation studies will be quoted directly without repeating the detailed explanations.

Analysis of the simulation results.

Group 1: In Studies 12-13, the *dynamic performance* of the LAWMV-PSS associated with the CSM1 is examined. It is seen from Figs. 3.18-3.19 that both the CPSS and the LAWMV-PSS can work well in dynamic conditions. This coincides with the performance of Studies 1-3 shown in Figs. 3.5-3.7. The LAWMV-PSS exhibits a better damping effect and a faster output tracking ability when compared with the CPSS.

Group 2: In Studies 14-15, the *transient performance* of the LAWMV-PSS associated with the CSM1 is illustrated in Figs. 3.20-3.21. Though the CPSS eventually damps the system oscillations in Study 14, it gives unstable performance for the severe fault in Study 15. This indicates that the CPSS designed for the CSM3 can not be used to control the actual power system (CSM1) for the large or major disturbances considered in these studies. The LAWMV-PSS, however, leads the CSM1 to be stable in each case and provides more damping to the system oscillations.

Conclusions.

The above analysis reveals the following facts:

1. The LAWMV-PSS can cope with the unmodelled dynamics and the modelling errors at the various operating conditions, thus it is valid for controlling the higher-order actual power system.

2. The LAWMV-PSS can improve the system damping performance in dynamic and transient situations and can extend the system stability region.

3. The overall system performance associated with the LAWMV-PSS is superior to that with the CPSS.

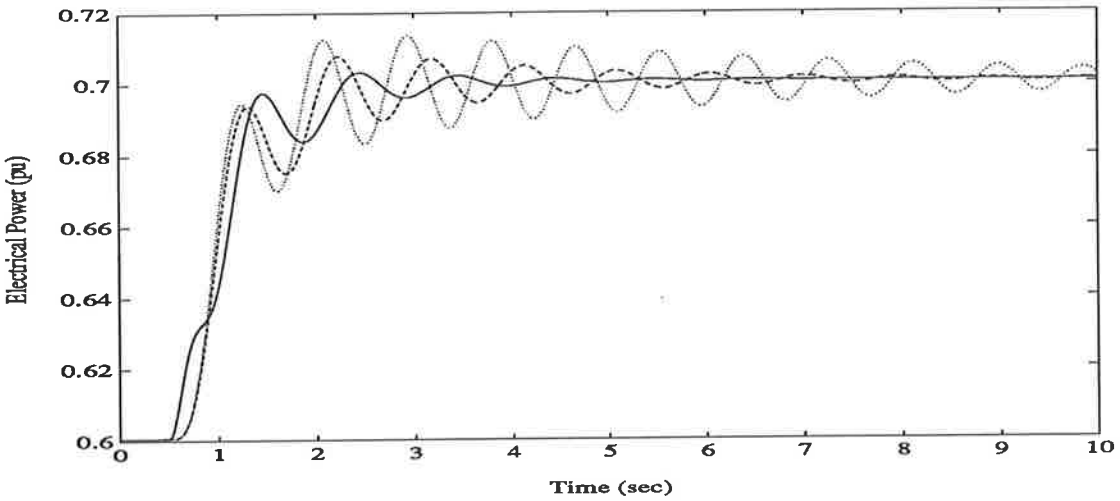

Figure 3.18: Electrical power response for Study 12 ($P_t = 0.6$ pu, $Q_t = 0.3$ pu; step change in reference power). CSM1 with the LAWMV-PSS - solid line, CSM1 with the CPSS - dashed line, CSM1 only - dotted line.

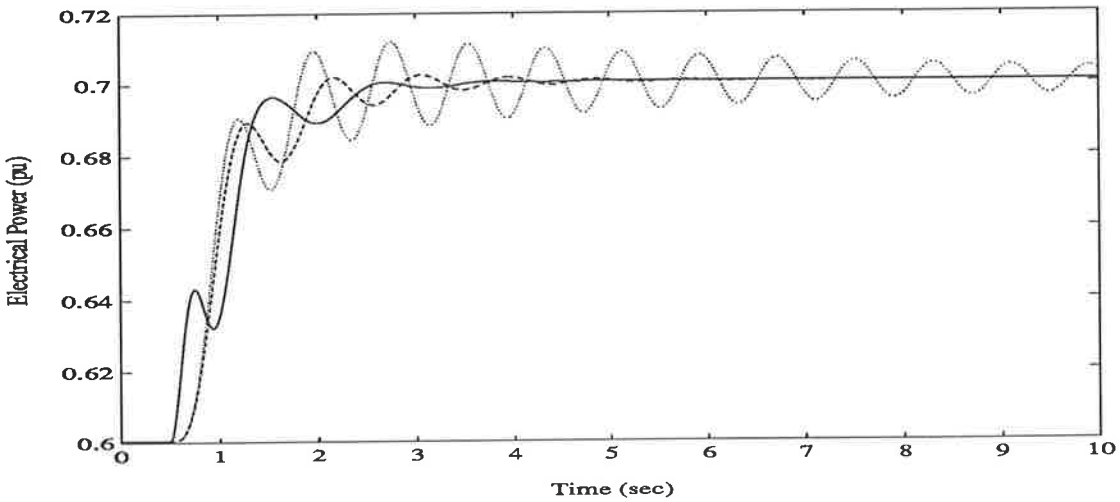

Figure 3.19: Electrical power response for Study 13 ($P_t = 0.6$ pu, $Q_t = -0.1$ pu; step change in reference power). CSM1 with the LAWMV-PSS - solid line, CSM1 with the CPSS - dashed line, CSM1 only - dotted line.

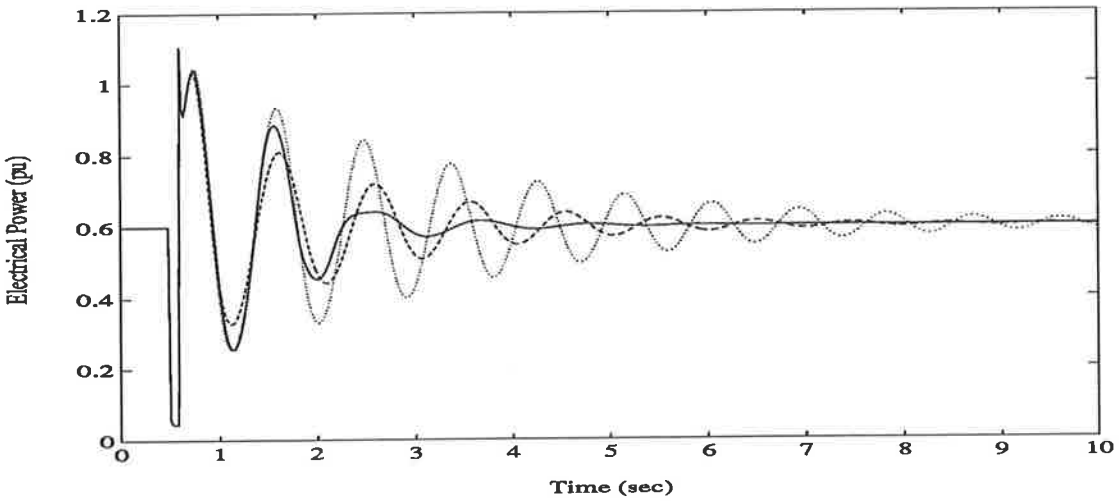

Figure 3.20: Electrical power response for Study 14 ($P_t = 0.6$ pu, $Q_t = 0.3$ pu; 100 ms short-circuit on the receiving end busbars). CSM1 with the LAWMV-PSS - solid line, CSM1 with the CPSS - dashed line, CSM1 only - dotted line.

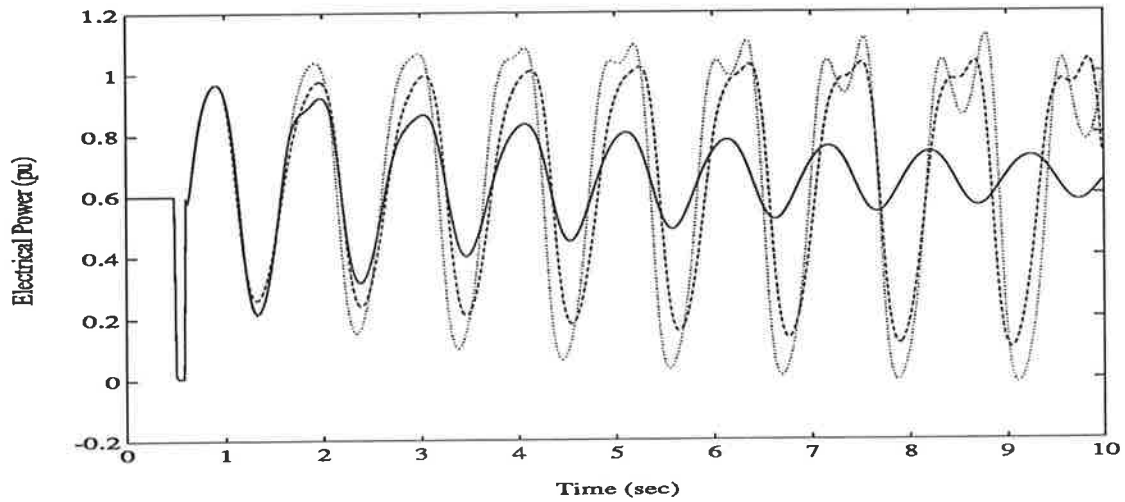

Figure 3.21: Electrical power response for Study 15 ($P_t = 0.6$ pu, $Q_t = -0.1$ pu; 100 ms short-circuit at the machine terminal). CSM1 with the LAWMV-PSS - solid line, CSM1 with the CPSS - dashed line, CSM1 only - dotted line.

3.7 Concluding Remarks.

In this chapter the design and implementation of a *linear adaptive* power system stabiliser for the SMIB power system modelled in Subsection 2.3.1 is discussed. The aim of this study is to establish a sound basis for the development and evaluation of the nonlinear optimal/adaptive power system stabilisers to be conducted in Chapters 4 to 6.

In Section 3.2 the linearised nominal model (LNM) of the nonlinear SMIB power system is derived from the simplified linearised analytical model (SLAM) given in Subsection 2.4.2. The order of the LNM is determined by making use of the conclusions drawn in Section 2.6. The derivation procedure shows clearly the insight of this model. The validity of this model to represent the nonlinear power system is further confirmed through the external equivalent studies presented in Subsection 3.6.1. The derived LNM provides a basis for the development of the linear adaptive power system stabiliser.

Linear stochastic optimal control laws are derived and discussed in Section 3.3 under a general form of the cost function. Aspects associated with the application of these control laws to the design of linear adaptive power system stabilisers are summarised under the general requirements essential for the design. The selection of the weighted minimum variance control law for the design of the linear adaptive power system stabiliser in this thesis is finalised. This control law is simple and robust, satisfying the general requirements mentioned above. Also, since a high-gain AVR is usually used in the excitation control system, the steady-state tracking error associated with this control law is very small. In the selection of this control law for the design of the linear adaptive power system stabiliser, special consideration is given to the feasibility of this control law for the development of the corresponding nonlinear control laws. This will facilitate the comparisons of the performance of the linear and nonlinear control approaches to be conducted in Chapters 4 and 6.

For the implementation of an adaptive power system stabiliser, parameter estimation algorithms suitable for on-line model identification of power systems are briefly

discussed in Section 3.4. The recursive least squares algorithm with the time-varying forgetting factor is adopted as the basic parameter estimation algorithm for the design of adaptive stabilisers in this thesis. A direct SISO linear adaptive generalised minimum variance control algorithm (Algorithm 3.1) is then developed from the combination of the optimal control law with the selected parameter estimation algorithm. This control algorithm establishes a basis for the development of the desired linear adaptive power system stabiliser.

A linear adaptive weighted minimum variance power system stabiliser (LAWMV-PSS) for the SMIB power system given in Subsection 2.3.1 is then proposed in Section 3.5. The LAWMV-PSS is implemented by an indirect control algorithm (Algorithms 3.2(A)-(B)) which produces the estimated parameters of the LNM and generates the control action by using directly the model estimates.

In Section 3.6 the performance of the SMIB power system with the LAWMV-PSS is assessed through simulation studies. A series of evaluation studies (Studies 1-11) and robustness studies (Studies 12-15) is described to form a systematic way of comparisons of system performance with different control approaches. These studies cover a wide range of system operating conditions and working environments. To provide a valid basis for the evaluation of the performance of the LAWMV-PSS, a robust conventional power system stabiliser (CPSS) is designed and implemented. The effectiveness of the LAWMV-PSS is then tested through the comparison of the system performance with the CPSS in the same simulation study. The simulation results shown in Figs. 3.5-3.21 indicate that the LAWMV-PSS is more robust and superior to the CPSS, particularly for more severe disturbances. The LAWMV-PSS significantly improves the system damping performance in the various dynamic and transient situations, and extends the system stability region effectively. The provision of the simulation results in this chapter establishes a valid reference to be used for the evaluation of system performance of the nonlinear control approaches in Chapters 4 to 6.

The extensions in this chapter to the previous work described in the literature have been listed in Section 3.1.

Chapter 4

SISO Nonlinear Optimal Power System Stabilisers.

4.1 Introduction.

In this chapter the design of *SISO nonlinear optimal* power system stabilisers is discussed. This establishes an important basis for the development of the nonlinear adaptive power system stabilisers to be conducted in Chapters 5 and 6. It also forms a link between the linear and nonlinear adaptive control approaches, the performance of which will be compared in Chapter 6.

As indicated in Section 3.1, linear adaptive control schemes have been proposed for the design of power system stabilisers in order to overcome the shortcomings of the conventional power system stabilisers in adapting to the variations of system operating conditions. By changing its parameters on-line, a linear adaptive power system stabiliser can cope with the nonlinearities and the time-varying properties associated with a nonlinear power system, so that it improves the system damping performance. However, since a linear adaptive power system stabiliser is based on a linearised nominal model for the design and implementation of the control law, the performance associated with the linear adaptive power system stabiliser may depend heavily on several factors, such as the order of the linearised nominal model, the convergence rate of the on-line

estimated parameters, etc.. For each variation in the operating conditions of the nonlinear power system, the parameters of the linearised nominal model have to change in order to track the changes in the system operating point. There exists, therefore, a transition in the identified parameters of the linearised nominal model between two system operating conditions. Before the identified parameters converge to their new values, the control action of the linear adaptive power system stabiliser may not be optimal, and the associated damping performance of the system may not be as good as expected.

The nonlinearities of power systems are often known. In Section 2.4 the nonlinearities associated with the power system given in Subsection 2.3.1 have been classified into the *inherent nonlinearities* and the *intentional nonlinearities*, and have been modelled accurately in the mathematical descriptions of the system. It is reasonable to expect that the system damping performance will be *better* if the nonlinear characteristics of the system are taken into account in the construction of the control law. The resulting control law would be *nonlinear* and should *inherently* possess the ability of stabilising the nonlinear power system over the range of the operating conditions of concern.

The design of such a nonlinear control law requires a nonlinear nominal model which should contain the nonlinearities of the system and should, inherently, track the changes in the system operating point without changing its parameters. A *nonlinear fixed-parameter* power system stabiliser designed on these principles is therefore expected to perform better than a *linear adaptive* power system stabiliser in that

- the control action should be optimal in the new operating point immediately;
- the system transition from one operating point to another should be optimal.

Different approaches that are utilised to incorporate the nonlinearities of the power system into the design of the control laws result in different nonlinear control schemes. In the literature, several attempts have been made to design power system controllers based on nonlinear models of the power systems [127]-[132]. For instance, a quasi-linearisation technique was used to obtain a nonlinear excitation controller [129], and

a nonlinear output-feedback control method was employed to construct an excitation control system for a fast acting static exciter [131]. As nonlinear control theory develops [77,174,175,176,177,178,179,180,76,181], advanced approaches are tested in the design of power system controllers [182,78,79,80,81,82,83,84,85,87]. For example, nonlinear decoupling theory has been applied to the design of nonlinear excitation and governor controllers using state-variable feedback [182]. A direct feedback linearising control technique [77] has been utilised to design an excitation controller which is composed of a complete linearising compensator and an output robust optimal feedback controller [80,82]. A similar control technique has been used to design a nonlinear variable structure excitation controller [83]. An exact linearisation design method for scalar nonlinear control systems has also been employed to construct a nonlinear excitation controller [85]. Using the feedback linearisation method, a multivariable linearising feedback controller has been derived and simulated for a synchronous generator [87]. In this chapter a *new* nonlinear optimal control law is developed for the design of the power system stabiliser for the SMIB power system given in Subsection 2.3.1. The nonlinear optimal control law will be given in a regression form which will facilitate the development of the corresponding nonlinear adaptive control laws to be discussed in Chapters 5 and 6.

Original work on the *analysis*, *design*, and *evaluation* of a nonlinear optimal power system stabiliser will be conducted in this chapter. The work involves the derivation of a nonlinear nominal model, the development of the nonlinear optimal control laws, the establishment of the closed-loop system stability conditions, the development of a nonlinear optimal power system stabiliser, and the assessment of the system damping performance with the nonlinear optimal stabiliser.

The organisation of this chapter is as follows. In Section 4.2 a nonlinear nominal model for the design of the nonlinear optimal and adaptive power system stabilisers is derived from the NAM given in Subsection 2.4.1. The SISO nonlinear stochastic generalised minimum variance control law is developed and its closed-loop stability conditions are established in Section 4.3. In Section 4.4 the nonlinear stochastic weighted minimum variance control law is presented and its global closed-loop stability conditions are analysed. A nonlinear optimal power system stabiliser is then proposed. In

Section 4.5 the performance of the proposed nonlinear optimal power system stabiliser is assessed through simulation studies, and is compared with that of the LAWMV-PSS developed in Chapter 3.

To the author's knowledge, the research reported in this chapter is **original**; the main contributions are:

1. A *new* SISO discrete-time input-output model (in terms of a nonlinear nominal model) is derived from the NAM given in Subsection 2.4.1. A rigorous mathematical derivation is presented, and the boundedness of the variables in the model is established. This model contains the inherent nonlinearities of the SMIB power system and is an accurate representation of the continuous-time nonlinear power system (CSM3) provided that certain assumptions are satisfied. The nonlinear model is formulated in a regression equation, linear in the parameters and in the control input. It thus provides an important basis for the development of the nonlinear optimal and adaptive control laws.

2. A *new* SISO nonlinear stochastic generalised minimum variance control law is derived from a general form of the cost function for the nonlinear nominal model. The closed-loop stability conditions with this control law are established and the associated proof is given in Section E.1 of Appendix E.

3. A *new* SISO nonlinear stochastic weighted minimum variance control law is developed and its global closed-loop stability conditions are established. The associated proof is presented in Section E.2 of Appendix E.

4. A *new* nonlinear optimal power system stabiliser based on the nonlinear weighted minimum variance control scheme is proposed, and its practical aspects are discussed. The control structure of the SMIB power system equipped with the proposed nonlinear optimal power system stabiliser is illustrated.

5. Simulation studies on the evaluation of the resulting nonlinear optimal power system stabiliser are conducted. A series of useful comparisons with the LAWMV-PSS is given.

It should be pointed out that while there is an extensive body of linear control theory for designing linear control systems, there are *no* general methods for specific nonlinear systems. For this reason, in this chapter nonlinear control laws have been developed *specifically* for the nonlinear nominal model proposed in Section 4.2, and the relevant proofs of lemmas and theorems have been established. This work provides a basis for extending these approaches to other forms of nonlinear power system models.

4.2 SISO Nonlinear Input-Output Power System Modelling.

In this section:

- a *new* SISO nonlinear *continuous-time* input-output model is derived from the NAM given in Subsection 2.4.1;
- the associated SISO nonlinear *discrete-time* input-output model is developed;
- a *new nonlinear* **nominal model** [1] is formed and will be used for the design of the nonlinear optimal and adaptive power system stabilisers;
- the boundedness of the system variables and noise in these models is discussed, and the *Bounded-Input Bounded-Output* **(BIBO)** stability of the nonlinear nominal model is established.

In a similar manner as for linear control methodologies, the first problem associated with nonlinear control methodologies is the development of the *nominal models* of the nonlinear dynamic systems. For the design of conventional power system stabilisers in the literature, the nominal model of the power system is usually taken as a linearised time-invariant form in which the parameters and/or the system operating conditions are fixed. In the design of the linear adaptive power system stabiliser discussed in Chapter 3, a linearised time-varying nominal model (LNM) is derived in order

[1] The definition of a "nominal model" used in this thesis has been given in Section 3.2.

to match more closely the practical nonlinear time-varying power system. However, no single *linearised* nominal model can represent the nonlinear power system *accurately*. A key feature in developing a nonlinear control scheme, be it a nonlinear optimal control scheme or a nonlinear adaptive control scheme, for the design of the power system stabiliser is that a *nonlinear nominal model* is derived *directly* from the mathematical description of the nonlinear power system itself. Thus, inherently, the nonlinear nominal model will represent the nonlinear system *accurately*, and track any changes in the system operating point *automatically*.

A general review of the nonlinear nominal models used to represent nonlinear dynamic systems for a wide range of applications is given in [75]. The models are mainly classified as

- Block-oriented models — the models consist of cascade connections of static nonlinearities followed by linear dynamic systems (e.g., [183]-[187]); [2]
- General models being linear in parameters — the models are described by a scalar (or vector) product of a parameter vector (or matrix) and a regression vector (or matrix) [3] independent of the parameter vector (or matrix) (e.g., [188]-[198]); [4]
- "Linear" models with signal-dependent parameters — the models have parameters that depend on a known vector of functional variable (e.g., [199]-[201]);
- "Linear" models with piece-wise constant parameters (multi-model) — the models have the characteristic that the parameter-dependence need not be known analytically, and the nonlinear models coincide with the approximate linearised models valid in the region under consideration (e.g., [202,201]).

For a nonlinear power system the main features considered in choosing a suitable structure of the nonlinear nominal model for the design of a nonlinear optimal (or adaptive) control law are:

[2] A typical example of this type of nonlinear models is the Hammerstein model.

[3] In the regression vector (or matrix), the nonlinear terms are normally restricted to quadratic nonlinearities [75].

[4] This representation comprises an important class of bilinear systems.

(1) the nonlinear nominal model should represent the inherent nonlinear features of the power system;

(2) if simplifications are involved in the derivation of the nonlinear nominal model, the nonlinear nominal model should contain enough information that is essential for the control purpose;

(3) both the parameter estimation algorithms and the control laws developed for the identification and control of linear dynamic systems should be capable of being extended to the nonlinear nominal model, which requires that

(4) the regression vector of the nonlinear nominal model be independent of its known (or unknown) parameters.

Based on these factors, it is decided that a *general model being linear in parameters* is the desirable representation of the nonlinear nominal model for the SMIB power system.

In deriving a *general model being linear in parameters* for the design of the nonlinear optimal (or adaptive) power system stabiliser for the SMIB power system described in Subsection 2.3.1, the system intentional nonlinearities (described by the term $\Xi(\mathbf{X}(t), \mathbf{Z}(t), \mathbf{U}_r(t))$ in (2.61)) are ignored. This is because proper design of the power system controllers requires that for normal operating conditions the system variables lie within the range of linear operation of the limiting nonlinearities. For this reason, in the following derivation of the nonlinear nominal model for the power system, Assumption 2.4.1 given in Subsection 2.4.1 is adopted. Consequently, the NAM developed in Subsection 2.4.1 forms the basis for deriving the nonlinear nominal model of the power system (CSM3).

The layout of the remainder of this section is as follows. A new SISO nonlinear continuous-time input-output model developed from the NAM is described in Subsection 4.2.1. The associated SISO nonlinear discrete-time input-output model is derived in Subsection 4.2.2. The nonlinear nominal model is then formulated and its BIBO stability is established in Subsection 4.2.3.

4.2.1 SISO Nonlinear Continuous-Time Input-Output Power System Modelling.

Consider the NAM given by (2.90)-(2.97) in Subsection 2.4.1. Following the elimination of the system auxiliary variable vector $\mathbf{Z}(t)$ from the system state equation (2.90) and the selection of the electrical torque $T_e(t)$ as the system output variable [5], a *SISO nonlinear continuous-time state-space model* is described by the equations below.

$$\dot{\mathbf{X}}(t) = \mathbf{A}(\mathbf{X}(t)) + \mathbf{B_r}\mathbf{R}(t) + \mathbf{b}_{\bar{u}}\bar{u}(t), \tag{4.1}$$

$$\bar{y}(t) = T_e(t) = \mathbf{c}(\mathbf{X}(t)), \tag{4.2}$$

where

$$\mathbf{X}(t)^T = \left[\begin{array}{cccccccc} \delta(t) & \omega_s(t) & E_q'(t) & E_{FD}(t) & P_{GV}(t) & P_{HP}(t) & P_{IP}(t) & P_{LP}(t) \end{array} \right], \tag{4.3}$$

$$\mathbf{R}(t)^T = \left[\begin{array}{cc} P_{ref}(t) & V_{ref}(t) \end{array} \right] = \left[\begin{array}{cc} \bar{y}^*(t) & \bar{d}(t) \end{array} \right], \tag{4.4}$$

$$\mathbf{A}(\mathbf{X}(t)) = \left[\begin{array}{l} \omega_0\omega_s(t) \\ -\frac{m_1}{2H}\sin 2\delta(t) - \frac{m_2}{2H}E_q'(t)\sin\delta(t) - \frac{D}{2H}\omega_s(t) + \frac{F_{HP}}{2H}P_{HP}(t) + \frac{F_{IP}}{2H}P_{IP}(t) + \frac{F_{LP}}{2H}P_{LP}(t) \\ \frac{m_3}{\tau_m}\cos\delta(t) - \frac{1}{\tau_m}E_q'(t) + \frac{m_4}{\tau_m}E_{FD}(t) \\ -\frac{K_A}{\tau_A}\bar{y}_F(t) - \frac{1}{\tau_A}E_{FD}(t) \\ -\frac{K_G}{\tau_G}\omega_s(t) - \frac{1}{\tau_G}P_{GV}(t) \\ \frac{1}{\tau_{CH}}P_{GV}(t) - \frac{1}{\tau_{CH}}P_{HP}(t) \\ \frac{1}{\tau_{RH}}P_{HP}(t) - \frac{1}{\tau_{RH}}P_{IP}(t) \\ \frac{1}{\tau_{CO}}P_{IP}(t) - \frac{1}{\tau_{CO}}P_{LP}(t) \end{array} \right] \tag{4.5}$$

with $\bar{y}_F(t)$ in (4.5) defined by

$$\bar{y}_F(t) = V_t(t) = \left(m_5\cos^2\delta(t) + m_6\sin^2\delta(t) + m_7E_q'(t)\cos\delta(t) + m_8E_q'(t)^2 \right)^{\frac{1}{2}}, \tag{4.6}$$

$$\mathbf{B_r}^T = \left[\begin{array}{cccccccc} 0 & 0 & 0 & 0 & \frac{1}{\tau_G} & 0 & 0 & 0 \\ 0 & 0 & 0 & \frac{K_A}{\tau_A} & 0 & 0 & 0 & 0 \end{array} \right], \tag{4.7}$$

$$\mathbf{b}_{\bar{u}}^T = \left[\begin{array}{cccccccc} 0 & 0 & 0 & \frac{K_A}{\tau_A} & 0 & 0 & 0 & 0 \end{array} \right], \tag{4.8}$$

[5] The reason for using $T_e(t)$ as the stabilising signal has been explained in Section 2.5.

and

$$\mathbf{c}(\mathbf{X}(t)) = m_1 \sin 2\delta(t) + m_2 E_q'(t) \sin \delta(t). \tag{4.9}$$

In the above equations $\bar{y}^*(t)$ is the system output set point, $P_{ref}(t)$; $\bar{d}(t)$ is the measurable deterministic disturbance input, $V_{ref}(t)$; $\bar{y}_F(t)$ is the additional output signal, $V_t(t)$; $\bar{y}(t)$ is the system output variable, $T_e(t)$; [6] $\bar{u}(t)$ is the control signal generated by the nonlinear controller which will be designed later, and $\bar{u}(t)$ is injected into the voltage summing junction of the input of the AVR. The parameters m_i $(i = 1, 2, ..., 8)$ and the time constant τ_m in (4.5)-(4.9) are given by

$$m_1 = \frac{X_d' - X_q}{\left(X_e + X_d'\right)\left(X_e + X_q\right)} \frac{V_\infty^2}{2}, \tag{4.10}$$

$$m_2 = \frac{1}{X_e + X_d'} V_\infty, \tag{4.11}$$

$$m_3 = \frac{X_d - X_d'}{X_e + X_d} V_\infty, \tag{4.12}$$

$$m_4 = \frac{X_e + X_d'}{X_e + X_d}, \tag{4.13}$$

$$m_5 = \frac{X_d'^2}{\left(X_e + X_d'\right)^2} {V_\infty}^2, \tag{4.14}$$

$$m_6 = \frac{X_q^2}{\left(X_e + X_q\right)^2} {V_\infty}^2, \tag{4.15}$$

$$m_7 = \frac{2X_d' X_e}{\left(X_e + X_d'\right)^2} V_\infty, \tag{4.16}$$

$$m_8 = \frac{X_e^2}{\left(X_e + X_d'\right)^2}, \tag{4.17}$$

$$\tau_m = m_4 \tau_{d0}'. \tag{4.18}$$

where $m_i > 0$ for $(i = 2, \ldots, 8)$ and $m_1 < 0$.

A block diagram of the above system model is shown in Fig. 4.1. For this configuration, the system is *deterministic*. The scheduled variation of the system operating point due to the change of $P_{ref}(t)$ is considered as the change of the output set point, $\bar{y}^*(t)$. On the other hand, the scheduled variation of the system operating point due to the change of $V_{ref}(t)$ is viewed as the measurable deterministic disturbance, $\bar{d}(t)$.

[6] Note that $T_e(t) = P_e(t)$ due to Assumption 2.2.5.

Remark 4.2.1 *The model (4.1)-(4.18) is only an alternative expression for the NAM. As explained in Remark 2.4.1, the model (4.1)-(4.18) represents the CSM3 accurately within the range of linear operation of the system limiting nonlinearities.*

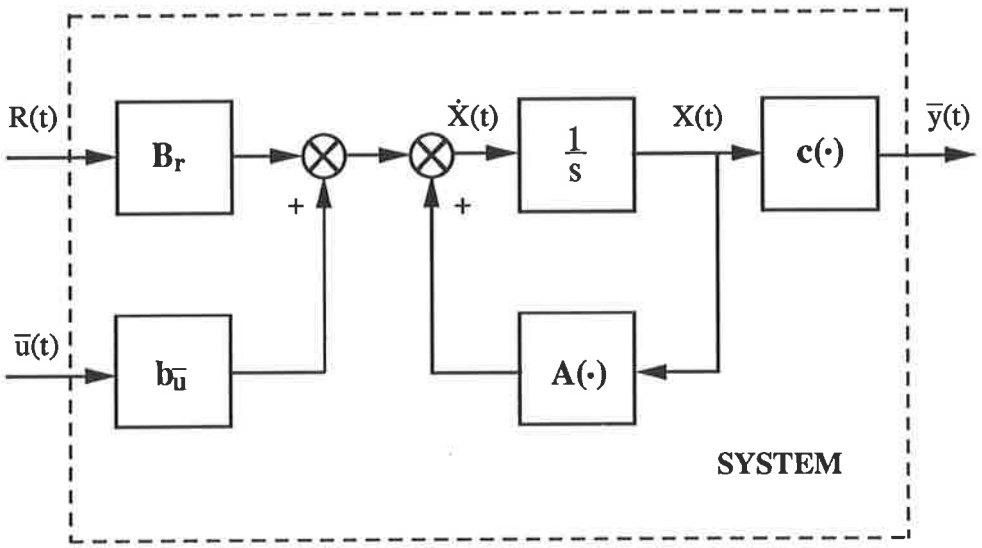

Figure 4.1: SISO nonlinear continuous-time state-space modelling of the SMIB power system.

Clearly, in the nonlinear continuous-time state-space representation (4.1)-(4.18), the output variable $\bar{y}(t)$ ($T_e(t)$ or $P_e(t)$) is an *implicit* function of the control input $\bar{u}(t)$. For control purposes, an *explicit* expression for $\bar{y}(t)$ in relation to $\bar{u}(t)$ is required. To find the desired input-output relationship between $\bar{y}(t)$ and $\bar{u}(t)$ from the model (4.1)-(4.18), the following mathematical rule is introduced

$$(1+p)\{x_i x_j\} = x_i(1+p)\{x_j\} + x_j p\{x_i\}$$

where x_i and x_j are arbitrary, continuously differentiable time variables. Premultiplying the output equation (4.2) by $(1+\tau_m p)$ and using the following state equations from (4.1) and (4.5)

$$\begin{aligned} p\delta(t) &= \omega_0\omega_s(t), \\ (1+\tau_m p)E_q'(t) &= m_3\cos\delta(t) + m_4 E_{FD}(t), \end{aligned} \tag{4.19}$$

one writes

$$\begin{aligned}
(1+\tau_m p)\,\bar{y}(t) &= m_1\,(1+\tau_m p)\,\{\sin 2\delta(t)\} + m_2 \sin\delta(t)\,(1+\tau_m p)\left\{E_q'(t)\right\} \\
&\quad + m_2\tau_m E_q'(t) p\,\{\sin\delta(t)\} \\
&= m_1\,(1+\tau_m p)\,\{\sin 2\delta(t)\} \\
&\quad + m_2 \sin\delta(t)\,[m_3\cos\delta(t) + m_4 E_{FD}(t)] \\
&\quad + m_2\tau_m E_q'(t)\cos\delta(t) p\,\{\delta(t)\} \\
&= \left[\left(m_1 + \frac{m_2 m_3}{2}\right) + m_1\tau_m p\right]\{\sin 2\delta(t)\} \\
&\quad + m_2 m_4\,\{E_{FD}(t)\sin\delta(t)\} \\
&\quad + m_2\omega_0\tau_m\left\{\omega_s(t)E_q'(t)\cos\delta(t)\right\}. \qquad (4.20)
\end{aligned}$$

Similarly, premultiplying (4.20) by $(1+\tau_A p)$ and using the state equation from (4.1) and (4.5)

$$(1+\tau_A p)\,E_{FD}(t) = K_A\left[\bar{d}(t) - \bar{y}_F(t) + \bar{u}(t)\right],$$

one obtains

$$\begin{aligned}
(1+\tau_A p)(1+\tau_m p)\,\bar{y}(t) &= (1+\tau_A p)\left[\left(m_1 + \frac{m_2 m_3}{2}\right) + m_1\tau_m p\right]\{\sin 2\delta(t)\} \\
&\quad + m_2\omega_0\tau_m\,(1+\tau_A p)\left\{\omega_s(t)E_q'(t)\cos\delta(t)\right\} \\
&\quad + m_2 m_4\tau_A E_{FD}(t) p\,\{\sin\delta(t)\} \\
&\quad + m_2 m_4 \sin\delta(t)\,(1+\tau_A p)\,\{E_{FD}(t)\} \\
&= \frac{2m_1 + m_2 m_3}{2}\,(1+\tau_A p)\left(1 + \frac{2m_1\tau_m}{2m_1 + m_2 m_3} p\right)\{\sin 2\delta(t)\} \\
&\quad + m_2\omega_0\tau_m\,(1+\tau_A p)\left\{\omega_s(t)E_q'(t)\cos\delta(t)\right\} \\
&\quad + m_2 m_4\omega_0\tau_A\,\{\omega_s(t)E_{FD}(t)\cos\delta(t)\} \\
&\quad + m_2 m_4 K_A\left\{\sin\delta(t)\left[\bar{d}(t) - \bar{y}_F(t) + \bar{u}(t)\right]\right\}. \qquad (4.21)
\end{aligned}$$

Now, define

$$\bar{z}_1(t) \triangleq \sin 2\delta(t), \qquad (4.22)$$

$$\bar{z}_2(t) \triangleq \omega_s(t)E_q'(t)\cos\delta(t), \qquad (4.23)$$

$$\bar{z}_3(t) \triangleq \omega_s(t)E_{FD}(t)\cos\delta(t), \qquad (4.24)$$

$$\bar{z}_4(t) \triangleq \sin\delta(t), \qquad (4.25)$$

and

$$\bar{A}(p) = 1 + (\tau_A + \tau_m)\, p + \tau_A \tau_m p^2, \tag{4.26}$$

$$\bar{B}(p) = k_1 \left[1 + \left(\tau_A + \tau_m^{'}\right) p + \tau_A \tau_m^{'} p^2\right], \tag{4.27}$$

$$\bar{C}(p) = k_2 \left(1 + \tau_A p\right), \tag{4.28}$$

$$\bar{D}(p) = k_3, \tag{4.29}$$

$$\bar{E}(p) = k_4, \tag{4.30}$$

where

$$k_1 = \frac{2m_1 + m_2 m_3}{2}, \tag{4.31}$$

$$k_2 = m_2 \omega_0 \tau_m, \tag{4.32}$$

$$k_3 = m_2 m_4 \omega_0 \tau_A, \tag{4.33}$$

$$k_4 = m_2 m_4 K_A, \tag{4.34}$$

$$\tau_m^{'} = \frac{2m_1 \tau_m}{2m_1 + m_2 m_3}. \tag{4.35}$$

Equation (4.21) is then re-organised in the following compact form:

$$\bar{A}(p)\bar{y}(t) = \bar{B}(p)\bar{z}_1(t) + \bar{C}(p)\bar{z}_2(t) + \bar{D}(p)\bar{z}_3(t) + \bar{E}(p)\bar{z}_4(t) \left[\bar{d}(t) - \bar{y}_F(t) + \bar{u}(t)\right]. \tag{4.36}$$

This high-order continuous-time differential equation describes the nonlinear relationship between the control input $\bar{u}(t)$ and the output $\bar{y}(t)$. It includes the additional feedback signals, $\bar{z}_i(t)$ $(i = 1, 2, 3, 4)$ and $\bar{y}_F(t)$, and the reference signal, $\bar{d}(t)$. Equations (4.22)-(4.36) form a *SISO nonlinear continuous-time input-output model* of the power system (CSM3). The block diagram of this model is shown in Figure 4.2.

Remark 4.2.2 *The derivation of the input-output model (4.22)-(4.36) from the state-space model (4.1)-(4.18) does not involve any mathematical assumptions. The former model is therefore a valid continuous-time input-output representation of the NAM.*

The boundedness of the variables in the nonlinear continuous-time input-output model (4.22)-(4.36) is important for the theoretical analysis of the nonlinear control schemes to be designed later. For most power system studies, the following assumption is generally accepted.

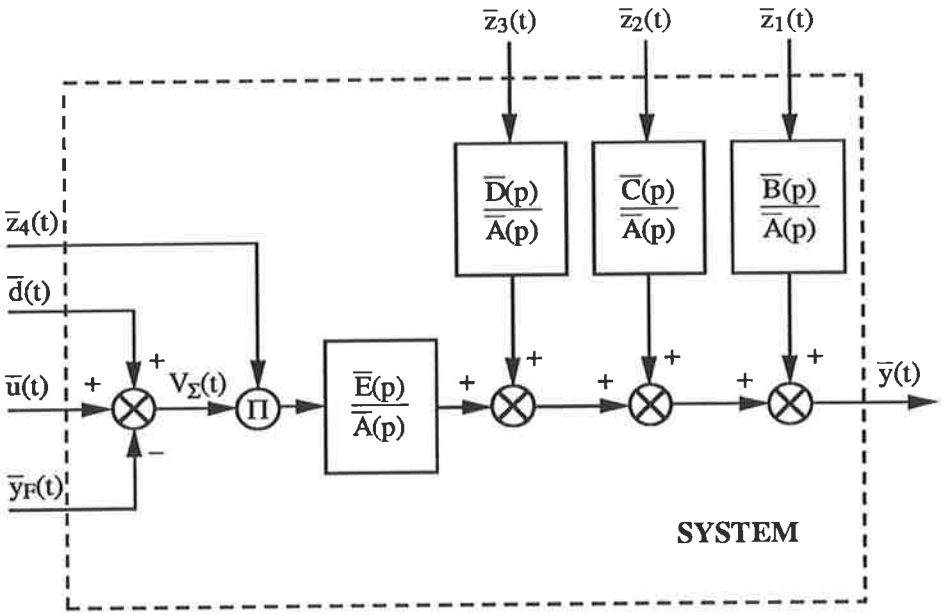

Figure 4.2: SISO nonlinear continuous-time input-output modelling of the SMIB power system.

Assumption 4.2.1 *The state variables $E_{FD}(t)$ and $P_{GV}(t)$ in the equations of the power system are all constrained as follows*

(i) $$|E_{FD}(t)| \leq \max\{|V_{R\,min}|, |V_{R\,max}|\} \triangleq K_1;$$

(ii) $$|P_{GV}(t)| \leq \max\{|P_{min}|, |P_{max}|\} \triangleq K_2,$$

for all t, where K_1 and K_2 are known.

This assumption is not critical since, in practice, the field voltage and the power at the gate (or valve) are always constrained by physical limitations as described by (A.14) and (A.18) respectively. Based on Assumption 4.2.1, the following lemma is established.

Lemma 4.2.1 *For the model (4.22)-(4.36), under Assumption 4.2.1,*

(i) $$\sup_{0 \leq t < \infty} |\bar{z}_1(t)| \leq 1;$$

(ii) $\sup_{0\leq t<\infty} |\bar{z}_2(t)| \leq \bar{z}_{2\,max}$;

(iii) $\sup_{0\leq t<\infty} |\bar{z}_3(t)| \leq \bar{z}_{3\,max}$;

(iv) $\sup_{0\leq t<\infty} |\bar{z}_4(t)| \leq 1$;

(v) $\sup_{0\leq t<\infty} |\bar{y}_F(t)| \leq V_{t\,max}$;

(vi) $\sup_{0\leq t<\infty} |\bar{y}(t)| \leq \bar{y}_{max}$,

where $\bar{z}_{2\,max}$, $\bar{z}_{3\,max}$, $V_{t\,max}$, *and* $\bar{y}_{max}$ *are either known or can be determined.*

Proof of Lemma 4.2.1

(1) From the definitions of $\bar{z}_1(t)$ and $\bar{z}_4(t)$ in (4.22) and (4.25) respectively, *(i)* and *(iv)* are obtained in a straightforward manner.

(2) From (4.19), it is seen that for bounded signals $\cos\delta(t)$ and $E_{FD}(t)$ (see Assumption 4.2.1(i)), $E_q'(t)$ is bounded, i.e.,

$$\sup_{0\leq t<\infty} \left|E_q'(t)\right| \leq m_3 + m_4 K_1 \triangleq K_3$$

where $m_3 > 0$ and $m_4 > 0$. Parts *(v)* and *(vi)* then follow from (4.6) and (4.2) respectively. $V_{t\,max}$ and $\bar{y}_{max}$ are given by

$$V_{t\,max} = \left(m_5 + m_6 + m_7 K_3 + m_8 K_3^2\right)^{\frac{1}{2}}$$

and

$$\bar{y}_{max} = m_2 K_3 - m_1 \tag{4.37}$$

where $m_i > 0$ for $(i = 2, 5, 6, 7, 8)$ and $m_1 < 0$.

(3) From the state equation (4.1) and eqn. (A.24) of Appendix A, the expression

$$\sup_{0\leq t<\infty} |F_{HP}P_{HP}(t) + F_{IP}P_{IP}(t) + F_{LP}P_{LP}(t)| \leq K_2 \tag{4.38}$$

follows from Assumption 4.2.1(ii). According to the equation

$$\left(1 + \frac{2H}{D}p\right)\omega_s(t) = \frac{1}{D}\left(F_{HP}P_{HP}(t) + F_{IP}P_{IP}(t) + F_{LP}P_{LP}(t) - \bar{y}(t)\right) \tag{4.39}$$

which is derived from the second differential equation of the state equation (4.1), the expression

$$\sup_{0\leq t<\infty} |\omega_s(t)| \leq \frac{1}{D}(K_2 - m_1 + m_2 K_3) \triangleq K_4 \tag{4.40}$$

arises as a result of applying the condition (4.38) and conclusion *(vi)* (with (4.37)) to (4.39). Hence, *(ii)* and *(iii)* are readily established by the definitions of $\bar{z}_2(t)$ and $\bar{z}_3(t)$ in (4.23) and (4.24), with $\bar{z}_{2\,max}$ and $\bar{z}_{3\,max}$ being chosen as

$$\bar{z}_{2\,max} = K_3 K_4$$

and

$$\bar{z}_{3\,max} = K_1 K_4$$

respectively.

Q.E.D.

Lemma 4.2.1 establishes the boundedness of the additional feedback signals, $\bar{z}_i(t)$ $(i = 1,2,3,4)$ and $\bar{y}_F(t)$, and the output variable, $\bar{y}(t)$, in the nonlinear continuous-time input-output model (4.22)-(4.36), in accordance with the physical limitations specified by Assumption 4.2.1. This lemma will be used when the boundedness of the variables in the corresponding discrete-time model is discussed in Subsection 4.2.2 and when the BIBO stability of the resulting nonlinear nominal model is established in Subsection 4.2.3.

Remark 4.2.3 *It should be emphasised that the boundedness of the state and output variables of the model (4.22)-(4.36) is obtained in Lemma 4.2.1* without *imposing an upper (or lower) bound on the control input* $\bar{u}(t)$.

4.2.2 SISO Nonlinear Discrete-Time Input-Output Power System Modelling.

In order to implement a discrete-time control law, the nonlinear continuous-time input-output model (4.22)-(4.36) developed in Subsection 4.2.1 is replaced by an *equivalent*

discrete-time one which is based on the approximation for the first and second derivatives given by

Assumption 4.2.2 *[141,193]*[7]

(i) $$px(t)\,|_{t=t_k} = \frac{x(t_k) - x(t_k - h)}{h} + \mu_x(t_k - h, t_k);$$

(ii) $$p^2x(t)\,|_{t=t_k} = \frac{x(t_k + h) - 2x(t_k) + x(t_k - h)}{h^2} + \eta_x(t_k - h, t_k, t_k + h),$$

where h is the sampling period and t_k is the sampling instant ($k \in [0,1,2,\ldots)$); $x(t)$ represents an arbitrary, continuously differentiable time variable that is sampled (or computed) through a zero-order hold; $\mu_x(t_k - h, t_k)$ and $\eta_x(t_k - h, t_k, t_k + h)$ are sufficiently small, satisfying the condition that at each sampling instant t_k

$$\lim_{h \to 0} \mu_x(t_k - h, t_k) = 0 \tag{4.41}$$

and

$$\lim_{h \to 0} \eta_x(t_k - h, t_k, t_k + h) = 0. \tag{4.42}$$

By applying Assumption 4.2.2 to (4.36), the nonlinear continuous-time input-output model (4.22)-(4.36) is discretised, and its approximate discrete-time model is derived as

$$\begin{aligned} \bar{y}(t_k + h) + a_1\bar{y}(t_k) + a_2\bar{y}(t_k - h) \;=\; & \bar{b}_0\bar{z}_1(t_k + h) + \bar{b}_1\bar{z}_1(t_k) + \bar{b}_2\bar{z}_1(t_k - h) \\ & + c_1\bar{z}_2(t_k) + c_2\bar{z}_2(t_k - h) + d_1\bar{z}_3(t_k) \\ & + e_1\bar{z}_4(t_k)\left[\bar{d}(t_k) - \bar{y}_F(t_k) + \bar{u}(t_k)\right] \\ & + \bar{v}(t_k + h) \end{aligned} \tag{4.43}$$

where

$$a_1 \;=\; \frac{h^2 + (\tau_A + \tau_m)\,h - 2\tau_A\tau_m}{\tau_A\tau_m}, \tag{4.44}$$

[7] It is possible to use a higher order approximation, e.g., the fourth-order Runge-Kutta, to derive the corresponding discrete-time model. However, for simplicity, the approximations introduced by Assumption 4.2.2 are considered adequate for the studies in this thesis.

$$a_2 = \frac{\tau_A\tau_m - (\tau_A + \tau_m)\,h}{\tau_A\tau_m}, \tag{4.45}$$

$$\bar{b}_0 = k_1\frac{\tau_m^{'}}{\tau_m}, \tag{4.46}$$

$$\bar{b}_1 = k_1\frac{h^2 + \left(\tau_A + \tau_m^{'}\right)h - 2\tau_A\tau_m^{'}}{\tau_A\tau_m}, \tag{4.47}$$

$$\bar{b}_2 = k_1\frac{\tau_A\tau_m^{'} - \left(\tau_A + \tau_m^{'}\right)h}{\tau_A\tau_m}, \tag{4.48}$$

$$c_1 = k_2\frac{h\,(h + \tau_A)}{\tau_A\tau_m}, \tag{4.49}$$

$$c_2 = -k_2\frac{h}{\tau_m}, \tag{4.50}$$

$$d_1 = k_3\frac{h^2}{\tau_A\tau_m}, \tag{4.51}$$

$$e_1 = k_4\frac{h^2}{\tau_A\tau_m}, \tag{4.52}$$

and

$$\begin{aligned}\bar{v}(t_k + h) \triangleq\ & -\frac{h^2\,(\tau_A + \tau_m)}{\tau_A\tau_m}\mu_{\bar{y}}(t_k - h, t_k) - h^2\eta_{\bar{y}}(t_k - h, t_k, t_k + h) \\ & + k_1\frac{h^2\left(\tau_A + \tau_m^{'}\right)}{\tau_A\tau_m}\mu_{\bar{z}_1}(t_k - h, t_k) + k_1\frac{h^2\tau_m^{'}}{\tau_m}\eta_{\bar{z}_1}(t_k - h, t_k, t_k + h) \\ & + k_2\frac{h^2}{\tau_m}\mu_{\bar{z}_2}(t_k - h, t_k).\end{aligned}$$

Note that $\bar{v}(t_k + h)$ represents the error due to the discretisation introduced by Assumption 4.2.2. According to (4.41) and (4.42), $\bar{v}(t_k + h)$ satisfies

$$\lim_{h\to 0}\bar{v}(t_k + h) = 0 \tag{4.53}$$

for each sampling instant t_k.

Clearly, for purposes of prediction and control of the output variable, the future value of $\bar{z}_1(t_k)$, $\bar{z}_1(t_k + h)$, in (4.43) needs to be expressed in terms of its present and/or past values $\{\bar{z}_1(t_k), \bar{z}_1(t_k - h), \ldots\}$. This results in the following assumption.

Assumption 4.2.3 [8] *A linearised prediction $\bar{z}_1(t_k + h)$ at time t_k is given by*

$$\bar{z}_1(t_k + h) = 2\bar{z}_1(t_k) - \bar{z}_1(t_k - h) + h\bar{\epsilon}_{t_k} \tag{4.54}$$

[8] Again, it is possible to use a higher order approximation to derive the prediction $\bar{z}_1(t_k + h)$ at time t_k. However, according to the definition of $\bar{z}_1(t)$ in (4.22), the adopted first-order linearisation (4.54) is found to be adequate, provided that the condition (4.57) is satisfied.

where $\bar{\epsilon}_{t_k}$ *represents the error due to the prediction and satisfies*

$$\lim_{h\to 0} \bar{\epsilon}_{t_k} = 0 \tag{4.55}$$

for each sampling instant t_k.

Remark 4.2.4 *Assumption 4.2.3 is based on the relation*

$$p\bar{z}_1(\tau)\,|_{\tau=t_k+h} = p\bar{z}_1(\tau)\,|_{\tau=t_k} + \epsilon_{t_k} \tag{4.56}$$

where, according to (4.22),

$$\epsilon_{t_k} \triangleq 2\omega_0\left[\omega_s(t_k+h)\cos 2\delta(t_k+h) - \omega_s(t_k)\cos 2\delta(t_k)\right]$$

satisfies the condition that

$$\lim_{h\to 0} \epsilon_{t_k} = 0 \tag{4.57}$$

for each sampling instant t_k. *Application of Assumption 4.2.2(i) to (4.56) leads to the following expression*

$$\frac{\bar{z}_1(t_k+h) - \bar{z}_1(t_k)}{h} = \frac{\bar{z}_1(t_k) - \bar{z}_1(t_k-h)}{h} + \bar{\epsilon}_{t_k}$$

where

$$\bar{\epsilon}_{t_k} \triangleq \epsilon_{t_k} + \mu_{\bar{z}_1}(t_k-h, t_k) - \mu_{\bar{z}_1}(t_k, t_k+h).$$

According to the conditions (4.41) and (4.57), $\bar{\epsilon}_{t_k}$ *satisfies the condition (4.55).*

Substituting from (4.54) for the prediction $\bar{z}_1(t_k+h)$ into (4.43), one writes

$$\begin{aligned}\bar{y}(t_k+h) + a_1\bar{y}(t_k) + a_2\bar{y}(t_k-h) &= b_1\bar{z}_1(t_k) + b_2\bar{z}_1(t_k-h)\\ &\quad + c_1\bar{z}_2(t_k) + c_2\bar{z}_2(t_k-h) + d_1\bar{z}_3(t_k)\\ &\quad + e_1\bar{z}_4(t_k)\left[\bar{d}(t_k) - \bar{y}_F(t_k) + \bar{u}(t_k)\right]\\ &\quad + v(t_k+h)\end{aligned} \tag{4.58}$$

where

$$b_1 = 2\bar{b}_0 + \bar{b}_1, \tag{4.59}$$

$$b_2 = \bar{b}_2 - \bar{b}_0, \tag{4.60}$$

$$v(t_k+h) = \bar{v}(t_k+h) + \bar{b}_0 h\bar{\epsilon}_{t_k},$$

and

$$\lim_{h \to 0} v(t_k + h) = 0 \tag{4.61}$$

due to the conditions (4.53) and (4.55).

From a practical point of view one allows for measurement errors, actuator errors, and in some instances computer round-off errors in (4.58) by writing

Assumption 4.2.4 *For the variables in (4.58),*

$$y(t_k) = \bar{y}(t_k) + w_1(t_k), \tag{4.62}$$

$$z_1(t_k) = \bar{z}_1(t_k) + w_2(t_k), \tag{4.63}$$

$$z_2(t_k) = \bar{z}_2(t_k) + w_3(t_k), \tag{4.64}$$

$$z_3(t_k) = \bar{z}_3(t_k) + w_4(t_k), \tag{4.65}$$

$$z_4(t_k) = \bar{z}_4(t_k) + w_5(t_k), \tag{4.66}$$

$$y_F(t_k) = \bar{y}_F(t_k) + w_7(t_k), \tag{4.67}$$

$$d(t_k) = \bar{d}(t_k) + w_6(t_k), \tag{4.68}$$

$$u(t_k) = \bar{u}(t_k) + w_8(t_k), \tag{4.69}$$

where the terms of the left-hand side of (4.62)-(4.69) represent measured or computed values, and the terms, $w_i(t_k)$ $(i = 1, \ldots, 8)$, of the right-hand side of (4.62)-(4.69) represent the measurement errors, actuator errors, and computer round-off errors that are assumed bounded, such that

$$\sup_{0 \le t_k < \infty} |w_i(t_k)| \le \Delta_i \qquad (i = 1, \ldots, 8), \tag{4.70}$$

with Δ_i $(i = 1, \ldots, 8)$ being some fixed, known values.

Remark 4.2.5 *Under the condition (4.70), from Lemma 4.2.1(iv) and (4.66), it follows that*

$$\sup_{0 \le t_k < \infty} |z_4(t_k)| \le 1 + \Delta_5. \tag{4.71}$$

The condition (4.71) will be used for the stability analysis of the nonlinear optimal and adaptive controllers in Sections 4.3, 4.4, and 5.3. It will also be used for the convergence analysis of the parameter estimation algorithms in Section 5.2.

A *SISO nonlinear discrete-time input-output model* of the power system is finally derived by applying Assumption 4.2.4 ((4.62)-(4.69)) to (4.58), resulting in

$$\begin{aligned} y(t_k+h)+a_1y(t_k)+a_2y(t_k-h) &= b_1z_1(t_k)+b_2z_1(t_k-h) \\ &\quad +c_1z_2(t_k)+c_2z_2(t_k-h)+d_1z_3(t_k) \\ &\quad +e_1z_4(t_k)\left[d(t_k)-y_F(t_k)+u(t_k)\right] \\ &\quad +w(t_k+h) \end{aligned} \tag{4.72}$$

where $w(t_k+h)$ represents the combined effect of errors due to discretisation (see Assumption 4.2.2), linearisation (see Assumption 4.2.3), and measurements, etc. (see Assumption 4.2.4), which together shall be designated as *noise*; $w(t_k+h)$ is defined as

$$\begin{aligned} w(t_k+h) \triangleq\ & w_1(t_k+h)+a_1w_1(t_k)+a_2w_1(t_k-h)-b_1w_2(t_k)-b_2w_2(t_k-h) \\ & -c_1w_3(t_k)-c_2w_3(t_k-h)-d_1w_4(t_k)-e_1\bar{z}_4(t_k)\left[w_6(t_k)-w_7(t_k)+w_8(t_k)\right] \\ & -e_1w_5(t_k)\left[\bar{d}(t_k)-\bar{y}_F(t_k)+\bar{u}(t_k)\right]+v(t_k+h). \end{aligned} \tag{4.73}$$

Remark 4.2.6 *The model (4.72)-(4.73) is derived from the nonlinear continuous-time input-output model (4.22)-(4.36) subject to Assumptions 4.2.2-4.2.4. In view of Remarks 4.2.1 and 4.2.2, it can be concluded that*

(i) the model (4.72)-(4.73) is a valid discrete-time input-output representation of the NAM, provided that the conditions in Assumptions 4.2.2-4.2.4 are all satisfied;

(ii) the model (4.72)-(4.73) is an accurate representation of the continuous-time nonlinear SMIB power system (CSM3), provided that the conditions in Assumptions 2.4.1 and 4.2.2-4.2.4 are all satisfied.

The characteristic of $w(t+h)$ in the model (4.72)-(4.73) is important for the theoretical analyses of the parameter estimation algorithm and the adaptive control law under a nonlinear control scheme. Considering that in practice the voltage reference signal and the control signal from a power system stabiliser are usually constrained by operation or design, one may assume that

Assumption 4.2.5 *In the model (4.72)-(4.73) the external measurable disturbance input* $\bar{d}(t_k)$ *and the control input* $\bar{u}(t_k)$ *are constrained to be*

(i) $$\left|\bar{d}(t_k)\right| \leq \bar{V}_{max};$$

(ii) $$|\bar{u}(t_k)| \leq \bar{u}_{max},$$

for each sampling instant t_k, *where* $\bar{V}_{max}$ *and* $\bar{u}_{max}$ *are known.*

Based on Assumptions 4.2.1-4.2.5, the following property of $w(t_k + h)$ is readily established.

Lemma 4.2.2 *For the model (4.72)-(4.73), subject to Assumptions 4.2.1-4.2.5, there exists a* Δ_w *such that*

$$\sup_{0 \leq t_k < \infty} |w(t_k)| < \Delta_w. \tag{4.74}$$

Proof of Lemma 4.2.2

Signals $\bar{d}(t_k)$ and $\bar{u}(t_k)$ are all bounded due to Assumption 4.2.5(i) and (ii). Also, the boundedness of $\bar{z}_4(t_k)$ and $\bar{y}_F(t_k)$ is provided by Lemma 4.2.1(iv) and (v). Therefore, the conclusion (4.74) is readily obtained from the expression for $w(t_k + h)$ in (4.73), subject to the condition (4.70) in Assumption 4.2.4 as well as the condition (4.61).

Q.E.D.

The boundedness of $w(t_k + h)$ in Lemma 4.2.2 is essential for the proof of convergence of the parameter estimation algorithms in Section 5.2 and for the analysis of the closed-loop stability associated with the nonlinear control laws to be designed in Sections 4.3, 4.4, and 5.3.

4.2.3 Nonlinear Nominal Model of the Power System and Its BIBO Stability.

For a fixed sampling period h, the sampling instant t_k is expressed as

$$t_k = kh, \qquad (k \in [0, 1, 2, \ldots)).$$

Equation (4.72) is then rewritten as

$$\begin{aligned} y(kh+h) + a_1 y(kh) + a_2 y(kh-h) \;=\; & b_1 z_1(kh) + b_2 z_1(kh-h) \\ & + c_1 z_2(kh) + c_2 z_2(kh-h) + d_1 z_3(kh) \\ & + e_1 z_4(kh)\,[d(kh) - y_F(kh) + u(kh)] \\ & + w(kh+h). \end{aligned} \tag{4.75}$$

For convenience of notation, the sampling period h in (4.75) will be implied in the following equations. A compact form of the SISO nonlinear discrete-time input-output model (4.72)-(4.73) developed in Subsection 4.2.2 is then given by the following regression equation

$$y(k+1) = \phi(k)^T \Theta_0 + w(k+1) \tag{4.76}$$

where $\phi(k)$ is the regression vector, the components of which are functions of the sequences of the inputs and the output as well as the additional feedback signals. $\phi(k)$ is given by

$$\begin{aligned} \phi(k)^T \;\triangleq\; \Big[& -y(k) \quad -y(k-1) \quad z_1(k) \quad z_1(k-1) \\ & z_2(k) \quad z_2(k-1) \quad z_3(k) \quad z_4(k)\,(d(k) - y_F(k) + u(k)) \Big]. \end{aligned} \tag{4.77}$$

Θ_0 is the parameter vector, the elements of which are the model parameters, i.e.,

$$\Theta_0 \triangleq \Big[\; a_1 \quad a_2 \quad b_1 \quad b_2 \quad c_1 \quad c_2 \quad d_1 \quad e_1 \; \Big]^T. \tag{4.78}$$

The parameters in (4.78) are given, in the order written, by (4.44)-(4.45), (4.59)-(4.60), and (4.49)-(4.52). It is assumed that

Assumption 4.2.6 *For the SMIB power system described in Subsection 2.3.1,*

(i) the values of the parameters of the generating unit and the tie-line (such as X_d, X_e, etc.) are known;

(ii) for a given steady-state operating condition, the infinite bus voltage V_∞ is constant over the time period of a simulation study.

Referring to the definitions of a_1, etc., one may conclude that the model parameters (a_1, etc.) in the vector Θ_0 are all *'known'*, and that Θ_0 is independent of $\phi(k)$. Hence, equations (4.76)-(4.78) represent a SISO nonlinear discrete-time input-output model which is linear in its parameters. In the following analysis this model is referred to as the *Nonlinear Nominal Model* (NNM) of the power system (CSM3), and is to be used for the design of not only the parameter estimation algorithms in Section 5.2 but also the nonlinear optimal and adaptive control algorithms in Sections 4.3, 4.4, and 5.3, respectively. Figure 4.3 shows the configuration of the NNM.

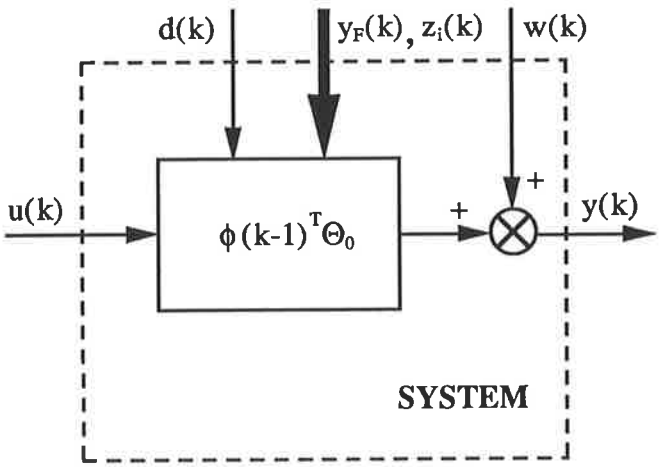

Figure 4.3: SISO nonlinear discrete-time input-output modelling of the SMIB power system.

Remark 4.2.7 *The NNM (4.76)-(4.78) is an alternative form of the model (4.72)-(4.73), and therefore accurately represents the continuous-time nonlinear power system (CSM3), provided that the conditions in Assumptions 2.4.1 and 4.2.2-4.2.5 are all*

satisfied (referring to Remark 4.2.6(ii)). This point will be verified in Subsection 4.5.1 through simulation studies.

Remark 4.2.8 *Since the electrical torque output, $T_e(k)$, of the system (CSM3) is related to the state variables (such as $E'_q(k)$ and $\delta(k)$) through the nonlinear relationship (4.9), $z_i(k)$ $(i = 1,2,3,4)$ (see (4.22)-(4.25)) are implicit functions of $y(k)$. This determines the nonlinear nature of the NNM (4.76)-(4.78).*

There are several important features in the NNM:

(1) The model (4.76)-(4.78) is derived from the mathematical description of the nonlinear power system (CSM3), and represents the inherent nonlinearities (i.e., the product nonlinearities and the trigonometric nonlinearities) associated with the electrical torque (or power) output (see (4.9)). Therefore, the inclusion of the measurable disturbance input, $d(k)$, as well as the additional feedback variables, $z_i(k)$ $(i = 1,2,3,4)$ and $y_F(k)$, in the model will result in an *accurate* prediction of the output variable, $y(k)$, and potentially *better* control of the system dynamics. This point will be demonstrated in Section 4.5 (see Remark 4.5.1).

(2) Since the model (4.76)-(4.78) includes the measurable deterministic disturbance input signal $\{d(k)\}$ *explicitly*, the influence of this disturbance on the system performance can be reduced as soon as it acts on the system. From this point of view, the model (4.76)-(4.78) provides a *feedforward* path for the control of the system. The simulation results shown in Subsection 4.5.2 will verify this point (see Remark 4.5.6). Being a reference signal, the disturbance input sequence $\{d(k)\}$ is known or exactly predictable.

(3) Since the model (4.76)-(4.78) is described in a regression form, the parameter estimation algorithms and the optimal (or adaptive) control strategies that are developed for linear systems can be extended to this nonlinear model. Also, since $\phi(k)$ is a linear function of the control input $u(k)$, the solution of $u(k)$ from the optimal (or adaptive) control laws to be designed later will be relatively

straightforward. This aspect is essential for the implementation of the nonlinear control schemes.

It should be pointed out that the *discrete-time* nonlinear input-output model (NNM) of the power system (CSM3) has been developed from the *continuous-time* nonlinear input-output equations (4.22)-(4.36). Consequently, the nature of the input-output model of the power system has been changed from deterministic (see Fig. 4.2) to random or stochastic (see Fig. 4.3), with the term $w(k+1)$ representing the nondeterministic quantity of the NNM.

The BIBO stability [9] of the NNM is given by

Lemma 4.2.3 *Subject to Assumptions 4.2.1, 4.2.4, and 4.2.5, for the NNM*

(i) the output $y(k)$, and the additional feedback signals $z_i(k)$ $(i = 1, 2, 3, 4)$ and $y_F(k)$, are bounded for all k;

(ii) the measurable deterministic disturbance input $d(k)$ is bounded for all k;

(iii) the control input $u(k)$ is bounded for all k.

Proof of Lemma 4.2.3

Conclusion *(i)* is the consequence of Lemma 4.2.1 and Assumption 4.2.4. Also, conclusions *(ii)-(iii)* are the result of the combination of Assumption 4.2.4 with Assumption 4.2.5.

Q.E.D.

Remark 4.2.9 *According to Lemma 4.2.3(i) the output and the additional feedback signals of the NNM are bounded* without *imposing an upper (or lower) bound on the control input $u(k)$.*

[9] See Definition 4.2 in [170].

Lemma 4.2.3 forms a key lemma for the proofs of the convergence of the parameter estimation algorithms in Section 5.2, the analyses of the closed-loop stability associated with the nonlinear optimal control laws in Sections 4.3 and 4.4, and the proofs of the convergence of the nonlinear adaptive control algorithms in Section 5.3.

4.3 SISO Nonlinear Stochastic Generalised Minimum Variance Control and Stability Analysis.

In this section:

- the optimal prediction of the output variable of the NNM is developed;
- the nonlinear stochastic generalised minimum variance control of the NNM is discussed, and the closed-loop characteristics are presented;
- the closed-loop stability conditions with the nonlinear stochastic generalised minimum variance control law are established.

The discrete-time NNM (4.76)-(4.78) derived in Subsection 4.2.3 is used for the development of the nonlinear optimal power system stabiliser for the SMIB power system described in Subsection 2.3.1. The model (4.76)-(4.78) can be rewritten in a *left difference operator representation* [157] expressed in terms of the backward-shift operator q^{-1}, i.e.,

$$A(q^{-1})y(k+1) = f(k) + w(k+1) \tag{4.79}$$

where $A(q^{-1})$ is a linear scalar polynomial in q^{-1}

$$A(q^{-1}) = 1 + a_1 q^{-1} + a_2 q^{-2} \tag{4.80}$$

and $f(k)$ is a nonlinear function of the form

$$f(k) = \begin{bmatrix} b_1 & b_2 & c_1 & c_2 & d_1 & e_1 \end{bmatrix} \begin{bmatrix} z_1(k) \\ z_1(k-1) \\ z_2(k) \\ z_2(k-1) \\ z_3(k) \\ z_4(k)\,(d(k) - y_F(k) + u(k)) \end{bmatrix}. \tag{4.81}$$

The backward-shift operator, q^{-1}, is defined as

$$q^{-1}y(k) \triangleq y(k-1), \quad \text{for } k \geq 1; \qquad\qquad q^{-1}y(0) \triangleq y(0)$$

and so on.

As indicated in Subsection 4.2.3, the derivation of the NNM introduces a nondeterministic disturbance term that is expressed by the scalar sequence $\{w(k)\}$. For theoretical analyses, it is desirable to define the properties of this noise term. Thus, three types of noise models are proposed:

Noise Model 1: Assume that the noise is negligible. With the omission of the term $w(k+1)$, the model (4.79)-(4.81) becomes a *Nonlinear Deterministic AutoRegressive Moving-Average* **(NDARMA)** *model* of the form

$$A(q^{-1})y(k+1) = f(k).$$

The analysis of the nonlinear prediction and control of the NNM will thus be carried out in a deterministic environment. However, this assumption may not be reasonable since the model (4.79)-(4.81) does possess a significant noise term $w(k+1)$ during and shortly after a severe disturbance (e.g., a three-phase short-circuit). This is because in such an event limiting actions may occur on the power system, so that Assumption 2.4.1 which is used for the development of the NNM is violated. This phenomenon will be demonstrated in Subsection 4.5.1 (see Remark 4.5.3).

Noise Model 2: Assume that the statistical properties of the scalar sequence $\{w(k)\}$ can be described in terms of one kind of stochastic process, e.g., a white noise sequence $\{\varepsilon(k)\}$, or a coloured noise sequence such as

$$w(k+1) = C_\varepsilon(q^{-1})\varepsilon(k+1)$$

where $C_\varepsilon(q^{-1})$ is assumed to be a linear filter having its roots strictly inside the unit circle of the z-domain. The model (4.79)-(4.81) can then be written as

$$A(q^{-1})y(k+1) = f(k) + C_\varepsilon(q^{-1})\varepsilon(k+1) \tag{4.82}$$

which is called a *Nonlinear AutoRegressive Moving-Average model with auXiliary input* (**NARMAX**). [10] If $C_\varepsilon(q^{-1}) = 1$, then $w(k+1)$ is white, and equation (4.82) reduces to (4.79).

Noise Model 3: Consider $\{w(k)\}$ to be any bounded nondeterministic noise sequence (satisfying Lemma 4.2.2), without specifying its statistical properties. The model (4.79)-(4.81) remains. The optimal prediction and control of the NNM are then subjected to conditions, such as the condition (4.74) in Lemma 4.2.2.

For the discussion of the nonlinear optimal prediction and control of the NNM in this chapter, the second noise model (4.82) is adopted, in which the term $w(k+1)$ is defined to be a white noise sequence so that $C_\varepsilon(q^{-1}) = 1$ in (4.82). Optimal prediction and control of the NNM will be developed from (4.79)-(4.81). The third noise model (i.e., (4.79)-(4.81)) will be employed in Sections 5.2 and 5.3 in which the boundedness of $w(k+1)$ (established by Lemma 4.2.2) will be used to prove the convergence of the parameter estimation algorithms as well as the convergence of the nonlinear adaptive control algorithms.

The layout of the remainder of this section is as follows. In Subsection 4.3.1 an optimal predictor of the output of the NNM is derived. In Subsection 4.3.2 the nonlinear stochastic generalised minimum variance control of the NNM and its closed-loop characteristics are presented. The closed-loop stability conditions are then established.

[10] The definition of a NARMAX model without additional feedback signals can be found in [157] (eqn. (7.4.20), p. 267).

4.3.1 SISO Optimal One-Step-Ahead Predictor.

The optimal prediction of the NNM discussed in this subsection is concerned with extrapolating a time series of the output variable into the future from the model (4.79)-(4.81). Since the NNM has been structured in a regression form, linear in the parameters, the prediction of the future output of the NNM can be constructed through simple algebraic manipulations of (4.79)-(4.81).

The assumption about the noise sequence $\{w(k)\}$ in the model (4.79)-(4.81) is formalised as follows.

Assumption 4.3.1 *Let the scalar sequence $\{w(k)\}$ in the model (4.79)-(4.81) be a real-valued stochastic process defined in a probability space $(\Omega, \mathcal{F}, \mathcal{P})$ [157] and adapted to the sequence of increasing sub-sigma algebras $(\mathcal{F}_k, k \in \mathcal{N})$, where $\mathcal{F}_k$ is generated by the observations up to and including time k. ($\mathcal{F}_0$ is assumed to contain all initial condition information.) The sequence $\{w(k)\}$ satisfies*

(i) $$E\{w(k+1)\,|\mathcal{F}_k\} = 0, \qquad a.s., \quad k \geq 0;$$

(ii) $$E\{w(k+1)^2\,|\mathcal{F}_k\} = \sigma_w^2, \qquad a.s., \quad k \geq 0,$$

where the symbol "a.s." means almost surely, i.e., save on a set having probability measure zero [157].

Under Assumption 4.3.1, $\{w(k)\}$ is a white noise sequence. The optimal prediction of the output of the NNM is then given by the following lemma.

Lemma 4.3.1 *Consider the model (4.79)-(4.81) in which $w(k+1)$ is subjected to Assumption 4.3.1 and $f(k)$ is $\mathcal{F}_k$ measurable. The optimal one-step-ahead prediction, $y^0(k+1 \mid k)$, of $y(k+1)$ satisfies*

$$y^0(k+1 \mid k) = G(q^{-1})y(k) + F(q^{-1})f(k) \tag{4.83}$$

where

$$y^0(k+1 \mid k) \triangleq y(k+1) - F(q^{-1})w(k+1). \tag{4.84}$$

$F(q^{-1})$ and $G(q^{-1})$ are the unique polynomials satisfying

$$F(q^{-1})A(q^{-1}) + q^{-1}G(q^{-1}) = 1, \tag{4.85}$$

$$F(q^{-1}) \equiv 1, \tag{4.86}$$

$$G(q^{-1}) \equiv \left[1 - A(q^{-1})\right] q. \tag{4.87}$$

The optimality of $y^0(k+1 \mid k)$ is established by

$$y^0(k+1 \mid k) = E\left\{y(k+1) \,|\mathcal{F}_k\right\}.$$

Also

$$E\left\{\left[y(k+1) - y^0(k+1 \mid k)\right]^2\right\} = \sigma_w^2.$$

Proof of Lemma 4.3.1

Refer to the proofs of Lemma 7.4.1 and Lemma 7.4.5 of [157].

Q.E.D.

Remark 4.3.1 *From (4.83) it is noted that*

(i) since the model (4.79)-(4.81) is linear in $y(k+1)$, the optimal predictor (4.83)-(4.87) has a simple closed-form expression for the prediction of the electrical torque (or power) output of the generator;

(ii) the inclusion in the model (4.79)-(4.81) of the measurable disturbance input as well as the additional feedback signals in $f(k)$ enhances the predictability of the output. This concept has been outlined in Subsection 4.2.3 with regard to the features of the NNM, and will be verified in Subsection 4.5.1.

The optimal predictor (4.83)-(4.87) will be used for the development of the nonlinear optimal control law in Subsection 4.3.2.

4.3.2 SISO Nonlinear Stochastic Generalised Minimum Variance Control Law.

The aim of optimal stochastic control of the NNM is to compensate for the stochastic noise $\{w(k)\}$ of zero mean (see Assumption 4.3.1(i)). The control input is chosen so as to minimise a cost function, $J(k+1)$, of the form

$$J(k+1) = E\left\{\left[W_y(q^{-1})y(k+1) - W_r(q^{-1})y^*(k+1)\right]^2 + \left[W_u(q^{-1})u(k)\right]^2\right\} \quad (4.88)$$

where $y^*(k+1)$ is the desired output trajectory; $W_y(q^{-1})$, $W_r(q^{-1})$, and $W_u(q^{-1})$ are the preselected weighting polynomials in the backward-shift operator

$$W_y(q^{-1}) = w_{y0} + w_{y1}q^{-1} + w_{y2}q^{-2} + \cdots, \quad (4.89)$$

$$W_r(q^{-1}) = w_{r0} + w_{r1}q^{-1} + w_{r2}q^{-2} + \cdots, \quad (4.90)$$

$$W_u(q^{-1}) = w_{u0} + w_{u1}q^{-1} + w_{u2}q^{-2} + \cdots, \quad (4.91)$$

with w_{y0} being taken to be 1 without loss of generality. The expectation is conditional upon the system input and output data acquired up to time k. Using the optimal predictor (4.83)-(4.87), the control $u(k)$ that minimises the cost function (4.88)-(4.91) is given by the following lemma.

Lemma 4.3.2 *For the model (4.79)-(4.81), the input $u(k)$ that minimises the cost function (4.88)-(4.91) is given by*

$$w_{u0}W_u(q^{-1})u(k) = \frac{df(k)}{du(k)}\left[W_r(q^{-1})y^*(k+1) - W_y(q^{-1})G(q^{-1})y(k) - W_y(q^{-1})f(k)\right]. \quad (4.92)$$

Proof of Lemma 4.3.2

Substituting for $y(k+1)$ from (4.84) into (4.88) and using Assumption 4.3.1, one finds

$$J(k+1) = \left[1 + \sum_{i=1} w_{yi}\right]\sigma_w{}^2 + \left[W_y(q^{-1})y^0(k+1 \mid k) - W_r(q^{-1})y^*(k+1)\right]^2 + \left[W_u(q^{-1})u(k)\right]^2. \quad (4.93)$$

Differentiating (4.93) with respect to $u(k)$ and setting the result equal to zero, one writes

$$\left[W_y(q^{-1})y^0(k+1 \mid k) - W_r(q^{-1})y^*(k+1)\right] \frac{\partial y^0(k+1 \mid k)}{\partial u(k)} + w_{u0}W_u(q^{-1})u(k) = 0. \tag{4.94}$$

Equation (4.92) immediately follows by substituting (4.83) into (4.94) and noting that

$$\frac{\partial y^0(k+1 \mid k)}{\partial u(k)} = \frac{df(k)}{du(k)}.$$

Q.E.D.

According to (4.81), $f(k)$ is also a function of $\bar{z}_i(k)$ $(i = 1, 2, 3, 4)$ and $\bar{y}_F(k)$ defined by (4.22)-(4.25) and (4.6), respectively. The solution of $\frac{df(k)}{du(k)}$ in (4.92) can then be written as

$$\begin{aligned}\frac{df(k)}{du(k)} &= \frac{\partial f(k)}{\partial z_1(k)}\frac{\partial z_1(k)}{\partial \bar{z}_1(k)}\frac{d\bar{z}_1(k)}{du(k)} + \frac{\partial f(k)}{\partial z_2(k)}\frac{\partial z_2(k)}{\partial \bar{z}_2(k)}\frac{d\bar{z}_2(k)}{du(k)} \\ &+ \frac{\partial f(k)}{\partial z_3(k)}\frac{\partial z_3(k)}{\partial \bar{z}_3(k)}\frac{d\bar{z}_3(k)}{du(k)} + \frac{\partial f(k)}{\partial z_4(k)}\frac{\partial z_4(k)}{\partial \bar{z}_4(k)}\frac{d\bar{z}_4(k)}{du(k)} \\ &+ \frac{\partial f(k)}{\partial y_F(k)}\frac{\partial y_F(k)}{\partial \bar{y}_F(k)}\frac{d\bar{y}_F(k)}{du(k)} + \frac{\partial f(k)}{\partial u(k)}\end{aligned} \tag{4.95}$$

where, due to (4.63)-(4.67),

$$\frac{\partial z_i(k)}{\partial \bar{z}_i(k)} = 1, \qquad (i = 1, 2, 3, 4), \tag{4.96}$$

$$\frac{\partial y_F(k)}{\partial \bar{y}_F(k)} = 1, \tag{4.97}$$

and

$$\frac{\partial f(k)}{\partial z_1(k)} = b_1, \tag{4.98}$$

$$\frac{d\bar{z}_1(k)}{du(k)} = 2\cos 2\delta(k)\frac{d\delta(k)}{du(k)}, \tag{4.99}$$

$$\frac{\partial f(k)}{\partial z_2(k)} = c_1, \tag{4.100}$$

$$\begin{aligned}\frac{d\bar{z}_2(k)}{du(k)} &= \frac{\partial \bar{z}_2(k)}{\partial \omega_s(k)}\frac{d\omega_s(k)}{du(k)} + \frac{\partial \bar{z}_2(k)}{\partial E_q'(k)}\frac{dE_q'(k)}{du(k)} + \frac{\partial \bar{z}_2(k)}{\partial \delta(k)}\frac{d\delta(k)}{du(k)} \\ &= E_q'(k)\cos\delta(k)\frac{d\omega_s(k)}{du(k)} + \omega_s(k)\cos\delta(k)\frac{dE_q'(k)}{du(k)}\end{aligned}$$

$$-\omega_s(k)E_q'(k)\sin\delta(k)\frac{d\delta(k)}{du(k)}, \tag{4.101}$$

$$\frac{\partial f(k)}{\partial z_3(k)} = d_1, \tag{4.102}$$

$$\begin{aligned}\frac{d\bar{z}_3(k)}{du(k)} &= \frac{\partial \bar{z}_3(k)}{\partial \omega_s(k)}\frac{d\omega_s(k)}{du(k)} + \frac{\partial \bar{z}_3(k)}{\partial E_{FD}(k)}\frac{dE_{FD}(k)}{du(k)} + \frac{\partial \bar{z}_3(k)}{\partial \delta(k)}\frac{d\delta(k)}{du(k)} \\ &= E_{FD}(k)\cos\delta(k)\frac{d\omega_s(k)}{du(k)} + \omega_s(k)\cos\delta(k)\frac{dE_{FD}(k)}{du(k)} \\ &\quad -\omega_s(k)E_{FD}(k)\sin\delta(k)\frac{d\delta(k)}{du(k)},\end{aligned} \tag{4.103}$$

$$\frac{\partial f(k)}{\partial z_4(k)} = e_1\left[d(k) - y_F(k) + u(k)\right], \tag{4.104}$$

$$\frac{d\bar{z}_4(k)}{du(k)} = \cos\delta(k)\frac{d\delta(k)}{du(k)}, \tag{4.105}$$

$$\frac{\partial f(k)}{\partial y_F(k)} = -e_1 z_4(k), \tag{4.106}$$

$$\begin{aligned}\frac{d\bar{y}_F(k)}{du(k)} &= \frac{\partial \bar{y}_F(k)}{\partial E_q'(k)}\frac{dE_q'(k)}{du(k)} + \frac{\partial \bar{y}_F(k)}{\partial \delta(k)}\frac{d\delta(k)}{du(k)} \\ &= \frac{1}{2}\bar{y}_F(k)^{-1}\left\{\left[m_7\cos\delta(k) + 2m_8E_q'(k)\right]\frac{dE_q'(k)}{du(k)}\right. \\ &\quad \left. + \left[(m_6 - m_5)\sin 2\delta(k) - m_7E_q'(k)\sin\delta(k)\right]\frac{d\delta(k)}{du(k)}\right\},\end{aligned} \tag{4.107}$$

$$\frac{\partial f(k)}{\partial u(k)} = e_1 z_4(k). \tag{4.108}$$

Substituting (4.96)-(4.108) into (4.95), one writes

$$\frac{df(k)}{du(k)} = \chi(k) + \beta_0(k) \triangleq \tilde{\beta}_0(k) \tag{4.109}$$

where

$$\begin{aligned}\chi(k) \triangleq\ & \left\{2b_1\cos 2\delta(k) - \omega_s(k)\sin\delta(k)\left[c_1E_q'(k) + d_1E_{FD}(k)\right]\right. \\ & + e_1\left[d(k) - y_F(k) + u(k)\right]\cos\delta(k) \\ & \left. - \frac{e_1}{2}z_4(k)\bar{y}_F(k)^{-1}\left[(m_6 - m_5)\sin 2\delta(k) - m_7E_q'(k)\sin\delta(k)\right]\right\}\frac{d\delta(k)}{du(k)} \\ & + \left\{\cos\delta(k)\left[c_1E_q'(k) + d_1E_{FD}(k)\right]\right\}\frac{d\omega_s(k)}{du(k)} \\ & + \left\{c_1\omega_s(k)\cos\delta(k) - \frac{e_1}{2}z_4(k)\bar{y}_F(k)^{-1}\left[m_7\cos\delta(k) + 2m_8E_q'(k)\right]\right\}\frac{dE_q'(k)}{du(k)} \\ & + \left\{d_1\omega_s(k)\cos\delta(k)\right\}\frac{dE_{FD}(k)}{du(k)},\end{aligned} \tag{4.110}$$

$$\beta_0(k) \triangleq e_1 z_4(k). \tag{4.111}$$

Remark 4.3.2 *From the definition of $\beta_0(k)$ in (4.111) and the condition (4.71), it follows that*

$$\sup_{0\leq k<\infty} |\beta_0(k)| \leq e_1 (1 + \Delta_5) \triangleq \beta_{0max} \tag{4.112}$$

where $e_1 > 0$ according to (4.52).

For the solution of $\chi(k)$ in (4.110), the SISO nonlinear continuous-time state-space equation (4.1) introduced in Subsection 4.2.1 is utilised. Using the *Backward Difference Approximation* **(BDA)** [11] (i.e., Assumption 4.2.2(i)) to approximate the derivatives of the state variables in (4.1) at time $t_k = kh$, the following difference equation of (4.1) is obtained

$$\mathbf{X}(kh) = \mathbf{X}(kh - h) + h\mathbf{A}(\mathbf{X}(kh)) + h\mathbf{B}_\mathbf{r}\mathbf{R}(kh) + h\mathbf{b}_{\bar{u}}\bar{u}(kh) \tag{4.113}$$

where h is the sampling period. From (4.113) and the definition of $\mathbf{b}_{\bar{u}}$ in (4.8), the expression for $\dfrac{d\mathbf{X}(k)}{d\bar{u}(k)}$ (where for convenience of notation kh is written as k, as described previously) can be found

$$\frac{d\mathbf{X}(k)}{d\bar{u}(k)} = h\mathbf{b}_{\bar{u}} = \begin{bmatrix} 0 & 0 & 0 & \frac{hK_A}{\tau_A} & 0 & 0 & 0 & 0 \end{bmatrix}^T. \tag{4.114}$$

Thus, according to the definition of $\mathbf{X}(t)$ in (4.3) as well as (4.69) in Assumption 4.2.4,

$$\frac{d\delta(k)}{du(k)} = \frac{d\delta(k)}{d\bar{u}(k)}\frac{d\bar{u}(k)}{du(k)} = 0, \tag{4.115}$$

$$\frac{d\omega_s(k)}{du(k)} = \frac{d\omega_s(k)}{d\bar{u}(k)}\frac{d\bar{u}(k)}{du(k)} = 0, \tag{4.116}$$

$$\frac{dE'_q(k)}{du(k)} = \frac{dE'_q(k)}{d\bar{u}(k)}\frac{d\bar{u}(k)}{du(k)} = 0, \tag{4.117}$$

$$\frac{dE_{FD}(k)}{du(k)} = \frac{dE_{FD}(k)}{d\bar{u}(k)}\frac{d\bar{u}(k)}{du(k)} = \frac{hK_A}{\tau_A} \tag{4.118}$$

are obtained from (4.114), by noting that $\dfrac{d\bar{u}(k)}{du(k)} = 1$. Therefore, the solution of $\chi(k)$ is readily derived by substituting (4.115)-(4.118) into (4.110), and results in

$$\chi(k) = \frac{d_1 hK_A}{\tau_A}\omega_s(k)\cos\delta(k). \tag{4.119}$$

[11] See, e.g., [141] p.176.

Consequently, the expression for $\frac{df(k)}{du(k)}$ in (4.109) (or (4.92)) is written as

$$\frac{df(k)}{du(k)} = \frac{d_1 h K_A}{\tau_A}\omega_s(k)\cos\delta(k) + e_1 z_4(k) = \tilde{\beta}_0(k) \tag{4.120}$$

due to (4.111) and (4.119).

Remark 4.3.3 *In view of (4.40) and (4.71), $\tilde{\beta}_0(k)$ in (4.120) is bounded for all k.*

Remark 4.3.4 *As an alternative to the BDA approach, the* Forward Difference Approximation **(FDA)** [12] *(or* Euler's method*) can be used to derive the expression for $\frac{df(k)}{du(k)}$. Using the FDA approach, the derivatives of the state variables in (4.1) are given by the following difference form*

$$\mathbf{X}(kh) = \mathbf{X}(kh-h) + h\mathbf{A}(\mathbf{X}(kh-h)) + h\mathbf{B_r}\mathbf{R}(kh-h) + h\mathbf{b}_{\bar{u}}\bar{u}(kh-h).$$

It is clear from the above equation that

$$\frac{d\mathbf{X}(k)}{d\bar{u}(k)} = 0.$$

Therefore, from (4.110) and (4.109) one immediately obtains that

$$\chi(k) = 0,$$

$$\frac{df(k)}{du(k)} = \beta_0(k) = \tilde{\beta}_0(k).$$

However, the BDA approach is adopted here because the same approach has been used for the derivation of the SISO nonlinear discrete-time input-output model (4.72)-(4.73) (see Assumption 4.2.2(i)).

In preparation for the derivation of the nonlinear optimal control law, a variable $g(k)$ is defined as

$$g(k) \triangleq f(k) - \beta_0(k)u(k). \tag{4.121}$$

The boundedness of $g(k)$ is given by

Lemma 4.3.3 *Subject to Assumptions 4.2.1, 4.2.4, and 4.2.5, $g(k)$ is bounded for all k.*

[12] See, e.g., [141] p.176.

Proof of Lemma 4.3.3

Lemma 4.3.3 is the consequence of the application of Lemma 4.2.3(i)-(ii) to (4.121).

Q.E.D.

The nonlinear optimal control law is now readily derived from Lemma 4.3.2, subject to the following assumption which ensures the solvability of the control input.

Assumption 4.3.2 *With proper selection of the leading coefficients of the weighting polynomials* $W_y(q^{-1})$ *and* $W_u(q^{-1})$,

(i) $\beta_0(k)\tilde{\beta}_0(k)w_{y0} + w_{u0}^2 \neq 0$, *for all* k.

(ii) $\sup\limits_{0\leq k<\infty} \left| \dfrac{1}{\beta_0(k)\tilde{\beta}_0(k)w_{y0} + w_{u0}^2} \right| < M_0$,

where $0 < M_0 < \infty$.

The nonlinear stochastic generalised minimum variance control law and its closed-loop characteristics are then given by

Theorem 4.3.1 *Subject to Assumption 4.3.2, for the model (4.79)-(4.81) having the optimal predictor (4.83)-(4.87),*

(a) the generalised minimum variance control $u^*(k)$ *minimising the cost function (4.88)-(4.91) is given by*

$$\left[\beta_0(k)\tilde{\beta}_0(k)W_y(q^{-1}) + w_{u0}W_u(q^{-1})\right] u^*(k)$$
$$= \tilde{\beta}_0(k)\left[W_r(q^{-1})y^*(k+1) - W_y(q^{-1})G(q^{-1})y(k) - W_y(q^{-1})g(k)\right]; \quad (4.122)$$

where

$$\beta_0(k) = e_1 z_4(k),$$
$$\tilde{\beta}_0(k) = \frac{d_1 h K_A}{\tau_A}\omega_s(k)\cos\delta(k) + e_1 z_4(k),$$
$$g(k) = f(k) - \beta_0(k)u(k);$$

(b) the effect of the control law (4.122) is to give

$$\tilde{\beta}_0(k)W_y(q^{-1})y^0(k+1 \mid k) = \tilde{\beta}_0(k)W_r(q^{-1})y^*(k+1) - w_{u0}W_u(q^{-1})u^*(k); \quad (4.123)$$

(c) with the control law given by (4.122), the closed-loop system is described by

$$\tilde{w}(q^{-1},k)\begin{bmatrix} y(k+1) \\ u^*(k) \end{bmatrix} = \tilde{H}(q^{-1},k)\begin{bmatrix} y^*(k+1) \\ g(k) \\ w(k+1) \end{bmatrix} \quad (4.124)$$

where

$$\tilde{w}(q^{-1},k) \triangleq \beta_0(k)\tilde{\beta}_0(k)W_y(q^{-1}) + w_{u0}W_u(q^{-1})A(q^{-1}) \quad (4.125)$$

and

$$\tilde{H}(q^{-1},k) \triangleq \begin{bmatrix} \beta_0(k)\tilde{\beta}_0(k)W_r(q^{-1}) & w_{u0}W_u(q^{-1}) \\ \tilde{\beta}_0(k)W_r(q^{-1})A(q^{-1}) & -\tilde{\beta}_0(k)W_y(q^{-1}) \\ \beta_0(k)\tilde{\beta}_0(k)W_y(q^{-1}) + w_{u0}W_u(q^{-1}) & \\ -\tilde{\beta}_0(k)W_y(q^{-1})G(q^{-1})q^{-1} & \end{bmatrix}; \quad (4.126)$$

(d) the resulting closed-loop system (4.124)-(4.126) is bounded-input bounded-output stable provided that:

(i) $\tilde{w}(z^{-1},k) \triangleq \beta_0(k)\tilde{\beta}_0(k)W_y(z^{-1}) + w_{u0}W_u(z^{-1})A(z^{-1})$

is bounded for all k;

(ii) $\sup_{0\le k<\infty} \| \Theta_{\tilde{w}}(k+1) - \Theta_{\tilde{w}}(k) \| \le \epsilon_{\tilde{w}}$

where $\epsilon_{\tilde{w}}$ *is sufficiently small and* $\Theta_{\tilde{w}}(k)$ *is the coefficient vector of* $\tilde{w}(z^{-1},k)$*, defined as*

$$\Theta_{\tilde{w}}(k)^T \triangleq \begin{bmatrix} 1 & \theta_{\tilde{w}1}(k) & \theta_{\tilde{w}2}(k) & \cdots & \theta_{\tilde{w}n}(k) \end{bmatrix}$$

with

$$\tilde{w}(z^{-1},k) \triangleq \theta_{\tilde{w}0}(k)\left[1 + \theta_{\tilde{w}1}(k)z^{-1} + \theta_{\tilde{w}2}(k)z^{-2} + \cdots + \theta_{\tilde{w}n}(k)z^{-n}\right]$$

where n denotes the order of the polynomial $\tilde{w}(z^{-1},k)$*;*

(iii) $\tilde{w}(z^{-1},k) \neq 0$

for all $| z^{-1} | \le 1$ *and all k.*

Proof of Theorem 4.3.1

See Section E.1 of Appendix E.

Q.E.D.

Remark 4.3.5 *In Theorem 4.3.1,*

(i) the stochastic control law (4.122) is based on the optimal predictor (4.83)-(4.87). The predictor allows one to determine, using past input/output data, the predictable part of the disturbance on the future response and hence to cancel it using the control action.

(ii) since the model (4.79)-(4.81) is linear in the control input, the solvability of $u^*(k)$ from (4.122) is ensured subject to Assumption 4.3.2(i)-(ii).

The closed-loop system stability established in Theorem 4.3.1(d) is essential for the implementation of the control law (4.122). It guarantees the existence of a *bounded* optimal control $u^*(k)$ such that the operation governed by (4.123) is feasible. Theorem 4.3.1 will be used in Subsection 4.4 to derive the nonlinear stochastic weighted minimum variance control law which forms the desired nonlinear optimal control strategy for the design of the nonlinear optimal power system stabiliser.

4.4 A Nonlinear Optimal Weighted Minimum Variance Power System Stabiliser and Stability Analysis.

In this section:

- the nonlinear stochastic weighted minimum variance control of the NNM is developed from Theorem 4.3.1 given in Subsection 4.3.2, and the closed-loop characteristics are presented;

- the closed-loop stability conditions with the nonlinear stochastic weighted minimum variance control law are established;
- a nonlinear weighted minimum variance power system stabiliser is proposed.
- the control structure of the SMIB power system equipped with the proposed nonlinear optimal power system stabiliser is given.

The nonlinear stochastic generalised minimum variance control law established in Theorem 4.3.1 is based on the cost function (4.88)-(4.91) for which a wide range of the weighting polynomials $W_y(q^{-1})$, $W_r(q^{-1})$, and $W_u(q^{-1})$ can be chosen. Different weighting polynomials result in different forms of the nonlinear optimal control law. Table 4.1 shows a few special cases.

Nonlinear Control Laws	$W_y(q^{-1})$	$W_r(q^{-1})$	$W_u(q^{-1})$
Minimum Variance	1	1	0
Weighted Minimum Variance	1	1	$\lambda^{\frac{1}{2}}$, $(\lambda > 0)$
Integrated Minimum Variance	1	1	$\lambda^{\frac{1}{2}}(1-q^{-1})$, $(\lambda > 0)$

Table 4.1: SISO nonlinear optimal control laws with their selections of weighting polynomials.

As a parallel study to the linear stochastic weighted minimum variance control approach discussed in Section 3.5, a nonlinear stochastic weighted minimum variance control law is considered in this section for the construction of the desired nonlinear optimal power system stabiliser. As shown in Table 4.1, such a control law is achieved simply by selecting $W_y(q^{-1}) = 1$, $W_r(q^{-1}) = 1$, and $W_u(q^{-1}) = \lambda^{\frac{1}{2}}$ in the cost function (4.88)-(4.91), which then reduces to

$$J(k+1) = E\left\{[y(k+1) - y^*(k+1)]^2 + \lambda u(k)^2\right\} \tag{4.127}$$

where the weighting coefficient $\lambda > 0$.

For the derivation of the nonlinear stochastic weighted minimum variance control law from Theorem 4.3.1, assumptions concerning $\chi(k)$ (4.119) and $\tilde{\beta}_0(k)$ (4.109) are made as follows.

Assumption 4.4.1 *Under Assumption 2.2.5, $\chi(k)$ (4.119) and $\tilde{\beta}_0(k)$ (4.109) satisfy*

$$\chi(k) \approx 0,$$

$$\tilde{\beta}_0(k) \approx \beta_0(k).$$

The nonlinear stochastic weighted minimum variance control law and its closed-loop characteristics are then given by

Theorem 4.4.1 *For the model (4.79)-(4.81) having the optimal predictor (4.83)-(4.87), subject to Assumption 4.4.1,*

(a) the weighted minimum variance control $u^*(k)$ minimising the cost function (4.127) is given by

$$\left[\beta_0(k)^2 + \lambda\right] u^*(k) = \beta_0(k)\left[y^*(k+1) - G(q^{-1})y(k) - g(k)\right] \tag{4.128}$$

which is equivalent to

$$\beta_0(k)y^0(k+1 \mid k) = \beta_0(k)y^*(k+1) - \lambda u^*(k);$$

(b) when the control law (4.128) is used for all k, the closed-loop system is described by

$$\tilde{w}(q^{-1},k)\begin{bmatrix} y(k+1) \\ u^*(k) \end{bmatrix} = \tilde{H}(q^{-1},k)\begin{bmatrix} y^*(k+1) \\ g(k) \\ w(k+1) \end{bmatrix} \tag{4.129}$$

where

$$\tilde{w}(q^{-1},k) \triangleq \beta_0(k)^2 + \lambda A(q^{-1}) \tag{4.130}$$

and

$$\tilde{H}(q^{-1},k) \triangleq \begin{bmatrix} \beta_0(k)^2 & \lambda & \beta_0(k)^2 + \lambda \\ \beta_0(k)A(q^{-1}) & -\beta_0(k) & -\beta_0(k)G(q^{-1})q^{-1} \end{bmatrix}; \tag{4.131}$$

(d) the resulting closed-loop system (4.129)-(4.131) is bounded-input bounded-output stable provided that:

(i) $\tilde{w}(z^{-1},k) \triangleq \beta_0(k)^2 + \lambda A(z^{-1})$

is bounded for all k*;*

(ii) $\sup_{0\le k<\infty} \| \Theta_{\tilde{w}}(k+1) - \Theta_{\tilde{w}}(k) \| \le \epsilon_{\tilde{w}}$

where $\epsilon_{\tilde{w}}$ *is sufficiently small and* $\Theta_{\tilde{w}}(k)$ *is defined as*

$$\Theta_{\tilde{w}}(k)^T \triangleq \left[\begin{array}{ccc} 1 & \frac{\lambda a_1}{\beta_0(k)^2+\lambda} & \frac{\lambda a_2}{\beta_0(k)^2+\lambda} \end{array}\right] \tag{4.132}$$

with

$$\tilde{w}(z^{-1},k) = \left[\beta_0(k)^2 + \lambda\right]\left[1 + \frac{\lambda a_1}{\beta_0(k)^2+\lambda} z^{-1} + \frac{\lambda a_2}{\beta_0(k)^2+\lambda} z^{-2}\right]; \tag{4.133}$$

(iii) $\tilde{w}(z^{-1},k) \neq 0$

for all $| z^{-1} | \le 1$ *and all* k.

Proof of Theorem 4.4.1

Exactly as for Theorem 4.3.1 (given by Section E.1 of Appendix E) on noting that $\tilde{\beta}_0(k) \approx \beta_0(k)$, $W_y(q^{-1}) = W_r(q^{-1}) = 1$, and $W_u(q^{-1}) = \lambda^{\frac{1}{2}}$.

Q.E.D.

Remark 4.4.1 *In Theorem 4.4.1, because* $\lambda > 0$, $\beta_0(k)^2 + \lambda > 0$ *is satisfied for all* k. *Hence, the solvability of* $u^*(k)$ *from (4.128) is guaranteed.*

Remark 4.4.2 *According to the definition of* $\beta_0(k)$ *in (4.111) (see also Remark 4.2.8),* $\beta_0(k)$ *is an implicit function of* $y(k)$. *This determines the nonlinear nature of the control law (4.128).*

The closed-loop stability of the control law (4.128) can be given by

Theorem 4.4.2 *For the system (4.79)-(4.81) having the nonlinear stochastic weighted minimum variance controller (4.128), there exists a choice of* λ *such that the closed-loop system (4.129)-(4.131) is bounded-input bounded-output stable.*

Proof of Theorem 4.4.2

See Section E.2 of Appendix E.

Q.E.D.

Theorem 4.4.2 gives a *sufficient* condition for the stability of the closed-loop system (4.129)-(4.131). It ensures the global stability of the closed-loop system associated with the control law (4.128). This control law can be used directly as the desired nonlinear optimal power system stabiliser. It will be used for the development of the corresponding nonlinear *adaptive* control laws in Section 5.3.

In practice, if the power system is operating under a no-load steady-state operating condition, then $\delta(k) \approx 0$, which leads to $\beta_0(k) \approx 0$ (since $\beta_0(k) = e_1 \sin \delta(k)$). For small disturbances around this operating point, the control action from (4.128) will be close to zero, which may result in an ineffective control action on the damping of small oscillations around the operating point. In order to prevent the control action from being close to zero for small disturbances, modifications to the control law (4.128) can be adopted. The consequent control algorithm which takes the physical limitations into account is then given by

Algorithm 4.1 [modified nonlinear weighted minimum variance control law.]

$$u^0(k) = \frac{\bar{\beta}_0(k)}{\beta_0(k)^2 + \lambda} \left[y^*(k+1) - G(q^{-1})y(k) - g(k) \right], \tag{4.134}$$

$$u^*(k) = \begin{cases} u_{max} & \text{if } u^0(k) \geq u_{max} \\ u^0(k) & \text{if } u_{min} < u^0(k) < u_{max} \\ u_{min} & \text{if } u^0(k) \leq u_{min} \end{cases}; \tag{4.135}$$

where

$$\bar{\beta}_0(k) = \begin{cases} \beta_0(k) & \text{if } |\beta_0(k)| > \beta_{0min} \\ \text{sign}[\beta_0(k)]\beta_{0min} & \text{otherwise} \end{cases}; \tag{4.136}$$

β_{0min} is a preselected constant, satisfying $0 < \beta_{0min} < \beta_{0max}$ where β_{0max} is defined by (4.112); λ is the weighting coefficient; u_{max} and u_{min} are known constants.

$\nabla\ \nabla\ \nabla$

Remark 4.4.3 *According to (4.112), $\bar{\beta}_0(k)$ in (4.136) satisfies*

$$0 < \beta_{0min} \leq \left|\bar{\beta}_0(k)\right| \leq \beta_{0max}, \qquad \text{for all } k. \tag{4.137}$$

Remark 4.4.4 *The suggested procedure for the selection of β_{0min} is:*

(i) choose a minimum value, $\Delta_\delta > 0$, of the rotor angle $\delta(k)$ (e.g., $\Delta_\delta = 1^o = 0.0175$ (rad));

(ii) calculate β_{0min} according to (4.111), i.e.,

$$\beta_{0min} = e_1 \sin \Delta_\delta \tag{4.138}$$

where $e_1 > 0$ is defined by (4.52).

Algorithm 4.1 ((4.134)-(4.136)) forms the *Nonlinear Optimal Weighted Minimum Variance Power System Stabiliser* **(NOWMV-PSS)** for the SMIB power system modelled in Subsection 2.3.1. The control structure of the system equipped with the NOWMV-PSS is given by Fig. 4.4. The stabilising signal $y(k)$ is the machine electrical power, $P_e(k)$ (or torque, $T_e(k)$). The performance of the NOWMV-PSS will be evaluated in Section 4.5.

Remark 4.4.5 *Referring to Remark 3.5.2, in practice the desired output trajectory $y^*(k)$ in Fig. 4.4 can be provided by feeding back the output variable $y(k)$ through a low-pass filter. However, for the sake of simplicity, $y^*(k)$ is set, artificially, to be the reference power ($P_{ref}(k)$) in the simulation studies of this chapter as well as Chapters 5 and 6. The same approach has been utilised in Chapter 3 (see Remark 3.5.2).*

Remark 4.4.6 *As indicated in Section 3.3, for a high-gain AVR-excitation control system, the steady-state value of the control action of the weighted minimum variance*

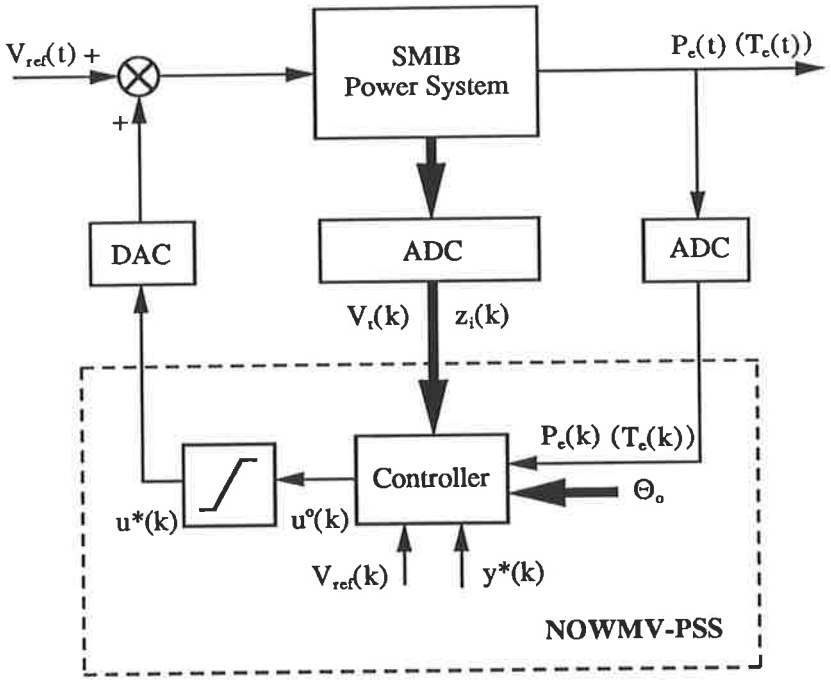

Figure 4.4: Control structure of the SMIB power system with the NOWMV-PSS.

power system stabiliser will converge to a very small value (see (3.42)). Therefore, the optimal control signal $u^*(k)$ (either in (4.128) or in (4.134)-(4.136)) satisfies

$$\lim_{k\to\infty} |u^*(k)| \leq \epsilon_{u^*} \tag{4.139}$$

where ϵ_{u^*} is a small constant, dependent of the value of the gain of the AVR. This condition will be employed in Section G.3 of Appendix G for the analysis of the convergence of the nonlinear adaptive control algorithms to be designed in Section 5.3.

4.5 Evaluation of the Performance of the Nonlinear Optimal Weighted Minimum Variance Power System Stabiliser.

In this section:

- the validity of the *discrete-time* NNM derived in Section 4.2 to represent the *continuous-time* nonlinear power system (CSM3) given in Subsection 2.3.1 is verified through simulation studies;
- the performance of the NOWMV-PSS proposed in Section 4.4 is investigated through the *evaluation studies* (Studies 1-11);
- the robustness of the NOWMV-PSS is tested with unmodelled dynamics and modelling errors (Studies 12-15).

The NOWMV-PSS proposed in Section 4.4 is realised by a digital computer which implements the calculations for generating the control signal. A sampling period of 20 ms is used.

Following the *procedure* described in Section 3.6, the simulation studies of this section will be conducted in three **Stages**:

Stage 1: Verification of the NNM — to examine the performance of the discrete-time NNM in tracking and predicting the dynamics and transients of the continuous-time nonlinear power system (CSM3) at different system operating conditions.

Stage 2: Evaluation of the performance of the NOWMV-PSS — to compare the dynamic and transient behaviour of the NOWMV-PSS with that of the LAWMV-PSS through Studies 1-11.

Stage 3: Studies on the robustness of the NOWMV-PSS — to test the performance of the NOWMV-PSS when the CSM3 is replaced by the CSM1 through Studies 12-15.

The implementation of the above three **Stages** will be discussed in Subsections 4.5.1, 4.5.2, and 4.5.3, which follow. The parameters and limits associated with the SMIB power system and the NOWMV-PSS are listed in Appendix C. The simulation results obtained from this section will be used as a *reference* for the comparison of the system performance of the nonlinear optimal and nonlinear adaptive control approaches in Chapter 5.

4.5.1 Verification of the Nonlinear Nominal Model of the Power System.

In this subsection the validity of using the *discrete-time* NNM (4.76)-(4.78) to represent the *continuous-time* nonlinear power system (CSM3 with $D = 4.0$ pu) is verified through simulation studies at different system operating conditions. The output signal is the machine electrical torque, $T_e(k)$. This subsection is the implementation of **Stage 1.**

Aims and structure of the simulation studies.

In the computer calculations, the electrical torque output of the NNM is the *optimal one-step-ahead prediction* of the actual electrical torque output of the CSM3, i.e.,

$$T_e^0(k \mid k-1) = \phi(k-1)^T \Theta_0. \tag{4.140}$$

According to (4.84), $T_e^0(k \mid k-1)$ is related to $T_e(k)$ through the relation

$$T_e^0(k \mid k-1) = T_e(k) - w(k). \tag{4.141}$$

Given the values of the parameters of the power system (CSM3) in Appendix C and the value of the infinite bus voltage (V_∞) at specified operating conditions, the values of the model parameters (a_1, etc., as defined by (4.44)-(4.45), (4.59)-(4.60), and (4.49)-(4.52)) of the NNM are pre-calculated. Let the control input $u(k)$ be an external test signal which is injected into the summing junction of the input of the AVR and the predictor, simultaneously. The model of the predictor is the fixed-parameter NNM. At each sampling instant, the predicted electrical torque output ($T_e^0(k \mid k-1)$) of the NNM is calculated by utilising the signals (such as $T_e(k-1)$, $z_i(k-1)$, etc.) obtained from the continuous-time nonlinear power system (CSM3) at the last sampling instant, and is compared with the current actual electrical torque output ($T_e(k)$) of the CSM3. The difference between $T_e^0(k \mid k-1)$ and $T_e(k)$ is denoted by $w(k)$ which is updated according to (4.141). The configuration for this study is illustrated in Fig. 4.5. The aims of this study are

- to confirm that the NNM is an accurate representation of the CSM3 when the system is operating within linear operation;
- to demonstrate that the NNM inherently possesses the ability to track the output accurately;
- to examine the validity of the NNM when the system is subjected to faults and/or changes in the system configuration.

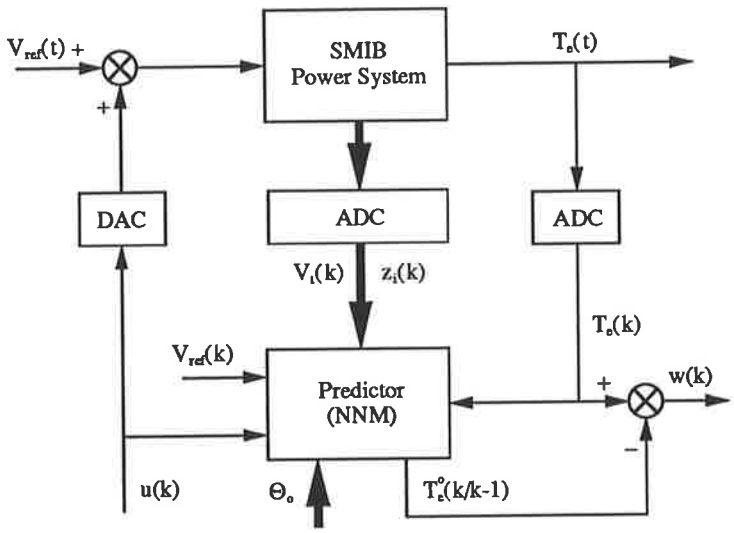

Figure 4.5: Structure of the verification of the NNM.

For the above purposes, two **Groups** of simulation studies are conducted:

Group 1: Let the same PRBS signal as that used in Subsection 3.6.1 be the signal $u(k)$ that is injected into the summing junction of the input of the AVR and the predictor. Two dynamic studies are performed:

Case 1: The system is operating at $P_t = 0.6$ pu and $Q_t = 0.3$ pu, and is subjected to a step change of 0.05 pu increase in reference power at time $t = 20$ second.

Case 2: The system is operating at $P_t = 0.6$ pu and $Q_t = -0.1$ pu, and is subjected to a step change of 0.05 pu decrease in reference power at time $t = 20$ second.

Group 2: Set the signal $u(k)$ to zero. Two transient studies are performed:

Case 3: The system is operating at $P_t = 0.6$ pu and $Q_t = 0.3$ pu, and is subjected to a three-phase fault on the receiving end busbars. The fault is cleared in 100 ms and the system returns to its pre-fault operating condition.

Case 4: The system is operating at $P_t = 0.6$ pu and $Q_t = -0.1$ pu, and is subjected to a three-phase fault of 100 ms duration at the machine terminal. The line is lost after the fault is cleared, and a new operating point is established.

The simulation results associated with Cases 1-4 are plotted in Figs. 4.6-4.9. The parameters of the NNM at the given lagging and leading operating points are listed in Table 4.2.

	lagging operating point ($V_\infty = 0.91214$)	**leading operating point** ($V_\infty = 1.0673$)
a_1	-1.7863	-1.7863
a_2	0.78857	0.78857
b_1	-8.03537E-02	-0.11002
b_2	8.03578E-02	0.11002
c_1	9.6592	11.302
c_2	-8.0494	-9.4186
d_1	2.84430E-02	3.32813E-02
e_1	9.05368E-02	0.10594

Table 4.2: Parameters of the NNM at the lagging ($P_t = 0.6$ pu, $Q_t = 0.3$ pu, $V_t = 1.0$ pu) and leading ($P_t = 0.6$ pu, $Q_t = -0.1$ pu, $V_t = 1.0$ pu) operating points.

Analysis of the simulation studies.

Group 1: The simulation studies in the first group involve the comparison of the time responses of $T_e^0(k \mid k-1)$ from the NNM and $T_e(k)$ from the CSM3 when the system is operating within linear operation. Subject to the PRBS input signal and the step change in reference power, the dynamic behaviour of $T_e^0(k \mid k-1)$ and $T_e(k)$ in Case 1 is plotted in Fig. 4.6. It is seen that the trajectories of $T_e^0(k \mid k-1)$ and $T_e(k)$ are almost identical. $T_e^0(k \mid k-1)$ tracks $T_e(k)$ perfectly, even at time $t = 20$ second, when the system operating point changes. In order to further demonstrate the output tracking ability of the NNM, the error $w(k)$ between $T_e^0(k \mid k-1)$ and $T_e(k)$ in Case 1 is plotted in Fig. 4.7 by the solid line. For the sake of comparison, Case 1 is applied to the identification of the LNM (proposed in Section 3.2), and the error between the predicted output of the LNM and the actual output of the CSM3 is plotted in the same graph (Fig. 4.7) by the dotted line. It is seen from Fig. 4.7 that while the estimated LNM presents a sudden increase in its error about $t = 20$ second when the system operating point has a step change, the NNM shows *consistently* a small error over the time horizon. It is then evident that the NNM *inherently* tracks the change in the system operating point. The same phenomenon can be observed in Case 2, the graphs of which are therefore omitted.

Remark 4.5.1 *The significant difference between the NNM and the estimated LNM is shown clearly in Fig. 4.7. With the NNM, there is no time delay in tracking the system output during the transients (e.g., about $t = 20$ second) and a smaller error in the dynamics (e.g., after $t = 20$ second) when compared with the response of the estimated LNM. This fact indicates that the NNM provides a* better *prediction of the output than the estimated LNM. Therefore, it is reasonable to expect that a nonlinear optimal control approach which is based on the NNM will give a* better *control action than a linear adaptive control approach, the model of which is the estimated LNM. This point will be verified by the comparison of the performance of the NOWMV-PSS and the LAWMV-PSS to be conducted in Subsection 4.5.2.*

Remark 4.5.2 *Figure 4.7 provides evidence of the boundedness of the noise term, $w(k)$, established in Lemma 4.2.2.*

Group 2: The second group of simulation studies tests the validity of the discrete-time NNM when the continuous-time CSM3 is subjected to faults and/or changes in the system configuration. The faults specified in Cases 3 and 4 cause limiting to occur on certain system variables, so that Assumption 2.4.1 which is used for the development of the NNM is violated. It is seen from Figs. 4.8-4.9 that the NNM gives a poor prediction of the electrical torque output of the CSM3 during the occurrence of the faults (0.5 second - 0.6 second). However, it quickly tracks back the dynamics of the system shortly after the faults are cleared. Good post-fault output tracking ability of the NNM is shown in Fig. 4.8 in which the CSM3 returns to its pre-fault operating condition. In Fig. 4.9 a small error between $T_e^0(k \mid k-1)$ and $T_e(k)$ can be found after the clearance of the fault. This is due to the fact that the CSM3 has changed its pre-fault configuration by losing the faulted line, causing the value of the transmission line reactance X_e to be doubled. With fixed parameters, the NNM updates the post-fault output prediction which is still based on the pre-fault values of the model parameters, and this results in the post-fault output tracking error as shown in Fig. 4.9.

Remark 4.5.3 *Since the NNM is derived from the NAM which excludes the system intentional nonlinearities introduced by the limits, the NNM has a potential shortcoming in representing the CSM3 during the faults. Hence the phenomenon of poor output prediction of the NNM, exhibited in Figs. 4.8-4.9 during 0.5 second - 0.6 second, is expected. As a result, the noise term $w(k)$ is significant during this period of time.*

Remark 4.5.4 *The post-fault output tracking error shown in Fig. 4.9 indicates that the NNM does not have the ability to follow the changes in the system parameters and configuration. Nevertheless, NNM still follows the post-fault dynamics of the system.*

Conclusions.

Summarising the simulation results of Cases 1-4, it is concluded that:

1. The discrete-time NNM represents the continuous-time CSM3 *accurately* within linear operation of the system. This fact verifies Remark 4.2.7.

2. The NNM *inherently* possesses the ability to track the output accurately in dynamics.

3. The NNM is a valid representation of the CSM3 after faults, provided that there are no configuration changes in the system.

The use of the NNM to represent the CSM3 for the design of the nonlinear optimal power system stabiliser is thus verified.

4.5.2 Evaluation of the Performance of the NOWMV-PSS for the CSM3.

In this subsection the evaluation of the performance of the NOWMV-PSS is conducted for the CSM3 (with $D = 4.0$ pu) through the series of *evaluation studies* (Studies 1-11) defined in Subsection 3.6.2. This subsection is the implementation of **Stage 2**.

Aims and structure of the simulation studies.

The control structure of the CSM3 equipped with the NOWMV-PSS is illustrated in Fig. 4.4. The machine electrical torque is used as the stabilising signal. For each simulation study, the performance of the CSM3 equipped with the NOWMV-PSS is compared with that of the CSM3 equipped with the LAWMV-PSS proposed in Chapter 3. The aims of this study are

- to confirm that the proposed NOWMV-PSS has good characteristics.
- to establish a reference for the comparison of the performance of the nonlinear optimal and nonlinear adaptive control strategies to be conducted in Subsection 5.4.2.

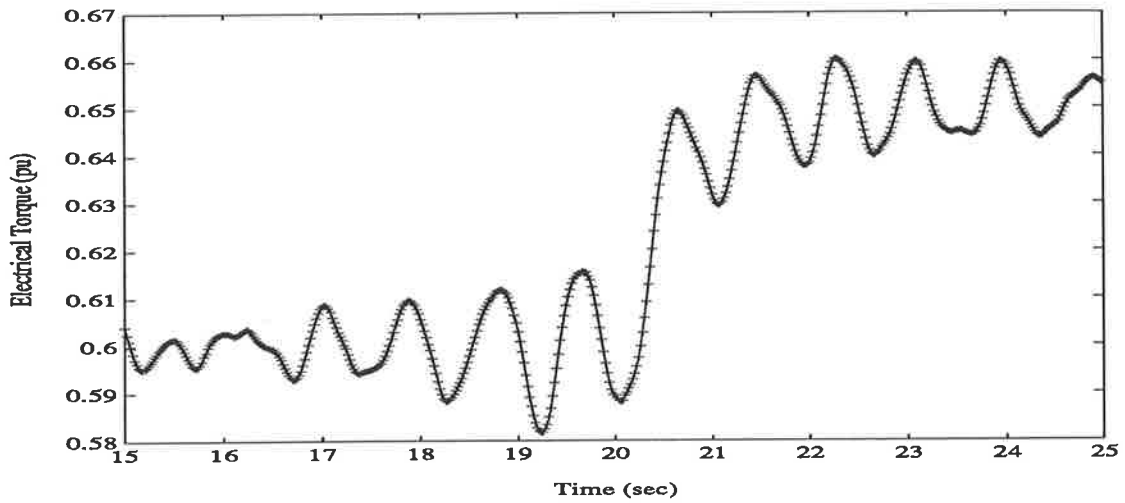

Figure 4.6: Electrical torque response for Case 1 ($P_t = 0.6$ pu, $Q_t = 0.3$ pu; 0.05 pu increase in reference power). CSM3 - solid line, NNM - line marked by '+'.

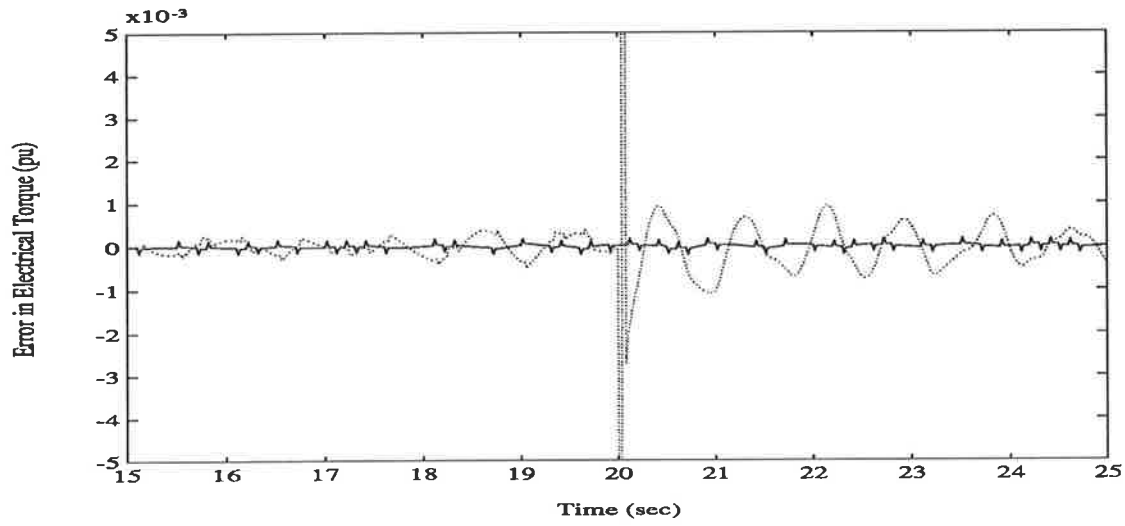

Figure 4.7: Error in electrical torque for Case 1 ($P_t = 0.6$ pu, $Q_t = 0.3$ pu; 0.05 pu increase in reference power). NNM - solid line, estimated LNM - dotted line.

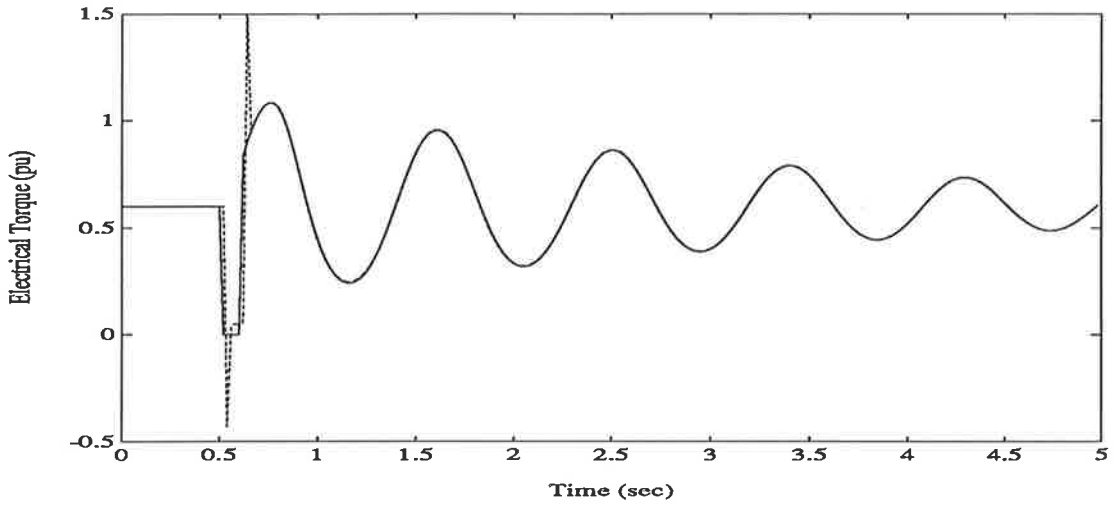

Figure 4.8: Electrical torque response for Case 3 ($P_t = 0.6$ pu, $Q_t = 0.3$ pu; 100 ms short-circuit on the receiving end busbars). CSM3 - solid line, NNM - dashed line.

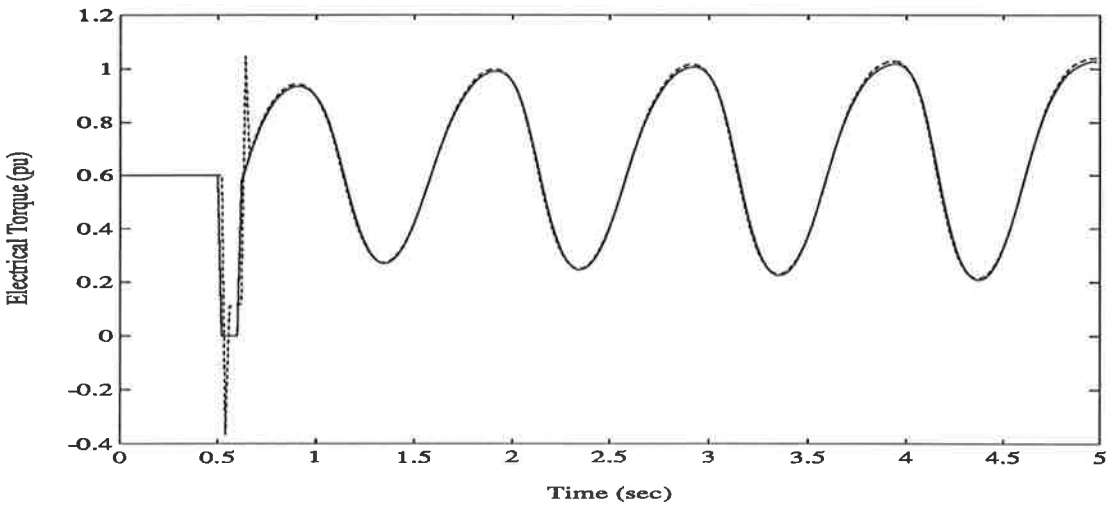

Figure 4.9: Electrical torque response for Case 4 ($P_t = 0.6$ pu, $Q_t = -0.1$ pu; 100 ms short-circuit at the machine terminal). CSM3 - solid line, NNM - dashed line.

Studies 1-11 allocated to the five **Groups** specified in Subsection 3.6.2 are implemented. The simulation results are given by Figs. 4.10-4.21 in which the performance of the LAWMV-PSS is provided by Figs. 3.5-3.12 and 3.14-3.17. The parameters of the NOWMV-PSS are: $u_{min} = -0.05$ pu, $u_{max} = 0.05$ pu, $\lambda = 0.4$ (these values are the same as those used in the LAWMV-PSS), and $\beta_{0min} = 0.0001$.

Analysis of the simulation studies.

Group 1: The *dynamic performance* of the NOWMV-PSS is examined in Studies 1-3 by simulating the periodic changes in the system operating point. The simulation results are shown in Figs. 4.10-4.12. In Studies 1-2, with the step changes in reference power, the estimated parameters of the LNM converge rapidly. Therefore, as shown in Figs. 4.10-4.11, the system responses with the NOWMV-PSS and the LAWMV-PSS are similar. However, in Study 3 (shown in Fig. 4.12), in which the reactive power of the system is changed between the lagging and leading conditions, the convergence rate of the estimated parameters of the LNM is relatively slow. The damping performance associated with the LAWMV-PSS shows a deterioration when compared with the NOWMV-PSS. As indicated in Remark 4.5.1, since the NNM inherently tracks the changes in the system operating point, the control action of the NOWMV-PSS is optimal at each new operating point immediately. Hence, the NOWMV-PSS provides better damping of the rotor oscillations than the LAWMV-PSS.

Group 2: The *transient performance* of the NOWMV-PSS following three-phase faults on a transmission line is examined in Studies 4-6. The simulation results are plotted in Figs. 4.13-4.16. In Study 4 (shown in Fig. 4.13), the settling times associated with the LAWMV-PSS and the NOWMV-PSS are almost the same. However, the amplitude of the first few swings associated with the LAWMV-PSS is greater than that with the NOWMV-PSS. This is due to the fact that the LAWMV-PSS needs to readjust its parameters, and its control action is not optimal before the convergence of the estimated parameters. The NOWMV-PSS, however, provides an optimal control action to damp the rotor oscillations as soon as the fault is removed. In Study 5 (shown in Fig. 4.14), the LAWMV-PSS takes time to identify the new operating point with the

new system configuration following the clearance of the faulted line. Consequently, the performance of the LAWMV-PSS is inferior to that of the NOWMV-PSS. As indicated in Remark 4.5.4 (see also Fig. 4.9), because the NOWMV-PSS can still follow the system dynamics, even with the use of the pre-fault model parameters, the NOWMV-PSS provides more rapid damping than the LAWMV-PSS. The above explanations of the behaviour of the NOWMV-PSS and the LAWMV-PSS in Studies 4-5 can also be applied to Study 6 (shown in Fig. 4.16).

Remark 4.5.5 *Figure 4.15 illustrates the field voltage $E_{FD}(t)$ response for the test in Study 5. The conclusions regarding the field voltage responses of the different power system stabilisers support those made for the torque responses. Further to this, the field voltage response of the NOWMV-PSS shows that the NOWMV-PSS can provide a control action with appropriate amplitude and phase, resulting in the stronger damping of the rotor oscillations as revealed by the responses.*

Group 3: The *ability* of the NOWMV-PSS to track the changes in the system parameters and configuration is examined in Study 7. The LAWMV-PSS can sense the change in the value of X_e (from 0.4 pu to 0.8 pu) by readjusting its parameters on-line. With fixed parameters, the NOWMV-PSS does *no* on-line adjustment. Therefore, as shown in Fig. 4.17, the NOWMV-PSS shows lighter damped performance than that of the LAWMV-PSS when one transmission line is switched out (during the time period 10.5 second - 20.5 second). However, when the lost line is switched back (after $t = 20.5$ second), the control action of the NOWMV-PSS is superior to that of the LAWMV-PSS, the parameters of which need to be readjusted again (see also Fig. 3.13).

Group 4: In Studies 8-9, the *ability* of the NOWMV-PSS to overcome the measurable deterministic disturbances in reference voltage is examined. It shows clearly, in Figs. 4.18-4.19, that the NOWMV-PSS provides faster damping than the LAWMV-PSS.

Remark 4.5.6 *As discussed in Section 4.2 concerning the features of the NNM, the NNM includes the voltage reference signal, $d(k)$,* explicitly. *Therefore, once a step*

change of $d(k)$ is applied to the system, the NOWMV-PSS immediately acts to damp the predicted output oscillations even before *the influence of this disturbance actually affects the system output. Based on this fact, the NOWMV-PSS can provide some feedforward compensation for the disturbance $d(k)$ and, consequently, better control performance than the LAWMV-PSS.*

Group 5: The *ability* of the NOWMV-PSS to extend the system stability region is examined in Studies 10-11, shown in Figs. 4.20-4.21. The behaviour of the NOWMV-PSS is as good as that of the LAWMV-PSS. It is then evident that both the NOWMV-PSS and the LAWMV-PSS are well designed.

Conclusions.

From the analysis of the simulation results in this subsection, it is concluded that:

1. With the use of the same value of the weighting coefficient λ, the NOWMV-PSS is more effective than the LAWMV-PSS in most cases:
   - In dynamic situations, the NOWMV-PSS possesses the inherent ability to track the changes in the system operating point, thus it provides a better damping effect than the LAWMV-PSS.
   - Following a three-phase fault, the NOWMV-PSS can offer a fast optimal control action for damping system oscillations. This is due to the fact that the NOWMV-PSS does not involve any on-line parameter adjustment; its optimal control action has no time delay.
2. The lack of a facility for on-line parameter adjustment associated with the NOWMV-PSS deleteriously affects its damping performance, when the system parameters or the operating conditions (and hence the parameters of the NNM) change.

Remark 4.5.7 *The above shortcoming of the NOWMV-PSS will initiate the further development of a nonlinear adaptive power system stabiliser which will be discussed in Chapter 5.*

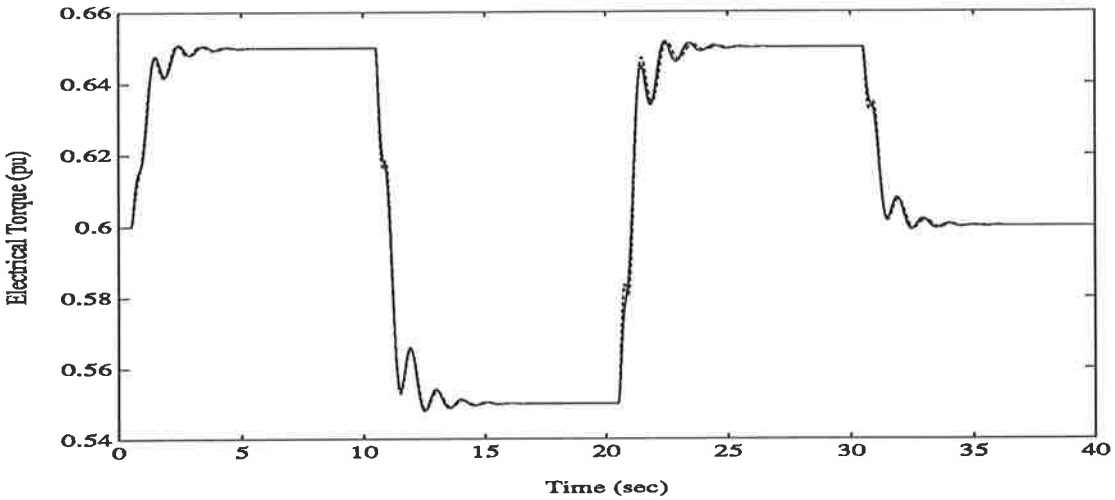

Figure 4.10: Electrical torque response for Study 1 ($P_t = 0.6$ pu, $Q_t = 0.3$ pu; periodic variations in reference power). CSM3 with the NOWMV-PSS - solid line, CSM3 with the LAWMV-PSS - dashed line.

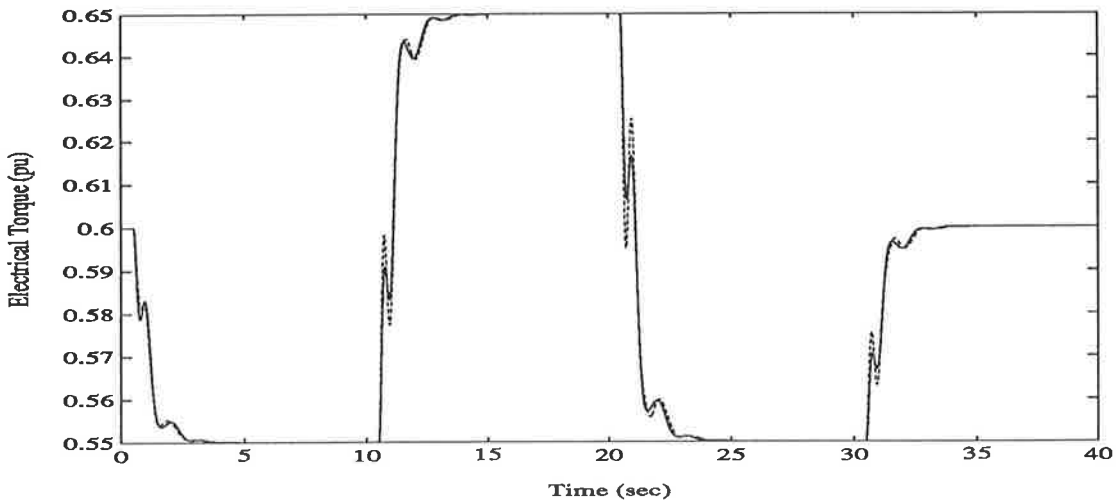

Figure 4.11: Electrical torque response for Study 2 ($P_t = 0.6$ pu, $Q_t = -0.1$ pu; periodic variations in reference power). CSM3 with the NOWMV-PSS - solid line, CSM3 with the LAWMV-PSS - dashed line.

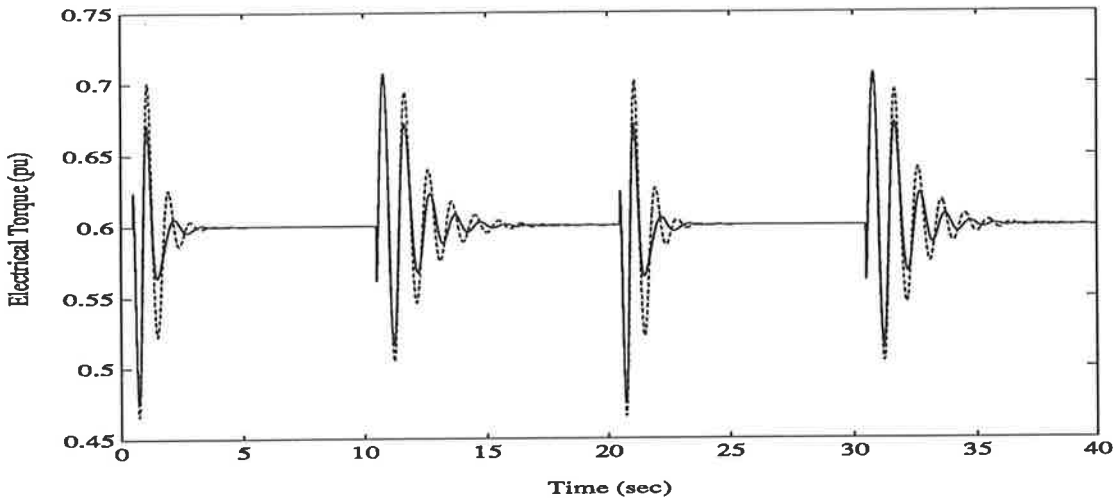

Figure 4.12: Electrical torque response for Study 3 ($P_t = 0.6$ pu, $Q_t = 0.3$ pu; periodic variations in reactive power between lagging and leading operating conditions). CSM3 with the NOWMV-PSS - solid line, CSM3 with the LAWMV-PSS - dashed line.

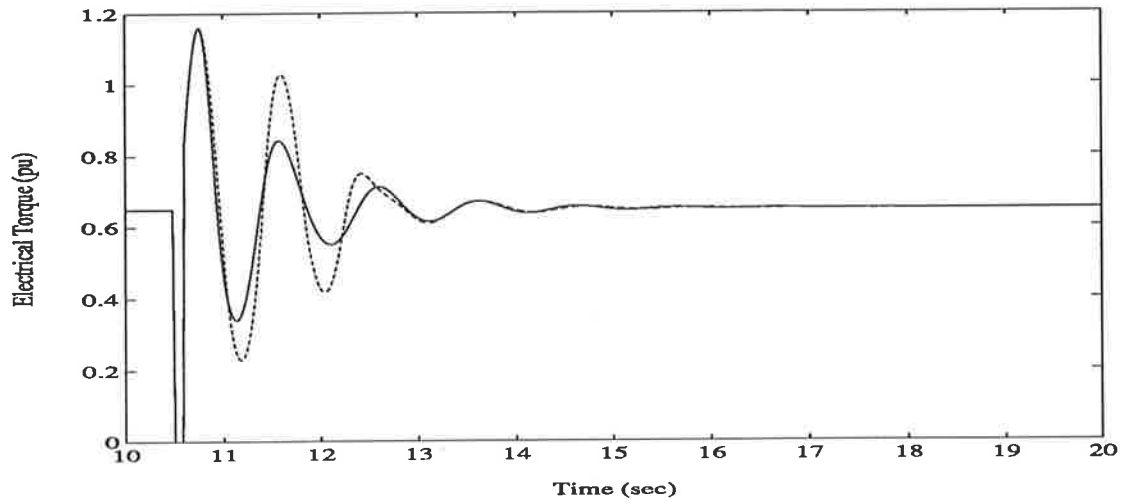

Figure 4.13: Electrical torque response for Study 4 ($P_t = 0.65$ pu, $Q_t = 0.3$ pu; 100 ms short-circuit on the receiving end busbars). CSM3 with the NOWMV-PSS - solid line, CSM3 with the LAWMV-PSS - dashed line.

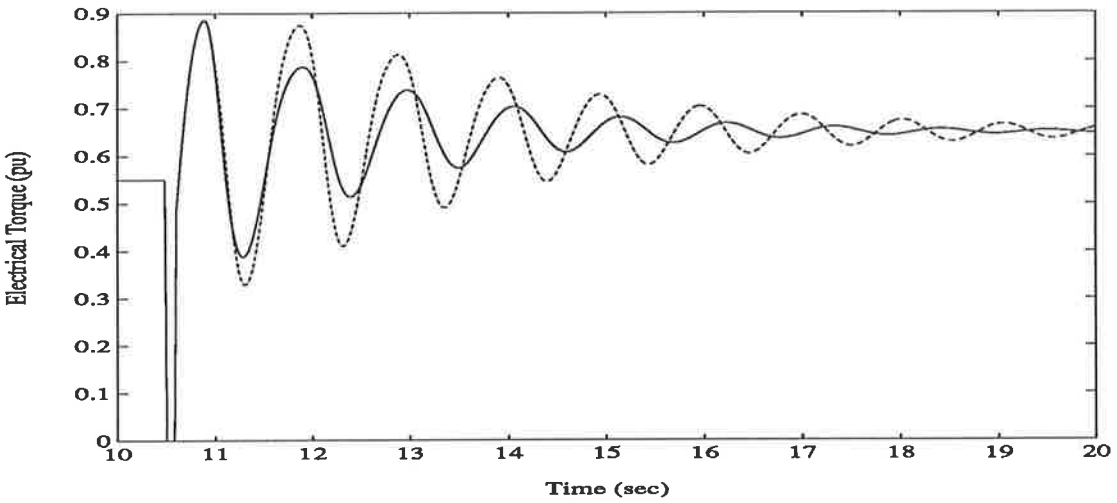

Figure 4.14: Electrical torque response for Study 5 ($P_t = 0.55$ pu, $Q_t = -0.1$ pu; 100 ms short-circuit at the machine terminal). CSM3 with the NOWMV-PSS - solid line, CSM3 with the LAWMV-PSS - dashed line.

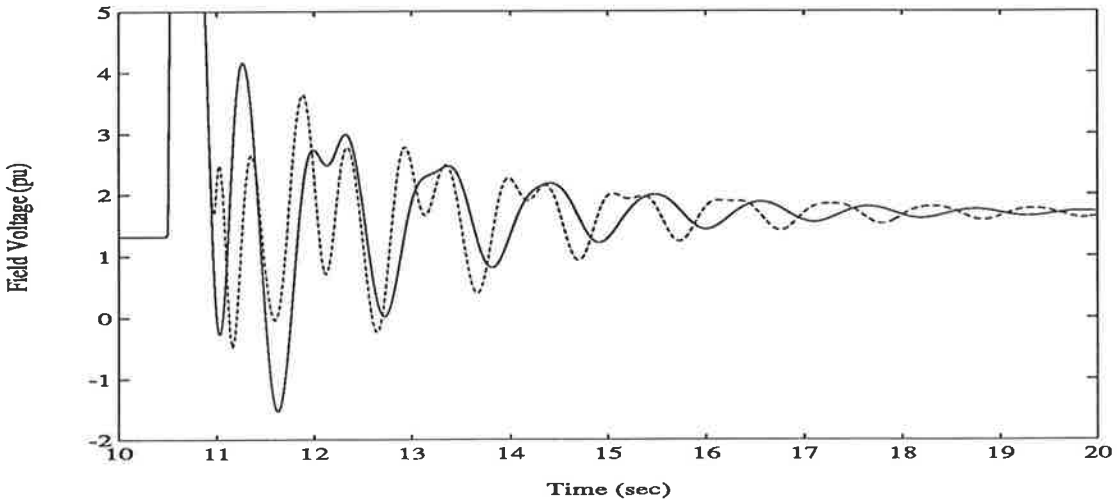

Figure 4.15: Field voltage response for Study 5 ($P_t = 0.55$ pu, $Q_t = -0.1$ pu; 100 ms short-circuit at the machine terminal). CSM3 with the NOWMV-PSS - solid line, CSM3 with the LAWMV-PSS - dashed line.

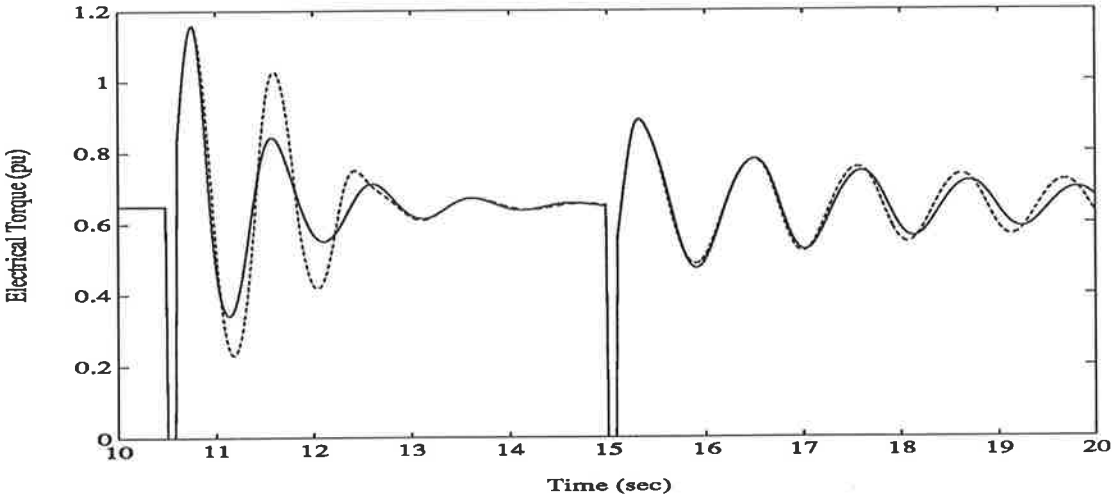

Figure 4.16: Electrical torque response for Study 6 ($P_t = 0.65$ pu, $Q_t = 0.3$ pu; two successive faults of 100 ms duration on the receiving end busbars). CSM3 with the NOWMV-PSS - solid line, CSM3 with the LAWMV-PSS - dashed line.

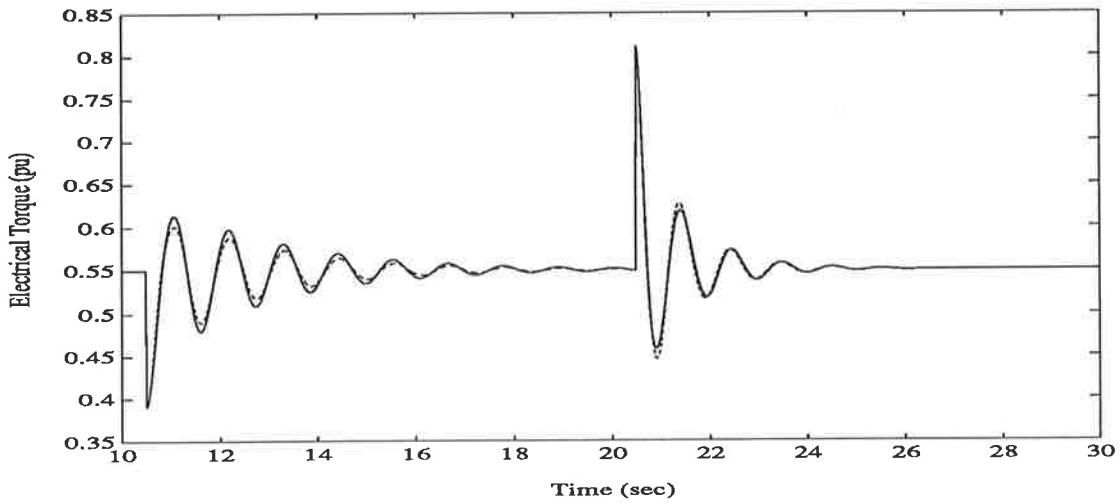

Figure 4.17: Electrical torque response for Study 7 ($P_t = 0.55$ pu, $Q_t = 0.3$ pu; one transmission line is opened and then reclosed). CSM3 with the NOWMV-PSS - solid line, CSM3 with the LAWMV-PSS - dashed line.

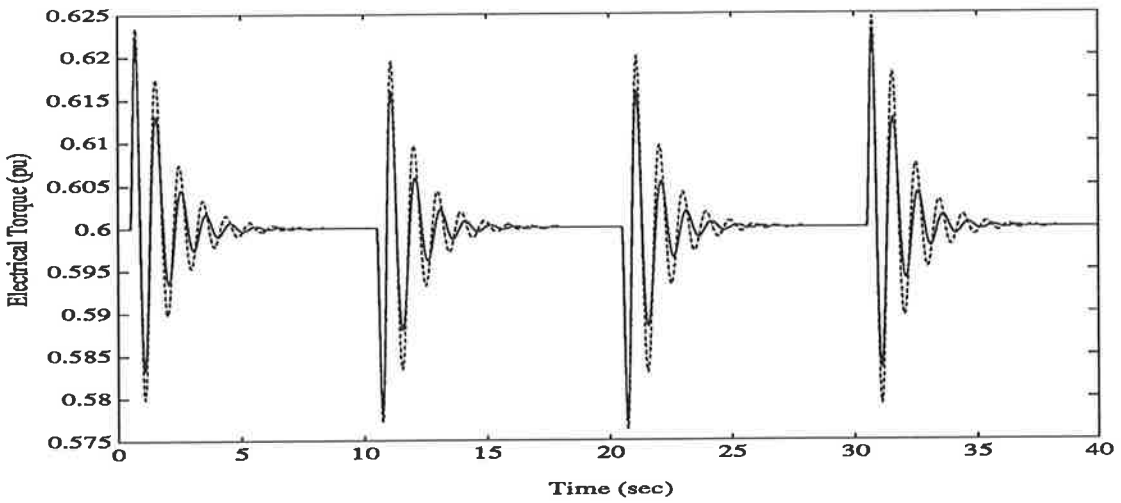

Figure 4.18: Electrical torque response for Study 8 ($P_t = 0.6$ pu, $Q_t = 0.3$ pu; periodic disturbances in reference voltage). CSM3 with the NOWMV-PSS - solid line, CSM3 with the LAWMV-PSS - dashed line.

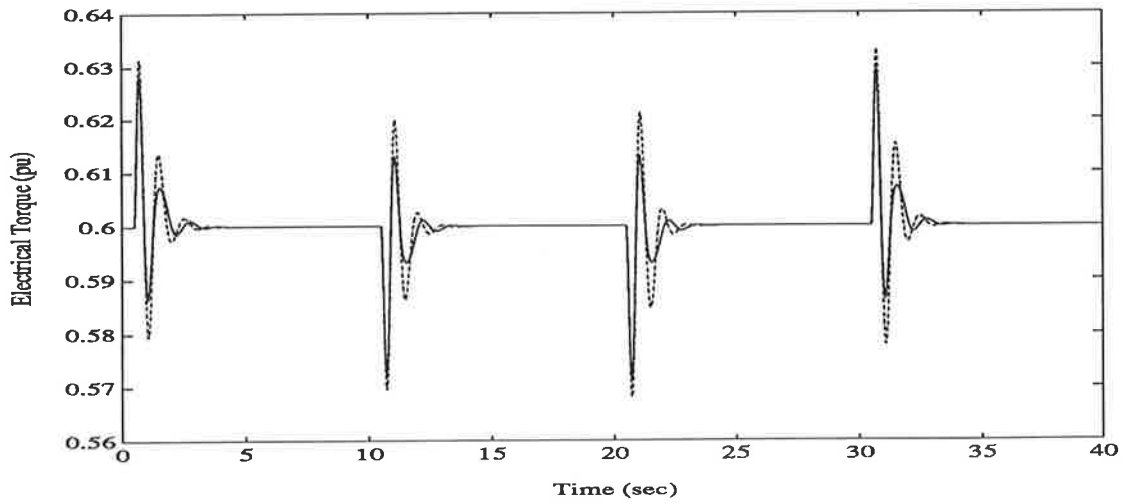

Figure 4.19: Electrical torque response for Study 9 ($P_t = 0.6$ pu, $Q_t = -0.1$ pu; periodic disturbances in reference voltage). CSM3 with the NOWMV-PSS - solid line, CSM3 with the LAWMV-PSS - dashed line.

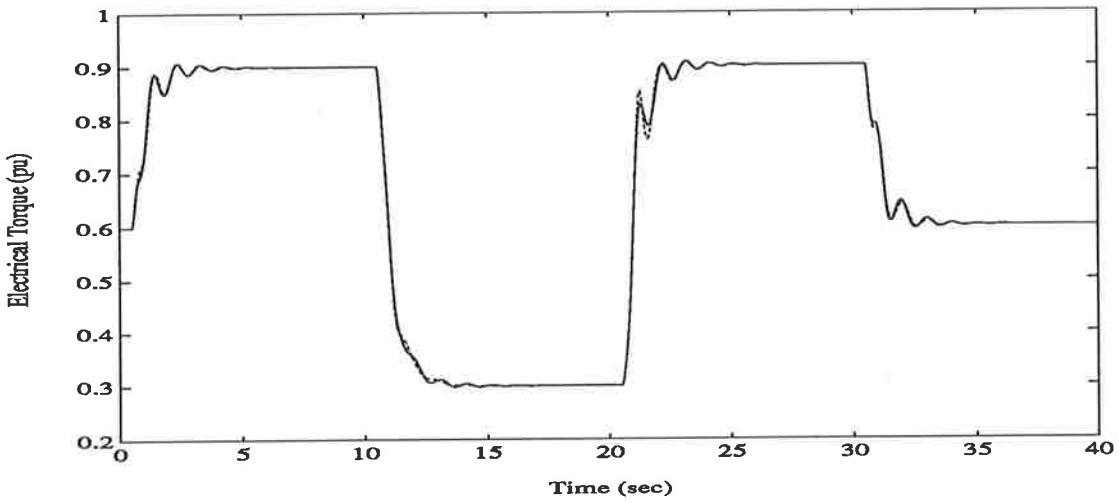

Figure 4.20: Electrical torque response for Study 10 ($P_t = 0.6$ pu, $Q_t = 0.3$ pu; large periodic excursions in reference power). CSM3 with the NOWMV-PSS - solid line, CSM3 with the LAWMV-PSS - dashed line.

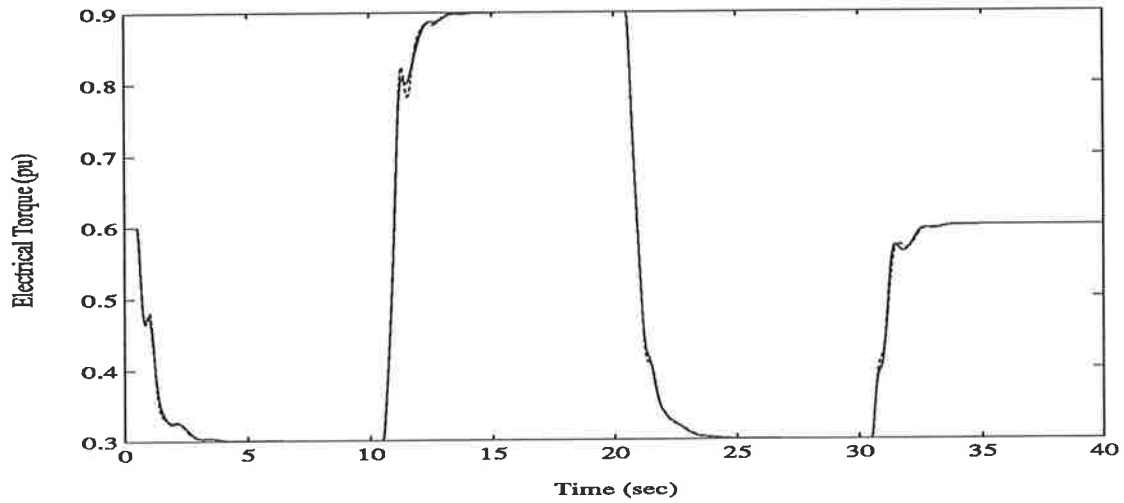

Figure 4.21: Electrical torque response for Study 11 ($P_t = 0.6$ pu, $Q_t = -0.1$ pu; large periodic excursions in reference power). CSM3 with the NOWMV-PSS - solid line, CSM3 with the LAWMV-PSS - dashed line.

4.5.3 Studies on the Robustness of the NOWMV-PSS for the CSM1.

In this subsection the robustness of the NOWMV-PSS is confirmed through the series of *robustness studies* (Studies 12-15) defined in Subsection 3.6.3. The performance of the NOWMV-PSS is tested with unmodelled dynamics and modelling errors. This subsection is the implementation of **Stage 3.**

Aims and structure of the simulation studies.

The performance of the NOWMV-PSS and the LAWMV-PSS is further compared with the CSM3 ($D = 4.0$ pu) replaced by the CSM1 ($D = 0.1$ pu). The stabilising signal is the electrical power $P_e(k)$. The aims of this study are

- to verify the validity of the NOWMV-PSS for the power system represented by the more accurate model (CSM1);
- to establish a reference for the comparison of the performance of the nonlinear optimal and nonlinear adaptive control strategies with unmodelled dynamics and modelling errors to be conducted in Subsection 5.4.3.

Studies 12-15 allocated to the two **Groups** specified in Subsection 3.6.3 are implemented. The simulation results are given by Figs. 4.22-4.25 in which the performance of the LAWMV-PSS is provided by Figs. 3.18-3.21.

Analysis of the simulation studies.

Group 1: The *dynamic performance* of the NOWMV-PSS associated with the CSM1 is examined in Studies 12-13. The results are plotted in Figs. 4.22-4.23. It is seen that the NOWMV-PSS gives damping performance similar to that of the LAWMV-PSS. This concides with the results shown in Figs. 4.10-4.11.

Group 2: The *transient performance* of the NOWMV-PSS associated with the CSM1 is examined in Studies 14-15. In Fig. 4.24 the damping performance of the NOWMV-PSS shows a slight deterioration as compared to its behaviour in Fig. 4.13 for the identical disturbance. This can be attributed to the influence of the subtransients of the CSM1 (i.e., the unmodelled dynamics of the NOWMV-PSS). Nevertheless, the performance of the NOWMV-PSS is still better than that of the LAWMV-PSS in Study 15, as shown in Fig. 4.25. This agrees with the result shown in Fig. 4.14. Thus, the fast control effect associated with the NOWMV-PSS is still evident.

Conclusions.

The above studies confirm that:

1. The NOWMV-PSS which is well designed for the CSM3 is also valid for the higher-order actual power system represented by the CSM1.
2. In terms of the damping performance, the NOWMV-PSS is at least comparable with, and typically better than, the LAWMV-PSS.

4.6 Concluding Remarks.

In this chapter *original* work on the design and implementation of a *nonlinear optimal* power system stabiliser for the SMIB power system modelled in Subsection 2.3.1 is conducted. This work forms the basis for the theoretical and practical development of the nonlinear adaptive power system stabilisers to be discussed in Chapters 5 and 6.

In order to deal with a nonlinear control problem, the development of a suitable nonlinear model for controller analysis and design is essential. For this reason, in Section 4.2 a *new* nonlinear nominal model (NNM) in a discrete-time input-output representation is derived from the nonlinear analytical model (NAM) given in Subsection 2.3.1. The NNM includes the inherent nonlinearities associated with the machine

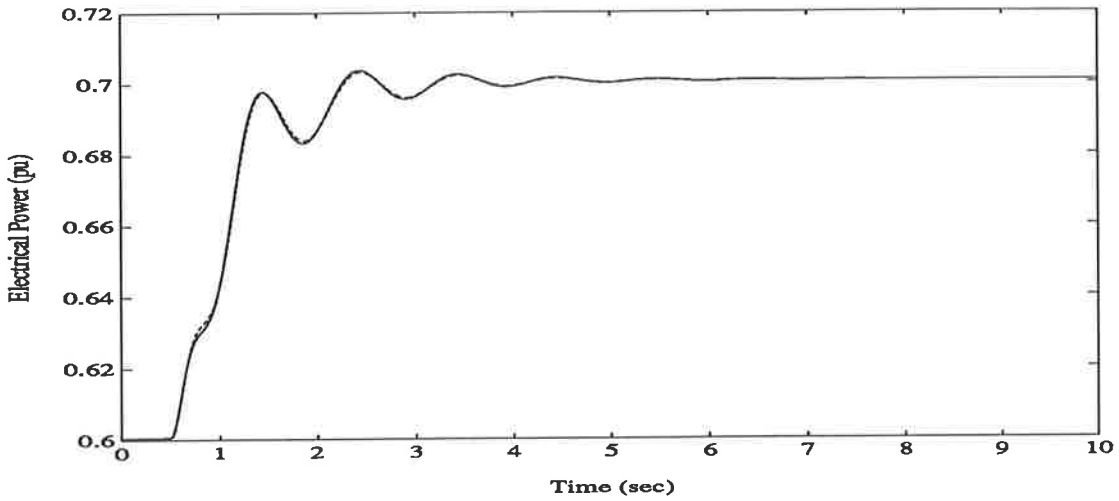

Figure 4.22: Electrical power response for Study 12 ($P_t = 0.6$ pu, $Q_t = 0.3$ pu; step change in reference power). CSM1 with the NOWMV-PSS - solid line, CSM1 with the LAWMV-PSS - dashed line.

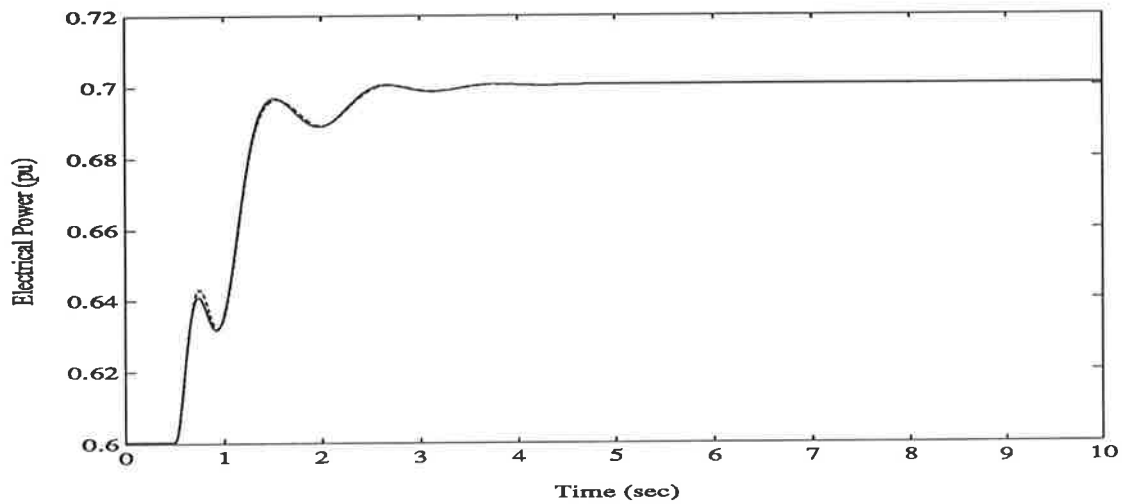

Figure 4.23: Electrical power response for Study 13 ($P_t = 0.6$ pu, $Q_t = -0.1$ pu; step change in reference power). CSM1 with the NOWMV-PSS - solid line, CSM1 with the LAWMV-PSS - dashed line.

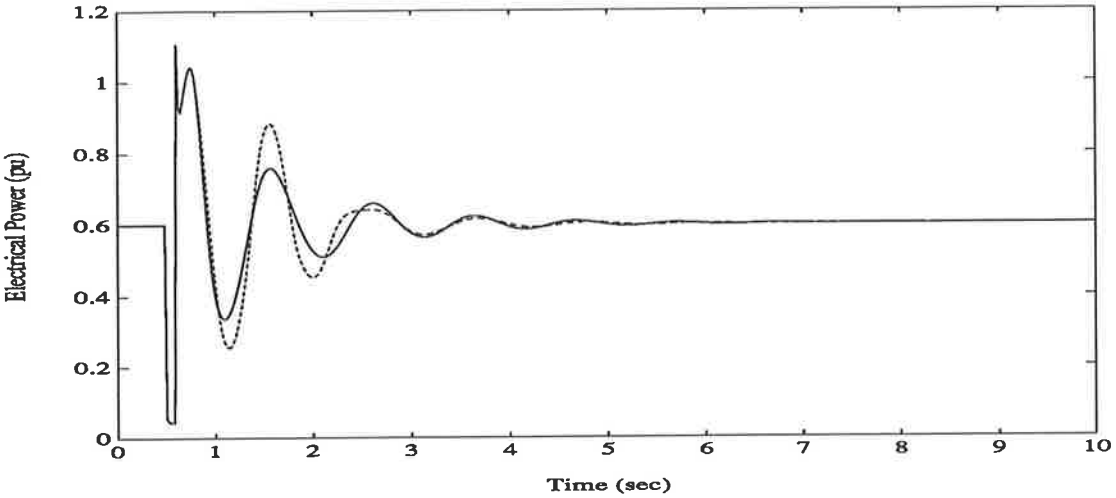

Figure 4.24: Electrical power response for Study 14 ($P_t = 0.6$ pu, $Q_t = 0.3$ pu; 100 ms short-circuit on the receiving end busbars). CSM1 with the NOWMV-PSS - solid line, CSM1 with the LAWMV-PSS - dashed line.

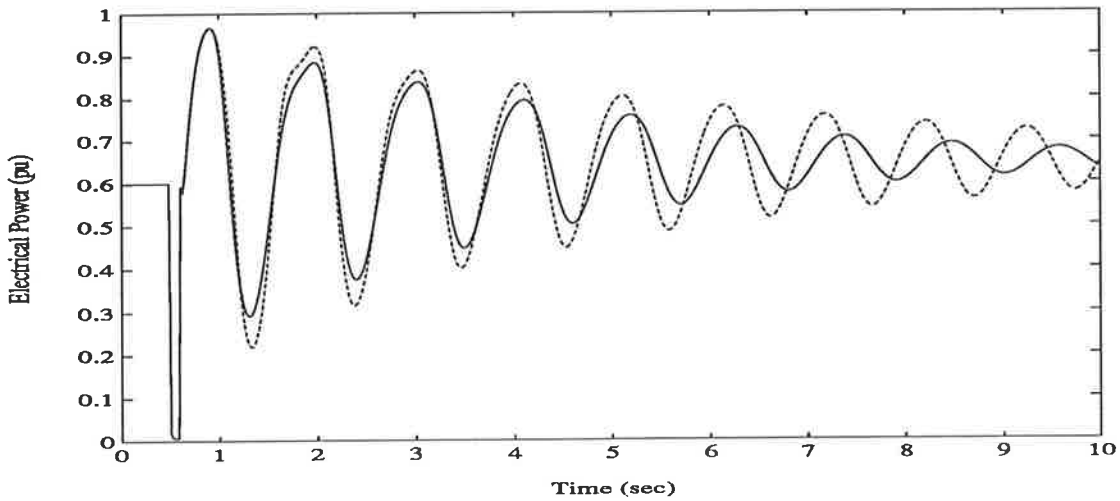

Figure 4.25: Electrical power response for Study 15 ($P_t = 0.6$ pu, $Q_t = -0.1$ pu; 100 ms short-circuit at the machine terminal). CSM1 with the NOWMV-PSS - solid line, CSM1 with the LAWMV-PSS - dashed line.

electrical torque (or power) *accurately*. Hence, it tracks the changes in the operating point of the nonlinear power system *automatically*. The validity of the NNM to represent the CSM3 at various system operating conditions is verified through simulation studies in Subsection 4.5.1.

The NNM, given in a regression form, is linear in the parameters and in the control input. This feature of the NNM is important, since the linear theory of estimation, prediction, and control, can then be developed for this nonlinear model. The BIBO stability of the NNM has been established in Lemma 4.2.3 for use in the theoretical analyses associated with the nonlinear optimal and adaptive control laws developed in this chapter and Chapter 5.

A *new* nonlinear stochastic generalised minimum variance control law is developed for the NNM in Section 4.3, and its closed-loop stability conditions are established in Theorem 4.3.1. By choosing different weighting polynomials in the cost function, different forms of the nonlinear optimal control law are obtained. The noise term in the NNM is specified as a white noise with zero mean. This specification facilitates the theoretical development of the nonlinear optimal control laws for the NNM. The boundedness and the dynamic characteristics of this noise term are examined in Subsection 4.5.1.

In Section 4.4 a *new* nonlinear stochastic weighted minimum variance control law is derived. The sufficient condition for the global stability of the closed-loop system associated with this control law is given by Theorem 4.4.2. The application of this control law to the design of a nonlinear optimal power system stabiliser is then discussed. In taking practical implementation into account, a *new* nonlinear optimal weighted minimum variance power system stabiliser (NOWMV-PSS) is proposed for the SMIB power system given in Subsection 2.3.1. The NOWMV-PSS would be realised in practice by a digital computer, and its control action updated by the implementation of Algorithm 4.1.

In Section 4.5 the performance of the proposed NOWMV-PSS is investigated and its robustness in stabilising the higher-order actual power system is tested through the series of evaluation studies and robustness studies specified in Subsections 3.6.2

and 3.6.3, respectively. The effectiveness of the NOWMV-PSS is demonstrated by the comparison of the system damping performance with the LAWMV-PSS proposed in Chapter 3. The simulation results in this chapter indicate that the NOWMV-PSS is properly designed; it is comparable with the LAWMV-PSS and improves the system damping performance with the LAWMV-PSS in most cases. Due to the property that the NOWMV-PSS is *fixed-parameter* and *nonlinear*, the NOWMV-PSS provides a faster control action for damping rotor oscillations than the LAWMV-PSS with an identical weighting coefficient λ. Moreover, since the voltage reference signal is included in the control law *explicitly*, some feedforward compensation for this measurable deterministic disturbance is provided by the NOWMV-PSS. The provision of the dynamic and transient behaviour of the NOWMV-PSS in this chapter establishes a basis for the evaluation of the system performance with the nonlinear adaptive control scheme yet to be designed in Chapter 5.

The contributions in this chapter are **original**, and have been listed in Section 4.1.

Chapter 5

SISO Nonlinear Adaptive Power System Stabilisers.

5.1 Introduction.

In this chapter the design of *SISO nonlinear adaptive* power system stabilisers is discussed. This follows on from the development of the nonlinear optimal power system stabilisers discussed in Chapter 4. It will establish a basis for the further development of a dedicated bilinear adaptive power system stabiliser to be discussed in Chapter 6.

In order to deal with the nonlinearities in a power system, nonlinear optimal control approaches have been proposed in Chapter 4. The inherent nonlinearities of the power system are incorporated into the design of the control laws. A nonlinear nominal model (NNM) was derived from the mathematical description of the nonlinear SMIB power system for the purposes of the design and implementation of the nonlinear optimal power system stabiliser. The parameters associated with the NNM are defined by (4.44)-(4.45), (4.59)-(4.60), and (4.49)-(4.52). From these definitions, it is clear that for a given generating unit (with fixed system parameters), the values of the parameters of the NNM will depend on the following factors:

- the value of the transmission line parameters, such as X_e etc., which change following a change in the system configuration;

- the value of the infinite bus voltage, V_∞, which is assumed to be time-invariant for a given lagging or leading operating condition, but will be time-varying as the system operating condition changes from lagging to leading or vice versa.

If the above factors were *unchanged*, then a *fixed-parameter* NNM would be an accurate representation of the nonlinear power system. However, in practice, these factors *do* change over a period of time. Consequently, the nature of the NNM (4.76)-(4.78) is *time-varying*. As indicated in the Conclusions of Subsection 4.5.2, the NOWMV-PSS designed by the use of the fixed-parameter NNM is not capable of tracking the system changes on-line.

In order to overcome the shortcoming associated with the NOWMV-PSS, *nonlinear adaptive* control schemes are considered in this chapter. Based on the *certainty equivalence principle*, the derivation of a nonlinear adaptive control law from an existing nonlinear optimal control law developed in Chapter 4 will be straightforward. A parameter estimation algorithm will be required for the purpose of on-line identification of the time-varying NNM. Since the model is nonlinear, it will be necessary to separate the estimation of the parameters and the calculation of the control law. Therefore, *indirect* control methods will be considered for the development of the nonlinear adaptive control algorithms.

From the review of the literature, the study of nonlinear adaptive control algorithms for the design of power system stabilisers has *not* been reported widely. One example of a nonlinear controller, designed on direct feedback linearisation, has been employed to implement adaptive control laws for studies on the transient stabilisation of power systems [86]. However, in some other fields of scientific research, nonlinear adaptive control approaches have been developed and implemented. Typical applications are documented in [75,44]. For example, nonlinear minimum variance control strategies have been designed in [192] for use in dissolved oxygen control in activated sludge waste water treatment and in control of pH in acidic waste water. Similar approaches have been developed in [196] for substrate concentration control and production rate control of time-varying bacterial growth systems. A nonlinear model reference control approach has been proposed in [193] for control of the nonlinear dynamics relating

joint angles to motor torques in robot control. Because there are a great variety of representations of nonlinear systems in practice, nonlinear adaptive control approaches differ significantly in formulation. However, there is a common principle behind each design, that is to account for the nonlinearities and the time-varying features of the systems. Moreover, a nonlinear adaptive control approach is usually proposed for a specific problem. The application of a nonlinear adaptive control law designed for one specific nonlinear system to other control problems is limited.

In this chapter *new* nonlinear adaptive control algorithms are developed for the design of the power system stabiliser for the SMIB power system modelled in Subsection 2.3.1. Original work on the *analysis*, *design*, and *evaluation* of nonlinear adaptive power system stabilisers will be conducted in the following sections of this chapter. The work involves the development of the parameter estimation algorithms for identification of the time-varying NNM, the derivation of the nonlinear adaptive control laws, the convergence analyses of both parameter estimation and adaptive control algorithms, the formulation of a nonlinear adaptive power system stabiliser, and the assessment of the system damping performance with the proposed nonlinear adaptive stabiliser.

The organisation of this chapter is as follows. In Section 5.2 parameter estimation algorithms for identification of the time-varying NNM are proposed and the relevant convergence analyses are briefly discussed. In Section 5.3 the SISO nonlinear adaptive weighted minimum variance control laws are developed from the optimal control law (4.128), and the convergence of the resulting bounded nonlinear adaptive control algorithms is established. A nonlinear adaptive power system stabiliser is then proposed. In Section 5.4 the performance of the proposed nonlinear adaptive power system stabiliser is assessed through simulation studies, and is compared with that of the NOWMV-PSS developed in Chapter 4.

To the author's knowledge, the research reported in this chapter is **original**; the main contributions are:

1. The recursive least squares algorithm with the time-varying forgetting factor and dead zone is applied to the NNM for the identification of the time-varying

parameters on-line. Based on Lemma 4.2.3 established in Subsection 4.2.3, convergence analyses of the resulting parameter estimation algorithms are given in Sections G.1-G.2 of Appendix G.

2. *New* SISO nonlinear adaptive weighted minimum variance control laws are derived from the nonlinear stochastic optimal control law (4.128). The convergence of the resulting bounded nonlinear adaptive control algorithms is established. A rigorous mathematical proof of the convergence is presented in Section G.3 of Appendix G.

3. A *new* nonlinear adaptive power system stabiliser based on the bounded nonlinear adaptive weighted minimum variance control algorithm is proposed, and the control structure of the SMIB power system equipped with the proposed nonlinear adaptive power system stabiliser is illustrated.

4. Simulation studies on the evaluation of the nonlinear adaptive power system stabiliser are conducted. A series of useful comparisons with the NOWMV-PSS is given.

It should be pointed out that while the convergence analysis of a standard linear adaptive control algorithm has been well-documented, there is *no* general proof of the convergence of a *particular* nonlinear adaptive control algorithm. For this reason, proofs of lemmas and theorems to be established for the theoretical development of the nonlinear adaptive power system stabiliser under design are given in this chapter. These analyses are *necessary* to ensure the closed-loop system stability associated with the proposed nonlinear adaptive power system stabiliser.

5.2 Parameter Estimation Algorithms for the Nonlinear Nominal Model of the Power System and Convergence Analyses.

In this section:

- the recursive least squares algorithm with the time-varying forgetting factor and dead zone is proposed for the estimation of the parameters of the NNM;
- convergence analyses of the proposed parameter estimation algorithms are given.

The NNM given in Subsection 4.2.3 is written as

$$y(k+1) = \phi(k)^T \Theta_0 + w(k+1) \tag{5.1}$$

where $\phi(k)$ and Θ_0 are given by (4.77) and (4.78), respectively. It has been shown in (4.83) and (4.86) that the optimal one-step-ahead prediction of the output of the above model is given by

$$y^0(k+1 \mid k) = G(q^{-1})y(k) + f(k) = \phi(k)^T \Theta_0$$

in which $\{w(k)\}$ is assumed to be a white noise sequence satisfying Assumption 4.3.1. In this chapter, as indicated in Section 4.3, the *third* noise model is considered and $\{w(k)\}$ is a general bounded nondeterministic noise sequence which satisfies Lemma 4.2.2. This treatment will result in a more general form of the nonlinear adaptive controller applicable to different noise characteristics, provided that the noise term is bounded (i.e., satisfying Lemma 4.2.2).

Given an estimate $\hat{\Theta}(k)$ of Θ_0, the *adaptive one-step-ahead prediction*, $\hat{y}(k+1)$, of $y(k+1)$ in (5.1) is defined as

$$\hat{y}(k+1) \triangleq \phi(k)^T \hat{\Theta}(k) \tag{5.2}$$

where

$$\hat{\Theta}(k)^T \triangleq \left[\begin{array}{cccccccc} \hat{a}_1(k) & \hat{a}_2(k) & \hat{b}_1(k) & \hat{b}_2(k) & \hat{c}_1(k) & \hat{c}_2(k) & \hat{d}_1(k) & \hat{e}_1(k) \end{array} \right]. \tag{5.3}$$

Since the model (5.1) is linear in its parameters, the parameter estimation algorithms developed for the identification of linear models can be applied to this nonlinear model. Therefore, the *recursive least squares algorithm with the time-varying forgetting factor*, used in Chapter 3 to construct the linear adaptive control algorithms, is employed in this chapter as the basic parameter estimation algorithm for the NNM. The use of the time-varying forgetting factor is to allow tracking of the time-varying parameters

of the NNM due to the changes in the system parameters and/or in the value of the infinite bus voltage. It is also used to prevent the covariance matrix $P(k)$ from 'blowing-up' (the reason for which has been explained in Subsection 3.4.1). Moreover, since the model (5.1) contains a bounded noise term $w(k+1)$, the technique of a *dead zone* [157] is recommended. A switching function, $\sigma(k)$, is incorporated into the parameter estimation algorithms [192,196]. The switching function $\sigma(k)$ is used to hold the parameter estimates constant whenever the prediction errors become smaller than a prespecified bound, Δ_w. The introduction of $\sigma(k)$ into the algorithms is necessary for the theoretical analysis of the parameter convergence of the algorithms. It may be omitted in practice or in simulation studies when this precaution is unnecessary. The resulting parameter estimation algorithm for the model (5.1) is then given as follows.

Algorithm 5.1(A) [recursive least squares algorithm with the time-varying forgetting factor and dead zone for the model (5.1).]

Estimate:

$$\hat{\Theta}(k) = \hat{\Theta}(k-1) + \sigma(k-1)P(k-1)\phi(k-1)\left[y(k) - \hat{y}(k)\right] \tag{5.4}$$

Covariance:

$$P(k-1) = \left[P(k-2) - \frac{\sigma(k-1)P(k-2)\phi(k-1)\phi(k-1)^T P(k-2)}{\mu(k-1) + \sigma(k-1)\phi(k-1)^T P(k-2)\phi(k-1)}\right]\frac{1}{\mu(k-1)} \tag{5.5}$$

Prediction:

$$\hat{y}(k) = \phi(k-1)^T\hat{\Theta}(k-1) \tag{5.6}$$

Error:

$$e(k) = y(k) - \hat{y}(k) \tag{5.7}$$

Switching Function:

$$\sigma(k-1) = \begin{cases} 1 & \text{if } \dfrac{\mu(k-1)e(k)^2}{\mu(k-1) + \phi(k-1)^T P(k-2)\phi(k-1)} > \Delta_w^2 \\ 0 & \text{otherwise} \end{cases} \tag{5.8}$$

Forgetting Factor:

$$\mu_0(k) = 1 - \frac{\sigma(k-1)e(k)^2}{1+\phi(k-1)^T P(k-2)\phi(k-1)}\frac{1}{\Sigma_0} \tag{5.9}$$

$$\bar{\mu}(k) = \begin{cases} \mu_0(k) & \text{if } \mu_0(k) \geq \mu_{min} > 0 \\ \mu_{min} & \text{otherwise} \end{cases} \tag{5.10}$$

$$\mu(k) = \begin{cases} \bar{\mu}(k) & \text{if } \dfrac{\text{trace}(P(k-1))}{\bar{\mu}(k)} < C \\ 1 & \text{otherwise} \end{cases} \tag{5.11}$$

where $k \geq 1$, $P(-1) = K_0 I$ $(0 < K_0 < C)$, and $\mu(0) = 1$. Δ_w, Σ_0, μ_{min}, and C are preselected positive constants. $\hat{\Theta}(k)$ and $\phi(k)$ are defined by (5.3) and (4.77), respectively. $\hat{\Theta}(0)$ is given.

$\nabla\ \nabla\ \nabla$

The parameter estimate $\hat{\Theta}(k)$ from Algorithm 5.1(A) will be used to calculate the corresponding nonlinear adaptive control law (Algorithm 5.1(B)) in Section 5.3.

Remark 5.2.1 *Algorithm 5.1(A) is obtained by minimising the quadratic cost function (F.1) given in Appendix F.*

The convergence of Algorithm 5.1(A) is given by the following theorem, based on [192,196]. This theorem ensures that: if the noise term $w(k+1)$ in the model (5.1) is bounded, then (i) the convergence of the parameter estimate $\hat{\Theta}(k)$ is guaranteed through the use of the switching function $\sigma(k)$ in the algorithm; (ii) the boundedness of the adaptive one-step-ahead prediction, $\hat{y}(k)$, of $y(k)$ as well as the error between $y(k)$ and $\hat{y}(k)$ is also guaranteed.

Theorem 5.2.1 *For the least squares algorithm (5.4)-(5.11), subject to Assumptions 4.2.1-4.2.5,*

(a) $\limsup_{t\to\infty} |\hat{y}(k)| \leq \tilde{K}_3 + \tilde{K}_4\Delta_w$,

(b) $\limsup_{t\to\infty} |y(k) - \hat{y}(k)| \leq \tilde{K}_4\Delta_w$,

(c) $\limsup_{t\to\infty} \left|\hat{\Theta}(k) - \hat{\Theta}(k-1)\right| \leq \tilde{K}_5 \Delta_w,$

(d) $\| \hat{\Theta}(k) - \Theta_0 \| \leq \tilde{K}_6 \| \hat{\Theta}(0) - \Theta_0 \|, \qquad$ *for* $k \geq 1,$

where $\tilde{K}_3$, $\tilde{K}_4$, $\tilde{K}_5$, *and* $\tilde{K}_6$ *are known constants, independent of* Δ_w.

Proof of Theorem 5.2.1

See Section G.1 of Appendix G.

Q.E.D.

Theorem 5.2.1(b) will be used to prove the convergence of the corresponding non-linear adaptive control algorithm (Algorithm 5.1(B)) in Section 5.3.

Alternatively, the model (5.1) can be written as

$$y(k+1) = \tilde{\phi}(k)^T \Theta_0 + \beta_0(k) u(k) + w(k+1) \tag{5.12}$$

where

$$\tilde{\phi}(k)^T \triangleq \Big[-y(k) \quad -y(k-1) \quad z_1(k) \quad z_1(k-1) \quad z_2(k) \quad z_2(k-1) \quad z_3(k) \quad z_4(k)\,(d(k) - y_F(k)) \Big]. \tag{5.13}$$

Define $\tilde{y}(k+1)$ by

$$\tilde{y}(k+1) \triangleq \tilde{\phi}(k)^T \Theta_0 + w(k+1). \tag{5.14}$$

The model (5.12) can then be rewritten as

$$y(k+1) = \tilde{y}(k+1) + \beta_0(k) u(k). \tag{5.15}$$

As far as the model (5.14)-(5.15) is concerned, the adaptive one-step-ahead prediction, $\hat{\tilde{y}}(k+1)$, of $\tilde{y}(k+1)$ can be defined as

$$\hat{\tilde{y}}(k+1) \triangleq \tilde{\phi}(k)^T \hat{\Theta}(k). \tag{5.16}$$

Hence, for the model (5.14)-(5.15) the parameter estimation algorithm proposed in Algorithm 5.1(A) can be modified to give

Algorithm 5.2(A) [recursive least squares algorithm with the time-varying forgetting factor and dead zone for the model (5.14)-(5.15).]

Estimate:

$$\hat{\Theta}(k) = \hat{\Theta}(k-1) + \sigma(k-1)P(k-1)\tilde{\phi}(k-1)\left[\tilde{y}(k) - \hat{\tilde{y}}(k)\right] \tag{5.17}$$

Covariance:

$$P(k-1) = \left[P(k-2) - \frac{\sigma(k-1)P(k-2)\tilde{\phi}(k-1)\tilde{\phi}(k-1)^T P(k-2)}{\mu(k-1) + \sigma(k-1)\tilde{\phi}(k-1)^T P(k-2)\tilde{\phi}(k-1)}\right]\frac{1}{\mu(k-1)} \tag{5.18}$$

Output:

$$\tilde{y}(k) = y(k) - \beta_0(k-1)u(k-1); \tag{5.19}$$

Prediction:

$$\hat{\tilde{y}}(k) = \tilde{\phi}(k-1)^T\hat{\Theta}(k-1) \tag{5.20}$$

Error:

$$\tilde{e}(k) = \tilde{y}(k) - \hat{\tilde{y}}(k) \tag{5.21}$$

Switching Function:

$$\sigma(k-1) = \begin{cases} 1 & \text{if } \dfrac{\mu(k-1)\tilde{e}(k)^2}{\mu(k-1) + \tilde{\phi}(k-1)^T P(k-2)\tilde{\phi}(k-1)} > \Delta_w^2 \\ 0 & \text{otherwise} \end{cases} \tag{5.22}$$

Forgetting Factor:

$$\mu_0(k) = 1 - \frac{\sigma(k-1)\tilde{e}(k)^2}{1 + \tilde{\phi}(k-1)^T P(k-2)\tilde{\phi}(k-1)}\frac{1}{\Sigma_0} \tag{5.23}$$

$$\bar{\mu}(k) = \begin{cases} \mu_0(k) & \text{if } \mu_0(k) \geq \mu_{min} > 0 \\ \mu_{min} & \text{otherwise} \end{cases} \tag{5.24}$$

$$\mu(k) = \begin{cases} \bar{\mu}(k) & \text{if } \dfrac{\text{trace}(P(k-1))}{\bar{\mu}(k)} < C \\ 1 & \text{otherwise} \end{cases} \tag{5.25}$$

where $k \geq 1$, $P(-1) = K_0 I$ $(0 < K_0 < C)$, and $\mu(0) = 1$. Δ_w, Σ_0, μ_{min}, and C are preselected positive constants. $\hat{\Theta}(k)$ and $\tilde{\phi}(k)$ are defined by (5.3) and (5.13), respectively. $\hat{\Theta}(0)$ is given.

$\nabla\ \nabla\ \nabla$

The parameter estimate $\hat{\Theta}(k)$ from Algorithm 5.2(A) will be used to calculate the corresponding nonlinear adaptive control law (Algorithm 5.2(B)) in Section 5.3.

Remark 5.2.2 *In Algorithm 5.2(A),*

(i) at each sampling instant k, $\tilde{y}(k)$ is obtained from the measured input/output data sequences according to (5.19);

(ii) the parameter e_1 is set to be constant in (5.19) in order to calculate $\tilde{y}(k)$, while the estimated e_1, $\hat{e}_1(k)$, is still retained in $\hat{\Theta}(k)$ for updating the prediction $\hat{\tilde{y}}(k)$. This approach will be used in Section 5.3 to derive the modified nonlinear adaptive control law (Algorithm 5.2(B)) for the sake of ensuring the convergence of the resulting control algorithm over the time horizon.

The above points explain the essential differences between Algorithms 5.1(A) and 5.2(A).

In a similar way as for Theorem 5.2.1, the convergence of Algorithm 5.2(A) is given by the following theorem.

Theorem 5.2.2 *For the least squares algorithm (5.17)-(5.25), subject to Assumptions 4.2.1-4.2.5,*

(a) $\lim\limits_{t\to\infty} \sup \left|\hat{\tilde{y}}(k)\right| \leq \tilde{K}_3' + \tilde{K}_4'\Delta_w,$

(b) $\lim\limits_{t\to\infty} \sup \left|\tilde{y}(k) - \hat{\tilde{y}}(k)\right| \leq \tilde{K}_4'\Delta_w,$

(c) $\lim\limits_{t\to\infty} \sup \left|\hat{\Theta}(k) - \hat{\Theta}(k-1)\right| \leq \tilde{K}_5'\Delta_w,$

(d) $\| \hat{\Theta}(k) - \Theta_0 \| \leq \tilde{K}_6' \| \hat{\Theta}(0) - \Theta_0 \|, \qquad$ *for* $k \geq 1,$

where $\tilde{K}_3'$, $\tilde{K}_4'$, $\tilde{K}_5'$, and $\tilde{K}_6'$ are known constants, independent of Δ_w.

Proof of Theorem 5.2.2

See Section G.2 of Appendix G.

Q.E.D.

Theorem 5.2.2(b) will be used to prove the convergence of the corresponding nonlinear adaptive control algorithm (Algorithm 5.2(B)) in Section 5.3.

When Algorithm 5.2(A) is used, the adaptive prediction of $y(k+1)$ is defined as

$$\hat{y}(k+1) \triangleq \tilde{\phi}(k)^T \hat{\Theta}(k) + \beta_0(k)u(k). \tag{5.26}$$

Also, the error between $y(k+1)$ and $\hat{y}(k+1)$ can be calculated by $e(k+1)$ as

$$e(k+1) = y(k+1) - \hat{y}(k+1). \tag{5.27}$$

Clearly, from (5.12), (5.26), (5.14), and (5.16), it follows that

$$y(k) - \hat{y}(k) = \tilde{\phi}(k-1)^T \left[\Theta_0 - \hat{\Theta}(k-1)\right] + w(k) = \tilde{y}(k) - \hat{\tilde{y}}(k), \tag{5.28}$$

or

$$e(k) = \tilde{e}(k)$$

due to (5.27) and (5.21).

The parameter estimation algorithms (Algorithms 5.1(A) and 5.2(A)) developed in this section will be used to complete the *indirect* nonlinear adaptive control algorithms which will be designed in Section 5.3.

5.3 Nonlinear Adaptive Weighted Minimum Variance Power System Stabilisers and Convergence Analyses.

In this section:

- nonlinear adaptive weighted minimum variance control laws are developed from Theorem 4.4.1, given in Section 4.4;
- convergence analyses of the proposed bounded nonlinear adaptive control algorithms are presented;
- a nonlinear adaptive weighted minimum variance power system stabiliser is proposed;
- the control structure of the SMIB power system equipped with the proposed nonlinear adaptive power system stabiliser is given.

The nonlinear optimal weighted minimum variance control scheme proposed in Section 4.4 is used in this section for the development of the corresponding nonlinear adaptive control strategies. According to the *certainty equivalence principle*, the basic structure of a nonlinear adaptive control algorithm in an *indirect* form is obtained by the combination of the nonlinear optimal weighted minimum variance control law with one of the parameter estimation algorithms (Algorithms 5.1(A) and 5.2(A)) developed in Section 5.2.

Consider the model (5.1) for which the parameter estimation algorithm is given by Algorithm 5.1(A). From the nonlinear optimal weighted minimum variance control law (4.128) given in Theorem 4.4.1, a nonlinear adaptive weighted minimum variance control law is suggested by replacing the model parameters by their corresponding estimates in the following manner

$$\left[\hat{\beta}_0(k)^2 + \lambda\right] u(k) = \hat{\beta}_0(k) \left[y^*(k+1) - \hat{G}(q^{-1})y(k) - \hat{g}(k)\right] \tag{5.29}$$

where, according to (4.111), (4.87), and (4.121)

$$\hat{\beta}_0(k) \triangleq \hat{e}_1(k) z_4(k), \tag{5.30}$$

$$\hat{G}(q^{-1}) \triangleq -\hat{a}_1(k) - \hat{a}_2(k) q^{-1}, \tag{5.31}$$

$$\hat{g}(k) \triangleq \left[\begin{array}{cccccc} \hat{b}_1(k) & \hat{b}_2(k) & \hat{c}_1(k) & \hat{c}_2(k) & \hat{d}_1(k) & \hat{e}_1(k) \end{array}\right] \left[\begin{array}{c} z_1(k) \\ z_1(k-1) \\ z_2(k) \\ z_2(k-1) \\ z_3(k) \\ z_4(k)(d(k) - y_F(k)) \end{array}\right]. \quad (5.32)$$

In practice, the calculated control $u(k)$ from (5.29) is limited by design considerations. Therefore, a bounded nonlinear adaptive control algorithm is proposed for the model (5.1) as follows.

Algorithm 5.1(B) [bounded nonlinear adaptive weighted minimum variance control algorithm for the model (5.1).]

$$u^0(k) = \frac{\hat{\beta}_0(k)}{\hat{\beta}_0(k)^2 + \lambda} \left[y^*(k+1) - \hat{G}(q^{-1})y(k) - \hat{g}(k)\right], \quad (5.33)$$

$$u(k) = \begin{cases} u_{max} & \text{if } u^0(k) \geq u_{max} \\ u^0(k) & \text{if } u_{min} < u^0(k) < u_{max} \\ u_{min} & \text{if } u^0(k) \leq u_{min} \end{cases}; \quad (5.34)$$

where λ is the weighting coefficient; u_{max} and u_{min} are known constants; $\hat{\beta}_0(k)$, $\hat{G}(q^{-1})$, and $\hat{g}(k)$ are defined by (5.30), (5.31), and (5.32), respectively; the estimated parameters are obtained from Algorithm 5.1(A).

$\nabla \nabla \nabla$

To prove the convergence of Algorithm 5.1(B), the magnitude and sign of $[y(k+1) - y(k)]$ are required to satisfy certain conditions. For this purpose, the model (5.1) is rewritten as

$$y(k+1) = y(k) + R \quad (5.35)$$

where

$$\begin{aligned} R &= R(y(k), g(k), z_4(k), u(k), w(k+1)) \\ &\triangleq \left[G(q^{-1}) - 1\right] y(k) + g(k) + \beta_0(k)u(k) + w(k+1). \end{aligned} \quad (5.36)$$

According to Lemma 4.2.3(i) (see also Remark 4.2.9), $y(k)$ is bounded without imposing an upper or lower bound on the control input $u(k)$. Hence, there exist η_2 and η_1 such that

$$\eta_2 = \min_{u=u_{max}} [y(k+1) - y(k)],$$

$$\eta_1 = \max_{u=u_{min}} [y(k+1) - y(k)],$$

for all k. η_2 is the minimum value of $[y(k+1) - y(k)]$ when $u = u_{max}$. For the model (5.35)-(5.36)

$$\eta_2 \triangleq \min_{\substack{y(k) \\ g(k) \\ z_4(k)}} R(y(k), g(k), z_4(k), u_{max}, -\Delta_w). \tag{5.37}$$

Similarly, η_1 is the maximum value of $[y(k+1) - y(k)]$ when $u = u_{min}$. For the model (5.35)-(5.36)

$$\eta_1 \triangleq \max_{\substack{y(k) \\ g(k) \\ z_4(k)}} R(y(k), g(k), z_4(k), u_{min}, \Delta_w). \tag{5.38}$$

Consequently, when $y(k)$ is located in a specified region $[l_1, l_2] \in [y_{min}, y_{max}]$, it may be assumed that

Assumption 5.3.1 *there exist r_2 and r_1 for the model (5.35)-(5.36) such that*

$$r_2 \triangleq \min_{\substack{y \le l_2 - \eta_2 \\ g(k) \\ z_4(k)}} R(y(k), g(k), z_4(k), u_{max}, -\Delta_w) > 0, \tag{5.39}$$

$$r_1 \triangleq \max_{\substack{y \ge l_1 - \eta_1 \\ g(k) \\ z_4(k)}} R(y(k), g(k), z_4(k), u_{min}, \Delta_w) < 0. \tag{5.40}$$

Remark 5.3.1 *The existence of r_2 and r_1 is guaranteed for the same reason as the existence of η_2 and η_1. Assumption 5.3.1, therefore, only requires that the inequalities in (5.39) and (5.40) hold for the specified regions of $y(k)$ and $u(k)$.*

Remark 5.3.2 *The constant values of y_{max} and y_{min} can be found in (G.11) of Appendix G, and are*

$$[y_{min}, y_{max}] \in \left[-\tilde{K}_3, \tilde{K}_3\right].$$

The assumed inequalities (5.39)-(5.40) ensure that the increment of $[y(k+1)-y(k)]$ has the following sign and magnitude properties.

Lemma 5.3.1 *For the model (5.35)-(5.36), subject to Assumption 5.3.1,*

(i) if

$$y(k+1) \leq l_2 \qquad \text{and} \qquad u(k) = u_{max}, \tag{5.41}$$

then

$$y(k+1) \geq y(k) + r_2 > y(k); \tag{5.42}$$

(ii) if

$$y(k+1) \geq l_1 \qquad \text{and} \qquad u(k) = u_{min}, \tag{5.43}$$

then

$$y(k+1) \leq y(k) + r_1 < y(k); \tag{5.44}$$

where $l_2 > l_1$, $[l_1, l_2] \in [y_{min}, y_{max}]$, *and* y_{max} *and* y_{min} *are known constants.*

Proof of Lemma 5.3.1.

(1) With $u(k) = u_{max}$, the minimum increment of $[y(k+1)-y(k)]$ is given by (5.37). Thus, from (5.35) and (5.41)

$$y(k) \leq l_2 - \eta_2.$$

Using (5.39),

$$y(k+1) - y(k) \geq r_2 > 0. \tag{5.45}$$

Hence, inequality (5.42) follows from (5.45).

(2) With $u(k) = u_{min}$, the maximum increment of $[y(k+1)-y(k)]$ is given by (5.38). Thus, from (5.35) and (5.43)

$$y(k) \geq l_1 - \eta_1.$$

Using (5.40),

$$y(k+1) - y(k) \leq r_1 < 0. \tag{5.46}$$

Hence, inequality (5.44) follows from (5.46).

Q.E.D.

In order to further ensure the convergence of Algorithm 5.1(B), the following assumption is introduced.

Assumption 5.3.2 *For large enough* $k_0 > 0$,

(i) $\hat{\beta}_0(k) = \beta_0(k)$, *for all* $k > k_0$;

(ii) $0 < \Delta_\delta \leq \delta(k) \leq \pi - \Delta_\delta$, *for all* $k > k_0$,

where the constant Δ_δ *is such that*

$$e_1 \sin \Delta_\delta = \beta_{0min} > 0;$$

β_{0min} *is the same constant as in Algorithm 4.1.*

The desired convergence result of Algorithm 5.1(B) is given by the following theorem. References [192] and [196] provide some basic ideas concerning the proof of the theorem.

Theorem 5.3.1 *For Algorithms 5.1(A)-(B), subject to Assumptions 5.3.1-5.3.2 and 4.2.1-4.2.5,*

$$\lim_{k \to \infty} \sup |y(k) - y^*(k)| \leq \tilde{K}_u + \left(4\tilde{K}_4 + 1\right) \Delta_w \tag{5.47}$$

where

$$\tilde{K}_u \triangleq \frac{\lambda}{\beta_{0min}} \epsilon_{u^*}; \tag{5.48}$$

λ, β_{0min}, *and* ϵ_{u^*} *are known constants.* $\tilde{K}_4$ *is the same constant as in Theorem 5.2.1.*

Proof of Theorem 5.3.1

See Section G.3 of Appendix G.

Q.E.D.

The convergence of Algorithm 5.1(B) requires that $\hat{\beta}_0(k) = \beta_0(k)$ (or $\hat{e}_1(k) = e_1$) be satisfied when $k > k_0$. In order to ensure the global convergence of the proposed

adaptive control law for any possible set of values of the estimate $\hat{\Theta}(k)$ over the time horizon, a modification to the control law (5.29) can be adopted. The basic idea is to replace the estimated $\hat{e}_1(k)$ in (5.30) by its true value e_1 (i.e., to use $\beta_0(k)$ instead of $\hat{\beta}_0(k)$), while the estimated $\hat{e}_1(k)$ is still retained in $\hat{g}(k)$ (5.32). Such an approach has been proposed in Section 5.2 (see Remark 5.2.2(ii)) in preparation for this modification to the adaptive control law. The model (5.14)-(5.15) has been given to accommodate this approach, and Algorithm 5.2(A) has been developed for the parameter estimation of the model (5.14)-(5.15). The resulting modified bounded nonlinear adaptive control algorithm is then given by

Algorithm 5.2(B) [bounded nonlinear adaptive weighted minimum variance control algorithm for the model (5.14)-(5.15).]

$$u^0(k) = \frac{\beta_0(k)}{\beta_0(k)^2 + \lambda} \left[y^*(k+1) - \hat{G}(q^{-1}) y(k) - \hat{g}(k) \right], \tag{5.49}$$

$$u(k) = \begin{cases} u_{max} & \text{if } u^0(k) \geq u_{max} \\ u^0(k) & \text{if } u_{min} < u^0(k) < u_{max} \\ u_{min} & \text{if } u^0(k) \leq u_{min} \end{cases} ; \tag{5.50}$$

where λ is the weighting coefficient; u_{max} and u_{min} are known constants; $\beta_0(k)$, $\hat{G}(q^{-1})$, and $\hat{g}(k)$ are defined by (4.111), (5.31), and (5.32), respectively; the estimated parameters are obtained from Algorithm 5.2(A).

$\nabla \nabla \nabla$

Accordingly, the desired convergence of Algorithm 5.2(B) is presented in the following theorem.

Theorem 5.3.2 *For Algorithms 5.2(A)-(B), subject to Assumptions 5.3.1, 5.3.2(ii), and 4.2.1-4.2.5,*

$$\lim_{k \to \infty} \sup |y(k) - y^*(k)| \leq \tilde{K}_u + \left(4\tilde{K}_4' + 1 \right) \Delta_w \tag{5.51}$$

where $\tilde{K}_u$ is the same constant as in Theorem 5.3.1 and $\tilde{K}_4'$ is the same constant as in Theorem 5.2.2.

Proof of Theorem 5.3.2

Exactly as for the proof of Theorem 5.3.1 (given by Section G.3 of Appendix G), on noting that

(1) Assumption 5.3.2(i) is not required;

(2) equations (5.26) and (5.28) hold for all k;

(3) Theorem 5.2.2(b) is used.

Q.E.D.

Remark 5.3.3 *Note that since Assumption 5.3.2(i) is not included in Theorem 5.3.2, this theorem gives the global convergence of Algorithm 5.2(B) for any value of the estimate* $\hat{e}_1(k)$ *at* $k > k_0$. *However, due to the replacement of* $\hat{\beta}_0(k)$ *by* $\beta_0(k)$ *for all* k, *the control action* $u(k)$ *given by Algorithm 5.2(B) is expected to be less 'adaptive' than that given by Algorithm 5.1(B). Thus, the system performance associated with the use of Algorithm 5.2(B) may not be as good as that with Algorithm 5.1(B). Nevertheless, since* $\hat{e}_1(k)$ *is still used for updating* $\hat{g}(k)$, *the deterioration in system performance due to the use of* e_1 *(instead of* $\hat{e}_1(k)$*) in calculating* $u^0(k)$ *in (5.49) can then be minimised. Simulation studies have been conducted, which confirm this point. For the sake of brevity, however, these studies are not included in this thesis.*

The combination of Algorithm 5.1(A) (Algorithm 5.2(A)) with Algorithm 5.1(B) (Algorithm 5.2(B)) gives the desired *Nonlinear Adaptive Weighted Minimum Variance Power System Stabiliser* **(NAWMV-PSS)** for the SMIB power system modelled in Subsection 2.3.1. The calculation of the control action of the NAWMV-PSS is a two-step procedure:

- the recursive least squares algorithm with the time-varying forgetting factor and dead zone (Algorithm 5.1(A) or Algorithm 5.2(A)) provides the estimated parameters of the NNM;

- the control law ((5.33)-(5.34) of Algorithm 5.1(B) or (5.49)-(5.50) of Algorithm 5.2(B)) generates the control signal $u(k)$ by making use of the estimates of the NNM.

The control structure of the system equipped with the NAWMV-PSS is illustrated in Fig. 5.1. The stabilising signal $y(k)$ is the machine electrical power, $P_e(k)$ (or torque, $T_e(k)$). For the purpose of demonstrating the effect of the proposed nonlinear adaptive control scheme, Algorithms 5.1(A)-(B) are chosen to be the desired NAWMV-PSS, the performance of which will be evaluated in Section 5.4. For simulation studies, the desired output trajectory $y^*(k)$ in Fig. 5.1 is set to be the reference power $P_{ref}(k)$ as explained in Remarks 4.4.5 and 3.5.2.

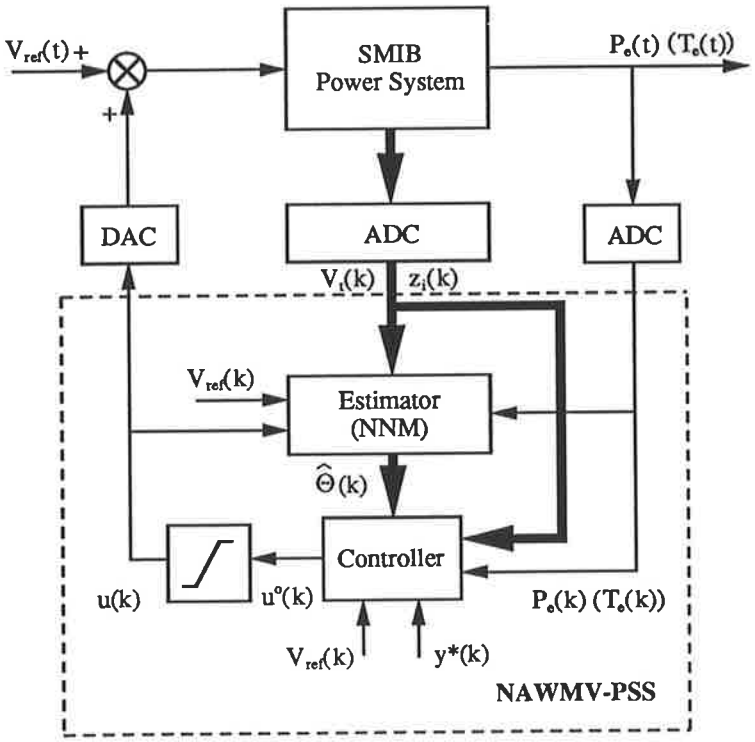

Figure 5.1: Control structure of the SMIB power system with the NAWMV-PSS.

5.4 Evaluation of the Performance of the Nonlinear Adaptive Weighted Minimum Variance Power System Stabiliser.

In this section:

- the dynamic behaviour of the *estimated* NNM in representing the *time-varying* nonlinear power system (CSM3) is examined through simulation studies;
- the performance of the NAWMV-PSS proposed in Section 5.3 is investigated through the *evaluation studies* (Studies 1-11);
- the robustness of the NAWMV-PSS is tested with unmodelled dynamics and modelling errors (Studies 12-15).

The NAWMV-PSS proposed in Section 5.3 is operated in the same environment as the NOWMV-PSS and the LAWMV-PSS, that is via excitation control of the SMIB power system modelled in Subsection 2.3.1. The sampling period h is 20 ms.

The simulation studies of this section will follow the *procedure* described in Section 3.6, and will be conducted in three **Stages**:

Stage 1: Identification of the NNM — to examine the behaviour of the estimated NNM in tracking and predicting the dynamics of the time-varying nonlinear power system (CSM3).

Stage 2: Evaluation of the performance of the NAWMV-PSS — to compare the dynamic and transient behaviour of the NAWMV-PSS with that of the NOWMV-PSS through Studies 1-11.

Stage 3: Studies on the robustness of the NAWMV-PSS — to test the performance of the NAWMV-PSS when the CSM3 is replaced by the CSM1 through Studies 12-15.

The implementation of the above three **Stages** will be discussed in Subsections 5.4.1, 5.4.2, and 5.4.3, respectively. The parameters and limits associated with the SMIB power system and the NAWMV-PSS are listed in Appendix C. The simulation results obtained from this section will be used as a *reference* for the comparisons of the system performance of the NAWMV-PSS and its simplified versions in Chapter 6.

5.4.1 Identification of the Nonlinear Nominal Model of the Power System.

In this subsection the behaviour of the *estimated* NNM in tracking and predicting the dynamics of the *time-varying* nonlinear power system (CSM3 with $D = 4.0$ pu) at different operating conditions is examined through simulation studies. The output signal is the machine electrical torque, $T_e(k)$. This subsection is the implementation of **Stage 1**.

Aims and structure of the simulation studies.

The PRBS signal, which has been used in Subsections 3.6.1 and 4.5.1 for the verification of the estimated LNM and the fixed-parameter NNM, is taken as the external control input $u(k)$ that is injected into the summing junction of the input of the AVR and the estimator, simultaneously. The model of the estimator is the NNM. At each sampling instant, the estimator generates the estimated parameters, $\hat{\Theta}(k)$, and the predicted electrical torque output, $\hat{T}_e(k)$, by the implementation of Algorithm 5.1(A). [1] The error, $e(k)$, between the predicted output, $\hat{T}_e(k)$, of the estimated NNM and the actual output, $T_e(k)$, of the CSM3 is updated. The configuration for this study is given by Fig. 5.2. The aims of this study are

- to confirm the inherent output tracking ability of the estimated NNM;
- to demonstrate the difference between the estimated NNM and the estimated LNM in representing the CSM3 at different operating points;

[1] The switching function $\sigma(k)$ is not used in the simulation studies.

- to examine the ability of the estimated NNM in tracking changes in the system parameters.

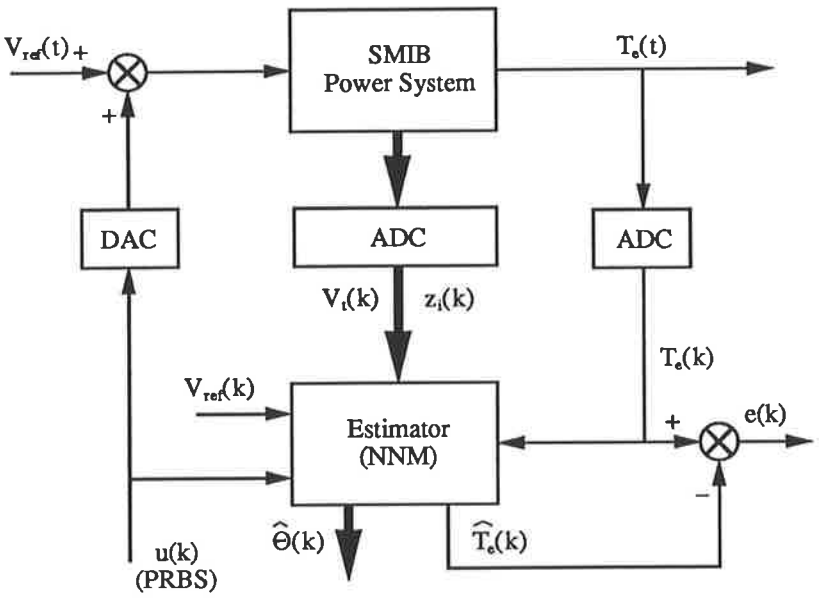

Figure 5.2: Structure of the identification of the NNM.

For the above purposes, two cases of simulation studies are chosen:

Case 1: The system is operating at $P_t = 0.6$ pu and $Q_t = 0.3$ pu, and is subjected to a step change of 0.05 pu increase in reference power at time $t = 20$ second. This case is the same as Case 1 given in Subsection 4.5.1.

Case 2: The system is operating at $P_t = 0.6$ pu and $Q_t = 0.3$ pu, and is subjected to a change in the system configuration — one transmission line is switched out at time $t = 20$ second, causing the value of the parameter X_e to double.

The simulation results associated with Cases 1-2 are shown in Figs. 5.3-5.7 and Tables 5.1-5.2. The estimator parameters are: $K_0 = 10^2$, $C = 10^3$, $\mu_{min} = 0.2$, and $\Sigma_0 = 0.8$. The initial value of the estimate, $\hat{\Theta}(0)$, is set to be the pre-calculated true value, Θ_0 (see column 2 of Table 4.2). The results for the fixed-parameter NNM (studied in Subsection 4.5.1) and the estimated LNM (studied in Subsection 3.6.1) are compared with the simulation results in the discussion that follows.

Analysis of the simulation studies.

Case 1: The simulation study in this case involves the confirmation of the inherent output tracking ability of the estimated NNM. Subject to the PRBS input signal and the step change in reference power, the dynamic responses of the predicted output, $\hat{T}_e(k)$, of the *estimated* NNM and the actual output, $T_e(k)$, of the CSM3 in Case 1 are superimposed in Fig. 5.3. The error, $e(k)$, between $T_e(k)$ and $\hat{T}_e(k)$ is plotted in Fig. 5.4 by the solid line. In order to form a comparison, the error, $w(k)$, between the predicted output, $T_e^0(k \mid k-1)$, of the *fixed-parameter* NNM and the actual output, $T_e(k)$, of the CSM3 in the same case (as shown in Fig. 4.7) is re-plotted in Fig. 5.4 by the dotted line. It is seen from Figs. 5.3-5.4 that the estimated NNM inherently tracks the dynamics of the CSM3 and represents the CSM3 at different operating points as accurately as the fixed-parameter NNM; both errors, $w(k)$ and $e(k)$, are of the same order of magnitude. This implies that in small dynamics where the power system parameters are time-invariant, the performance of the NAWMV-PSS will closely match that of the NOWMV-PSS. This point will be demonstrated in the simulation studies of Subsections 5.4.2 and 5.4.3.

The inherent output tracking ability of the estimated NNM is further demonstrated by the comparison of the variation in the estimates of both the *estimated* NNM and the *estimated* LNM when the system operating point changes. For this purpose, Case 1 is applied to the estimated LNM. The estimated parameters of the LNM and the NNM in the same case are then plotted in Figs. 5.5 and 5.6, respectively. It is seen that while the estimated LNM has to modify its parameters in order to cope with the change in the system operating point, the parameters of the estimated NNM are kept almost constant. Tables 5.1-5.2 give the variation of the estimates of the LNM and the NNM when a step change in the system operating point occurs at time $t = 20$ second. The parameters of the estimated NNM vary very little when the system operating point changes, which confirms the fact that the estimated NNM inherently tracks the change in the system operating point. Consequently, using the parameters of the estimated NNM, the NAWMV-PSS is expected to provide superior control action.

Case 2: This simulation study examines the ability of the estimated NNM to

track the changes in the system parameters. The same study is applied to the fixed-parameter NNM. The errors, $w(k)$ and $e(k)$, after a transmission line is switched out are plotted in Fig. 5.7. Since the fixed-parameter NNM cannot adapt to the change in the system configuration, the output tracking error $w(k)$ is seen to be much larger than $e(k)$.

Conclusions.

Based on the simulation results given by Cases 1-2, it is concluded that:

1. The estimated NNM has similar performance to the fixed-parameter NNM in that it accurately models the dynamics of the continuous-time CSM3 when the system parameters are constant and the system configuration does not change.

2. The estimated NNM possesses the ability to adapt on-line to the changes in the system parameters and configuration.

3. Because the estimated NNM tracks the changes in the nonlinear power system, the control action based on the estimated NNM in damping system dynamic oscillations should be superior to that based on the fixed-parameter NNM.

Estimates	**True Values**	$\hat{\theta}_i(1000)$	$\hat{\theta}_i(2000)$	$\lvert\hat{\theta}_i(2000) - \hat{\theta}_i(1000)\rvert$
$\hat{\theta}_1 = \hat{a}_1$	*	-1.2624	-1.2732	1.08×10^{-2}
$\hat{\theta}_2 = \hat{a}_2$	*	-0.2932	-0.02957	2.64×10^{-1}
$\hat{\theta}_3 = \hat{a}_3$	*	0.5976	0.3360	2.62×10^{-1}
$\hat{\theta}_4 = \hat{b}_0$	*	0.04238	0.03526	7.11×10^{-3}
$\hat{\theta}_5 = \hat{b}_1$	*	0.04721	0.05020	3.00×10^{-3}
$\hat{\theta}_6 = \hat{b}_2$	*	-0.02459	-0.0006131	2.40×10^{-2}

Table 5.1: Estimated parameters of the LNM for Case 1.

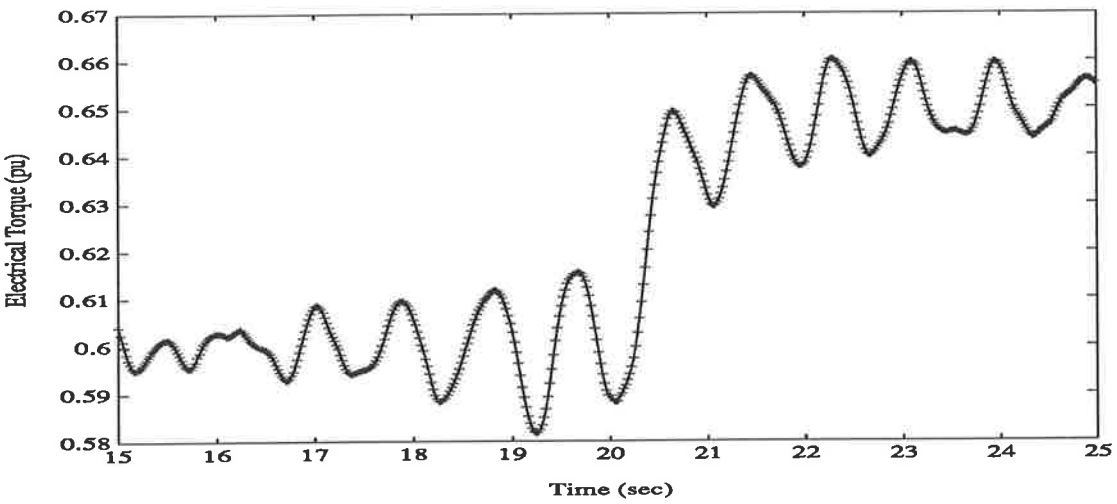

Figure 5.3: Electrical torque response for Case 1 ($P_t = 0.6$ pu, $Q_t = 0.3$ pu; 0.05 pu increase in reference power). CSM3 - solid line, estimated NNM - line marked by '+'.

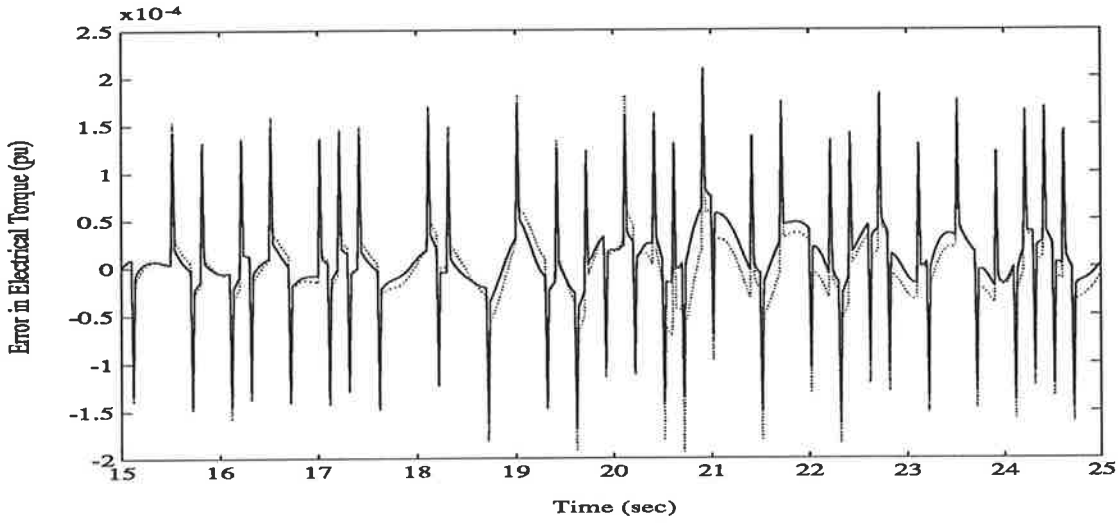

Figure 5.4: Error in electrical torque for Case 1 ($P_t = 0.6$ pu, $Q_t = 0.3$ pu; 0.05 pu increase in reference power). estimated NNM - solid line, fixed-parameter NNM - dotted line.

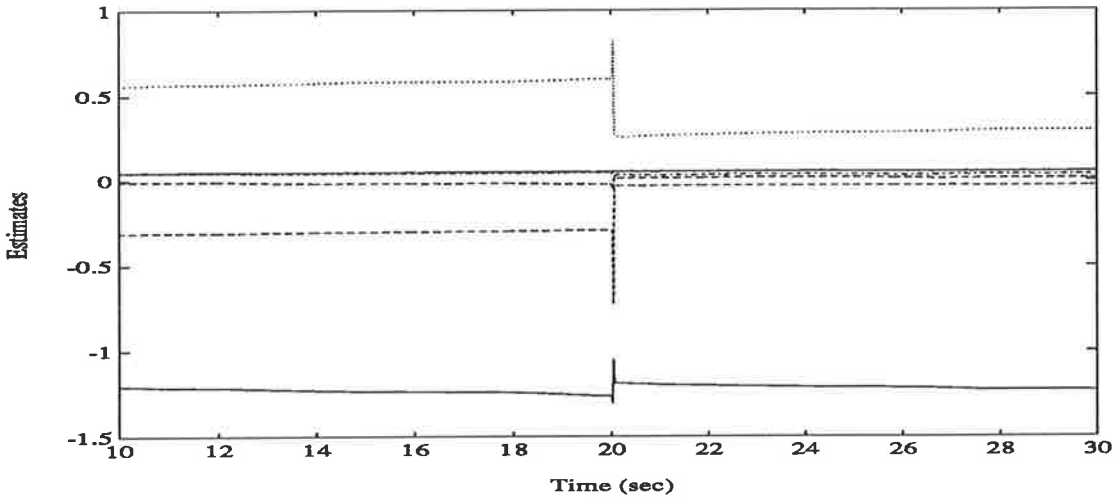

Figure 5.5: Estimated parameters of the LNM for Case 1 ($P_t = 0.6$ pu, $Q_t = 0.3$ pu; 0.05 pu increase in reference power).

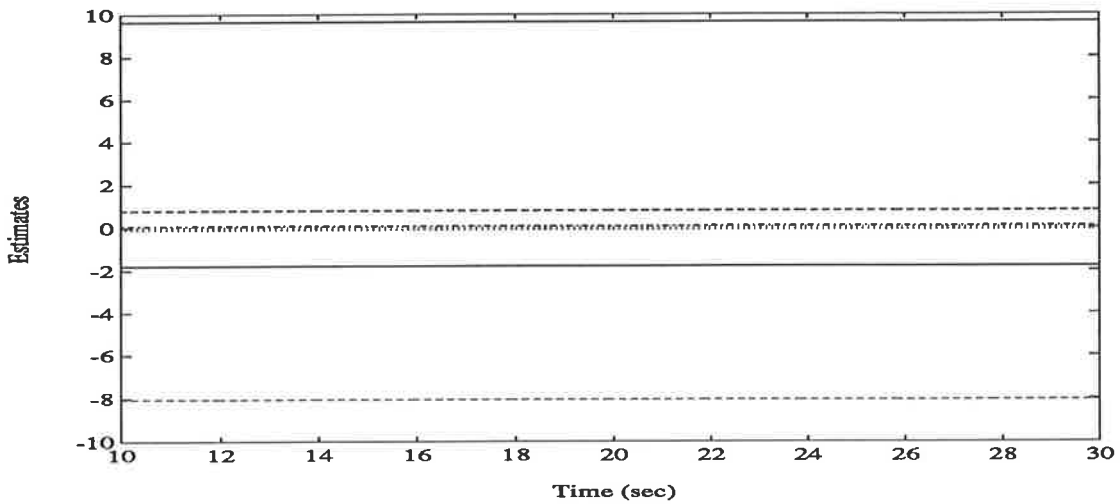

Figure 5.6: Estimated parameters of the NNM for Case 1 ($P_t = 0.6$ pu, $Q_t = 0.3$ pu; 0.05 pu increase in reference power).

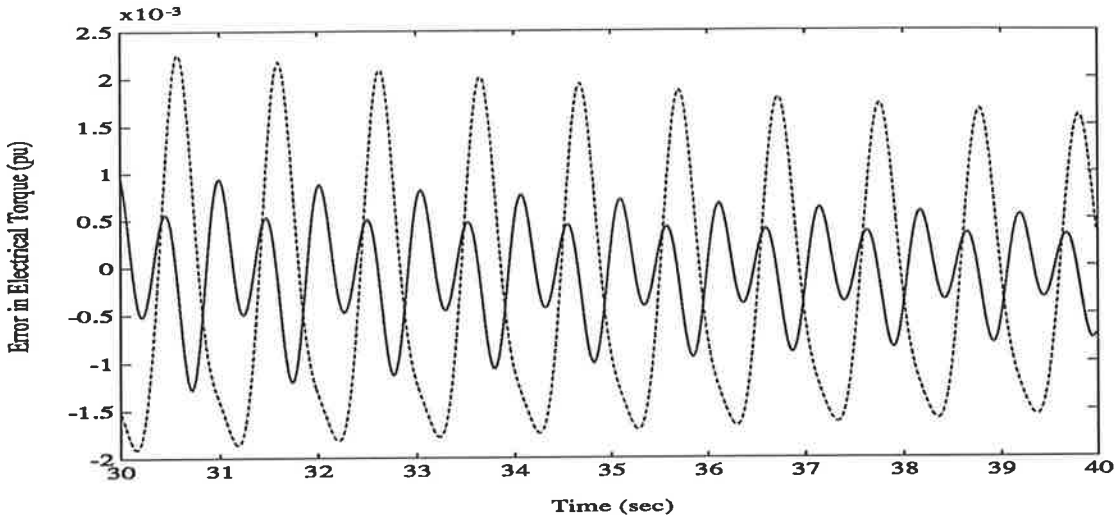

Figure 5.7: Error in electrical torque for Case 2 (P_t = 0.6 pu, Q_t = 0.3 pu; one transmission line switching-out). estimated NNM - solid line, fixed-parameter NNM - dashed line.

Estimates	**True Values**	$\hat{\theta}_i(1000)$	$\hat{\theta}_i(2000)$	$\lvert\hat{\theta}_i(2000) - \hat{\theta}_i(1000)\rvert$
$\hat{\theta}_1 = \hat{a}_1$	-1.7863	-1.7857	-1.7858	1.00×10^{-4}
$\hat{\theta}_2 = \hat{a}_2$	0.7886	0.7887	0.7881	5.80×10^{-4}
$\hat{\theta}_3 = \hat{b}_1$	-0.08035	-0.07990	-0.07978	1.21×10^{-4}
$\hat{\theta}_4 = \hat{b}_2$	0.08036	0.08039	0.07986	5.26×10^{-4}
$\hat{\theta}_5 = \hat{c}_1$	9.6592	9.6592	9.6591	1.00×10^{-4}
$\hat{\theta}_6 = \hat{c}_2$	-8.0494	-8.0494	-8.0495	1.00×10^{-4}
$\hat{\theta}_7 = \hat{d}_1$	0.02844	0.02825	0.02811	1.41×10^{-4}
$\hat{\theta}_8 = \hat{e}_1$	0.09054	0.08666	0.08435	2.31×10^{-3}

Table 5.2: Estimated parameters of the NNM for Case 1.

5.4.2 Evaluation of the Performance of the NAWMV-PSS for the CSM3.

In this subsection the evaluation of the performance of the NAWMV-PSS is conducted for the CSM3 (with $D = 4.0$ pu) through the series of *evaluation studies* (Studies 1-11) defined in Subsection 3.6.2. This subsection is the implementation of **Stage 2**.

Aims and structure of the simulation studies.

The control structure of the CSM3 equipped with the NAWMV-PSS is illustrated in Fig. 5.1. The machine electrical torque is used as the stabilising signal. For each simulation study, the performance of the CSM3 equipped with the NAWMV-PSS is compared with that of the CSM3 equipped with the NOWMV-PSS proposed in Chapter 4. The aims of this study are

- to confirm that the NAWMV-PSS overcomes the deficiencies in the NOWMV-PSS by adapting to the system changes and producing a superior control action during large transients;
- to establish a reference for comparisons of the performance of the NAWMV-PSS and its simplified versions to be designed in Chapter 6.

Studies 1-11 specified in the five **Groups** in Subsection 3.6.2 are performed. The simulation results are shown in Figs. 5.8-5.17 in which the performance of the NOWMV-PSS is provided by Figs. 4.10, 4.12-4.18, and 4.21. The parameters of the NAWMV-PSS are: $u_{min} = -0.05$ pu, $u_{max} = 0.05$ pu, and $\lambda = 0.4$, which are the same as those used in the NOWMV-PSS.

Remark 5.4.1 *In a similar manner to the LAWMV-PSS studies, a fixed-length freezing time period (explained in Remark 3.6.2) is employed in the estimator of the NAWMV-PSS to hold the estimates constant at their pre-fault values during the fault period.*

Analysis of the simulation studies.

Group 1: The *dynamic performance* of the NAWMV-PSS is examined in Studies 1-3 by simulating the periodic changes in the system operating point. In Studies 1-2, the system operating point changes with constant reactive power Q_t, and the infinite bus voltage V_∞ is assumed to be constant for each study. The true values of the parameters of the NNM are unchanged. Hence, the system responses with the NOWMV-PSS and the NAWMV-PSS are identical. As an example, the result of Study 1 is plotted in Fig. 5.8 (while the result of Study 2 is omitted). However, in Study 3 in which the system operating point changes *between* the lagging and leading conditions, the value of V_∞ varies in accordance with the variations in Q_t. Consequently, the true values of the parameters of the NNM are time-varying. As shown in Fig. 5.9, the damping performance associated with the NOWMV-PSS can be seen to deteriorate slightly when compared with that associated with the NAWMV-PSS. This is because the NAWMV-PSS can make on-line adjustment of its parameters, while the NOWMV-PSS cannot.

Group 2: The *transient performance* of the NAWMV-PSS following three-phase faults on a transmission line is examined in Studies 4-6. The simulation results are plotted in Figs. 5.10-5.13. It is seen that the NAWMV-PSS provides stronger damping than the NOWMV-PSS after the faults are cleared. With fixed parameters, the NOWMV-PSS can only generate the post-fault control action which is based on the assumption that the power system is operating within linear operation. The NAWMV-PSS, however, can not only take the inherent nonlinearities of the system into account for generating an adequate post-fault control action (as the NOWMV-PSS does), but can also adapt to the new operating conditions by changing its parameters on-line. Therefore, strong control actions are provided by the NAWMV-PSS, and the control goal — damping the output oscillations — is optimally achieved during the large transients.

Remark 5.4.2 *Figure 5.12 illustrates the field voltage $E_{FD}(t)$ response for the test in Study 5. The conclusions regarding the field voltage responses of the different power system stabilisers support those made for the torque responses. Further to this, the*

field voltage response of the NAWMV-PSS shows that the NAWMV-PSS can provide a control action with appropriate amplitude and phase, resulting in the stronger damping of the rotor oscillations as revealed by the responses.

Group 3: The *ability* of the NAWMV-PSS to track the changes in the system parameters and configuration is examined in Study 7. It is seen from Fig. 5.14 that the NAWMV-PSS provides better damping than the NOWMV-PSS in the event of one transmission line switching out and in. This is due to the fact that the NAWMV-PSS can adjust its parameters accordingly (see Fig. 5.15).

Group 4: In Studies 8-9, the *ability* of the NAWMV-PSS to overcome the measurable deterministic disturbances in reference voltage is examined. Under these circumstances, the true values of the parameters of the NNM are unchanged. Since both the NAWMV-PSS and the NOWMV-PSS include the voltage reference signal in the formulation of the NNM *explicitly* (see also Remark 4.5.6), the NAWMV-PSS and the NOWMV-PSS give *identical* system damping performance in these two studies. The result of Study 8 is shown in Fig. 5.16 to illustrate this. The result of Study 9 is omitted for simplicity.

Group 5: The *ability* of the NAWMV-PSS to extend the system stability region is examined in Studies 10-11. Since the infinite bus voltage V_∞ is kept constant during these studies, the true values of the parameters of the NNM are constant. The damping effect of the NAWMV-PSS is, therefore, equivalent to that of the NOWMV-PSS. An example is shown in Fig. 5.17 for Study 11 (while the result of Study 10 is omitted).

Conclusions.

From the analysis of the simulation results in this subsection, it is concluded that:

1. For the dynamic situations in which the power system parameters and the value of the infinite bus voltage are unchanged, the system responses with the NAWMV-PSS and the NOWMV-PSS are identical.

2. In the events of severe three-phase faults, the NAWMV-PSS is more effective in damping the system oscillations than the NOWMV-PSS. Unlike the NOWMV-PSS, the NAWMV-PSS can adapt to the changes in the system operating conditions during large transients.

3. When either the power system parameters change or the system lagging/leading operating condition changes (requiring a change in the value of the infinite bus voltage), the damping performance of the NAWMV-PSS is better than that of the NOWMV-PSS. This is because the parameters of the NAWMV-PSS can be adjusted on-line, while the parameters of the NOWMV-PSS are fixed.

The advantage of the *nonlinear adaptive* control strategy over the *nonlinear optimal* control strategy is thus evident.

5.4.3 Studies on the Robustness of the NAWMV-PSS for the CSM1.

In this subsection the robustness of the NAWMV-PSS is confirmed through the series of *robustness studies* (Studies 12-15) defined in Subsection 3.6.3. The performance of the NAWMV-PSS is tested with unmodelled dynamics and modelling errors. This subsection is the implementation of **Stage 3**.

Aims and structure of the simulation studies.

The CSM3 ($D = 4.0$ pu) is replaced by the CSM1 ($D = 0.1$ pu), and the performance of the NAWMV-PSS and the NOWMV-PSS is further compared. The stabilising signal is the electrical power $P_e(k)$. The aims of this study are

- to verify the design of the NAWMV-PSS in operation in a system represented by the more accurate model (CSM1);

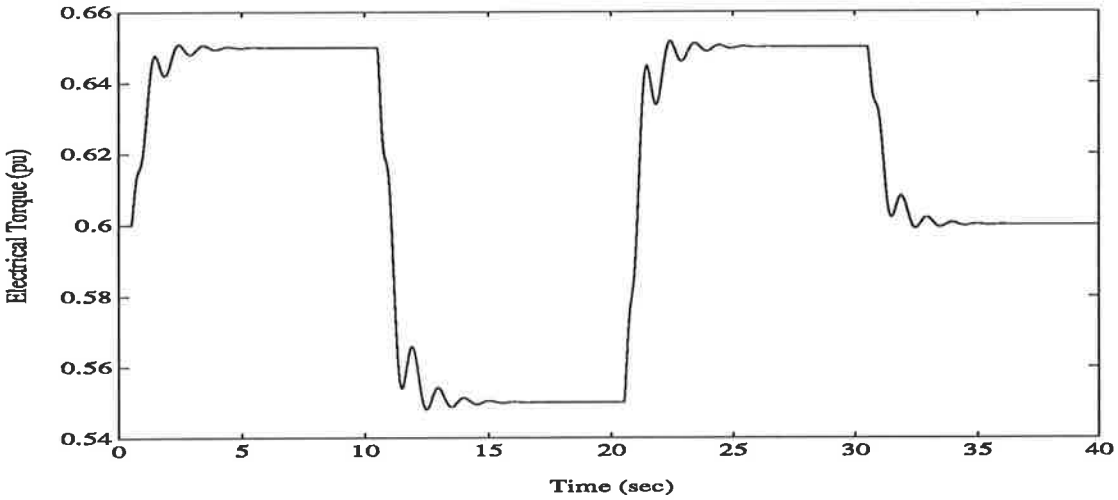

Figure 5.8: Electrical torque response for Study 1 ($P_t = 0.6$ pu, $Q_t = 0.3$ pu; periodic variations in reference power). CSM3 with the NAWMV-PSS - solid line, CSM3 with the NOWMV-PSS - dashed line.

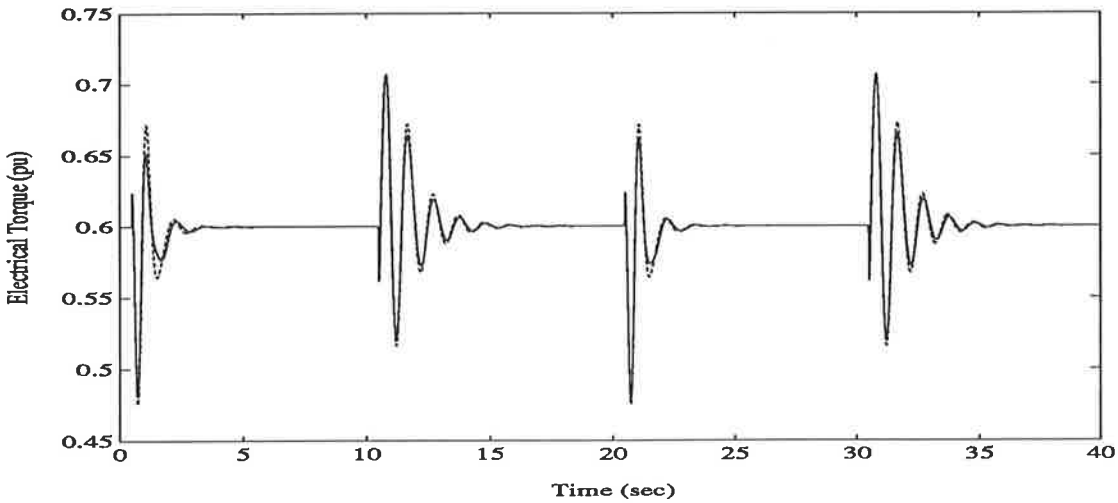

Figure 5.9: Electrical torque response for Study 3 ($P_t = 0.6$ pu, $Q_t = 0.3$ pu; periodic variations in reactive power between lagging and leading operating conditions). CSM3 with the NAWMV-PSS - solid line, CSM3 with the NOWMV-PSS - dashed line.

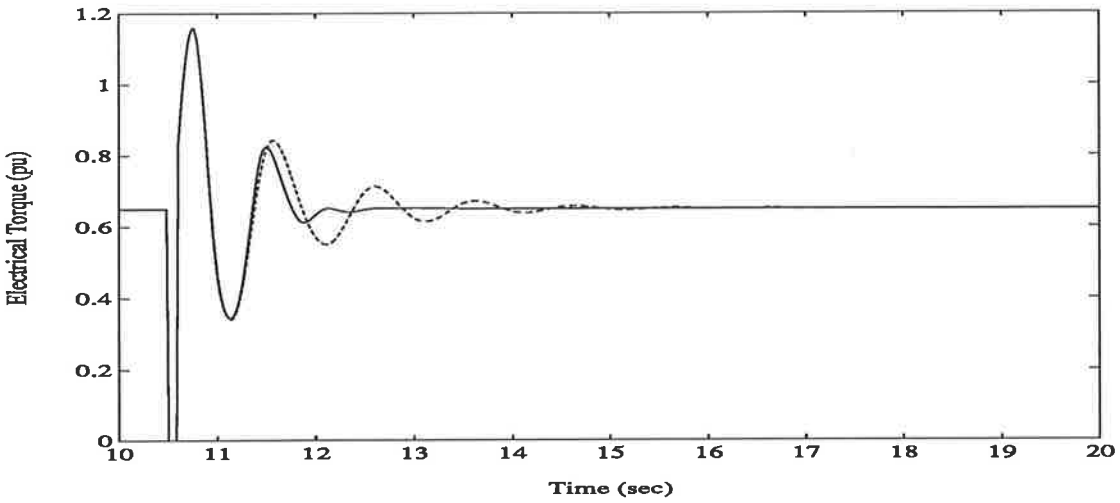

Figure 5.10: Electrical torque response for Study 4 ($P_t = 0.65$ pu, $Q_t = 0.3$ pu; 100 ms short-circuit on the receiving end busbars). CSM3 with the NAWMV-PSS - solid line, CSM3 with the NOWMV-PSS - dashed line.

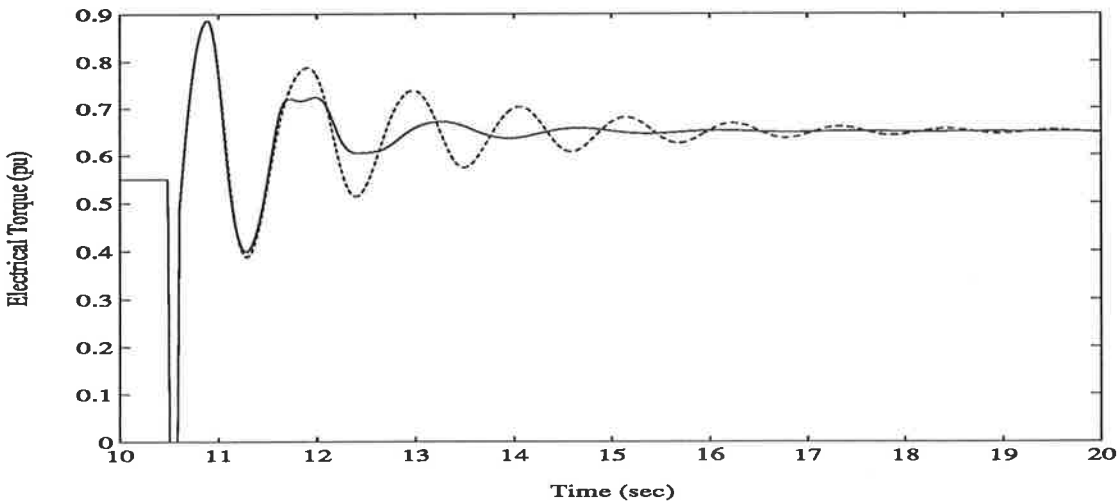

Figure 5.11: Electrical torque response for Study 5 ($P_t = 0.55$ pu, $Q_t = -0.1$ pu; 100 ms short-circuit at the machine terminal). CSM3 with the NAWMV-PSS - solid line, CSM3 with the NOWMV-PSS - dashed line.

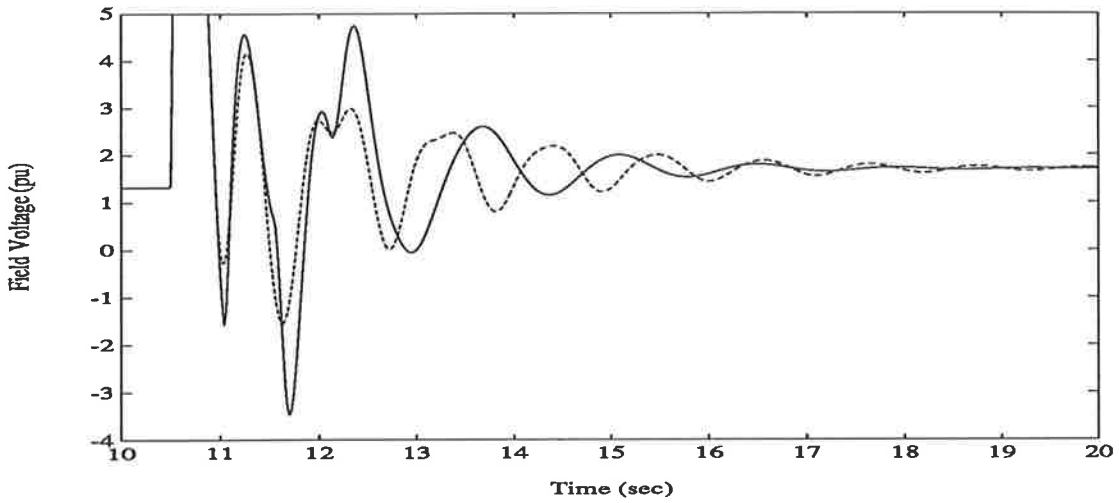

Figure 5.12: Field voltage response for Study 5 ($P_t = 0.55$ pu, $Q_t = -0.1$ pu; 100 ms short-circuit at the machine terminal). CSM3 with the NAWMV-PSS - solid line, CSM3 with the NOWMV-PSS - dashed line.

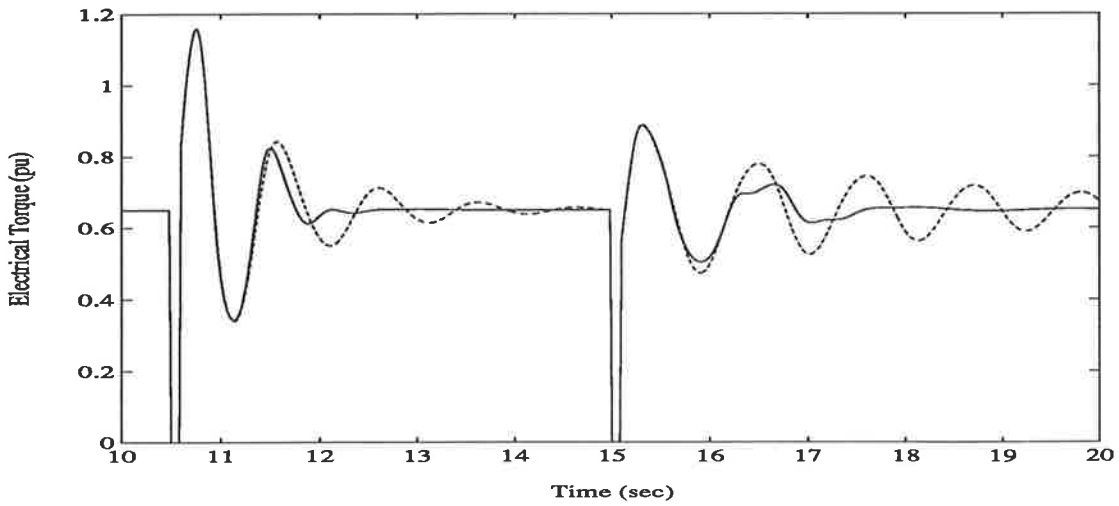

Figure 5.13: Electrical torque response for Study 6 ($P_t = 0.65$ pu, $Q_t = 0.3$ pu; two successive faults of 100 ms duration on the receiving end busbars). CSM3 with the NAWMV-PSS - solid line, CSM3 with the NOWMV-PSS - dashed line.

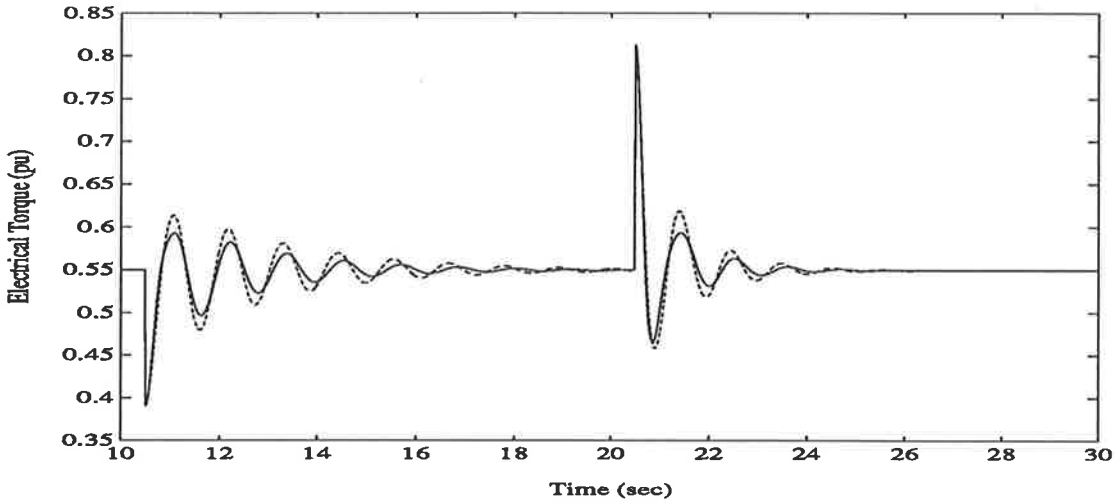

Figure 5.14: Electrical torque response for Study 7 ($P_t = 0.55$ pu, $Q_t = 0.3$ pu; one transmission line is opened and then reclosed). CSM3 with the NAWMV-PSS - solid line, CSM3 with the NOWMV-PSS - dashed line.

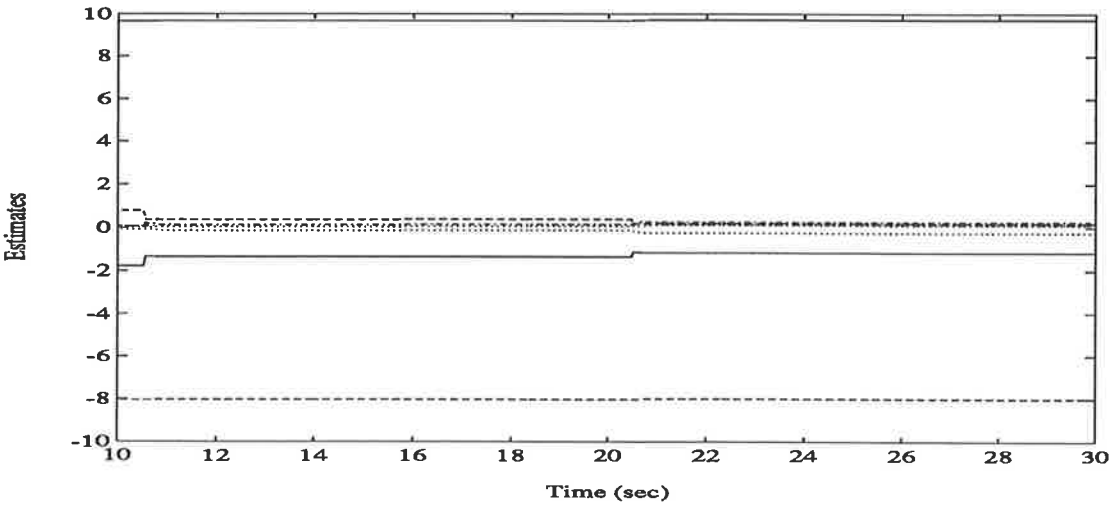

Figure 5.15: Estimated parameters of the NNM for Study 7 ($P_t = 0.55$ pu, $Q_t = 0.3$ pu; one transmission line is opened and then reclosed).

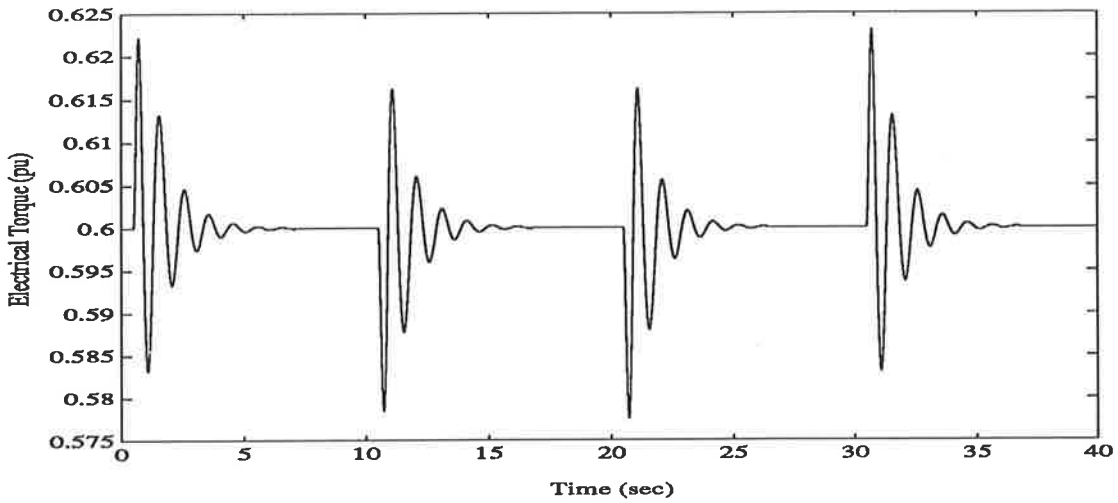

Figure 5.16: Electrical torque response for Study 8 ($P_t = 0.6$ pu, $Q_t = 0.3$ pu; periodic disturbances in reference voltage). CSM3 with the NAWMV-PSS - solid line, CSM3 with the NOWMV-PSS - dashed line.

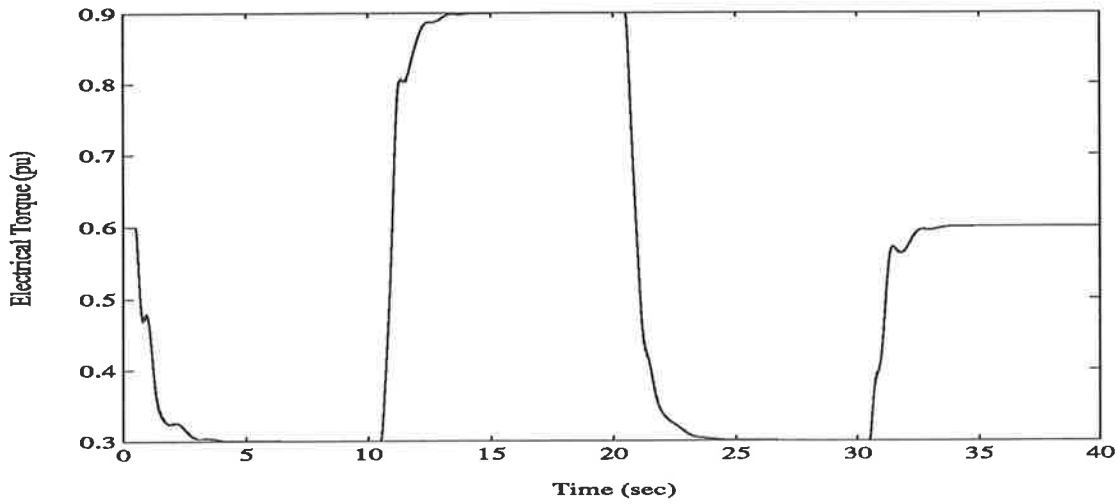

Figure 5.17: Electrical torque response for Study 11 ($P_t = 0.6$ pu, $Q_t = -0.1$ pu; large periodic excursions in reference power). CSM3 with the NAWMV-PSS - solid line, CSM3 with the NOWMV-PSS - dashed line.

- to establish a reference for the comparison of the performance of the NAWMV-PSS and its simplified versions with unmodelled dynamics and modelling errors to be conducted in Subsection 6.5.3.

Studies 12-15 specified in the two **Groups** in Subsection 3.6.3 are implemented. The simulation results are shown in Figs. 5.18-5.20 in which the performance of the NOWMV-PSS is provided by Figs. 4.23-4.25.

Analysis of the simulation studies.

Group 1: The *dynamic performance* of the NAWMV-PSS associated with the CSM1 is examined in Studies 12-13. It is found that the NAWMV-PSS and the NOWMV-PSS give almost identical damping performance. This agrees with the result shown in Figs. 5.8-5.9. The analysis of the simulation results of Studies 1-2 in **Stage 2** provides the explanation of this phenomenon. Besides, in dynamic situations the effect of the subtransients of the CSM1 (i.e., the unmodelled dynamics of the NNM) is negligible. The fixed-parameter NNM and the estimated NNM therefore provide the same damping effects to the system oscillations. The simulation result of Study 13 is shown in Fig. 5.18, while the result of Study 12 is omitted for the sake of simplicity.

Group 2: The *transient performance* of the NAWMV-PSS associated with the CSM1 is examined in Studies 14-15. The simulation results are plotted in Figs. 5.19-5.20. In transient situations, the unmodelled dynamics of the system become obvious. Due to its ability to adapt to system changes, the NAWMV-PSS provides better damping to the system oscillations than the NOWMV-PSS. This agrees with the results shown in Figs. 5.10-5.13.

Conclusions.

The above studies confirm that:

1. The NAWMV-PSS is a sound design for the higher-order actual power system.

2. The NAWMV-PSS is more effective than the NOWMV-PSS in the overall system performance.

From these conclusions, and the conclusions drawn in Subsections 3.6.3 and 4.5.3, it is evident that the NAWMV-PSS is superior to the NOWMV-PSS, the LAWMV-PSS, and the CPSS ($D_d = 20$ pu).

5.5 Concluding Remarks.

In this chapter *original* work on the design and implementation of a *nonlinear adaptive* power system stabiliser for the SMIB power system modelled in Subsection 2.3.1 is described. This work completes the theoretical development and assessment of a nonlinear adaptive power system stabiliser based on the nonlinear nominal model (NNM) derived in Subsection 4.2.3. The objective of this work is to establish a basis for the development of simplified versions of the nonlinear adaptive power system stabiliser and a bilinear adaptive power system stabiliser to be discussed in Chapter 6.

The development of the nonlinear adaptive power system stabiliser is initiated by the fact that the parameters of the NNM are time-varying. Several factors, such as a change in the system configuration and a change in operating conditions, will result in changes in the parameters of the NNM. The NOWMV-PSS which has been designed in Chapter 4 is based on the *fixed-parameter* NNM, and hence cannot adapt to changes in the parameters or configuration of the SMIB power system. For this reason, the nonlinear adaptive power system stabiliser which is based on the *estimated* NNM is introduced in this chapter. The performance of the estimated NNM in inherently tracking and predicting the time-varying nonlinear power system (CSM3) at different system operating points with different system parameters is confirmed through simulation studies in Subsection 5.4.1.

In Section 5.2 the recursive least squares algorithm with the time-varying forgetting factor, which has been proposed for the implementation of the linear adaptive power system stabiliser in Chapter 3, is applied to the identification of the time-varying

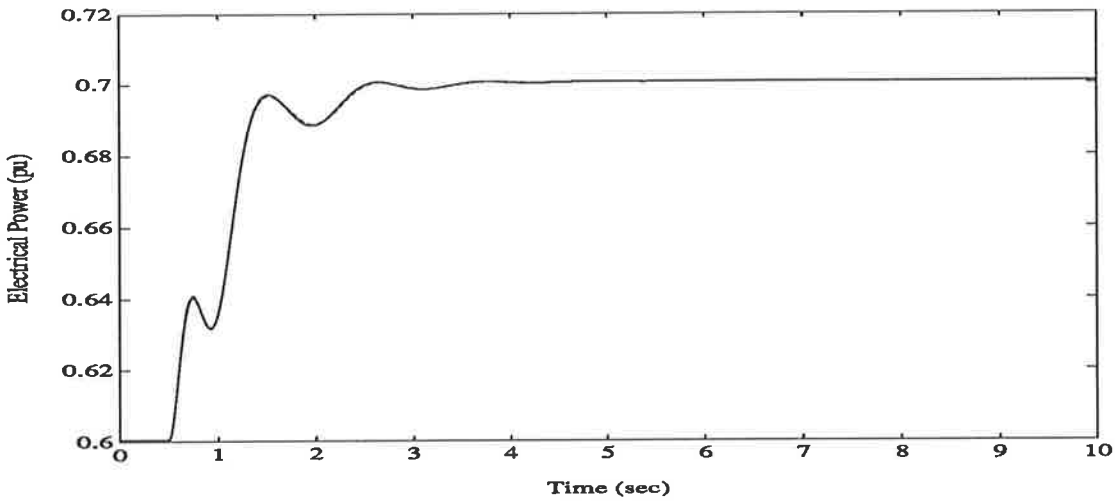

Figure 5.18: Electrical power response for Study 13 ($P_t = 0.6$ pu, $Q_t = -0.1$ pu; step change in reference power). CSM1 with the NAWMV-PSS - solid line, CSM1 with the NOWMV-PSS - dashed line.

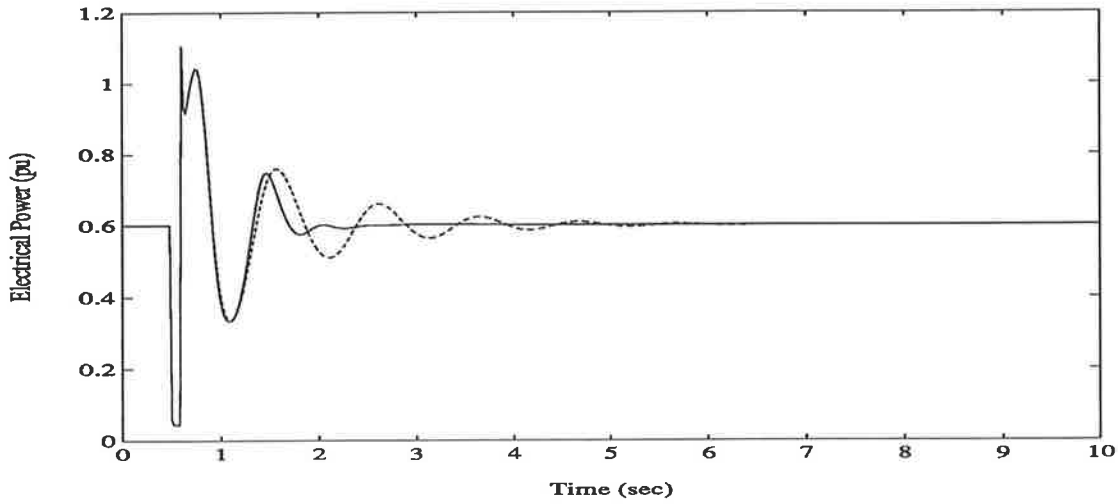

Figure 5.19: Electrical power response for Study 14 ($P_t = 0.6$ pu, $Q_t = 0.3$ pu; 100 ms short-circuit on the receiving end busbars). CSM1 with the NAWMV-PSS - solid line, CSM1 with the NOWMV-PSS - dashed line.

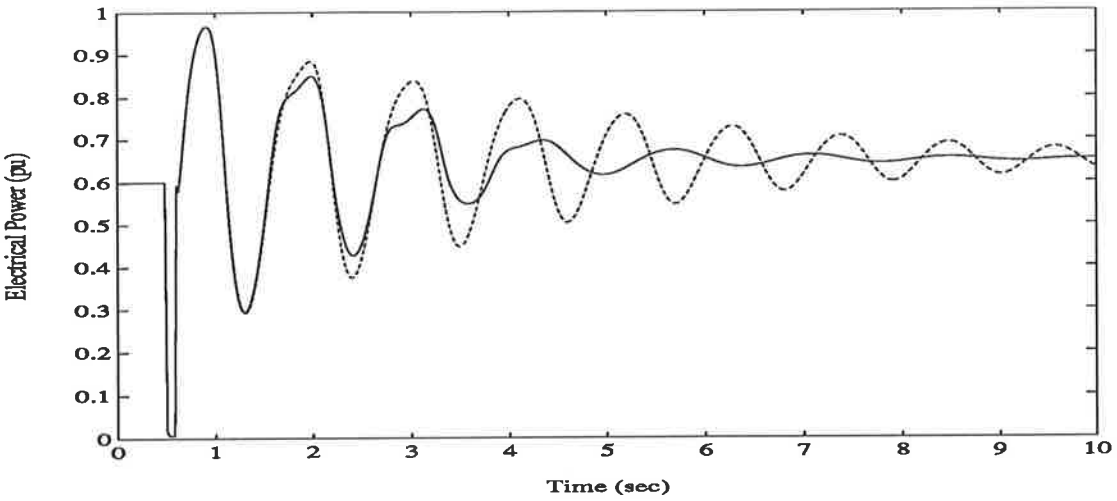

Figure 5.20: Electrical power response for Study 15 ($P_t = 0.6$ pu, $Q_t = -0.1$ pu; 100 ms short-circuit at the machine terminal). CSM1 with the NAWMV-PSS - solid line, CSM1 with the NOWMV-PSS - dashed line.

NNM. Since the noise term in the NNM is considered as a general bounded noise in this chapter, the dead zone technique is used in the parameter estimation algorithm to ensure the convergence of the algorithm. Algorithm 5.1(A) is then proposed, and its convergence is established in Theorem 5.2.1.

In Section 5.3 a *new* nonlinear adaptive weighted minimum variance control law is developed from the nonlinear stochastic weighted minimum variance control law (4.128), and the resulting bounded nonlinear adaptive control algorithm (Algorithm 5.1(B)) is proposed. The combination of Algorithm 5.1(A) with Algorithm 5.1(B) forms the desired *indirect* nonlinear adaptive weighted minimum variance power system stabiliser (NAWMV-PSS). The convergence of Algorithm 5.1(B) is established in Theorem 5.3.1, which ensures the closed-loop system stability associated with the proposed nonlinear adaptive power system stabiliser.

In order to guarantee the global convergence of the nonlinear adaptive control algorithm, a modification to the nonlinear adaptive control law (5.29) is proposed. The basic idea is to use a constant e_1 to calculate $\beta_0(k)$, while the estimate $\hat{e}_1(k)$ is

still retained in $\hat{g}(k)$. An alternative form of the estimated NNM is given by (5.14)-(5.15) to accommodate this modification. Algorithm 5.2(A) and Algorithm 5.2(B) are then developed for application to the model (5.14)-(5.15) for the estimation of the parameters and the calculation of the control law, respectively. The convergence of these algorithms is established in Theorems 5.2.2 and 5.3.2. The implementation of this modified nonlinear adaptive power system stabiliser is expected to give a less adaptive control effect, and is not included in this thesis for the sake of brevity (see Remark 5.3.3).

In Section 5.4 the performance of the proposed NAWMV-PSS is investigated and its robustness in stabilising the higher-order actual power system is tested through the simulation studies presented in Subsections 5.4.2 and 5.4.3. The performance of the NAWMV-PSS is compared with that of the NOWMV-PSS, and the effectiveness of the NAWMV-PSS in adapting to system changes and damping system oscillations is demonstrated by the comparison. The advantage of the nonlinear *adaptive* control strategy over the nonlinear *optimal* control strategy is clearly shown in Figs. 5.8-5.20. Through the systematic comparisons of performance of the CPSS, the LAWMV-PSS, the NOWMV-PSS, and the NAWMV-PSS, which have been conducted in Sections 3.6, 4.5, and 5.4, it is evident that, out of these power system stabilisers, the NAWMV-PSS gives superior damping performance. The evaluation of the dynamic behaviour of the system with the NAWMV-PSS establishes a basis for the evaluation of the system performance with simplified versions of the NAWMV-PSS and with a bilinear adaptive power system stabiliser which will be designed in Chapter 6.

Before concluding this chapter, it is necessary to make the following comments on the comparison of the *linear adaptive* control strategy discussed in Chapter 3 and the *nonlinear adaptive* control strategy proposed in this chapter. As far as the nominal model is concerned, the linear adaptive control strategy is based on the estimated LNM which has been derived by linearising the nonlinearities of the power system and assuming that the high-order time-varying nonlinear power system can be characterised by low-order time-varying linear dynamics. The nonlinear adaptive control strategy, however, is based on the estimated NNM which accurately represents the inherent nonlinearities of the SMIB power system and accommodates the system changes by its

time-varying parameters. Therefore,

1. the nonlinear adaptive control strategy has the advantage over the linear adaptive control strategy of not requiring parameter variations to adapt to different system operating points, when there is no change in the true values of the parameters of the NNM;

2. the damping performance with the nonlinear adaptive control strategy is potentially superior to that with the linear adaptive control strategy, when either the true values of the parameters of the NNM change or large transients occur.

In conclusion, a combination of *nonlinear* with *adaptive* control is more suitable for the stabilisation of the time-varying nonlinear power system than other more conventional approaches.

The contributions in this chapter are **original**, and have been listed in Section 5.1.

Chapter 6

Simplified SISO Nonlinear Adaptive Power System Stabilisers.

6.1 Introduction.

In this chapter *simplified versions* of the nonlinear adaptive power system stabiliser proposed in Chapter 5 are derived, and the design of a *bilinear adaptive* power system stabiliser is discussed. The development of this stabiliser is the objective of the analyses and studies conducted in Chapters 3 to 5 with the models of the SMIB power system derived in Chapter 2. The studies carried out in this chapter provide a basis for the practical implementation of a nonlinear adaptive power system stabiliser.

A *nonlinear adaptive* control strategy has been proposed in Chapter 5 in order to overcome the deficiencies associated with the *nonlinear optimal* power system stabiliser designed in Chapter 4. The NAWMV-PSS designed for this purpose has been shown to be more effective in improving the system performance than the NOWMV-PSS in situations where the true values of the parameters of the NNM are changed. As an ideal nonlinear adaptive power system stabiliser, the NAWMV-PSS has the advantage

of providing better damping of the system oscillations than the other three stabilisers (i.e., the NOWMV-PSS, the LAWMV-PSS, and the CPSS).

The implementation of the NAWMV-PSS (or the NOWMV-PSS) requires information about the additional feedback signals $z_i(k)$ $(i = 1, 2, 3, 4)$ at each sampling instant k. According to the definitions of these signals given by (4.22)-(4.25), $z_i(k)$ $(i = 1, 2, 3, 4)$ can be calculated from the values of the state variables $\delta(k)$, $\omega_s(k)$, $E_{FD}(k)$, and $E'_q(k)$. The provision of these state variables at each sampling instant k is, therefore, essential. Ideally, the state variables $\omega_s(k)$ and $E_{FD}(k)$ can be measured directly, while $\delta(k)$ and $E'_q(k)$ may be obtained indirectly by other means. However, in practice, the value of the rotor angle $\delta(k)$ is difficult to determine, since the infinite bus is taken as its reference. Furthermore, the measurement of the variable $E'_q(k)$ requires the access to the field flux, which may be difficult to obtain. Hence, from a practical point of view, *simplifications* of the NAWMV-PSS by the elimination of some of the additional feedback signals from the calculation of the control law are required.

The NAWMV-PSS is based on the NNM which has been derived directly from the mathematical description of the nonlinear power system (CSM3). The number of the parameters of the NNM is larger than that of the LNM employed by the LAWMV-PSS. From Figs 4.23 and 5.18, it is observed that for small disturbances the LAWMV-PSS performs as *well* as the NAWMV-PSS. This fact indicates that some parameters of the NNM represent the less significant dynamics which may be omitted by approximations. Due to the use of the *adaptive* control schemes, the effect of the omission of the less significant dynamics from the NNM will be compensated for by the rest of the time-varying estimated parameters. Hence, the system performance may not deteriorate. These considerations form the bases for the simplifications to be discussed in this chapter.

Another concern in designing an adaptive control scheme is to keep the number of the parameters to be estimated small. It is well known that the computation time grows with the number of the parameters to be estimated [193,203] and this factor may affect the practicality of the control strategy for real-time implementation. Moreover, the parameters which are related to the less significant dynamics of the system may

converge slowly due to small signal levels. From this point of view, the simplifications of the NAWMV-PSS are also required for simplifying the practical implementation of the control algorithm.

In this chapter the simplifications of the NAWMV-PSS are carried out in two steps:

- firstly, *simplified* nonlinear adaptive control algorithms are developed from the control algorithm on which the NAWMV-PSS is based;
- secondly, a *new* bilinear adaptive control algorithm is developed for the design of the power system stabiliser for the SMIB power system modelled in Subsection 2.3.1.

Original work on the *analysis*, *design*, and *evaluation* of these modified nonlinear adaptive power system stabilisers will be conducted in the following sections of this chapter. The work involves the isolation of the less significant dynamics in the output of the system from an analysis of the prediction of the NNM, the discussion of the simplification of the nonlinear adaptive weighted minimum variance control law (5.29), the derivation of the bilinear optimal and adaptive control laws, the proposal for a bilinear adaptive power system stabiliser, and the assessment of the system damping performance with the latter stabiliser.

The organisation of this chapter is as follows. In Section 6.2 the decomposition of the system dynamic and steady-state responses is discussed, and the role of the output components in constructing the system responses is analysed. In Section 6.3 simplified versions of the NAWMV-PSS are derived and the simulation results are briefly presented. In Section 6.4 a bilinear nominal model of the SMIB power system is developed from a simplified form of the NNM, and optimal and adaptive control laws are derived for the bilinear nominal model. A bilinear adaptive power system stabiliser is then proposed. In Section 6.5 the performance of the proposed bilinear adaptive power system stabiliser is assessed through simulation studies, and is compared with that of the NAWMV-PSS and the LAWMV-PSS.

To the author's knowledge, the research reported in this chapter is **original**; the main contributions are:

1. The electrical torque (or power) output of the power system modelled by the NNM is decomposed into four output components. The contribution of each component to the overall system response is then analysed.

2. Two simplified versions of the NAWMV-PSS are developed and their performance is assessed.

3. A *new* discrete-time bilinear nominal model of the power system is derived from the simplification of the NNM. This model, which uses a minimum set of feedback signals, tracks and predicts the dynamics of the continuous-time nonlinear power system satisfactorily.

4. The optimal and adaptive control of the bilinear nominal model is discussed, and a bilinear adaptive weighted minimum variance control law is derived.

5. A *new* bilinear weighted minimum variance power system stabiliser, which takes the operational aspects of the system into account in the design, is proposed. The control structure of the SMIB power system equipped with the proposed bilinear adaptive power system stabiliser is illustrated.

6. Simulation studies on the evaluation of the bilinear adaptive power system stabiliser are conducted. A series of useful comparisons with the NAWMV-PSS and the LAWMV-PSS is given.

6.2 Analysis of Contributions of the Output Components of the Nonlinear Nominal Model to the System Dynamic and Steady-State Responses.

In this section:

- the optimal one-step-ahead prediction of the output of the NNM proposed in Subsection 4.2.3 is reformulated in terms of a combination of four output components;

- the contribution of each component to the system dynamic and steady-state responses is analysed;
- conclusions regarding the relative importance of the components of the output prediction of the NNM are drawn.

The NAWMV-PSS proposed in Chapter 5 is based on the *complete* NNM. Clearly, for the simplification of the NAWMV-PSS, *simplified* forms of the NNM are required. The simplified NNM should represent the main dynamic and steady-state behaviour of the original model, while eliminating the use of the additional feedback signals as much as possible. Therefore, for the derivation of such simplified forms of the NNM, it is necessary to *decompose* the output prediction of the NNM into components and to *analyse* the contribution of each component to the overall dynamic and steady-state responses of the output.

From (4.83)-(4.87), the *optimal one-step-ahead predictor* of the NNM (4.76)-(4.78) can be rewritten as

$$\begin{aligned} y^0(k \mid k-1) &= H_B(q^{-1})z_1(k) + H_C(q^{-1})z_2(k) \\ &\quad + H_D(q^{-1})z_3(k) + H_E(q^{-1})z_4(k)\,[d(k) - y_F(k) + u(k)] \end{aligned}$$

where [1]

$$\begin{aligned} z_1(k) &= \sin 2\delta(k), \\ z_2(k) &= \omega_s(k)E'_q(k)\cos\delta(k), \\ z_3(k) &= \omega_s(k)E_{FD}(k)\cos\delta(k), \\ z_4(k) &= \sin\delta(k), \end{aligned}$$

and

$$\begin{aligned} H_B(q^{-1}) &\triangleq \frac{b_1q^{-1} + b_2q^{-2}}{1 + a_1q^{-1} + a_2q^{-2}}, \\ H_C(q^{-1}) &\triangleq \frac{c_1q^{-1} + c_2q^{-2}}{1 + a_1q^{-1} + a_2q^{-2}}, \end{aligned}$$

[1] Note that, for the sake of simplicity, the errors between $z_i(k)$ and $\bar{z}_i(k)$ $(i = 1, 2, 3, 4)$ (introduced by Assumption 4.2.4) are ignored in the theoretical analysis of this chapter.

$$H_D(q^{-1}) \triangleq \frac{d_1 q^{-1}}{1 + a_1 q^{-1} + a_2 q^{-2}},$$
$$H_E(q^{-1}) \triangleq \frac{e_1 q^{-1}}{1 + a_1 q^{-1} + a_2 q^{-2}}.$$

The prediction, $y^0(k \mid k-1)$, of the output of the NNM is then described by

$$y^0(k \mid k-1) = y_B(k) + y_C(k) + y_D(k) + y_E(k) \tag{6.1}$$

where $y_B(k)$, $y_C(k)$, $y_D(k)$, and $y_E(k)$ are the *output components*, defined as

$$y_B(k) \triangleq H_B(q^{-1}) z_1(k), \tag{6.2}$$
$$y_C(k) \triangleq H_C(q^{-1}) z_2(k), \tag{6.3}$$
$$y_D(k) \triangleq H_D(q^{-1}) z_3(k), \tag{6.4}$$
$$y_E(k) \triangleq H_E(q^{-1}) z_4(k) \left[d(k) - y_F(k) + u(k) \right], \tag{6.5}$$

respectively. From (6.1), it can be seen that $y^0(k \mid k-1)$ is a *linear combination* of $y_B(k)$, $y_C(k)$, $y_D(k)$, and $y_E(k)$. Hence, the time response of the output prediction of the NNM can be constructed by superposition of the corresponding time responses of the four output components generated by (6.2)-(6.5). The significance of each component's contribution to the output prediction can thus be examined by isolating the proportion of each component in the dynamic and steady-state responses.

For this purpose, simulation studies are conducted for the CSM3 ($D = 4.0$ pu) with (6.1)-(6.5) as the output predictor. The control input $u(k)$ is set to be zero. At each sampling instant k, the four output components $y_B(k)$, $y_C(k)$, $y_D(k)$, and $y_E(k)$ are calculated according to their definitions in (6.2)-(6.5); the output prediction, $y^0(k \mid k-1)$, of the NNM is then formed by the sum of the four components. The configuration for this study is illustrated in Fig. 6.1.

Two simulation studies are selected as examples:

Case 1: The system is initially operating at $P_t = 0.6$ pu and $Q_t = 0.3$ pu. It is then subjected to a step change of 0.05 pu increase in reference power at time $t = 0.5$ second, and a step change of 0.1 pu decrease in reference power at time $t = 10.5$ second.

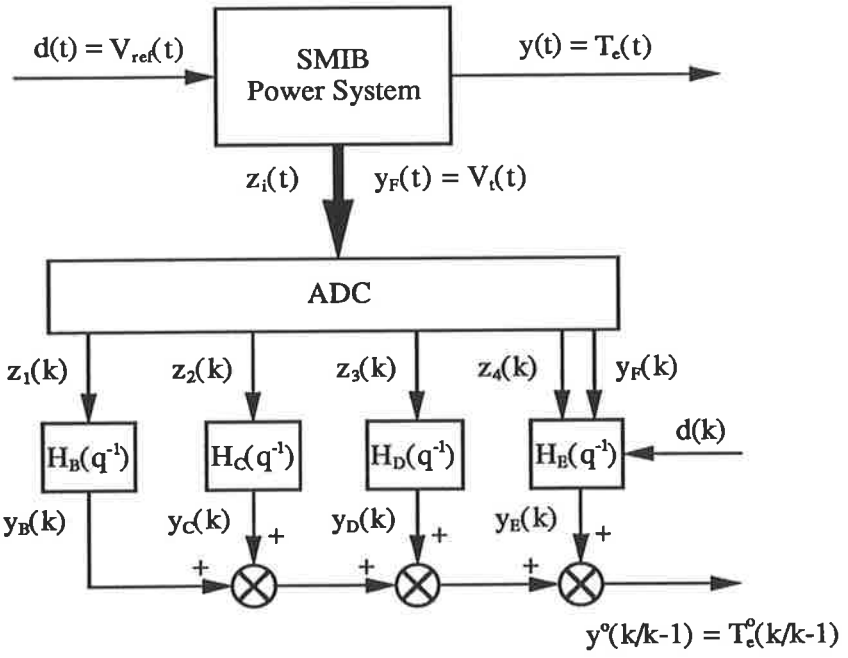

Figure 6.1: Decomposition of the output prediction of the NNM.

Case 2: The system is initially operating at $P_t = 0.6$ pu and $Q_t = -0.1$ pu. It is then subjected to a step change of 0.05 pu decrease in reference power at time $t = 0.5$ second, and a step change of 0.1 pu increase in reference power at time $t = 10.5$ second.

In each case, the time responses of the output prediction, $y^0(k \mid k-1)$, and its four components, $y_B(k)$, $y_C(k)$, $y_D(k)$, and $y_E(k)$, are obtained from the simulation and are plotted in the same graph for the evaluation of the contributions. The simulation results are given by Figs. 6.2-6.3.

From Figs. 6.2-6.3, it can be seen that

$y_B(k)$: contributes a negligible amount to the steady-state output, a very small proportion to the overall dynamic response at the lagging power factor (Fig. 6.2), and an increasing amount at the leading power factor (Fig. 6.3);

$y_C(k)$: has no contribution to the steady-state output, but contributes a relatively large proportion to the dynamic response at the lagging power factor, and a decreasing proportion at the leading power factor;

$y_D(k)$: does not contribute to the steady-state output, and contributes a negligible proportion to the dynamic response at both the lagging power factor and the leading power factor;

$y_E(k)$: provides the main contribution to the steady-state output and to the slow dynamics both at the lagging and the leading power factors.

Based on the above analysis, it is concluded that:

1. The elimination of the component $y_D(k)$ from the expression for $y^0(k \mid k-1)$ in (6.1) will not affect the system dynamic and steady-state performance.
2. The response $y_E(k)$ is the most significant component in the system dynamic and steady-state responses.
3. The response $y_C(k)$ is more significant than the response $y_B(k)$ in the dynamics, since it involves three state variables, $\omega_s(k)$, $E'_q(k)$, and $\delta(k)$, which may change significantly during large disturbances.

These conclusions provide a basis for the derivation of the simplified forms of the NNM as well as the resulting simplified versions of the NAWMV-PSS, to be discussed in Section 6.3.

6.3 Simplified Versions of the Nonlinear Adaptive Weighted Minimum Variance Power System Stabiliser.

In this section:

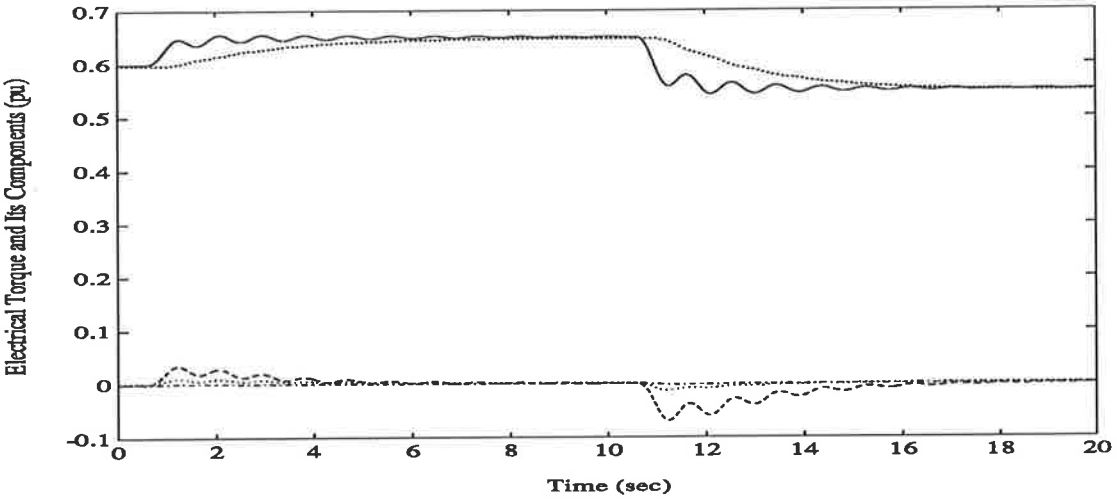

Figure 6.2: Electrical torque prediction and its components for Case 1 ($P_t = 0.6$ pu, $Q_t = 0.3$ pu; step changes in reference power). $y^0(k \mid k-1)$ - solid line, $y_B(k)$ - dotted line, $y_C(k)$ - dashed line, $y_D(k)$ - dot-dashed line, $y_E(k)$ - point line.

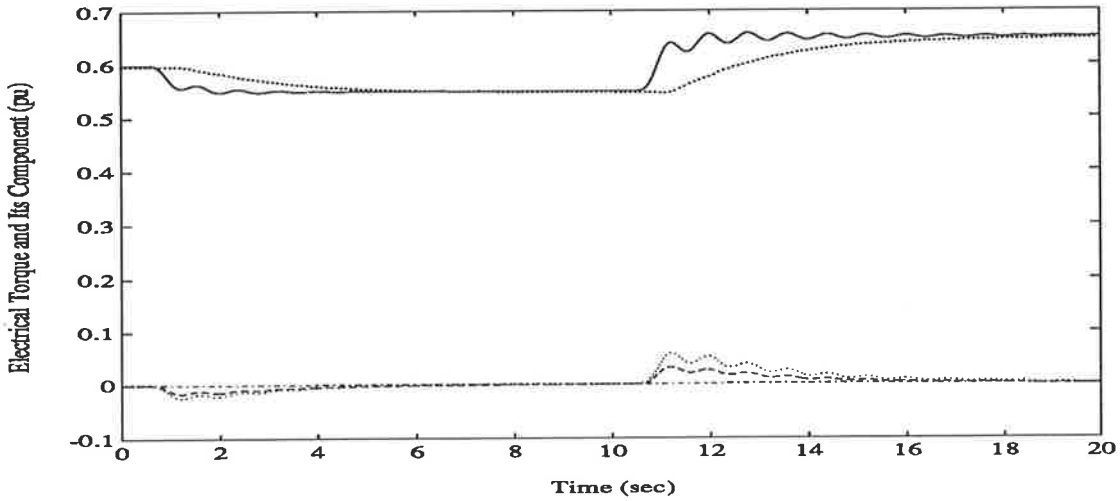

Figure 6.3: Electrical torque prediction and its components for Case 2 ($P_t = 0.6$ pu, $Q_t = -0.1$ pu; step changes in reference power). $y^0(k \mid k-1)$ - solid line, $y_B(k)$ - dotted line, $y_C(k)$ - dashed line, $y_D(k)$ - dot-dashed line, $y_E(k)$ - point line.

- two simplified versions of the NAWMV-PSS, derived from two versions of the simplified NNM, are proposed;
- examples of simulation studies are given to demonstrate the effects of the simplifications.

The contributions of the components (6.2)-(6.5) of the output prediction of the NNM to the overall system dynamic and steady-state responses have been analysed in Section 6.2. The conclusions drawn from the analysis are utilised in this section as a guide to the simplification of the NAWMV-PSS proposed in Chapter 5.

In the following, the derivations of the simplified NNM and the resulting simplified versions of the NAWMV-PSS are highlighted, in order of decreasing complexity:

Simplified Version I: Consider that the responses $y_D(k)$ and $y_B(k)$ are insignificant components in the system dynamic and steady-state responses. Eliminate $y_D(k)$ and $y_B(k)$ from the predictor (6.1). The *first* version of the simplified NNM is described by

$$\begin{aligned}\left(1+a_1q^{-1}+a_2q^{-2}\right)y(k) &= \left(c_1q^{-1}+c_2q^{-2}\right)z_2(k)+e_1q^{-1}z_4(k)\left[d(k)\right.\\ &\quad \left.-y_F(k)+u(k)\right]+w(k). \qquad (6.6)\end{aligned}$$

A simplified nonlinear adaptive weighted minimum variance control law is derived from the above model [2]

$$u^0(k)=\frac{\hat{\beta}_0(k)}{\hat{\beta}_0(k)^2+\lambda}\left[y^*(k+1)-\hat{G}(q^{-1})y(k)-\hat{g}_1(k)\right] \qquad (6.7)$$

where

$$\hat{g}_1(k)\triangleq\left[\hat{c}_1(k)+\hat{c}_2(k)q^{-1}\right]z_2(k)+\hat{e}_1(k)z_4(k)\left[d(k)-y_F(k)\right]; \qquad (6.8)$$

$\hat{\beta}_0(k)$ and $\hat{G}(q^{-1})$ are defined by (5.30) and (5.31), respectively. The combination of (6.7)-(6.8) and (5.34) forms the *Simplified Version I of the NAWMV-PSS* **(SVI-NAWMV-PSS)**.

[2] The symbol $u^0(k)$ is used to denote the unbounded control action in accordance with the notation in (5.33).

Simplified Version II: Consider that the time constant, τ'_{d0}, is long. From the machine differential equation (2.31) or (2.42), it may be assumed that for fast transients the state variable $E'_q(k)$ stays constant. Furthermore, $\cos\delta(k)$ is bounded in the region of $[-1, 1]$. Hence, these two variables in $z_2(k)$ can be incorporated into the parameters c_1 and c_2 of (6.6), so that the feedback signal $z_2(k)$ can be simplified as the speed deviation $\omega_s(k)$ only. The *second* version of the simplified NNM then takes the form

$$\begin{aligned}\left(1 + a_1 q^{-1} + a_2 q^{-2}\right) y(k) &= \left(\tilde{c}_1 q^{-1} + \tilde{c}_2 q^{-2}\right) \omega_s(k) + e_1 q^{-1} z_4(k) \left[d(k)\right. \\ &\quad \left. - y_F(k) + u(k)\right] + w(k), \end{aligned} \tag{6.9}$$

where

$$\tilde{c}_1 \triangleq c_1 E'_q(k-1) \cos\delta(k-1), \tag{6.10}$$

$$\tilde{c}_2 \triangleq c_2 E'_q(k-2) \cos\delta(k-2). \tag{6.11}$$

The resulting *Simplified Version II of the NAWMV-PSS* **(SVII-NAWMV-PSS)** has the same expression as (6.7)-(6.8) and (5.34), except that in (6.8) the parameters $\hat{c}_1(k)$ and $\hat{c}_2(k)$ are changed into $\hat{\tilde{c}}_1(k)$ and $\hat{\tilde{c}}_2(k)$ (which are defined as the estimated parameters $\hat{c}_1(k)$ and $\hat{c}_2(k)$) and the additional feedback signal $z_2(k)$ is simplified as $\omega_s(k)$.

Remark 6.3.1 *From the above derivation, it can be seen that the SVII-NAWMV-PSS is the simplest version of the NAWMV-PSS in this section. Although the two output components $y_B(k)$ and $y_D(k)$ have been eliminated from the complete NNM, and the additional feedback signal $z_2(k)$ has been simplified to $\omega_s(k)$, the main nonlinearities associated with the electrical torque (or power) output of the system are still retained in the SVII-NAWMV-PSS by the trigonometric term $z_4(k)$ and the product terms such as $z_4(k)\,[d(k) - y_F(k)]$.*

In order to investigate the performance of the above two simplified versions of the NAWMV-PSS, the *evaluation studies* (Studies 1-11) described in Subsection 3.6.2 are conducted for each of the simplified versions with the NAWMV-PSS as a reference.

In each simulation study, the output responses of the CSM3 equipped with the SVI-NAWMV-PSS and the SVII-NAWMV-PSS, respectively, are plotted in the same graph, along with the results for the NAWMV-PSS. The performance of the CSM3 equipped with the NAWMV-PSS is provided by the simulation results in Subsection 5.4.2. Examples of the dynamic performance and the transient performance of each simplified stabiliser are given by the results of Studies 1 and 5, shown in Figs. 6.4 and 6.5, respectively.

The simulation results demonstrate that:

- For dynamic operating conditions, the performance of the simplified versions of the NAWMV-PSS is almost *identical* to that of the NAWMV-PSS.
- In the event of a severe fault, the simplified versions of the NAWMV-PSS can provide damping effects to the system oscillations comparable to those provided by the NAWMV-PSS.

The above facts reveal that:

1. The analysis of the contributions of the components $y_B(k)$, $y_C(k)$, $y_D(k)$, and $y_E(k)$ in the dynamic performance of the system, given in Section 6.2, is valid.
2. The effect of the omission of the two components $y_B(k)$ and $y_D(k)$, as well as the change of $z_2(k)$ into $\omega_s(k)$, can be compensated for by the rest of the time-varying model parameters through the adaptive control scheme.
3. Though the SVII-NAWMV-PSS has been significantly simplified from the NAWMV-PSS, its performance is comparable with that of the NAWMV-PSS. This is because the SVII-NAWMV-PSS retains the inherent nonlinearities in the model of the SMIB power system.

Based on these conclusions, the simplification of the NAWMV-PSS will be continued in Section 6.4, where the SVII-NAWMV-PSS will be further developed into a bilinear adaptive power system stabiliser.

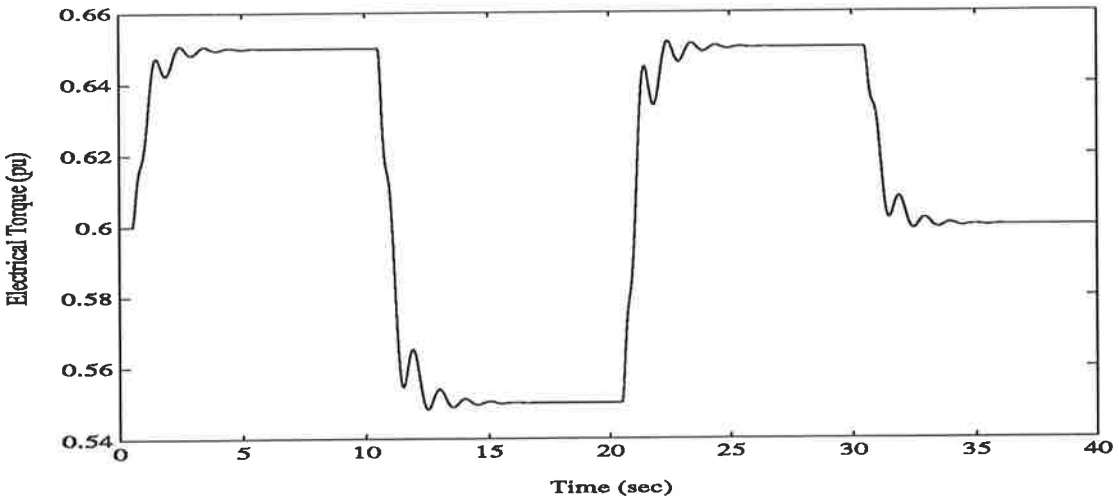

Figure 6.4: Electrical torque response for Study 1 ($P_t = 0.6$ pu, $Q_t = 0.3$ pu; periodic variations in reference power). CSM3 with NAWMV-PSS - solid line, CSM3 with SVI-NAWMV-PSS - dashed line, CSM3 with SVII-NAWMV-PSS - dotted line.

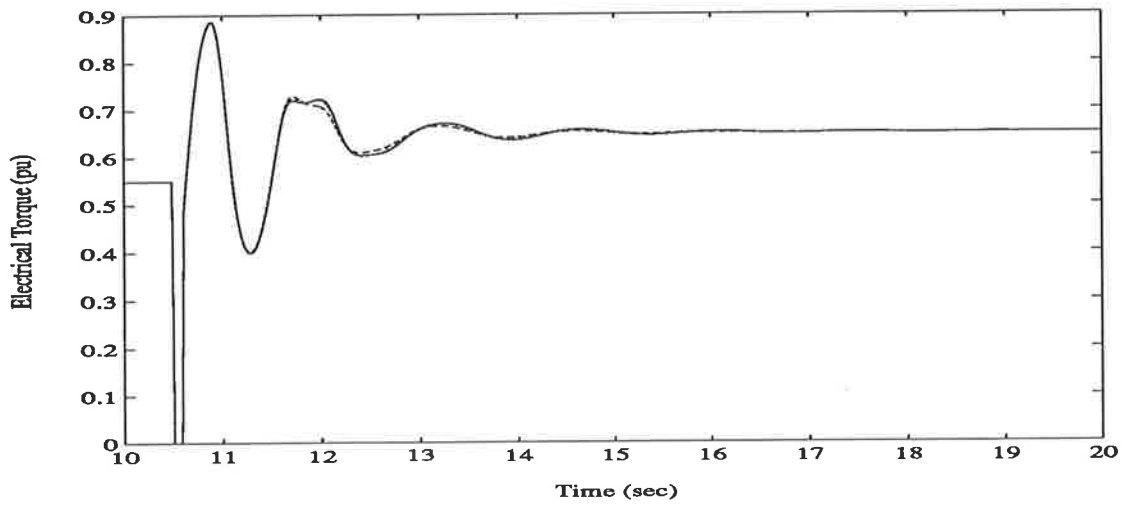

Figure 6.5: Electrical torque response for Study 5 ($P_t = 0.55$ pu, $Q_t = -0.1$ pu; 100 ms short-circuit at the machine terminal). CSM3 with NAWMV-PSS - solid line, CSM3 with SVI-NAWMV-PSS - dashed line, CSM3 with SVII-NAWMV-PSS - dotted line.

6.4 SISO Bilinear Optimal and Adaptive Power System Stabilisers.

In this section:

- a *new bilinear* **nominal model** [3] of the power system is derived from the second version of the simplified NNM, given by (6.9)-(6.11);
- the nonlinear stochastic generalised minimum variance control of the bilinear nominal model is discussed, and a bilinear optimal power system stabiliser is presented;
- a nonlinear adaptive weighted minimum variance control algorithm is developed for the bilinear nominal model;
- a bilinear adaptive weighted minimum variance power system stabiliser which takes the operational aspects of the power system into account is proposed;
- the control structure of the SMIB power system equipped with the proposed bilinear adaptive power system stabiliser is illustrated.

The performance of the SVII-NAWMV-PSS has been verified to be comparable with that of the NAWMV-PSS through the evaluation studies in Section 6.3. As indicated in Remark 6.3.1, the main feature of this simplest version of the NAWMV-PSS is that it contains the trigonometric and product nonlinearities associated with the electrical torque (or power) output of the power system by retaining the additional feedback signal $z_4(k)$ in its control law. However, since the rotor angle $\delta(k)$ is still used for calculating $z_4(k)$ and forming the control action of the SVII-NAWMV-PSS, a modification which replaces this state variable by a measurable output variable is required. This requirement results in the development of *bilinear* control schemes in the design of the power system stabiliser, to be undertaken in this section.

[3] See Section 3.2 for the definition of a "nominal model" used in this thesis.

The layout of this section is as follows. In Subsection 6.4.1 a bilinear nominal model is derived from the model (6.9)-(6.11) associated with the SVII-NAWMV-PSS. The nonlinear stochastic generalised minimum variance control of the bilinear nominal model is discussed and a bilinear optimal power system stabiliser is presented in Subsection 6.4.2. In Subsection 6.4.3 a nonlinear adaptive weighted minimum variance control algorithm is developed from the bilinear optimal control law, and a bilinear adaptive weighted minimum variance power system stabiliser with its control structure is proposed.

6.4.1 Bilinear Nominal Model of the Power System.

The aim of the development of a bilinear nominal model for the design of the power system stabiliser is to replace the additional feedback signal $z_4(k)$ (which involves the rotor angle $\delta(k)$) in (6.9) by the measurable output variable $y(k)$ (i.e., $T_e(k)$ or $P_e(k)$). For this purpose, the NAM given in Subsection 2.4.1 is reviewed. From (2.97), it readily follows that

$$T_e(t) = \frac{V_\infty}{X_e + X_q} \left[E(t) + (X_d - X_q)\, I_d(t)\right] \sin\delta(t) \tag{6.12}$$

where [4]

$$I_d(t) = \frac{V_\infty \cos\delta(t) - E'_q(t)}{X_e + X'_d},$$

$$E(t) \triangleq E'_q(t) - \left(X_d - X'_d\right) I_d(t).$$

It is assumed that

Assumption 6.4.1 [5] *In the equations of the synchronous generator,*

$$X_d \approx X_q.$$

Subject to Assumption 6.4.1, equation (6.12) becomes

$$T_e(t) = \frac{V_\infty E(t)}{X_e + X_q} \sin\delta(t). \tag{6.13}$$

[4] See, e.g., [3] p.99 for the definition of the variable $E(t)$.

[5] For round-rotor synchronous generators, the relationship $X_d = X_q$ is true.

The relationship between $z_4(k)$ and $y(k)$ in (6.9) can then be written as

$$z_4(k) = \tilde{K}(k)y(k) \tag{6.14}$$

where

$$\tilde{K}(k) \triangleq \frac{X_e + X_q}{V_\infty E(k)}. \tag{6.15}$$

Clearly, $\tilde{K}(k)$ contains the variable $E(k)$ and the time-varying quantity V_∞ (the value of which depends on the system operating condition), and can be treated as a time-varying parameter. The substitution of (6.14) and (6.15) into (6.9) results in the following expression

$$\begin{aligned}\left(1 + a_1 q^{-1} + a_2 q^{-2}\right) y(k) &= \left(\tilde{c}_1 q^{-1} + \tilde{c}_2 q^{-2}\right) \omega_s(k) \\ &\quad + e_{\tilde{K}} q^{-1} y(k) \left[d(k) - y_F(k) + u(k)\right] + w(k)\end{aligned} \tag{6.16}$$

where

$$e_{\tilde{K}} \triangleq e_1 \frac{X_e + X_q}{V_\infty E(k-1)}. \tag{6.17}$$

Equations (6.16)-(6.17) with (6.10)-(6.11) form a model which is called the *Bilinear Nominal Model* **(BNM)** of the power system (CSM3). It contains five parameters, of which $\tilde{c}_1$, $\tilde{c}_2$, and $e_{\tilde{K}}$ are time-varying and, perhaps, unknown. The BNM will be used to develop the bilinear control laws in the following subsections.

Remark 6.4.1 *It should be pointed out that the BNM retains the inherent nonlinearities of the output of the power system by the product term on the right-hand side of (6.16). The trigonometric nonlinearity of the output is taken into account in the relationship between $z_4(k)$ and $y(k)$ in (6.14).*

6.4.2 Bilinear Stochastic Generalised Minimum Variance Control.

In this subsection, the derivation of the stochastic generalised minimum variance control law for the BNM (6.16)-(6.17) (with (6.10)-(6.11)) makes use of the theories established in Section 4.3. For conciseness, the main results are highlighted as follows.

Assume that the noise sequence $\{w(k)\}$ in the BNM is white, satisfying Assumption 4.3.1. The optimal one-step-ahead prediction, $y^0(k+1 \mid k)$, of $y(k+1)$ of the BNM is then given by

$$\begin{aligned} y^0(k+1 \mid k) &\triangleq y(k+1) - w(k+1) \\ &= G(q^{-1})y(k) + \left(\tilde{c}_1 + \tilde{c}_2 q^{-1}\right)\omega_s(k) \\ &\quad + e_{\tilde{K}} y(k)\left[d(k) - y_F(k) + u(k)\right] \end{aligned}$$

where $G(q^{-1})$ is defined by (4.87). Hence, for the BNM, the generalised minimum variance control $u^*(k)$ which minimises the cost function (4.88)-(4.91) is derived as

$$\begin{aligned} &\left[e_{\tilde{K}}^2 y(k)^2 W_y(q^{-1}) + w_{u0} W_u(q^{-1})\right] u^*(k) \\ = \; & e_{\tilde{K}} y(k)\left\{W_r(q^{-1})y^*(k+1) - W_y(q^{-1})G(q^{-1})y(k)\right. \\ & \left. - W_y(q^{-1})\left(\tilde{c}_1 + \tilde{c}_2 q^{-1}\right)\omega_s(k) - W_y(q^{-1}) e_{\tilde{K}} y(k)\left[d(k) - y_F(k)\right]\right\} \end{aligned} \tag{6.18}$$

in which equations (4.97), (4.107), (4.115)-(4.117) are used, noting that $\dfrac{dy(k)}{du(k)} = 0$.

Clearly, with different selections of the polynomials $W_y(q^{-1})$, $W_r(q^{-1})$, and $W_u(q^{-1})$, different forms of the bilinear optimal control law will be obtained from (6.18). To be consistent with the linear and nonlinear optimal/adaptive power system stabilisers discussed in Chapters 3 to 5, the weighted minimum variance control scheme is considered for the design of the bilinear optimal power system stabiliser in this subsection. This control scheme is realised by selecting $W_y(q^{-1}) = W_r(q^{-1}) = 1$ and $W_u(q^{-1}) = \lambda^{\frac{1}{2}}$ with $\lambda > 0$ in (6.18). The resulting bilinear *optimal* weighted minimum variance control law is then described by

$$\begin{aligned} \left[e_{\tilde{K}}^2 y(k)^2 + \lambda\right] u^*(k) &= e_{\tilde{K}} y(k)\left\{y^*(k+1) - G(q^{-1})y(k)\right. \\ &\quad \left. - \left(\tilde{c}_1 + \tilde{c}_2 q^{-1}\right)\omega_s(k) - e_{\tilde{K}} y(k)\left[d(k) - y_F(k)\right]\right\}. \end{aligned} \tag{6.19}$$

This control law can be used as a bilinear optimal power system stabiliser. The derivation of this control law is for the further development of a bilinear adaptive power system stabiliser to be discussed in Subsection 6.4.3.

6.4.3 A Bilinear Adaptive Weighted Minimum Variance Power System Stabiliser.

The implementation of the bilinear optimal weighted minimum variance control law (6.19) requires the values of the parameters $\tilde{c}_1$, $\tilde{c}_2$, and $e_{\tilde{K}}$ to be known at each sampling instant. According to (6.10)-(6.11) and (6.17), the parameters $\tilde{c}_1$, $\tilde{c}_2$, and $e_{\tilde{K}}$ are generally time-varying and unknown. This feature of the control law (6.19) suggests the utilisation of an adaptive control method in which the estimated values of the unknown time-varying parameters are provided by the implementation of an on-line parameter estimation routine.

In this subsection, the development of a bilinear *adaptive* weighted minimum variance control algorithm for the BNM (6.16)-(6.17) (with (6.10)-(6.11)) utilises the theories established in Sections 5.2 and 5.3. Algorithm 5.1(A) which has been developed for the parameter estimation of the NNM in Section 5.2 can be used *directly* for the parameter estimation of the BNM, except that the vectors $\hat{\Theta}(k)$ and $\phi(k)$ are re-defined as

$$\hat{\Theta}(k)^T \triangleq \left[\begin{array}{ccccc} \hat{a}_1(k) & \hat{a}_2(k) & \hat{\tilde{c}}_1(k) & \hat{\tilde{c}}_2(k) & \hat{e}_{\tilde{K}}(k) \end{array} \right] \tag{6.20}$$

and

$$\phi(k)^T \triangleq \left[\begin{array}{cccccc} -y(k) & -y(k-1) & \omega_s(k) & \omega_s(k-1) & y(k)\left(d(k) - y_F(k) + u(k)\right) \end{array} \right]. \tag{6.21}$$

The parameter estimate $\hat{\Theta}(k)$ from Algorithm 5.1(A) can then be used to calculate the bilinear adaptive weighted minimum variance control law which, according to (6.19), is given by

$$\begin{aligned} \left[\hat{\theta}_5(k)^2 y(k)^2 + \lambda\right] u(k) \;=\; & \hat{\theta}_5(k)y(k)\left\{y^*(k+1) + \hat{\theta}_1(k)y(k) + \hat{\theta}_2(k)y(k-1)\right. \\ & -\hat{\theta}_3(k)\omega_s(k) - \hat{\theta}_4(k)\omega_s(k-1) \\ & \left. -\hat{\theta}_5(k)y(k)\left[d(k) - y_F(k)\right]\right\}. \end{aligned} \tag{6.22}$$

To design a bilinear adaptive power system stabiliser by the use of the above control law, special attention has to be given to

- the unmodelled nonlinearities of the system (caused by, e.g., three-phase faults) and
- the sudden losses of transmission lines (caused by, e.g., one transmission line switching-out).

This is because in both circumstances, the electrical torque (or power) output of the generator will suddenly become small or zero, resulting in an ineffective control input $u(k)$ or zero control action according to the control law (6.22) (note that in general $\hat{\theta}_5(k)^2 y(k)^2 \ll \lambda$). The consequence of the above phenomenon is poor damping performance or even instability of the system (see Remark 6.5.3). In order to avoid this, a function, $f_y(k)$, is introduced into the control law (6.22). $f_y(k)$ is defined by two piecewise functions: the first one uses a boundary $y_o > 0$ to prevent the value of the output $y(k)$ from being too small or zero; the second one uses a limit $C_y > 0$ to prevent the rate of decrease of the output $(y(k-1)-y(k))$ from being too large. $f_y(k)$ is described as

$$\bar{f}_y(k) = \begin{cases} y(k) & \text{if } y(k) > y_o \\ 1 & \text{otherwise} \end{cases},$$

$$f_y(k) = \begin{cases} \bar{f}_y(k) & \text{if } y(k-1) - y(k) < C_y \\ 1 & \text{otherwise} \end{cases},$$

where the boundary y_o can be determined by the value of the output $T_e(k)$ (or $P_e(k)$) during the occurrence of a fault, and the limit C_y can be determined based on the maximum rate of decrease of the output when one transmission line is suddenly switched out. The resulting bounded bilinear adaptive weighted minimum variance control algorithm is then given by

Algorithm 6.1 [bounded bilinear adaptive weighted minimum variance control algorithm for the BNM.]

$$\begin{aligned} u^0(k) \;=\; & \frac{\hat{\theta}_5(k) f_y(k)}{\hat{\theta}_5(k)^2 f_y(k)^2 + \lambda} \Big\{ y^*(k+1) + \hat{\theta}_1(k) y(k) + \hat{\theta}_2(k) y(k-1) \\ & - \hat{\theta}_3(k) \omega_s(k) - \hat{\theta}_4(k) \omega_s(k-1) - \hat{\theta}_5(k) y(k) \left[d(k) - y_F(k) \right] \Big\}, \end{aligned} \tag{6.23}$$

$$u(k) = \begin{cases} u_{max} & \text{if } u^0(k) \geq u_{max} \\ u^0(k) & \text{if } u_{min} < u^0(k) < u_{max} \\ u_{min} & \text{if } u^0(k) \leq u_{min} \end{cases} ; \tag{6.24}$$

where

$$\bar{f}_y(k) = \begin{cases} y(k) & \text{if } y(k) > y_o \\ 1 & \text{otherwise} \end{cases} , \tag{6.25}$$

$$f_y(k) = \begin{cases} \bar{f}_y(k) & \text{if } y(k-1) - y(k) < C_y \\ 1 & \text{otherwise} \end{cases} , \tag{6.26}$$

$y_o > 0$ and $C_y > 0$ are preselected constants; λ is the weighting coefficient; u_{max} and u_{min} are known constants; the estimated parameters are obtained from Algorithm 5.1(A), with $\hat{\Theta}(k)$ and $\phi(k)$ defined by (6.20) and (6.21) respectively.

$\nabla \nabla \nabla$

Remark 6.4.2 *In the design of the function $f_y(k)$,*

(i) the sudden increase in the electrical torque (or power) output due to the switching-in of transmission lines is not considered; this is because such a event will, in fact, reinforce the control action according to (6.22);

(ii) the value of 1 pu torque (or power) is used to replace $y(k)$ in the control law, when either $y(k) < y_o$ or $(y(k-1) - y(k)) > C_y$. This value has been found suitable since it will reinforce the control effort when it is most needed.

The combination of Algorithm 5.1(A) with Algorithm 6.1 results in the desired *Bilinear Adaptive Weighted Minimum Variance Power System Stabiliser* **(BAWMV-PSS)** for the SMIB power system modelled in Subsection 2.3.1. Since the control algorithm is designed in an *indirect* form, the calculation of the control action from the BAWMV-PSS is a two-step procedure:

- the recursive least squares algorithm with the time-varying forgetting factor and dead zone (Algorithm 5.1(A)) provides the estimated parameters of the BNM;

- the control law (6.23)-(6.26) (Algorithm 6.1) generates the control signal $u(k)$ by the use of the estimates of the BNM.

The BAWMV-PSS is the simplest nonlinear adaptive power system stabiliser proposed in this thesis. It contains five parameters and a minimum set of the additional feedback signals, all of which are measurable. The control structure of the SMIB power system equipped with the BAWMV-PSS is illustrated in Fig. 6.6, in which the desired output trajectory $y^*(k)$ is set to be the reference power $P_{ref}(k)$ (see Remarks 4.4.5 and 3.5.2). The stabilising signal $y(k)$ is the machine electrical power, $P_e(k)$ (or torque, $T_e(k)$). The performance of the BAWMV-PSS will be evaluated in Section 6.5.

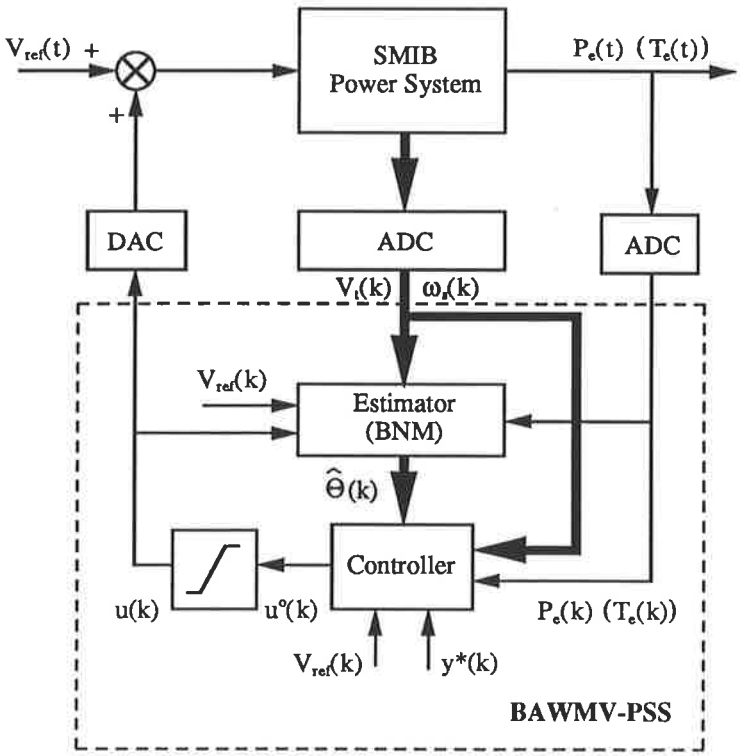

Figure 6.6: Control structure of the SMIB power system with the BAWMV-PSS.

6.5 Evaluation of the Performance of the Bilinear Adaptive Weighted Minimum Variance Power System Stabiliser.

In this section:

- the dynamic behaviour of the *estimated* BNM in tracking and predicting the dynamics of the nonlinear power system (CSM3) is examined through simulation studies;
- the performance of the BAWMV-PSS proposed in Subsection 6.4.3 is investigated through the *evaluation studies* (Studies 1-11);
- the robustness of the BAWMV-PSS is tested with unmodelled dynamics and modelling errors (Studies 12-15).

As the simplest nonlinear adaptive power system stabiliser discussed in this thesis, the BAWMV-PSS proposed in Subsection 6.4.3 is tested in this section with the NAWMV-PSS and the LAWMV-PSS as references. The differences between these three control strategies will be demonstrated through simulation studies. The results shown in this section provide a basis for the future practical implementation of the BAWMV-PSS.

For a systematic comparison, the simulation studies of this section will follow the same *procedure* arranged for the evaluations of the LAWMV-PSS, the NOWMV-PSS, and the NAWMV-PSS, conducted in Sections 3.6, 4.5, and 5.4, respectively. Three **Stages** will be conducted in this section:

Stage 1: Verification and identification of the BNM — to examine the behaviour of the estimated BNM in tracking and predicting the dynamics of the nonlinear power system (CSM3).

Stage 2: Evaluation of the performance of the BAWMV-PSS — to compare the dynamic and transient behaviour of the BAWMV-PSS with that of the NAWMV-PSS and the LAWMV-PSS through Studies 1-11.

Stage 3: Studies on the robustness of the BAWMV-PSS — to test the performance of the BAWMV-PSS when the CSM3 is replaced by the CSM1 through Studies 12-15.

The implementation of the above three **Stages** will be discussed in Subsections 6.5.1, 6.5.2, and 6.5.3, which follow. The parameters and limits associated with the SMIB power system and the BAWMV-PSS are listed in Appendix C. The sampling period h is 20 ms.

6.5.1 Verification and Identification of the Bilinear Nominal Model of the Power System.

In this subsection the validity of the *estimated* BNM in tracking and predicting the dynamics of the nonlinear power system (CSM3 with $D = 4.0$ pu) at different operating conditions is examined through simulation studies. The output signal is the machine electrical torque, $T_e(k)$. This subsection is the implementation of **Stage 1**.

Aims and structure of the simulation studies.

Let the PRBS signal described in Subsection 3.6.1 be an external control input $u(k)$ that is injected into the summing junction of the input of the AVR and the estimator, simultaneously. The model of the estimator is the BNM. At each sampling instant, the estimated parameters ,$\hat{\Theta}(k)$, and the predicted electrical torque output, $\hat{T}_e(k)$, of the BNM are generated by the implementation of Algorithm 5.1(A) in which the definitions of $\hat{\Theta}(k)$ and $\phi(k)$ are given by (6.20) and (6.21), respectively. The error, $e(k)$, between the predicted output, $\hat{T}_e(k)$, of the estimated BNM and the actual output, $T_e(k)$, of the CSM3 is updated. The configuration for this study is illustrated in Fig. 6.7. The aims of this study are

- to confirm the output tracking ability of the estimated BNM;
- to examine the convergence of the estimated parameters of the BNM;
- to demonstrate the differences between the estimated BNM, the estimated NNM, and the estimated LNM in representing the CSM3 at different operating points.

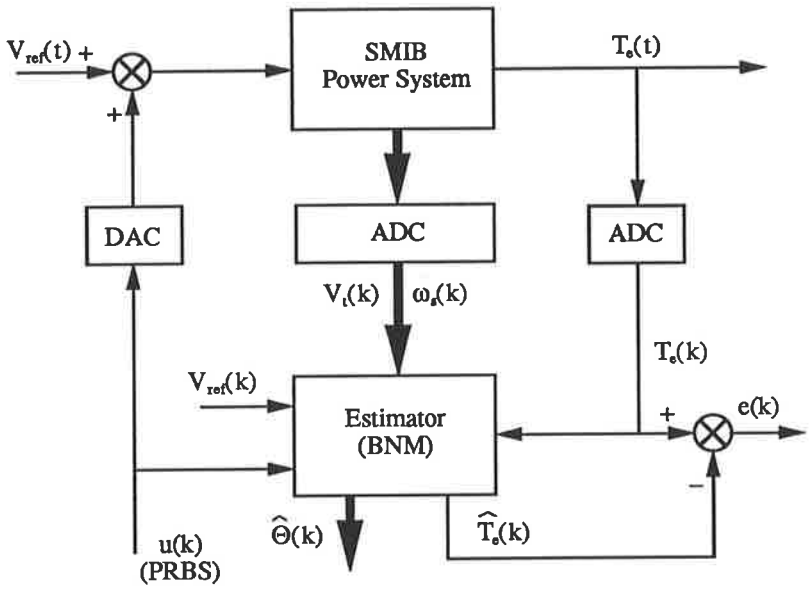

Figure 6.7: Structure of the verification and identification of the BNM.

For the above purposes, two cases of simulation studies are chosen as examples:

Case 1: The system is operating at $P_t = 0.6$ pu and $Q_t = 0.3$ pu, and is subjected to a step change of 0.05 pu increase in reference power at time $t = 20$ second. This case is the same as Case 1 given in Subsections 4.5.1 and 5.4.1.

Case 2: The system is operating at $P_t = 0.6$ pu and $Q_t = -0.1$ pu, and is subjected to a step change of 0.05 pu decrease in reference power at time $t = 20$ second.

The simulation results are shown in Figs. 6.8-6.10 and Table 6.1. The estimator parameters are: $K_0 = 10^2$, $C = 10^3$, $\mu_{min} = 0.2$, and $\Sigma = 0.8$. The initial value of the estimate, $\hat{\Theta}(0)$, is pre-calculated according to (6.20). For comparisons, the estimated

NNM and the estimated LNM, studied in Subsections 5.4.1 and 3.6.1 respectively, are incorporated into the analysis of the simulation results given below.

Analysis of the simulation studies.

Case 1: Subject to the PRBS input signal and the step change in reference power, the dynamic responses of the predicted output, $\hat{T}_e(k)$, of the *estimated* BNM and the actual output, $T_e(k)$, of the CSM3 in Case 1 are superimposed in Fig. 6.8. The error, $e(k)$, between $T_e(k)$ and $\hat{T}_e(k)$ is plotted in Fig. 6.9 by the dotted line. For a comparison, the error between the predicted output of the *estimated* NNM and the actual output of the CSM3 in the same case (as shown in Fig. 5.4) is re-plotted in Fig. 6.9 by the solid line. The estimated parameters of the BNM are shown in Fig. 6.10 in which the initial value of the estimate, $\hat{\Theta}(0)$, is set to be

$$\hat{\Theta}(0)^T = \begin{bmatrix} -1.7863 & 0.7886 & 6.0485 & -5.0404 & 0.1166 \end{bmatrix}.$$

It is seen from Fig. 6.8 that the estimated BNM tracks the dynamics of the CSM3 at the different operating points satisfactorily. The errors shown in Fig. 6.9 indicate that the accuracy of the estimated BNM in tracking the dynamics of the CSM3 is slightly lower than that of the estimated NNM. This is due to the simplifications involved in the modelling of the BNM. However, the estimated BNM still possesses the inherent output tracking ability, since its tracking error does not increase significantly following the step change in the system operating point at time $t = 20$ second. Further evidence of the inherent output tracking ability of the estimated BNM is shown in Fig. 6.10, in which the estimated parameters of the BNM do not appreciably change even after $t = 20$ second. Table 6.1 gives the converged values of the estimates of the BNM at each operating point and the variation of the estimates between the two operating points. With reference to the data shown in Tables 5.1-5.2, it is seen that although the difference $\left|\hat{\theta}_i(2000) - \hat{\theta}_i(1000)\right|$ of the estimates of the BNM is slightly larger than that of the NNM (shown in Table 5.2), it is still smaller than that of the LNM (shown in Table 5.1) for the same case. The estimated BNM is therefore better in tracking and predicting the nonlinear power system than the estimated LNM.

Case 2: The similar behaviour of the output prediction and the estimates of the BNM is observed from the study of Case 2. For the sake of brevity, these simulation results are omitted.

Conclusions.

Based on the above analysis, it is concluded that:

1. The BNM, with only five estimated parameters, can model the nonlinear power system (CSM3) satisfactorily at different operating points.
2. The estimated BNM retains the inherent output tracking ability as the estimated NNM.
3. The tracking accuracy of the estimated BNM is higher than that of the estimated LNM.

Remark 6.5.1 *In view of the above conclusions and those drawn in Subsections 4.5.1 and 5.4.1, it is evident that a nonlinear model (either the fixed-parameter NNM, or the estimated NNM, or the estimated BNM) more closely represents the nonlinear power system than a linearised model (e.g., the estimated LNM). This is because the nonlinear models retain the inherent nonlinearities of the system.*

6.5.2 Evaluation of the Performance of the BAWMV-PSS for the CSM3.

In this subsection the performance of the BAWMV-PSS is evaluated for the CSM3 ($D = 4.0$ pu) through the series of *evaluation studies* (Studies 1-11) defined in Subsection 3.6.2. This subsection is the implementation of **Stage 2**.

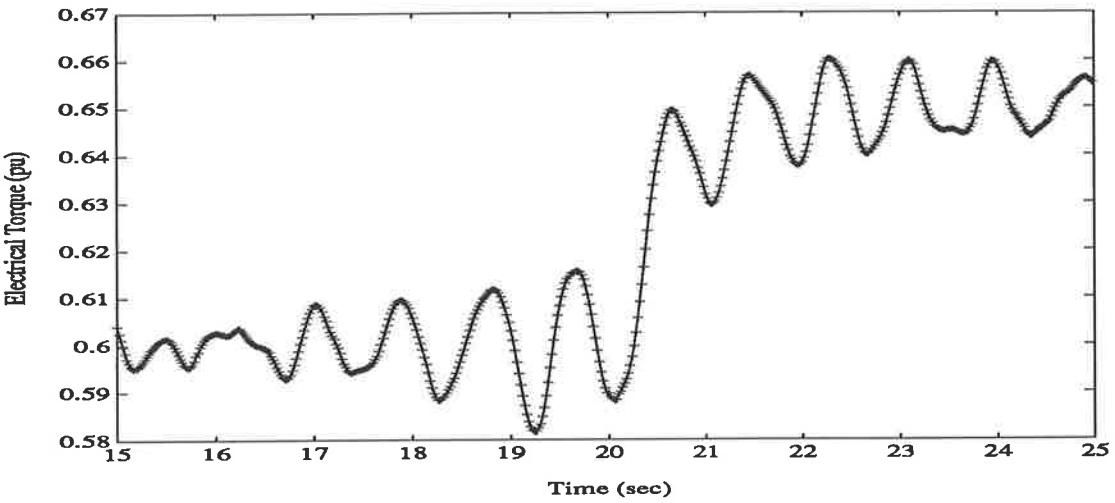

Figure 6.8: Electrical torque response for Case 1 ($P_t = 0.6$ pu, $Q_t = 0.3$ pu; 0.05 pu increase in reference power). CSM3 - solid line, estimated BNM - line marked by '+'.

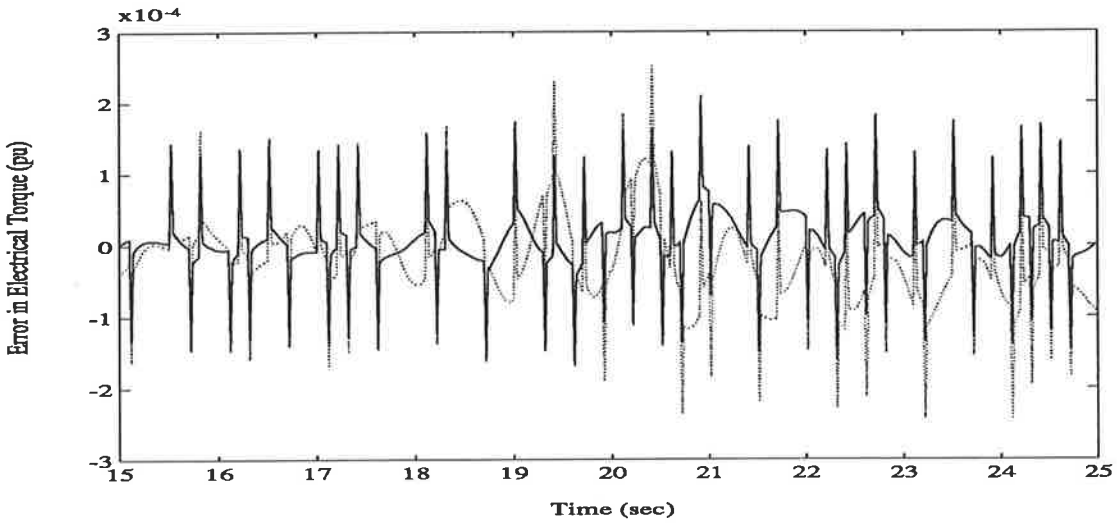

Figure 6.9: Error in electrical torque for Case 1 ($P_t = 0.6$ pu, $Q_t = 0.3$ pu; 0.05 pu increase in reference power). estimated NNM - solid line, estimated BNM - dotted line.

Estimates	True Values	$\hat{\theta}_i(1000)$	$\hat{\theta}_i(2000)$	$\lvert\hat{\theta}_i(2000) - \hat{\theta}_i(1000)\rvert$
$\hat{\theta}_1 = \hat{a}_1$	*	-1.7877	-1.7898	2.10×10^{-3}
$\hat{\theta}_2 = \hat{a}_2$	*	0.7900	0.7919	1.98×10^{-3}
$\hat{\theta}_3 = \hat{\tilde{c}}_1$	*	6.0489	6.0495	6.00×10^{-4}
$\hat{\theta}_4 = \hat{\tilde{c}}_2$	*	-5.0400	-5.0395	5.00×10^{-4}
$\hat{\theta}_5 = \hat{e}_{\bar{K}}$	*	0.1140	0.1103	3.74×10^{-3}

Table 6.1: Estimated parameters of the BNM for Case 1.

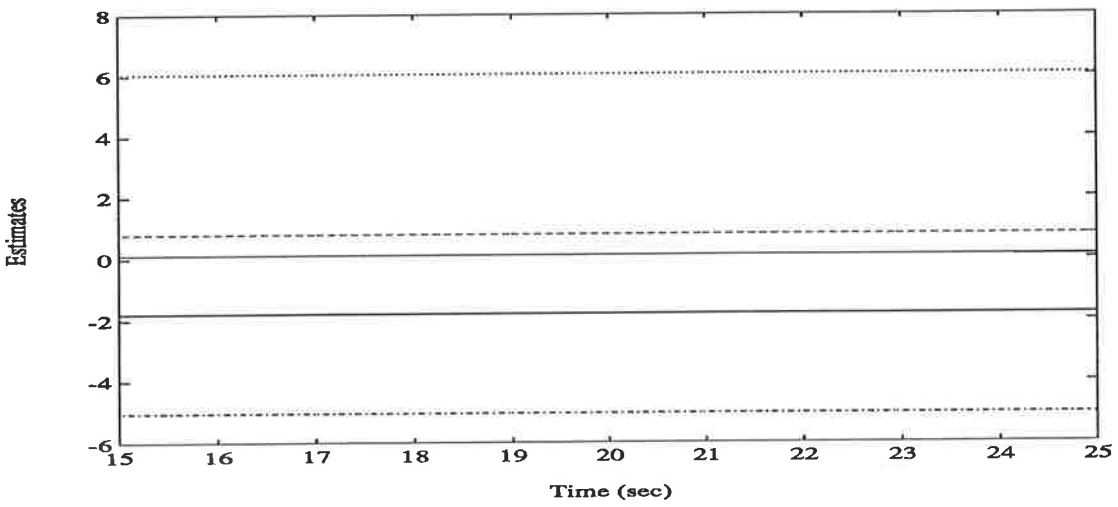

Figure 6.10: Estimated parameters of the BNM for Case 1 ($P_t = 0.6$ pu, $Q_t = 0.3$ pu; 0.05 pu increase in reference power).

Aims and structure of the simulation studies.

The control structure of the CSM3 equipped with the BAWMV-PSS is illustrated in Fig. 6.6. The machine electrical torque is used as the stabilising signal. For each simulation study, the performance of the CSM3 equipped with the BAWMV-PSS is compared with that of the CSM3 equipped with the NAWMV-PSS and the LAWMV-PSS proposed in Chapters 5 and 3, respectively. The aims of this study are

- to confirm that, with the significant simplifications in the control law, the BAWMV-PSS can provide comparable damping performance to the NAWMV-PSS for different operating conditions;
- to examine the effect of omitting the output components $y_B(k)$ and $y_D(k)$ in the design of the BAWMV-PSS on the system damping performance;
- to verify that even as the simplest nonlinear adaptive power system stabiliser proposed in this thesis, the BAWMV-PSS still provides better damping than the LAWMV-PSS in the simulation studies.

Studies 1-11 specified in the five **Groups** in Subsection 3.6.2 are implemented. The simulation results are shown in Figs. 6.11-6.24 in which the system responses associated with the NAWMV-PSS and the LAWMV-PSS are provided by the simulation studies conducted in Subsections 5.4.2 and 3.6.2, respectively. The parameters of the BAWMV-PSS are: $u_{min} = -0.05$ pu, $u_{max} = 0.05$ pu, $\lambda = 0.4$ (these are the same as those used in the NAWMV-PSS and the LAWMV-PSS), $y_o = 10^{-5}$, and $C_y = 0.1$.

Remark 6.5.2 *In a similar manner to the technique used in the estimators of the LAWMV-PSS and the NAWMV-PSS, the fixed-length freezing time (explained in Remarks 3.6.2 and 5.4.1) is applied to the estimator of the BAWMV-PSS to hold the estimates constant at their pre-fault values during the fault period.*

Analysis of the simulation studies.

Group 1: The *dynamic performance* of the BAWMV-PSS is examined in Studies 1-3 by simulating the periodic changes in the system operating point. The simulation results shown in Figs. 6.11-6.13 reveal that the system responses with the BAWMV-PSS and the NAWMV-PSS are similar. The difference between these two stabilisers is the variation of the estimated parameters following a step change in the system operating point. To illustrate this difference, the estimated parameter $\hat{a}_2(k)$ of both the NAWMV-PSS and the BAWMV-PSS in Studies 1-2 is plotted in Fig. 6.14. It is seen that while the estimate of the NAWMV-PSS has a small drift from its true value when the system operating point changes, the estimate of the BAWMV-PSS has a relatively large change from its previous value. This is because the BNM is less accurate than the NNM in tracking and predicting the system dynamics. However, the performance of the BAWMV-PSS is still better than that of the LAWMV-PSS in these studies.

Group 2: The *transient performance* of the BAWMV-PSS following three-phase faults on a transmission line is examined in Studies 4-6. The simulation results are plotted in Figs. 6.15-6.17. It is seen that the damping effects of the BAWMV-PSS and the NAWMV-PSS are almost the same for large transients, and that both can provide stronger damping of system oscillations than the LAWMV-PSS.

Group 3: The *ability* of the BAWMV-PSS to track changes in the system parameters and configuration is examined in Study 7. As shown in Fig. 6.18, the performance of the BAWMV-PSS is comparable with that of the NAWMV-PSS and is better than that of the LAWMV-PSS.

Remark 6.5.3 *When one transmission line is switched out, the system configuration is suddenly changed, resulting in a sudden decrease in the electrical torque (or power) output of the system. As indicated in Subsection 6.4.3, a large decreasing rate of the output will cause an ineffective control action (6.22). In order to overcome this problem, the function $f_y(k)$ (6.25)-(6.26) has been introduced into the control algorithm of the BAWMV-PSS in Subsection 6.4.3. To demonstrate the effectiveness of the function $f_y(k)$ in preventing the control action from being ineffective, the system responses with*

the unbounded control action $u^0(k)$ generated by (6.22) and (6.23), respectively, are compared in Study 7. The simulation results over the time period of 10-20 seconds, during which one transmission line is switched out, are plotted in Fig. 6.19. The corresponding control actions are shown in Fig. 6.20. The use of the function $f_y(k)$ improves the damping performance of the system significantly by increasing the control action through the functional calculation of (6.25)-(6.26). The effectiveness of this modification used in the control algorithm of the BAWMV-PSS is thus evident.

Group 4: In Studies 8-9, the *ability* of the BAWMV-PSS to overcome the measurable deterministic disturbances in reference voltage is examined. It is seen from Figs 6.21-6.22 that the performance of the BAWMV-PSS is slightly inferior to that of the NAWMV-PSS. This is because the BAWMV-PSS is based on the BNM in which the output components $y_B(k)$ and $y_D(k)$ have been omitted. Nevertheless, the system damping performance with the BAWMV-PSS is still better than that with the LAWMV-PSS.

Group 5: The *ability* of the BAWMV-PSS to extend the system stability region is examined in Studies 10-11. The simulation results are shown in Figs. 6.23-6.24. The damping performance of the BAWMV-PSS is as good as that of the NAWMV-PSS and the LAWMV-PSS.

Conclusions.

From the analysis of the simulation results in this subsection, it is concluded that:

1. With the elimination of some additional feedback signals (such as $\delta(k)$, $E_{FD}(k)$, and $E'_q(k)$) and the introduction of the function $f_y(k)$, the performance of the BAWMV-PSS is comparable with that of the NAWMV-PSS at different operating conditions.

2. The simplification involved in the modelling of the BNM results in a small deterioration of the system damping performance associated with the BAWMV-PSS in some cases.

3. Even as the simplest nonlinear adaptive power system stabiliser, the BAWMV-PSS is still superior to the LAWMV-PSS.

6.5.3 Studies on the Robustness of the BAWMV-PSS for the CSM1.

In this subsection the robustness of the BAWMV-PSS is confirmed through the series of *robustness studies* (Studies 12-15) defined in Subsection 3.6.3. The performance of the BAWMV-PSS is tested with unmodelled dynamics and modelling errors. This subsection is the implementation of **Stage 3**.

Aims and structure of the simulation studies.

The CSM3 ($D = 4.0$ pu) is replaced by the CSM1 ($D = 0.1$ pu), and the performance of the BAWMV-PSS, the NAWMV-PSS, and the LAWMV-PSS is further compared. The stabilising signal is the electrical power $P_e(k)$. The aims of this study are

- to examine the performance of the BAWMV-PSS for operation with a higher-order model representing the actual power system;
- to confirm the effectiveness of the BAWMV-PSS with unmodelled dynamics and modelling errors.

Studies 12-15 specified in the two **Groups** in Subsection 3.6.3 are implemented. The simulation results are shown in Figs. 6.25-6.28 in which the system responses associated with the NAWMV-PSS and the LAWMV-PSS are provided by the simulation studies conducted in Subsections 5.4.3 and 3.6.3, respectively.

Analysis of the simulation studies.

Group 1: The *dynamic performance* of the BAWMV-PSS associated with the CSM1 is examined in Studies 12-13. It is seen from Figs. 6.25-6.26 that the damping effects of

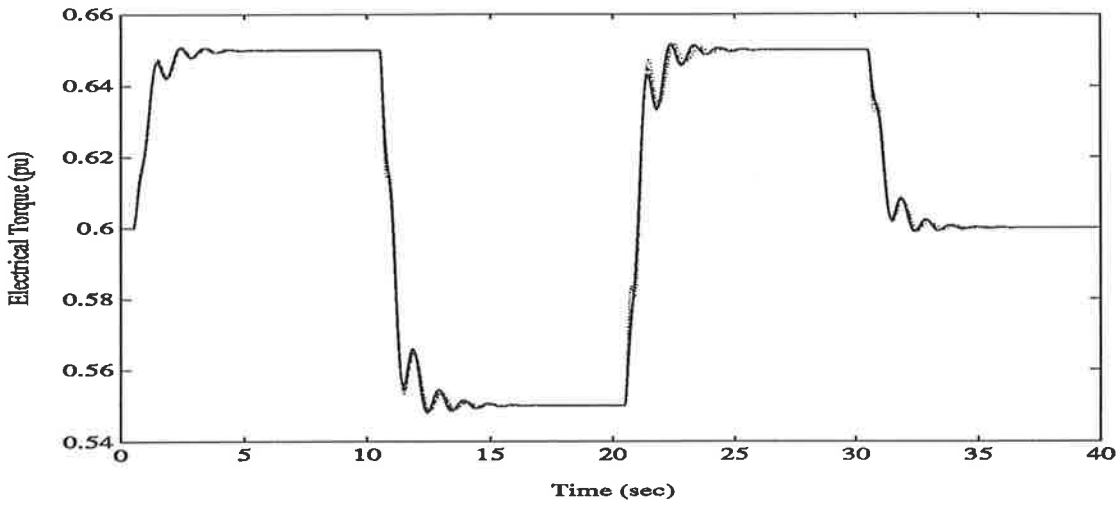

Figure 6.11: Electrical torque response for Study 1 ($P_t = 0.6$ pu, $Q_t = 0.3$ pu; periodic variations in reference power). CSM3 with the BAWMV-PSS - solid line, CSM3 with the NAWMV-PSS - dashed line, CSM3 with the LAWMV-PSS - dotted line.

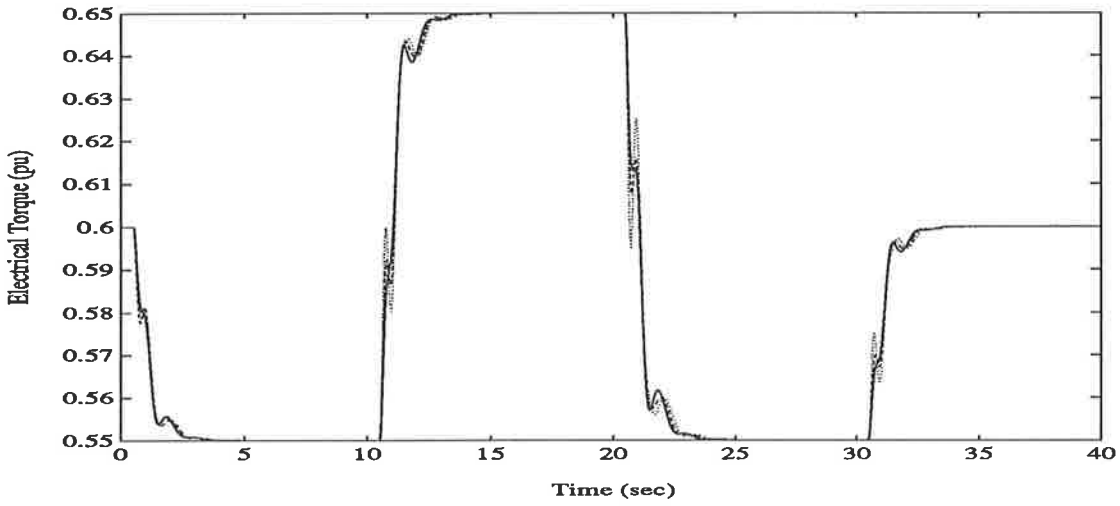

Figure 6.12: Electrical torque response for Study 2 ($P_t = 0.6$ pu, $Q_t = -0.1$ pu; periodic variations in reference power). CSM3 with the BAWMV-PSS - solid line, CSM3 with the NAWMV-PSS - dashed line, CSM3 with the LAWMV-PSS - dotted line.

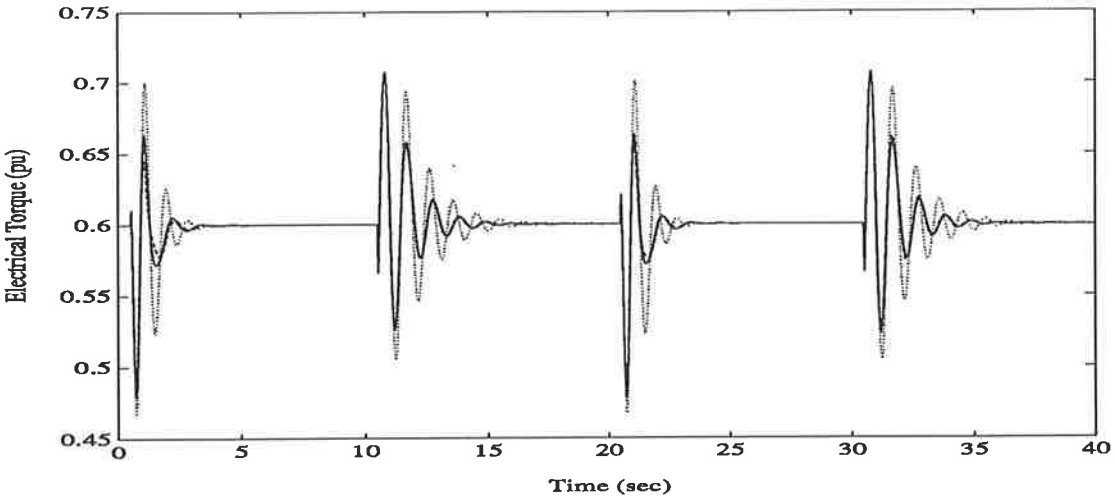

Figure 6.13: Electrical torque response for Study 3 ($P_t = 0.6$ pu, $Q_t = 0.3$ pu; periodic variations in reactive power between lagging and leading operating conditions). CSM3 with the BAWMV-PSS - solid line, CSM3 with the NAWMV-PSS - dashed line, CSM3 with the LAWMV-PSS - dotted line.

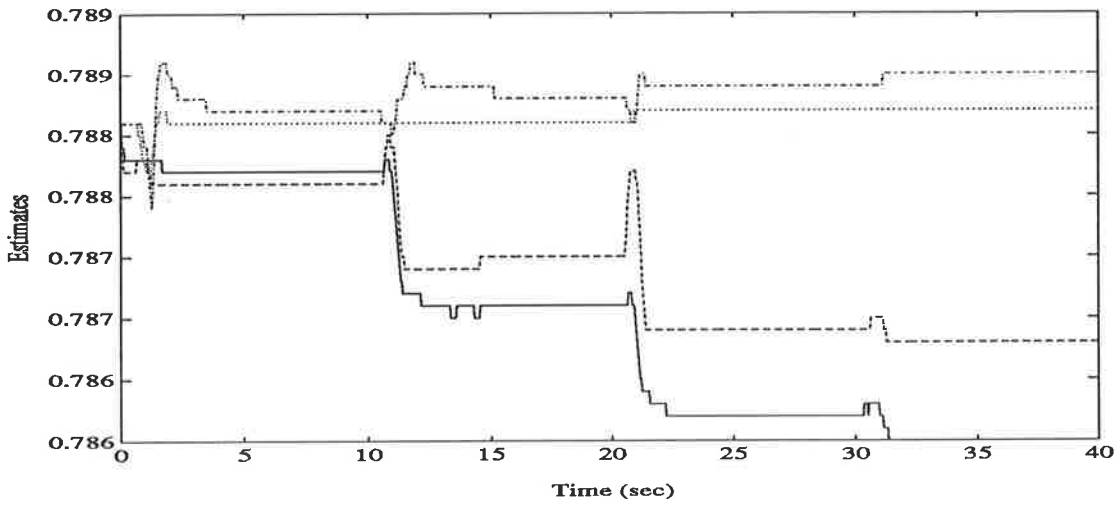

Figure 6.14: Estimated parameter $\hat{a}_2(k)$ of the NNM and the BNM for Studies 1-2 (step changes in the system operating point). BNM for Study 1 - solid line, BNM for Study 2 - dashed line, NNM for Study 1 - dotted line, NNM for Study 2 - dot-dashed line.

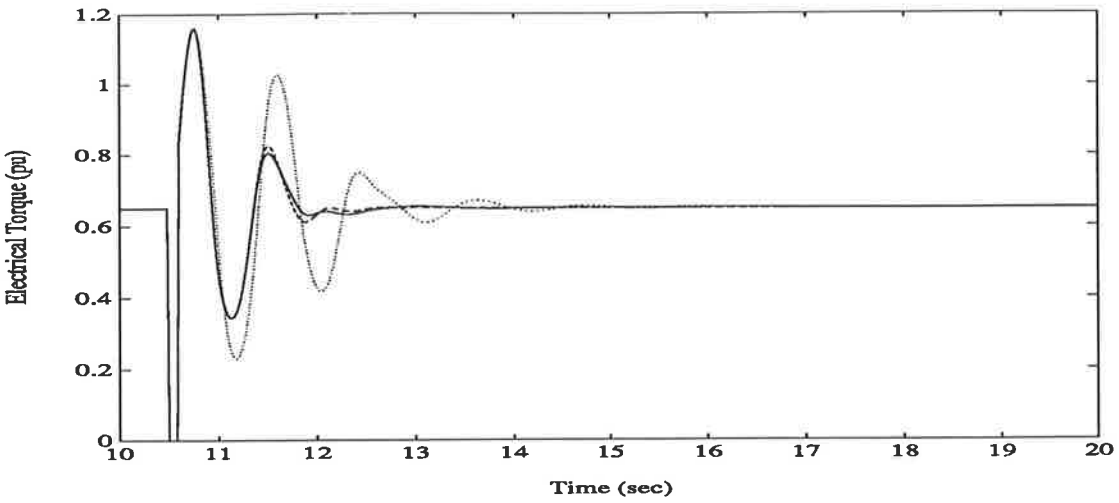

Figure 6.15: Electrical torque response for Study 4 ($P_t = 0.65$ pu, $Q_t = 0.3$ pu; 100 ms short-circuit on the receiving end busbars). CSM3 with the BAWMV-PSS - solid line, CSM3 with the NAWMV-PSS - dashed line, CSM3 with the LAWMV-PSS - dotted line.

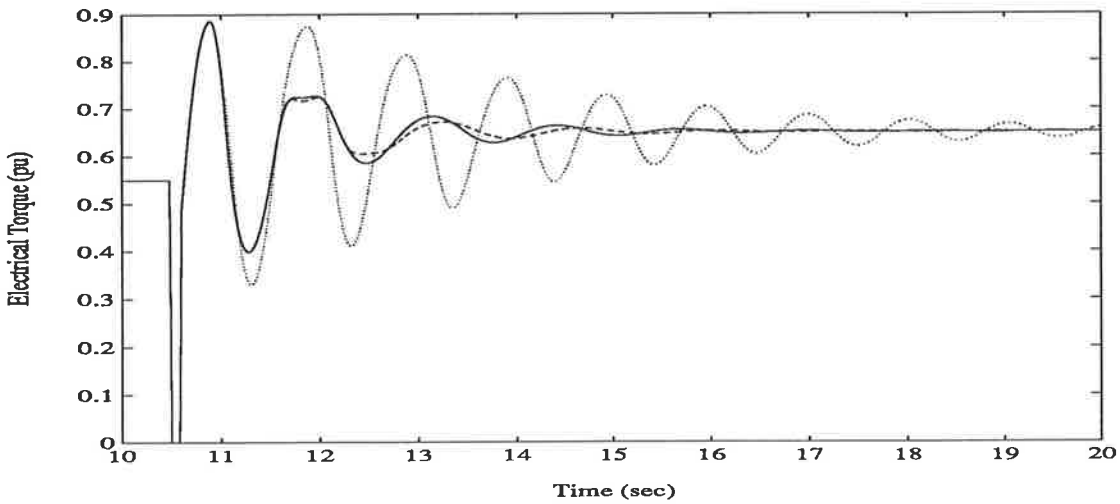

Figure 6.16: Electrical torque response for Study 5 ($P_t = 0.55$ pu, $Q_t = -0.1$ pu; 100 ms short-circuit at the machine terminal). CSM3 with the BAWMV-PSS - solid line, CSM3 with the NAWMV-PSS - dashed line, CSM3 with the LAWMV-PSS - dotted line.

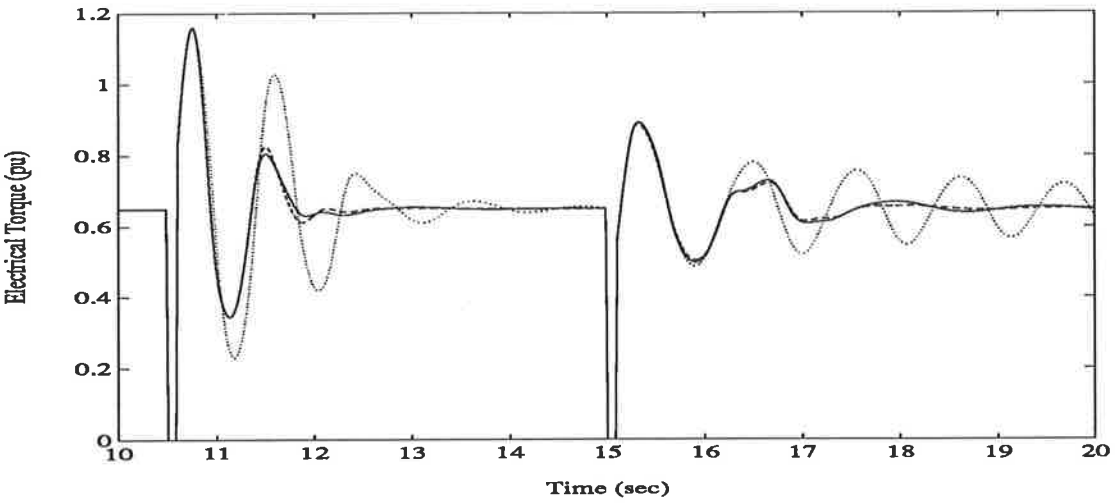

Figure 6.17: Electrical torque response for Study 6 ($P_t = 0.65$ pu, $Q_t = 0.3$ pu; two successive faults of 100 ms duration on the receiving end busbars). CSM3 with the BAWMV-PSS - solid line, CSM3 with the NAWMV-PSS - dashed line, CSM3 with the LAWMV-PSS - dotted line.

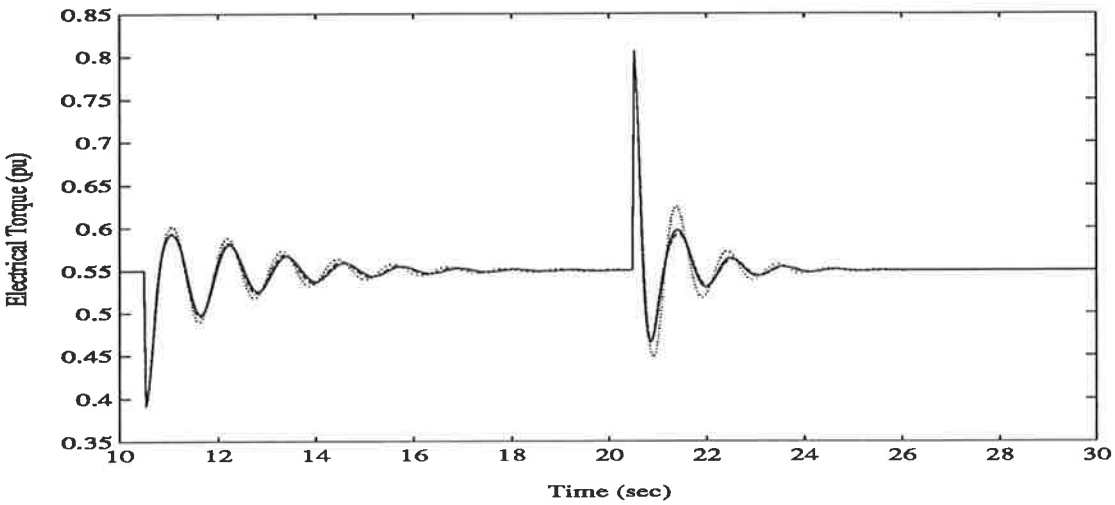

Figure 6.18: Electrical torque response for Study 7 ($P_t = 0.55$ pu, $Q_t = 0.3$ pu; one transmission line is opened and then reclosed). CSM3 with the BAWMV-PSS - solid line, CSM3 with the NAWMV-PSS - dashed line, CSM3 with the LAWMV-PSS - dotted line.

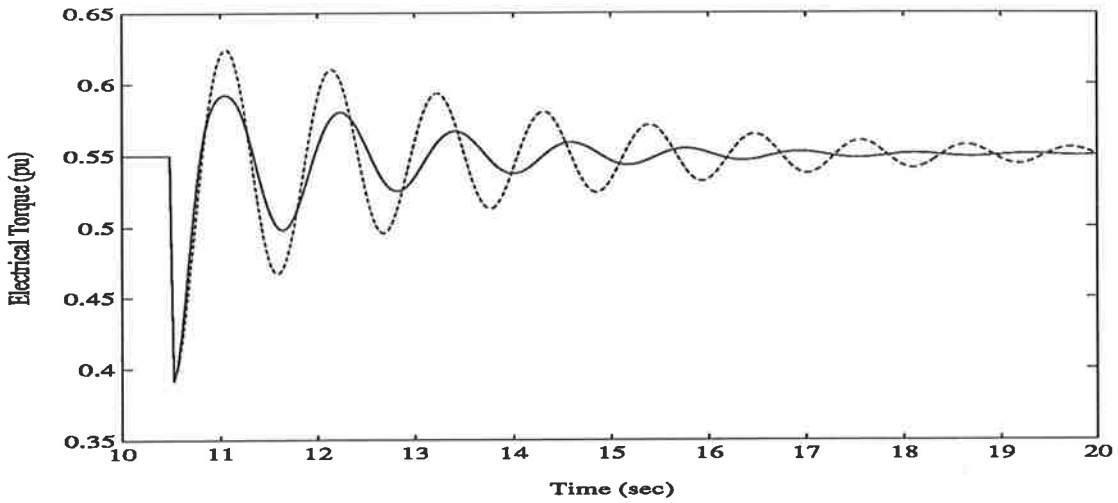

Figure 6.19: Electrical torque response for Study 7 in the first transient ($P_t = 0.55$ pu, $Q_t = 0.3$ pu; one transmission line is opened). BAWMV-PSS with the function $f_y(k)$ - solid line, BAWMV-PSS without the function $f_y(k)$ - dashed line.

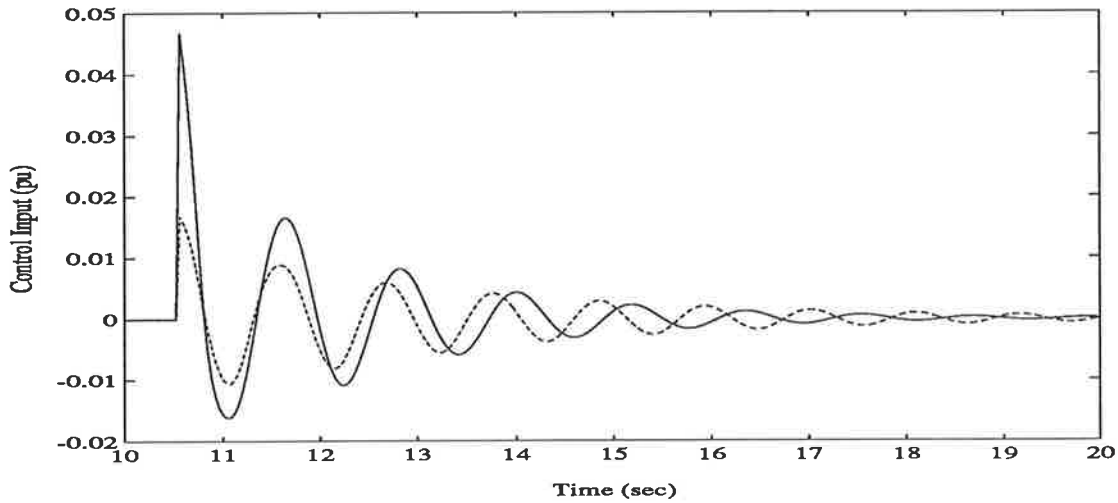

Figure 6.20: Control input for Study 7 in the first transient ($P_t = 0.55$ pu, $Q_t = 0.3$ pu; one transmission line is opened). BAWMV-PSS with the function $f_y(k)$ - solid line, BAWMV-PSS without the function $f_y(k)$ - dashed line.

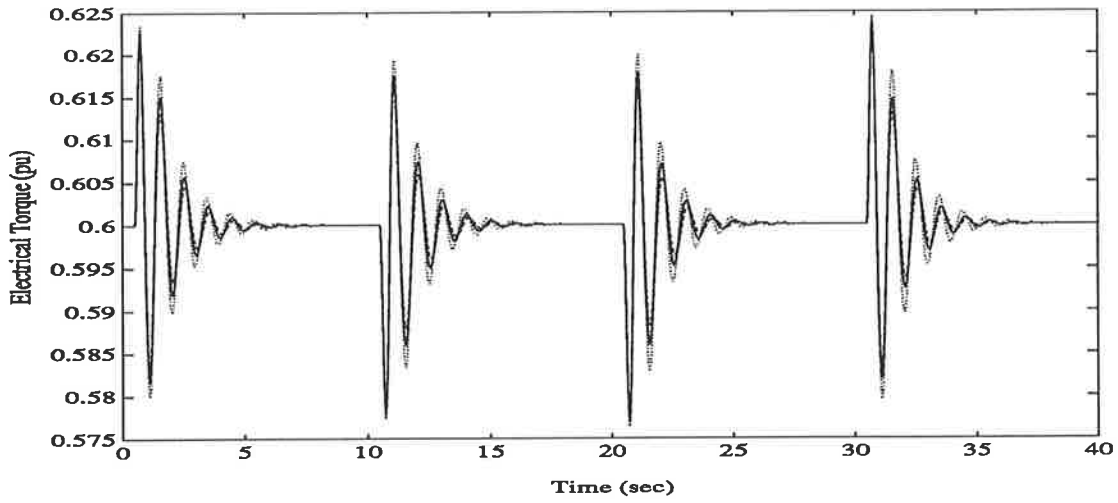

Figure 6.21: Electrical torque response for Study 8 ($P_t = 0.6$ pu, $Q_t = 0.3$ pu; periodic disturbances in reference voltage). CSM3 with the BAWMV-PSS - solid line, CSM3 with the NAWMV-PSS - dashed line, CSM3 with the LAWMV-PSS - dotted line.

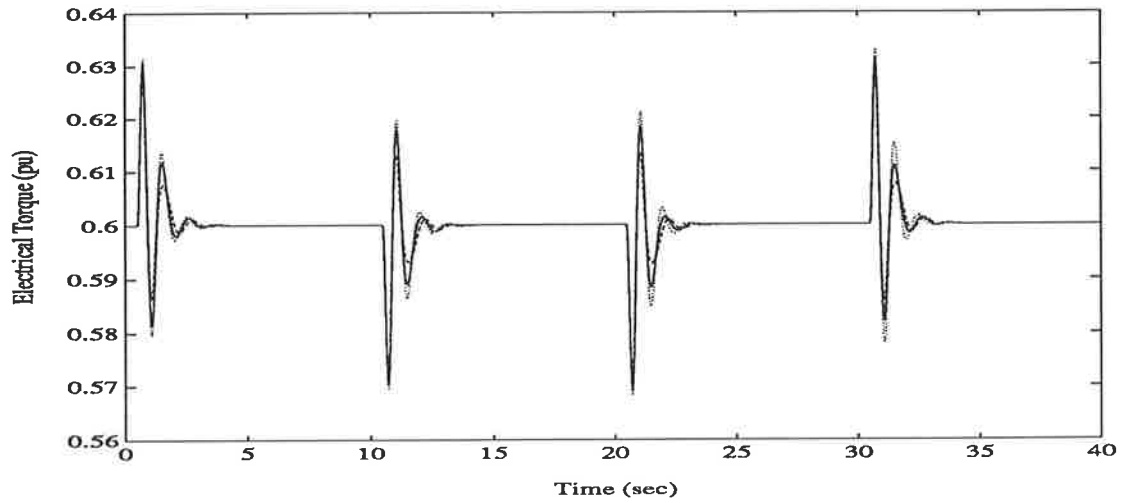

Figure 6.22: Electrical torque response for Study 9 ($P_t = 0.6$ pu, $Q_t = -0.1$ pu; periodic disturbances in reference voltage). CSM3 with the BAWMV-PSS - solid line, CSM3 with the NAWMV-PSS - dashed line, CSM3 with the LAWMV-PSS - dotted line.

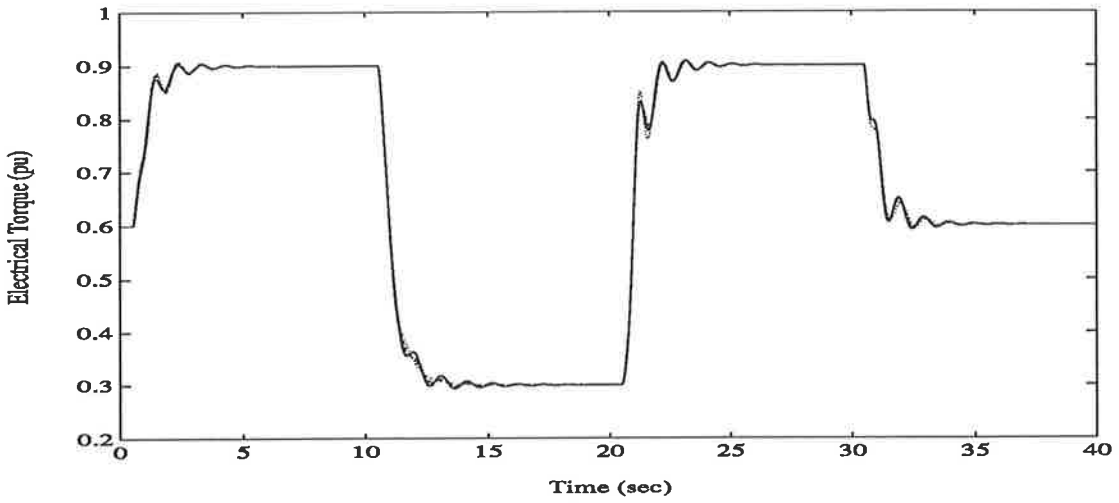

Figure 6.23: Electrical torque response for Study 10 ($P_t = 0.6$ pu, $Q_t = 0.3$ pu; large periodic excursions in reference power). CSM3 with the BAWMV-PSS - solid line, CSM3 with the NAWMV-PSS - dashed line, CSM3 with the LAWMV-PSS - dotted line.

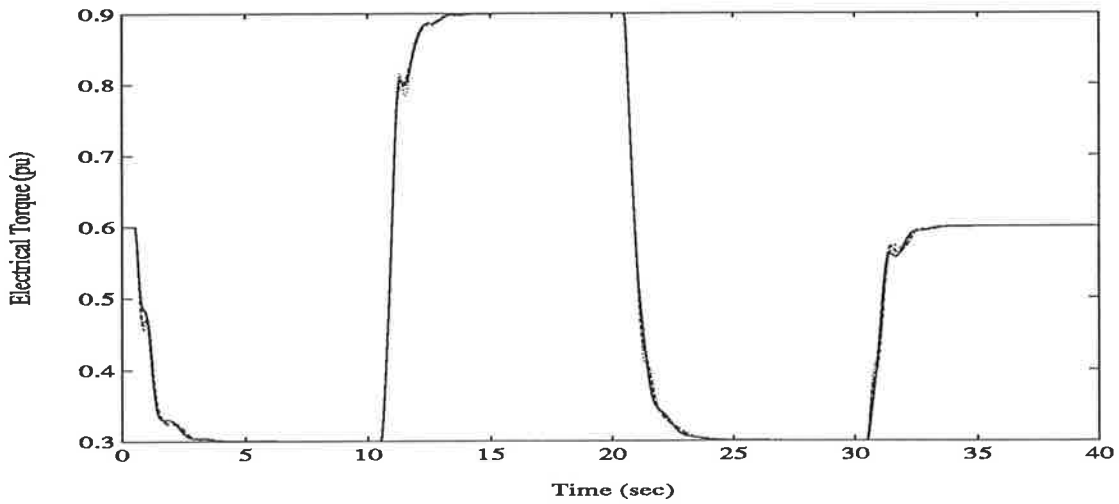

Figure 6.24: Electrical torque response for Study 11 ($P_t = 0.6$ pu, $Q_t = -0.1$ pu; large periodic excursions in reference power). CSM3 with the BAWMV-PSS - solid line, CSM3 with the NAWMV-PSS - dashed line, CSM3 with the LAWMV-PSS - dotted line.

the BAWMV-PSS and the NAWMV-PSS are similar. This agrees with the simulation results of Studies 1-3 in **Stage 2**.

Group 2: The *transient performance* of the BAWMV-PSS associated with the CSM1 is examined in Studies 14-15. The simulation results are plotted in Figs. 6.27-6.28. The performance of the BAWMV-PSS closely matches that of the NAWMV-PSS. The BAWMV-PSS is more effective than the LAWMV-PSS in damping system oscillations in these two studies. This result agrees with the simulation results of Studies 4-6 in **Stage 2**.

Conclusions.

The above studies confirm that:

1. The BAWMV-PSS is a simple but sound design for a SMIB power system.
2. The damping performance of the BAWMV-PSS is comparable with that of the NAWMV-PSS and more effective than that of the LAWMV-PSS.

The advantages of the *bilinear adaptive* control strategy in eliminating certain feedback signals and in providing good damping performance are therefore evident.

From the above conclusions and those drawn in Subsections 3.6.3, 4.5.3, and 5.4.3, it is seen that the BAWMV-PSS is superior to the NOWMV-PSS, the LAWMV-PSS, and the CPSS. Due to its simplicity, the BAWMV-PSS shows greater potential as a practical nonlinear adaptive power system stabiliser than the NAWMV-PSS.

6.6 Concluding Remarks.

In this chapter *original* work on *simplifications* of the nonlinear adaptive power system stabiliser (NAWMV-PSS) proposed in Chapter 5 is conducted. In particular, the design and implementation of a *bilinear adaptive* power system stabiliser for the SMIB power

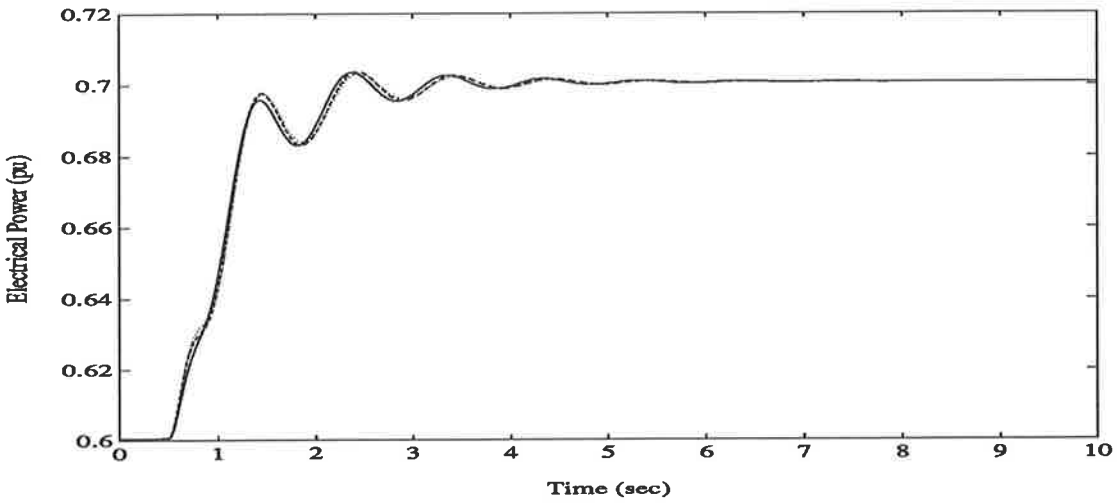

Figure 6.25: Electrical power response for Study 12 ($P_t = 0.6$ pu, $Q_t = 0.3$ pu; step change in reference power). CSM1 with the BAWMV-PSS - solid line, CSM1 with the NAWMV-PSS - dashed line, CSM1 with the LAWMV-PSS - dotted line.

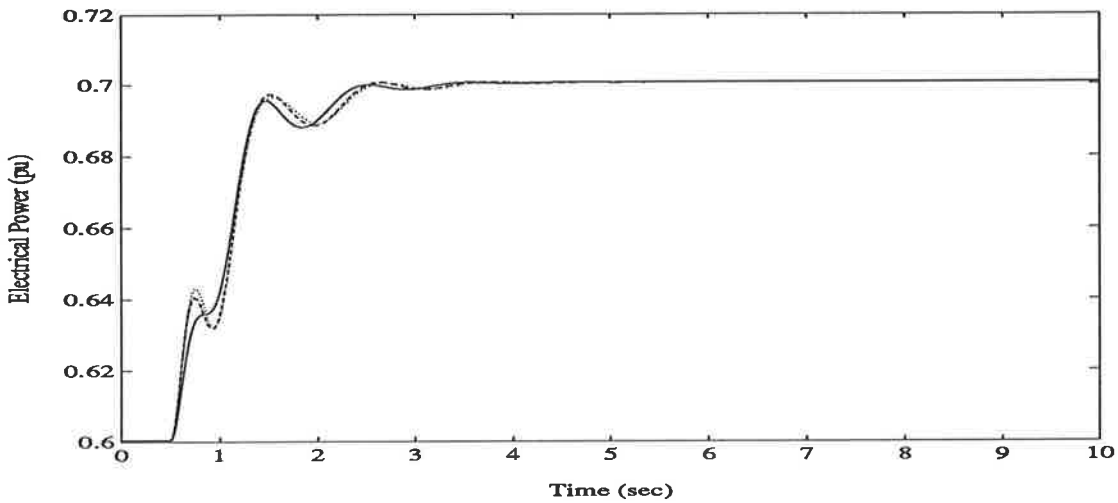

Figure 6.26: Electrical power response for Study 13 ($P_t = 0.6$ pu, $Q_t = -0.1$ pu; step change in reference power). CSM1 with the BAWMV-PSS - solid line, CSM1 with the NAWMV-PSS - dashed line, CSM1 with the LAWMV-PSS - dotted line.

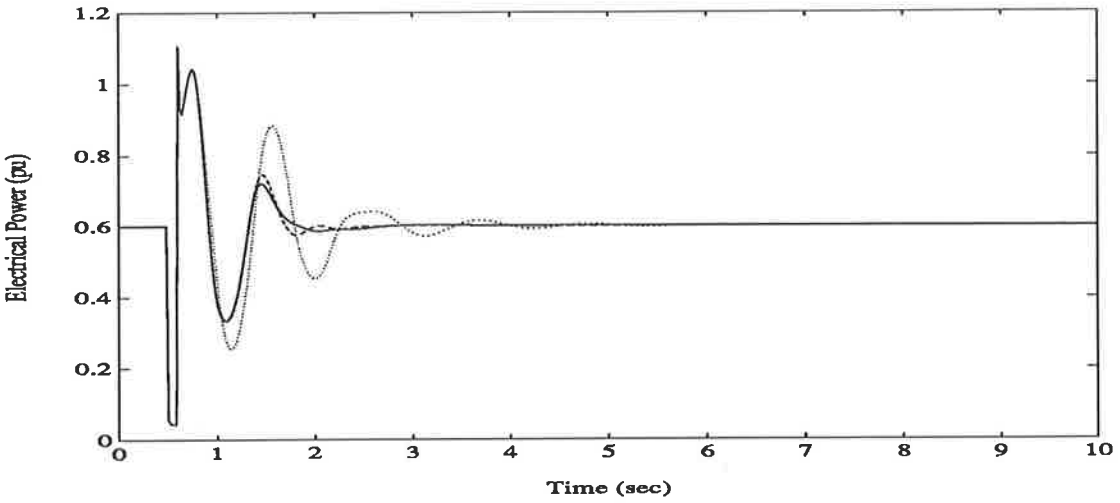

Figure 6.27: Electrical power response for Study 14 ($P_t = 0.6$ pu, $Q_t = 0.3$ pu; 100 ms short-circuit on the receiving end busbars). CSM1 with the BAWMV-PSS - solid line, CSM1 with the NAWMV-PSS - dashed line, CSM1 with the LAWMV-PSS - dotted line.

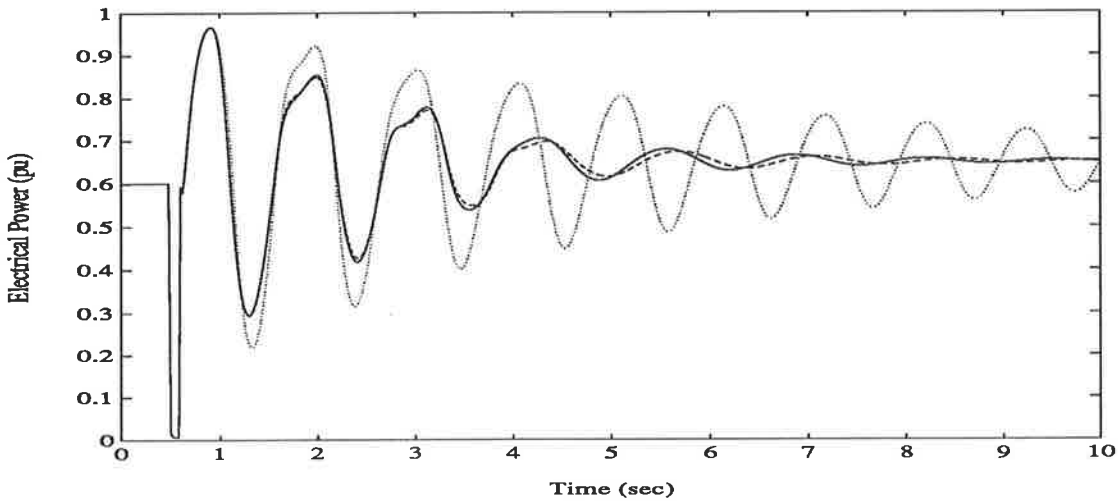

Figure 6.28: Electrical power response for Study 15 ($P_t = 0.6$ pu, $Q_t = -0.1$ pu; 100 ms short-circuit at the machine terminal). CSM1 with the BAWMV-PSS - solid line, CSM1 with the NAWMV-PSS - dashed line, CSM1 with the LAWMV-PSS - dotted line.

system modelled in Subsection 2.3.1 is discussed. This work completes the analysis and design of the nonlinear power system stabilisers carried out in Chapters 4 to 6. The significance of this work is to provide a theoretical basis confirmed by simulation studies for the future realisation of a practical nonlinear adaptive power system stabiliser for a SMIB power system.

The issue of simplifications of the NAWMV-PSS arises when aspects related to the practical implementation of the NAWMV-PSS are considered. The NAWMV-PSS is based on the complete NNM which requires the on-line measurements of the state variables $\delta(k)$, $\omega_s(k)$, $E_{FD}(k)$, and $E'_q(k)$ for its formulation. However, in practice, access to some of the state variables, such as $\delta(k)$ and $E'_q(k)$, is difficult. It is then necessary to eliminate the 'unmeasurable' state variables from the complete NNM and to simplify the calculation of the control law. It is primarily for this reason that simplifications of the NAWMV-PSS are discussed in this chapter.

Simplified versions of the NAWMV-PSS are based on simplified forms of the NNM. Simplified forms of the NMM can be obtained from the analysis of the output prediction of the complete NNM. In Section 6.2, through mathematical decompositions, the output prediction of the complete NNM is shown to be composed of four output components, $y_B(k)$, $y_C(k)$, $y_D(k)$, and $y_E(k)$, two of which ($y_B(k)$ and $y_D(k)$) are found to be less significant in contributing to the dynamic and steady-state responses of the system than the others. This analysis of the contributions of each output component to the overall response is *essential* for the simplification of the NAWMV-PSS, since, for control purposes, a simplified NNM must retain the main characteristics of the output variable while eliminating the need for the additional feedback signals as much as possible.

By the elimination of the less significant components $y_B(k)$ and $y_D(k)$ from the complete NNM and the change of the feedback signal $z_2(k)$ to $\omega_s(k)$, two simplified versions of the NAWMV-PSS (called the SVI-NAWMV-PSS and the SVII-NAWMV-PSS) are derived in Section 6.3. The evaluation studies conducted for these two simplified NAWMV-PSS confirm that the system damping performance does not deteriorate following the simplification. The SVII-NAWMV-PSS, as the simplest version of the

NAWMV-PSS in this thesis, retains the inherent nonlinearities of the power system, and hence possesses the potential to perform as *well* as the NAWMV-PSS.

Since the SVII-NAWMV-PSS still requires the access to the rotor angle $\delta(k)$, further modifications to the SVII-NAWMV-PSS are needed. This results in the discussion of the bilinear control strategies in Section 6.4. By replacing $\sin\delta(k)$ with $T_e(k)$ according to (6.13), a *new* bilinear nominal model (BNM (6.16)-(6.17) with (6.10)-(6.11)) which contains a minimum set of the measurable feedback signals is derived. The performance of the estimated BNM in inherently tracking and predicting the dynamics of the continuous-time nonlinear power system (CSM3) at different system operating points is verified through simulation studies in Subsection 6.5.1.

In line with the theories established in Chapters 4 and 5, the bilinear optimal and adaptive control of the BNM are discussed in Subsections 6.4.2 and 6.4.3, respectively. A *new* bilinear adaptive weighted minimum variance control law (6.22) is developed for the design of a bilinear adaptive power system stabiliser. To use this control law for on-line operation of a bilinear adaptive power system stabiliser, modifications have to be made in order to cope with the circumstances under which the output variable (i.e., the electrical torque or power) suddenly changes to a small value or zero. A three-phase fault or the sudden loss of a transmission line is a typical example of such an event. According to the control law (6.22), the control action is ineffective when such an event occurs. The consequence is poor damping performance of the system. The function $f_y(k)$ (6.25)-(6.26) is proposed in Subsection 6.4.3 to overcome this problem. The modified bilinear adaptive control law (6.23) which incorporates the function $f_y(k)$ into (6.22) is then derived. By proper selection of the parameters y_o and C_y, which are involved in the function $f_y(k)$, the modified bilinear adaptive control law (6.23) can provide a control action equivalent to that of the NAWMV-PSS when an event mentioned above occurs. The effectiveness of the function $f_y(k)$ in preventing the control action from being ineffective is demonstrated in Figs. 6.19-6.20.

Based on (6.23), a *new* bilinear adaptive weighted minimum variance power system stabiliser (BAWMV-PSS) is proposed by Algorithm 6.1. The estimator required by this control algorithm is provided by the implementation of Algorithm 5.1(A).

In Section 6.5 the performance of the proposed BAWMV-PSS is investigated and its robustness in stabilising the higher-order actual power system is tested through the simulation studies presented in Subsections 6.5.2 and 6.5.3. The performance of the BAWMV-PSS is compared with that of the NAWMV-PSS and the LAWMV-PSS. It is shown that the BAWMV-PSS is comparable with the NAWMV-PSS in providing good damping of system oscillations. In some cases there is a small deterioration in system damping performance associated with the BAWMV-PSS when compared with the NAWMV-PSS. However, the overall performance of the BAWMV-PSS is always better than that of the LAWMV-PSS. The advantage of the *bilinear* adaptive control strategy over the *linear* adaptive control strategy is clearly shown in Figs. 6.11-6.28. From these observations and the conclusions drawn in Chapter 5 concerning the evaluation of the performance of the stabilisers designed in this thesis, it is evident that the BAWMV-PSS is superior to the NOWMV-PSS, the LAWMV-PSS, and the CPSS. Due to the elimination of the 'unmeasurable' feedback signals from the formulation of the NAWMV-PSS, the potential of the BAWMV-PSS as a practical nonlinear adaptive power system stabiliser is greater than the NAWMV-PSS. In conclusion, the *bilinear adaptive* control approach is an appropriate design for the practical implementation of a nonlinear adaptive power system stabiliser.

The contributions in this chapter are **original**, and have been listed in Section 6.1.

Chapter 7

Conclusions and Recommendations for Future Research.

7.1 Conclusions.

In this thesis **original** research has been conducted on the analysis, design, and evaluation of *three* nonlinear power system stabilisers, namely the NOWMV-PSS, the NAWMV-PSS, and the BAWMV-PSS, for use with the SMIB models of the power system. The aim of this study is to explore the possibility of using a nonlinear adaptive control scheme for the design of power system stabilisers. In addition, a linear adaptive power system stabiliser (LAWMV-PSS) and a robust conventional power system stabiliser (CPSS) have been designed to assist in the assessment of the nonlinear power system stabilisers mentioned above.

The development of nonlinear power system stabilisers is motivated by the fact that a power system is a highly nonlinear system, and the inherent nonlinearities of the system are usually known. The use of a linear control approach for the design of the power system stabiliser will inevitably result in shortcomings related to the control methodology that is used. A linear *adaptive* control approach is no exception to this. It is only due to the fact that a linear adaptive controller is time-varying in nature (due to its on-line estimation of parameters), that a properly-designed linear adaptive power

system stabiliser can cope with the inherent nonlinearities of the power system and improve the system damping performance relative to that of a *fixed-parameter* linear power system stabiliser. However, the performance of a linear adaptive power system stabiliser may not be optimal in transients before the estimated parameters converge. Therefore, a linear adaptive power system stabiliser may not be the best design for the SMIB power system if the system nonlinearities are known analytically. The need to eliminate the shortcomings associated with linear control approaches immediately suggests the use of nonlinear control approaches which incorporate the inherent nonlinearities of the power system into the design of the power system stabiliser.

In order to carry out an investigation into the design of nonlinear power system stabilisers, the following three preparatory stages are essential:

- firstly, the modelling of the nonlinear power system being studied;
- secondly, the selection of the control scheme to be used for the design;
- thirdly, the establishment of a valid reference with which the performance of the resulting nonlinear power system stabiliser can be compared.

The above three aspects have been discussed (in Chapters 2 and 3) prior to the initiation of the design of the nonlinear power system stabilisers.

Firstly, the SMIB model of the power system, called the CSM1 (see Subsection 2.3.1), has been proposed as the model which closely matches the actual power system for which a power system stabiliser is required. For convenience in the theoretical development, the CSM3 with a properly-tuned rotor damping coefficient (see Subsection 2.3.2) has been used as a substitute for the CSM1 in the analysis and design of the control strategies. Nonlinear and linearised analytical models (NAM, LAM, and SLAM) have been developed from the CSM3 (see Subsections 2.4.1 and 2.4.2) for the derivation of the nominal models that are the characterisations of the nonlinear power system for the purpose of designing the control schemes. The development of these models facilitates the design of the power system stabilisers discussed in this thesis.

Secondly, the linear stochastic optimal control laws have been analysed under the general requirements essential for the design of power system stabilisers (see Section 3.3). The weighted minimum variance control scheme has been selected for the development of the nonlinear power system stabilisers for the sake of simplicity and consistence. The decision to select this control scheme is justified on the basis that it facilitates the comparisons and evaluations of *different* power system stabilisers under the *same* control scheme.

Thirdly, a linearised nominal model (LNM) has been derived from the SLAM for the development of the linear optimal and adaptive control laws (see Section 3.2). A linear adaptive weighted minimum variance power system stabiliser (LAWMV-PSS) (Algorithms 3.2(A)-(B)) has been proposed for the SMIB power system (see Section 3.5), and its performance has been taken as the *reference* for the assessment of the corresponding nonlinear power system stabilisers. The validity of this reference has been verified by the comparison of its damping effect with that of a well-designed robust conventional power system stabiliser (CPSS) at various system operating conditions (see Section 3.6).

The provision of the above three preparatory stages establishes a valid basis on which the nonlinear power system stabilisers have been designed.

A *new* nonlinear nominal model (NNM) has been derived from the NAM for the development of the nonlinear optimal and adaptive control laws (see Section 4.2). The main features of the NNM are

- it *accurately* represents the inherent nonlinearities associated with the electrical torque output of the power system;
- it is given in a regression form (linear in the parameters and in the control input), and hence provides the basis for the development of the nonlinear adaptive control algorithms from the linear ones.

For generality, a *new* nonlinear stochastic generalised minimum variance control law has been derived (see Section 4.3) and its closed-loop stability conditions have been given

by Theorem 4.3.1. The establishment of this control law and its stability conditions is important for the development of a variety of nonlinear optimal control schemes for the NNM, subject to the choice of the weighting polynomials of the associated cost function. A *new* nonlinear optimal weighted minimum variance power system stabiliser (NOWMV-PSS) (Algorithm 4.1) has been proposed for the SMIB power system (see Section 4.4). A sufficient condition for the global closed-loop system stability of the nonlinear stochastic weighted minimum variance control law used by the NOWMV-PSS has been guaranteed by Theorems 4.4.1-4.4.2. The theoretical proofs of the stability theorems associated with these nonlinear optimal control laws (see Appendix E) are *necessary*, since

- the property related to the closed-loop system stability of a control law *cannot* be determined simply by simulation studies;
- there is *no* general solution for the closed-loop system stability of a particular nonlinear control law.

The effectiveness of the proposed NOWMV-PSS has been demonstrated by the comparison of its performance with the reference, which has been taken to be the performance of the LAWMV-PSS, through simulation studies (see Section 4.5). It has been verified that

- because the NOWMV-PSS is based on the fixed-parameter NNM, its control action is optimal at any new operating points provided that the true values of the parameters of the NNM are unchanged;
- because the fixed-parameter NNM contains the inherent nonlinearities of the SMIB power system accurately, the transition from one operating point to another is optimal when the NOWMV-PSS is in operation.

The disadvantages of the NOWMV-PSS have been shown to be

- the parameters of the NOWMV-PSS are time-invariant. This implies a potential deficiency of the NOWMV-PSS in tracking the changes in operating conditions (which cause the true values of the parameters of the NNM to change).

- the generation of the control action of the NOWMV-PSS is based on the assumption that the limiting nonlinearities of the system are working within the linear region. Under this assumption the magnitude of the control action is limited when large disturbances, such as three-phase faults, occur.

The need for a solution to the above problems leads to the development of the corresponding nonlinear *adaptive* control approach.

A *new* nonlinear adaptive weighted minimum variance control law has been derived by combining the nonlinear stochastic weighted minimum variance control law and the recursive least squares algorithm with the time-varying forgetting factor and dead-zone (see Sections 5.2 and 5.3). The control algorithm is given in an indirect form. Two approaches have been considered. The first approach (Algorithms 5.1(A)-(B)) uses all of the estimated parameters of the NNM to calculate the adaptive control law. In order to ensure the convergence of the control algorithm, an assumption that the estimate $\hat{e}_1(k)$ associated with the term $u(k)$ converges to its true value is used. This precaution does not appear to be necessary in the simulation studies, although it is necessary for the theoretical analysis. The second approach (Algorithms 5.2(A)-(B)) sets the estimate $\hat{e}_1(k)$ associated with the term $u(k)$ to a constant value while using all of the estimates of the NNM for the calculations of the other terms in the control law. This approach removes the assumption involved in the first approach, but the control action of this approach becomes less 'adaptive' than that of the first one. The mathematical proofs of the convergence of Algorithms 5.1(A)-(B) and 5.2(A)-(B) associated with the above two control approaches have been given in Appendix G. These theoretical analyses are presented because there is *no* general guarantee of convergence for a particular nonlinear adaptive control algorithm.

A *new* nonlinear adaptive weighted minimum variance power system stabiliser (NAWMV-PSS), which is based on the first approach described above, has been proposed for the SMIB power system (see Section 5.3). The dynamic and transient performance of the NAWMV-PSS overcomes the deficiencies of the NOWMV-PSS, as demonstrated in simulation studies (see Section 5.4). The studies have confirmed that

- the adaptive feature of the NAWMV-PSS copes with the time-varying nature of the power system; the system damping performance with the NAWMV-PSS is thus better than that with the NOWMV-PSS;
- the nonlinear nature of the NAWMV-PSS takes the inherent nonlinearities of the power system into account; the system damping performance with the NAWMV-PSS is thus better than that with the LAWMV-PSS;
- the *nonlinear adaptive* power system stabiliser is, therefore, superior to the *nonlinear optimal* stabiliser and the *linear adaptive* stabiliser in damping the rotor oscillations of the *time-varying nonlinear* power system.

These advantages of the NAWMV-PSS demonstrate the potential of nonlinear adaptive control approaches for the design of power system stabilisers.

As an ideal nonlinear adaptive power system stabiliser, the NAWMV-PSS requires the entire set of feedback signals for the estimation of the parameters of the complete NNM and the calculation of the control law. Problems may arise when the practical implementation of the NAWMV-PSS is considered. This is because some state variables, which are required by the NAWMV-PSS as feedback signals, may be unmeasurable in practice. (This problem is shared by the NOWMV-PSS as well.) The direct method of dealing with this problem is to simplify the complete NNM, resulting in simplified versions of the NAWMV-PSS (see Sections 6.2 and 6.3). The discussion of the simplification of the NAWMV-PSS initiates the development of the bilinear controller for the design of nonlinear power system stabilisers.

A *new* bilinear nominal model (BNM) which requires a minimum set of measurable feedback signals has been derived (see Subsection 6.4.1). Due to the simplifications that are involved in the derivation of the BNM, the accuracy of the BNM in representing the nonlinear power system (CSM3) is lower than that of the NNM. However, with the implementation of an on-line parameter estimation algorithm, the inaccuracy of the BNM can be compensated for by the time-varying parameters of its estimated model (see Subsection 6.5.1). A *new* bilinear adaptive weighted minimum variance control law (6.22) has been developed from the discussion of the optimal and adaptive control

of the BNM (see Subsections 6.4.2 and 6.4.3). Since the BNM contains a product term of the control input $u(k)$ and the output $y(k)$, the control action of the control law (6.22) is significantly reduced following a sudden decrease of the output (caused, e.g., by a three-phase fault) or a sudden increase of the decreasing rate of the output (caused, e.g., by a transmission line switching-out). A measurement to prevent the control action from being ineffective in such an event has been incorporated into the controller by means of the function $f_y(k)$. This results in a *new* bilinear adaptive weighted minimum variance power system stabiliser (BAWMV-PSS). The BAWMV-PSS is described by Algorithms 5.1(A) and 6.1 (see Subsection 6.4.3). An investigation of the performance of the BAWMV-PSS has demonstrated that

- being *inherently nonlinear* and *adaptive* in its control law, the performance of the BAWMV-PSS is superior to that of the LAWMV-PSS;
- being *simple* in its structure, the BAWMV-PSS is more practical than the NAWMV-PSS, although in some instances it is subject to small deteriorations in its damping performance when compared with the NAWMV-PSS.

In conclusion, the *bilinear adaptive* control approach is an appropriate, and potentially a practical, design of the nonlinear adaptive power system stabiliser for the SMIB power system.

The original contributions in this thesis have been summarised in Section 1.9 (or see Sections 4.1, 5.1, and 6.1). The extensions to earlier work described in the literature have been listed in Sections 2.1 and 3.1.

7.2 Recommendations of Future Research.

For the investigation of nonlinear adaptive control schemes in the design of power system stabilisers, the *SISO nonlinear weighted minimum variance* control scheme has been studied for the NNM and the BNM proposed in this thesis. The nonlinear power

system stabilisers developed in this thesis, namely the NOWMV-PSS, the NAWMV-PSS, and the BAWMV-PSS, are for use in the excitation control loop of the SMIB power system. The studies reported in this thesis involve the theoretical analyses and the simulation studies only. In view of the development of *linear* adaptive control strategies in the design of power system stabilisers, the following aspects relating to future research into the *nonlinear* adaptive control strategies in the design of power system stabilisers are suggested:

1. The BAWMV-PSS designed in this thesis through theoretical analyses and simulation studies can be further developed in the laboratory as a *practical* nonlinear adaptive power system stabiliser.

2. The studies of the BAWMV-PSS in the SMIB power system environment, presented in this thesis, can be extended to a *multi-machine* power system environment in which each (or some) of the individual generating units in the system is equipped with a BAWMV-PSS that utilises local measurements only.

3. By the use of the NNM or the BNM developed in this thesis, the design of the *pole-shifting* control scheme is recommended for study. In the literature, studies of this control scheme in the field of *linear* adaptive control have shown the effectiveness of this scheme in improving the system damping performance, despite the heavy burden involved in the calculation of the associated control algorithm [49,50,53, 54,55,56,70]. For *nonlinear* adaptive control studies, the computational burden related to this control scheme is expected to be higher than that in the linear case. However, with the use of new fast micro-processors or parallel processor architectures in practical implementations, the problem of the computational burden may be solved. The effort in developing this control scheme for the design of a nonlinear adaptive power system stabiliser would be applied to the *solvability* of the control action from the control law and/or the *convergence analysis* of the resulting control algorithm. Since the NNM or the BNM is nonlinear, the above two issues may be difficult to solve.

4. *Multi-input multi-output* nonlinear adaptive control strategies can be developed by the utilisation of the NNM or the BNM for the representation of the excitation

control loop of the power system with a new development of another representation of the governor control loop. This involves a progression from SISO nonlinear adaptive power system stabilisers to MIMO nonlinear adaptive power system stabilisers (or controllers). As indicated in [71], for a modern fast-governing and fast-exciting power system, a MIMO control strategy is more suitable than a SISO one for the co-ordination of the control actions of the exciter and the governor. In the field of linear adaptive control, much research has been reported for the development of MIMO power system stabilisers (or controllers) in the literature [68]-[74]. However, in the field of nonlinear adaptive control, there appears to have been nothing forthcoming. A promising MIMO nonlinear control scheme for the design of a MIMO nonlinear adaptive power system stabiliser would be a MIMO nonlinear weighted minimum variance control law, since the solvability of the control action from the control law is expected to be relatively simple. However, difficulties may occur in establishing the convergence of the resulting MIMO adaptive control algorithm.

Since the study of nonlinear adaptive control algorithms for the design of power system stabilisers is rather new, considerable development is required in this field. It is the author's hope that the development of nonlinear adaptive control strategies for implementation in real time will bear fruit. The studies performed for this thesis have provided a promising basis for this.

Appendix A

The Basic Model of a Single Machine Infinite Bus Power System.

Consider a synchronous generator power system equipped with a conventional excitation system and conventional governor and steam turbine, connected to an infinite bus through a double-circuit transmission line having resistance R_e and inductance L_e. The remote infinite busbar is taken as the phasor reference.

A.1 Equations of the Synchronous Generator.

The synchronous generator under consideration is assumed to have three stator windings, one field winding, and two amortisseur (damper) windings. These six windings are magnetically coupled. The type of the generator chosen is the salient pole type.

Let the positive directions of stator currents be the directions of *leaving* the machine terminals. The sign convention of torque is that a positive mechanical (driving) torque $T_m(t)$ *accelerates* the shaft, whereas a positive electrical (retarding or load) torque $T_e(t)$ *decelerates* the shaft. The definition of the position of the d-axis adopted is that in [3].

For the six-winding salient-pole synchronous generator, it is assumed that

Assumption A.1.1

(i) There is no saturation and there is no distributed conducting material in which eddy currents can flow [125].

(ii) The harmonics above second-order can be neglected, thus all the inductances vary sinusoidally with an additional constant term in some cases [125,120].

(iii) The machine is operating under balanced conditions [3].

Using Park's transformation technique, the general equations describing the relationship between voltages, currents and flux linkages in the synchronous generator are given as follows [3].

Flux Linkage Equations

$$\begin{bmatrix} \Lambda_d(t) \\ \Lambda_F(t) \\ \Lambda_D(t) \\ \Lambda_q(t) \\ \Lambda_Q(t) \end{bmatrix} = \begin{bmatrix} L_d & L_{md} & L_{md} & & \\ L_{md} & L_F & L_{md} & \mathbf{0} & \\ L_{md} & L_{md} & L_D & & \\ & \mathbf{0} & & L_q & L_{mq} \\ & & & L_{mq} & L_Q \end{bmatrix} \begin{bmatrix} I_d(t) \\ I_F(t) \\ I_D(t) \\ I_q(t) \\ I_Q(t) \end{bmatrix}. \tag{A.1}$$

Voltage Equations

$$\begin{bmatrix} V_d(t) \\ -V_F(t) \\ 0 \\ V_q(t) \\ 0 \end{bmatrix} = -\begin{bmatrix} r & & & & \\ & r_F & & \mathbf{0} & \\ & & r_D & & \\ & \mathbf{0} & & r & \\ & & & & r_Q \end{bmatrix} \begin{bmatrix} I_d(t) \\ I_F(t) \\ I_D(t) \\ I_q(t) \\ I_Q(t) \end{bmatrix} - \frac{1}{\omega_0} \begin{bmatrix} \dot{\Lambda}_d(t) \\ \dot{\Lambda}_F(t) \\ \dot{\Lambda}_D(t) \\ \dot{\Lambda}_q(t) \\ \dot{\Lambda}_Q(t) \end{bmatrix} - \begin{bmatrix} \omega(t)\Lambda_q(t) \\ 0 \\ 0 \\ -\omega(t)\Lambda_d(t) \\ 0 \end{bmatrix}. \tag{A.2}$$

Swing Equations

$$\dot{\delta}(t) = \omega_0 \omega_s(t), \tag{A.3}$$

$$\dot{\omega}_s(t) = \frac{1}{2H}\left(T_m(t) - T_e(t) - D\omega_s(t)\right) \tag{A.4}$$

where

$$T_m(t) = \frac{P_m(t)}{\omega(t)}. \tag{A.5}$$

Electrical Torque and Power Equations

$$T_e(t) = I_q(t)\Lambda_d(t) - I_d(t)\Lambda_q(t), \tag{A.6}$$

$$P_e(t) = T_e(t)\omega(t). \tag{A.7}$$

External Connection

The external connection of the synchronous generator to the infinite bus can be described by the following equations

$$\omega(t) = \omega_s(t) + 1, \tag{A.8}$$

$$V_d(t) = -V_\infty \sin\delta(t) + R_e I_d(t) + \frac{1}{\omega_0} L_e \dot{I}_d(t) + L_e \omega(t) I_q(t), \tag{A.9}$$

$$V_q(t) = V_\infty \cos\delta(t) + R_e I_q(t) + \frac{1}{\omega_0} L_e \dot{I}_q(t) - L_e \omega(t) I_d(t), \tag{A.10}$$

$$V_t(t)^2 = V_d(t)^2 + V_q(t)^2, \tag{A.11}$$

$$I_t(t)^2 = I_d(t)^2 + I_q(t)^2, \tag{A.12}$$

where the transmission system is represented as a lumped series resistance and inductance, R_e being the effective resistance and L_e the effective inductance. The transformer parameters are included in R_e and L_e.

In the above equations all quantities are normalised in per unit except that $\delta(t)$ is expressed in radians and time t is in seconds. The base speed ω_B is taken as the synchronous (nominal) speed ω_0 in radians per second. The mechanical torque $T_m(t)$ and the electrical torque $T_e(t)$ are normalised on a three-phase base. Park's transformation matrix as in [3] (eqn. (4.5)) is adopted. The voltages, currents, and flux linkages are expressed by their *r.m.s.* equivalents [3].

A.2 Equations of the Excitation System.

There are a variety of excitation system models presented in two IEEE committee reports [204,205]. In this thesis the standard conventional *Type 1 continuously acting excitation system representation* [204] is employed for modelling. Figure A.1 shows the basic configuration.

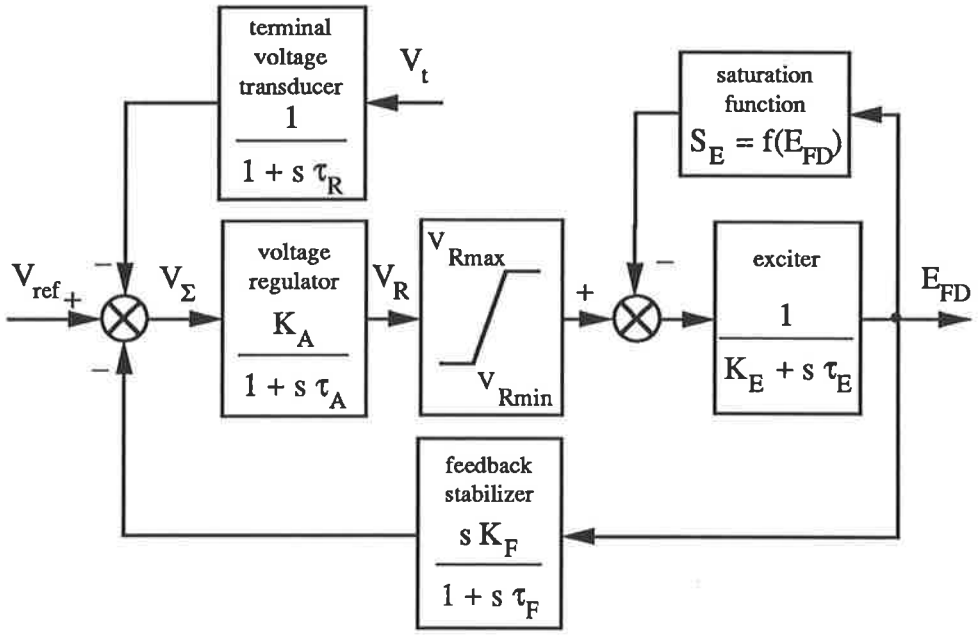

Figure A.1: IEEE Type 1 excitation system representation.

For most power systems, a general assumption for the terminal voltage transducer in Fig. A.1 can be made.

Assumption A.2.1 *The terminal voltage transducer is linear and introduces no delays, i.e.* $\tau_R = 0$ *[204,206].*

To simplify the Type 1 excitation system representation, an additional assumption made for the *Type 1S system* (a special case of the Type 1 system) in [204] is accepted.

Assumption A.2.2

(i) The exciter constant $K_E = 1$, and the exciter time constant $\tau_E = 0$.

(ii) The exciter saturation function is omitted by setting $S_E = 0$.

Furthermore, the feedback stabiliser can be eliminated by assuming that [3]

Assumption A.2.3

(i) There is no feedback filter ($\tau_F = 0$).

(ii) There is no rate feedback ($K_F = 0$).

Therefore, the equations of the simplified Type 1 continuously acting excitation system representation are written as

Conventional Excitation System

$$V_R(t) = \frac{K_A}{1 + p\tau_A} V_\Sigma(t), \tag{A.13}$$

$$E_{FD}(t) = \begin{cases} V_{R\,max} & \text{if } V_R(t) \geq V_{R\,max} \\ V_R(t) & \text{if } V_{R\,min} < V_R(t) < V_{R\,max} \\ V_{R\,min} & \text{if } V_R(t) \leq V_{R\,min} \end{cases}, \tag{A.14}$$

with

$$V_\Sigma(t) = V_{ref}(t) - V_t(t), \tag{A.15}$$

where p is the differential operator. The voltage regulator output is bounded by the magnitude limits $[V_{R\,min}, V_{R\,max}]$ which are determined as a proportion of the machine terminal voltage [204].

Remark A.2.1 *The simplified excitation system (A.13)-(A.15) may in practice be a typical thyristor-type excitation system. The stabilisation that is normally required by this type of excitation system is assumed to be an integral part of the control law to be designed [207,88]. It is for this reason that Assumption A.2.3 is introduced.*

A.3 Equations of the Governor and Steam Turbine.

A general model of a conventional governor for steam turbines proposed in [208] is illustrated in Fig. A.2. This model may be used to represent either a mechanical-hydraulic system or an electro-hydraulic system depending on an appropriate selection of the parameters [208]. The synchronous speed ω_0 is set *a priori.*

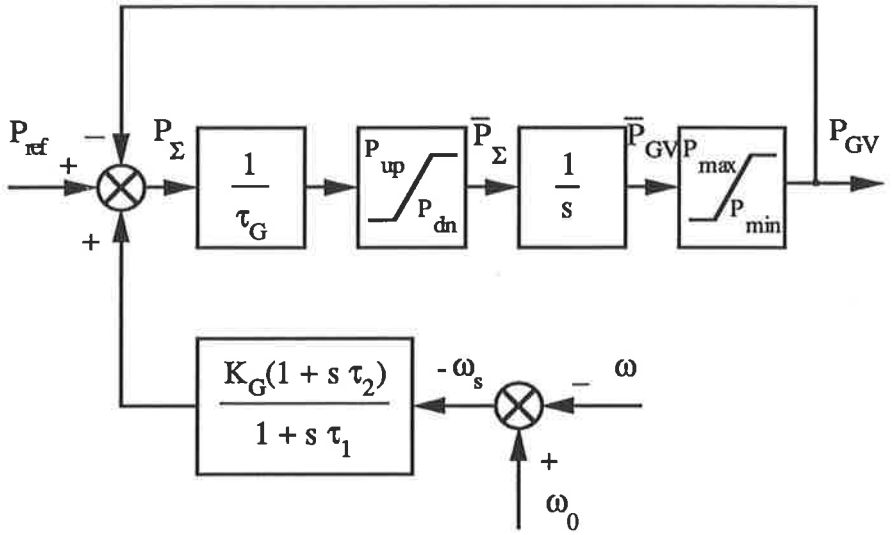

Figure A.2: General model of a governor/valve system for a steam turbine.

For a governor without acceleration feedback, the speed deviation $\omega_s(t)$ is simply amplified by the gain K_G [120]. This is equivalent to assuming that

Assumption A.3.1 *In the speed deviation feedback filter,* τ_1 *and* τ_2 *are negligible.*

The output power from the governor is constrained by the rate limits $[P_{dn}, P_{up}]$ and the magnitude limits $[P_{min}, P_{max}]$. The simplified governor model is then described as

Conventional Governor/Valve System

$$\overline{P}_{\Sigma}(t) = \begin{cases} P_{up} & \text{if } \frac{1}{\tau_G}P_{\Sigma}(t) \geq P_{up} \\ \frac{1}{\tau_G}P_{\Sigma}(t) & \text{if } P_{dn} < \frac{1}{\tau_G}P_{\Sigma}(t) < P_{up} \\ P_{dn} & \text{if } \frac{1}{\tau_G}P_{\Sigma}(t) \leq P_{dn} \end{cases}, \tag{A.16}$$

$$\overline{P}_{GV}(t) = \frac{1}{p}\overline{P}_{\Sigma}(t), \tag{A.17}$$

$$P_{GV}(t) = \begin{cases} P_{max} & \text{if } \overline{P}_{GV}(t) \geq P_{max} \\ \overline{P}_{GV}(t) & \text{if } P_{min} < \overline{P}_{GV}(t) < P_{max} \\ P_{min} & \text{if } \overline{P}_{GV}(t) \leq P_{min} \end{cases}, \tag{A.18}$$

with

$$P_{\Sigma}(t) = P_{ref}(t) - K_G\omega_s(t) - P_{GV}(t). \tag{A.19}$$

Among the six common configurations of steam turbines summarised in [208], two useful (simple) models for simulation studies are a three-stage tandem-compound single-reheat turbine model and a nonreheat turbine model. Their approximate linear representations are given in Figs. A.3 and A.4 respectively.

The equations that formulate the three-stage tandem-compound single-reheat turbine system in Fig. A.3 are

Conventional Steam Turbine (With Reheat)

$$P_{HP}(t) = \frac{1}{1+p\tau_{CH}}P_{GV}(t), \tag{A.20}$$

$$P_{IP}(t) = \frac{1}{1+p\tau_{RH}}P_{HP}(t), \tag{A.21}$$

$$P_{LP}(t) = \frac{1}{1+p\tau_{CO}}P_{IP}(t), \tag{A.22}$$

$$P_m(t) = F_{HP}P_{HP}(t) + F_{IP}P_{IP}(t) + F_{LP}P_{LP}(t), \tag{A.23}$$

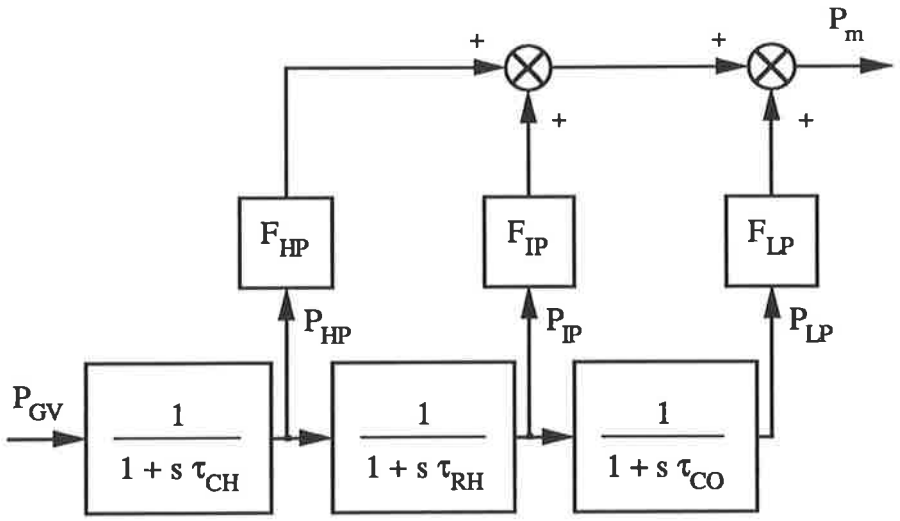

Figure A.3: Linear model of a tandem-compound single-reheat turbine.

with

$$F_{HP} + F_{IP} + F_{LP} = 1. \tag{A.24}$$

Usually $\tau_{RH} \gg \tau_{CH}$ and $\tau_{RH} \gg \tau_{CO}$, and it is assumed that

Assumption A.3.2 *The steam chest time constant τ_{CH} and the crossover time constant τ_{CO} are negligible compared to the reheat time constant τ_{RH}.*

The equation that represents the simplified form of block diagram of Fig. A.3 can be written as

$$P_m(t) = \left(F_{HP} + \frac{1 - F_{HP}}{1 + p\tau_{RH}}\right) P_{GV}(t). \tag{A.25}$$

For the nonreheat turbine system in Fig. A.4, the equation of the model can be directly obtained by setting the time constants τ_{RH} in (A.21) and τ_{CO} in (A.22) to zero and summing the power fractions F_{HP}, F_{IP}, and F_{LP} in (A.23) to 1. This results in the following expression

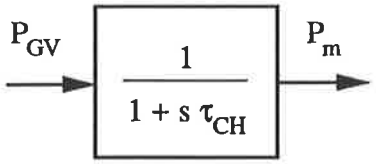

Figure A.4: Linear model of a nonreheat turbine.

Conventional Steam Turbine (Nonreheat)

$$P_m(t) = \frac{1}{1 + p\tau_{CH}} P_{GV}(t). \tag{A.26}$$

Remark A.3.1 *Both the simplified reheat turbine (A.25) and the nonreheat turbine (A.26) can be included in the general expression for the conventional steam turbine (with reheat) in (A.20)-(A.24) by selecting appropriate values of the time constants and the power fractions.*

Remark A.3.2 *Normally, an appropriate boiler model should be chosen to complete the mathematical description of a prime mover system in a power system. However, since the time constants associated with the boiler are usually very large compared to those associated with the other components in a power system, the boiler can be considered to be an infinite steam source that delivers steam at constant temperature and presure when transient disturbances to the power system occur [206,120]. Therefore, the dynamic modelling of a boiler has been omitted in this thesis.*

Appendix B

Derivation of the Operational Functions $G_F(p)$ and $H_F(p)$ in Section 2.2.

The derivation of the expressions for the operational functions $G_F(p)$ and $H_F(p)$ in (2.1) makes use of the following machine equations from (A.1)-(A.2) of Appendix A.

$$\Lambda_F(t) = L_{md}I_d(t) + L_F I_F(t) + L_{md}I_D(t), \tag{B.1}$$

$$\Lambda_D(t) = L_{md}I_d(t) + L_{md}I_F(t) + L_D I_D(t), \tag{B.2}$$

$$V_F(t) = r_F I_F(t) + \frac{1}{\omega_0}\dot{\Lambda}_F(t), \tag{B.3}$$

$$0 = r_D I_D(t) + \frac{1}{\omega_0}\dot{\Lambda}_D(t). \tag{B.4}$$

Eliminating $I_F(t)$ from (B.1) and (B.2), one writes

$$\Lambda_D(t) = \frac{L_{md}}{L_F}\Lambda_F(t) + \left(L_D - \frac{L_{md}^2}{L_F}\right) I_D(t) + \left(L_{md} - \frac{L_{md}^2}{L_F}\right) I_d(t). \tag{B.5}$$

Similarly, from (B.1) and (B.3) one has

$$I_D(t) = \frac{L_F}{\omega_0 r_F}\frac{1}{L_{md}}\dot{\Lambda}_F(t) + \frac{1}{L_{md}}\Lambda_F(t) - \frac{L_F}{r_F L_{md}}V_F(t) - I_d(t). \tag{B.6}$$

Differentiating (B.5) with respect to time and substituting the resulting equation into (B.4), one obtains

$$\frac{1}{\omega_0 r_D}\left(L_D - \frac{L_{md}^2}{L_F}\right)\dot{I}_D(t) + I_D(t) + \frac{1}{\omega_0 r_D}\frac{L_{md}}{L_F}\dot{\Lambda}_F(t) + \frac{1}{\omega_0 r_D}\left(L_{md} - \frac{L_{md}^2}{L_F}\right)\dot{I}_d(t) = 0. \tag{B.7}$$

An expression for $\Lambda_F(t)$ is formed by substituting $I_D(t)$ (B.6) and its time derivative $\dot{I}_D(t)$ into (B.7)

$$\begin{aligned}\Lambda_F(t) &= \frac{1 + p\tau_{d7}}{1 + p(\tau_{d1} + \tau_{d2}) + p^2\tau_{d1}\tau_{d3}} L_{md}\left(I_d(t)\right) \\ &\quad + \frac{1 + p\tau_{d3}}{1 + p(\tau_{d1} + \tau_{d2}) + p^2\tau_{d1}\tau_{d3}} \frac{L_F}{L_{md}}\left(\frac{L_{md}}{r_F} V_F(t)\right)\end{aligned} \tag{B.8}$$

where p is the differential operator. The time constants $\tau_{d1}, \tau_{d2}, \tau_{d3}$, and τ_{d7} are defined in (2.3), (2.4), (2.5), and (2.6) respectively.

The expressions for the operational functions $G_F(p)$ and $H_F(p)$ in (2.1) result directly from (B.8).

Appendix C

System Parameters.

The following system parameters are used for the modelling of the CSM1, the CSM2, and the CSM3 defined in subsection 2.3.1, unless stated otherwise. All parameters are in per unit.

Synchronous Generator:

$r = 0.0012$	$H = 3.36$	
$\tau'_{d0} = 5.66$	$\tau''_{d0} = 0.041$	$\tau''_{q0} = 0.065$
$X_d = 1.904$	$X'_d = 0.312$	$X''_d = 0.26$
$X_q = 1.881$	$X''_q = 0.26$	
$D = 0.1$	$D = 4.0$	(for the CSM3 only)

Transmission Lines:

$R_e = 0.02$ $\quad$ $X_e = 0.4$

Excitation System:

$K_A = 100.0$ $\quad$ $\tau_A = 0.1$ $\quad$ $V_{Rmax} = 5.0$ $\quad$ $V_{Rmin} = -5.0$

Governor:

$K_G = 25.0 \qquad \tau_G = 0.1$

$P_{up} = 9.9 \qquad P_{dn} = -9.9 \qquad P_{max} = 1.2 \qquad P_{min} = 0.0$

Steam Turbine (Nonreheat):

$\tau_{CH} = 0.4 \qquad F_{HP} = 1.0$

Power System Stabilisers:

controller output limits:

$u_{max} = 0.05 \qquad u_{min} = -0.05$

CPSS:

$D_d = 20.0 \qquad K_m = 2.5 \qquad \tau_p = 0.1$

$\tau_{pss1}, \tau_{pss2} = 0.0795 \pm j0.0811 \qquad \tau_{pss3}, \tau_{pss4} = 0.01$

LAWMV-PSS:

$K_0 = 10^4 \qquad C = 10^5 \qquad \mu_{min} = 0.2 \qquad \Sigma_0 = 0.8 \qquad \lambda = 0.4$

NOWMV-PSS:

$\lambda = 0.4 \qquad \beta_{0min} = 0.0001$

NAWMV-PSS:

$K_0 = 10^2 \qquad C = 10^3 \qquad \mu_{min} = 0.2 \qquad \Sigma_0 = 0.8 \qquad \lambda = 0.4$

BAWMV-PSS:

$K_0 = 10^2 \qquad C = 10^3 \qquad \mu_{min} = 0.2 \qquad \Sigma_0 = 0.8 \qquad \lambda = 0.4$

$y_o = 10^{-5} \qquad C_y = 0.1$

Appendix D

Derivation of the Linearised System State Matrix A_0 in Subsection 2.4.2 and Section 2.5.

D.1 Derivation of A_0 in Equation (2.116).

Eliminate the dynamic models of the governor and the steam turbine from the equations of the LAM. The Jacobian matrices of the LAM become

$$\mathbf{\Phi_{X_0}} = \begin{bmatrix} 0 & \omega_0 & 0 & 0 \\ 0 & -\frac{D}{2H} & 0 & 0 \\ 0 & 0 & -\frac{1}{T'_{d0}} & \frac{1}{T'_{d0}} \\ 0 & 0 & 0 & -\frac{1}{\tau_A} \end{bmatrix},$$

$$\mathbf{\Phi_{Z_0}} = \begin{bmatrix} 0 & 0 & 0 \\ 0 & -\frac{1}{2H} & 0 \\ \frac{X_d - X'_d}{T'_{d0}} & 0 & 0 \\ 0 & 0 & -\frac{K_A}{\tau_A} \end{bmatrix},$$

$$\mathbf{\Psi_{X_0}} = \begin{bmatrix} -V_\infty \sin\delta_0 & 0 & -1 & 0 \\ \bar{K}_1 & 0 & \bar{K}_2 & 0 \\ \bar{K}_5 & 0 & \bar{K}_6 & 0 \end{bmatrix},$$

and

$$\mathbf{\Psi_{Z_0}} = \begin{bmatrix} -\left(X_e + X_d'\right) & 0 & 0 \\ 0 & -1 & 0 \\ 0 & 0 & -2V_{t0} \end{bmatrix}, \tag{D.1}$$

where (D.1) is the same as (2.106). $\mathbf{A_0}$ in (2.116) is then derived from its definition in (2.113), subject to the definitions of $\bar{K}_3$ and $\bar{K}_4$ in (2.119) and (2.120) respectively.

D.2 Derivation of $\mathbf{A_0}$ in Equation (2.126).

An alternative expression for the SLAM can be written as

$$\Delta\dot{\delta}(t) = \omega_0\Delta\omega_s(t), \tag{D.2}$$

$$\Delta\dot{\omega}_s(t) = -\frac{D}{2H}\Delta\omega_s(t) - \frac{1}{2H}\Delta T_e(t) + \frac{1}{2H}\Delta T_m(t), \tag{D.3}$$

$$\Delta\dot{E}_q'(t) = -\frac{\bar{K}_4}{\tau_{d0}'}\Delta\delta(t) - \frac{1}{\tau_{d0}'\bar{K}_3}\Delta E_q'(t) + \frac{1}{\tau_{d0}'}\Delta E_{FD}(t), \tag{D.4}$$

$$\Delta\dot{E}_{FD}(t) = -\frac{K_A}{\tau_A}\Delta V_t(t) - \frac{1}{\tau_A}\Delta E_{FD}(t) + \frac{K_A}{\tau_A}\Delta V_{ref}(t), \tag{D.5}$$

with

$$\Delta T_e(t) = \bar{K}_1\Delta\delta(t) + \bar{K}_2\Delta E_q'(t), \tag{D.6}$$

$$\Delta V_t(t) = \frac{\bar{K}_5}{2V_{t0}}\Delta\delta(t) + \frac{\bar{K}_6}{2V_{t0}}\Delta E_q'(t). \tag{D.7}$$

By eliminating $\Delta E_q'(t)$ from (D.6) and (D.7) with the use of (D.2) and (D.4), one writes

$$\Delta\dot{T}_e(t) = \bar{K}_1\omega_0\Delta\omega_s(t) + \frac{\bar{K}_1 - \bar{K}_2\bar{K}_3\bar{K}_4}{\tau_{d0}'\bar{K}_3}\Delta\delta(t) - \frac{1}{\tau_{d0}'\bar{K}_3}\Delta T_e(t) + \frac{\bar{K}_2}{\tau_{d0}'}\Delta E_{FD}(t) \tag{D.8}$$

and

$$\Delta\dot{V}_t(t) = \frac{\bar{K}_5}{2V_{t0}}\omega_0\Delta\omega_s(t) - \frac{1}{\tau_{d0}'\bar{K}_3}\Delta V_t(t) + \frac{\bar{K}_5 - \bar{K}_3\bar{K}_4\bar{K}_6}{2V_{t0}\tau_{d0}'\bar{K}_3}\Delta\delta(t) + \frac{\bar{K}_6}{2V_{t0}\tau_{d0}'}\Delta E_{FD}(t). \tag{D.9}$$

Similarly, by eliminating $\Delta E_q'(t)$ from (D.6) and (D.7), one obtains

$$\Delta\delta(t) = \frac{1}{\bar{K}_1\bar{K}_6 - \bar{K}_2\bar{K}_5}\left(\bar{K}_6\Delta T_e(t) - 2V_{t0}\bar{K}_2\Delta V_t(t)\right). \tag{D.10}$$

The final forms of the linear differential equations of $\Delta\dot{T}_e(t)$ and $\Delta\dot{V}_t(t)$ are obtained by substituting (D.10) into (D.8) and (D.9), resulting in

$$\begin{aligned}\Delta\dot{T}_e(t) &= \bar{K}_1\omega_0\Delta\omega_s(t) + \frac{\bar{K}_2}{\tau'_{d0}\bar{K}_3}\frac{\bar{K}_5 - \bar{K}_3\bar{K}_4\bar{K}_6}{\bar{K}_1\bar{K}_6 - \bar{K}_2\bar{K}_5}\Delta T_e(t) \\ &\quad -\frac{2V_{t0}\bar{K}_2}{\tau'_{d0}\bar{K}_3}\frac{\bar{K}_1 - \bar{K}_2\bar{K}_3\bar{K}_4}{\bar{K}_1\bar{K}_6 - \bar{K}_2\bar{K}_5}\Delta V_t(t) + \frac{\bar{K}_2}{\tau'_{d0}}\Delta E_{FD}(t) \qquad \text{(D.11)}\end{aligned}$$

and

$$\begin{aligned}\Delta\dot{V}_t(t) &= \frac{\bar{K}_5}{2V_{t0}}\omega_0\Delta\omega_s(t) + \frac{\bar{K}_6}{2V_{t0}\tau'_{d0}\bar{K}_3}\frac{\bar{K}_5 - \bar{K}_3\bar{K}_4\bar{K}_6}{\bar{K}_1\bar{K}_6 - \bar{K}_2\bar{K}_5}\Delta T_e(t) \\ &\quad -\frac{\bar{K}_6}{\tau'_{d0}\bar{K}_3}\frac{\bar{K}_1 - \bar{K}_2\bar{K}_3\bar{K}_4}{\bar{K}_1\bar{K}_6 - \bar{K}_2\bar{K}_5}\Delta V_t(t) + \frac{\bar{K}_6}{2V_{t0}\tau'_{d0}}\Delta E_{FD}(t). \qquad \text{(D.12)}\end{aligned}$$

From the definition of $\Delta\mathbf{X}(t)$ in (2.125), $\mathbf{A_0}$ in (2.126) follows from (D.3), (D.11), (D.12), and (D.5) immediately.

Appendix E

Proofs of Theorems in Chapter 4.

E.1 Proof of Theorem 4.3.1.

(a) Equation (4.122) is immediately obtained by substituting (4.120) and (4.121) into (4.92).

(b) Equation (4.123) follows from substituting (4.83), (4.86), and (4.120) into (4.92).

(c) Premultiplying (4.123) by $A(q^{-1})$ and using (4.84) and (4.86), one writes

$$\begin{aligned} w_{u0}W_u(q^{-1})A(q^{-1})u^*(k) &= \tilde{\beta}_0(k)\left[W_r(q^{-1})A(q^{-1})y^*(k+1)\right. \\ &\quad -W_y(q^{-1})A(q^{-1})y(k+1) \\ &\quad \left.+W_y(q^{-1})A(q^{-1})w(k+1)\right]. \end{aligned} \tag{E.1}$$

Substituting (4.79) and (4.121) into (E.1) and using (4.87), one has

$$\begin{aligned} &\left[\beta_0(k)\tilde{\beta}_0(k)W_y(q^{-1}) + w_{u0}W_u(q^{-1})A(q^{-1})\right]u^*(k) \\ &= \tilde{\beta}_0(k)\left[W_r(q^{-1})A(q^{-1})y^*(k+1) - W_y(q^{-1})g(k)\right. \\ &\quad \left.- W_y(q^{-1})G(q^{-1})w(k)\right]. \end{aligned} \tag{E.2}$$

Similarly, premultiplying (4.123) by $\beta_0(k)$ and using (4.84) and (4.86), one writes

$$\begin{aligned} w_{u0}W_u(q^{-1})\beta_0(k)u^*(k) &= \beta_0(k)\tilde{\beta}_0(k)\left[W_r(q^{-1})y^*(k+1) - W_y(q^{-1})y(k+1)\right. \\ &\quad \left.+W_y(q^{-1})w(k+1)\right]. \end{aligned} \tag{E.3}$$

Substituting (4.79) and (4.121) into (E.3) and rearranging, one has

$$\begin{aligned}
&\left[\beta_0(k)\tilde{\beta}_0(k)W_y(q^{-1}) + w_{u0}W_u(q^{-1})A(q^{-1})\right] y(k+1) \\
= \;& \beta_0(k)\tilde{\beta}_0(k)W_r(q^{-1})y^*(k+1) + w_{u0}W_y(q^{-1})g(k) \\
&+ \left[\beta_0(k)\tilde{\beta}_0(k)W_y(q^{-1}) + w_{u0}W_u(q^{-1})\right] w(k+1). \qquad \text{(E.4)}
\end{aligned}$$

The closed-loop system (4.124)-(4.126) is then obtained from (E.2) and (E.4).

(d) Step 1: Define

$$\begin{bmatrix} r_1^*(k+1) \\ r_2^*(k+1) \end{bmatrix} \triangleq \tilde{H}(q^{-1},k) \begin{bmatrix} y^*(k+1) \\ g(k) \\ w(k+1) \end{bmatrix}.$$

Note that the boundedness of $\beta_0(k)$ and $\tilde{\beta}_0(k)$ is given by Remarks 4.3.2 and 4.3.3 respectively. Hence, for bounded sequences $\{y^*(k)\}$, $\{w(k)\}$, and $\{g(k)\}$, the sequences $\{r_1^*(k)\}$ and $\{r_2^*(k)\}$ are bounded. The closed-loop system (4.124) then becomes

$$\tilde{w}(q^{-1},k) \begin{bmatrix} y(k+1) \\ u^*(k) \end{bmatrix} = \begin{bmatrix} r_1^*(k+1) \\ r_2^*(k+1) \end{bmatrix}. \qquad \text{(E.5)}$$

Consider the first equation of (E.5). It can be rewritten as

$$\left[z^n + \theta_{\tilde{w}1}(k)z^{n-1} + \theta_{\tilde{w}2}(k)z^{n-2} + \cdots + \theta_{\tilde{w}n}(k)\right] y(k) = \frac{1}{\theta_{\tilde{w}0}(k)} r_1^*(k+1) \qquad \text{(E.6)}$$

where, according to Assumption 4.3.2(i)-(ii),

$$\theta_{\tilde{w}0}(k) = \beta_0(k)\tilde{\beta}_0(k)w_{y0} + w_{u0}^2 \neq 0, \qquad \text{for all } k,$$

and

$$\sup_{0\leq k<\infty} \left|\frac{1}{\theta_{\tilde{w}0}(k)}\right| < M_0.$$

Clearly, with the selection of n state variables such as

$$\begin{aligned}
x_1(k) &= y(k) - \frac{1}{\theta_{\tilde{w}0}(k)} r_1^*(k), \\
x_2(k) &= \theta_{\tilde{w}1}(k)y(k) + x_1(k+1), \\
x_3(k) &= \theta_{\tilde{w}2}(k)y(k) + x_2(k+1), \\
&\vdots \\
x_n(k) &= \theta_{\tilde{w}n}(k)y(k) + x_{n-1}(k+1),
\end{aligned}$$

equation (E.6) can be written in the following observable form

$$X(k+1) = A_o(k)X(k) + b_o(k)r_1^*(k), \tag{E.7}$$

$$y(k) = c_o(k)X(k) + d_o(k)r_1^*(k), \tag{E.8}$$

where

$$A_o(k) = \begin{bmatrix} -\theta_{\tilde{w}1}(k) & 1 & 0 & \cdots & 0 \\ -\theta_{\tilde{w}2}(k) & 0 & 1 & \cdots & 0 \\ \vdots & \vdots & \vdots & \cdots & \vdots \\ -\theta_{\tilde{w}(n-1)}(k) & 0 & 0 & \cdots & 1 \\ -\theta_{\tilde{w}n}(k) & 0 & 0 & \cdots & 0 \end{bmatrix}, \tag{E.9}$$

$$b_o(k)^T = \begin{bmatrix} -\frac{\theta_{\tilde{w}1}(k)}{\theta_{\tilde{w}0}(k)} & -\frac{\theta_{\tilde{w}2}(k)}{\theta_{\tilde{w}0}(k)} & \cdots & -\frac{\theta_{\tilde{w}n}(k)}{\theta_{\tilde{w}0}(k)} \end{bmatrix},$$

$$c_o(k) = \begin{bmatrix} 1 & 0 & \cdots & 0 \end{bmatrix},$$

$$d_o(k) = -\frac{1}{\theta_{\tilde{w}0}(k)}.$$

Step 2: Consider the zero-input response of the system (E.7)

$$X(k+1) = A_o(k)X(k). \tag{E.10}$$

(i) Since $\tilde{w}(z^{-1}, k)$ is bounded for all k,

$$\sup_{0 \le k < \infty} \| \Theta_{\tilde{w}}(k) \| \le K_{\tilde{w}}$$

where $0 < K_{\tilde{w}} < \infty$. Hence, the sequence of matrices $\{A_o(k)\}$ (E.9) is bounded for all k, i.e., there is some finite a_M such that

$$\sup_{0 \le k < \infty} \| A_o(k) \| = a_M < \infty. \tag{E.11}$$

(ii) Due to

$$\sup_{0 \le k < \infty} \| \Theta_{\tilde{w}}(k+1) - \Theta_{\tilde{w}}(k) \| \le \epsilon_{\tilde{w}},$$

it follows from (E.9) that

$$\sup_{0 \le k < \infty} \| A_o(k+1) - A_o(k) \| \le \epsilon_o \tag{E.12}$$

where ϵ_o is sufficiently small.

(iii) Since $\tilde{w}(z,k)$ has its roots strictly inside the unit circle of the z-domain, the eigenvalues, $\tilde{\lambda}_i$ $(i = 1, 2, \cdots, n)$, of $A_o(k)$ are strictly inside the stability boundary, i.e.,

$$\left|\tilde{\lambda}_i[A_o(k)]\right| < 1 \qquad (i = 1, 2, \cdots, n), \qquad \text{for all } k. \tag{E.13}$$

Under the conditions (E.11), (E.12), and (E.13), the system (E.10) is exponentially stable (see [209,210]).

Step 3: The solution of the output of the system (E.7)-(E.8) is given by

$$\begin{aligned} y(k) &= c_o(k)\Phi(k,k_0)X(k_0) + d_o(k)r_1^*(k) \\ &\quad + \sum_{j=k_0+1}^{k} c_o(k)\Phi(k,j)b_o(j-1)r_1^*(j-1), \quad \text{for } k \geq k_0+1, \end{aligned} \tag{E.14}$$

where $X(k_0)$ is the initial state and $\Phi(k,k_0)$ is the system state transition matrix [156]. Since the system (E.10) is exponentially stable, it follows that [211,210]

$$\| \Phi(k,k_0) \| \leq M_1\mu^{k-k_0}, \qquad \text{for any } k_0 \geq 0 \text{ and for all } k \geq k_0,$$

where M_1 and μ are independent of k; $0 < M_1 < \infty$ and $0 < \mu < 1$. Thus, from (E.14),

$$\begin{aligned} \| y(k) \|^2 &\leq 3\Big\{\| c_o(k) \|^2 \| \Phi(k,k_0) \|^2 \| X(k_0) \|^2 + \| d_o(k) \|^2 \| r_1^*(k) \|^2 \\ &\quad + \left[\sum_{j=k_0+1}^{k} \| c_o(k) \| \| \Phi(k,j) \| \| b_o(j-1) \| \| r_1^*(j-1) \|\right]^2\Big\} \\ &\leq M_2\mu^{2(k-k_0)} + M_3 \| r_1^*(k) \|^2 + M_4 \sum_{j=k_0+1}^{k} \mu^{k-j} \| r_1^*(j-1) \|^2 \end{aligned}$$

where

$$\begin{aligned} 0 \leq M_2 &\triangleq 3M_1^2 \| X(k_0) \|^2 < \infty, \\ 0 < M_3 &\triangleq 3M_0^2 < \infty, \\ 0 < M_4 &\triangleq \frac{3M_0^2M_1^2K_{\tilde{w}}^2}{1-\mu} < \infty; \end{aligned}$$

M_2, M_3, and M_4 are independent of k. Hence, for any $N \geq k_0+1$, it follows that

$$\sum_{k=k_0+1}^{N} \| y(k) \|^2 \leq M_5 + M_6 \sum_{\tau=k_0}^{N} \| r_1^*(\tau) \|^2 \tag{E.15}$$

where

$$0 \leq M_5 \triangleq \frac{M_2}{1-\mu} < \infty,$$
$$0 < M_6 \triangleq M_3 + \frac{M_4}{1-\mu} < \infty.$$

Clearly, M_5 and M_6 are independent of N. Also, from (E.14),

$$\begin{aligned} \| y(k) \| &\leq \| c_o(k) \| \| \Phi(k,k_0) \| \| X(k_0) \| + \| d_o(k) \| \| r_1^*(k) \| \\ &\quad + \sum_{j=k_0+1}^{k} \| c_o(k) \| \| \Phi(k,j) \| \| b_o(j-1) \| \| r_1^*(j-1) \| \\ &\leq M_7 + M_8 \max_{k_0 \leq \tau \leq k} \| r_1^*(\tau) \|, \qquad \text{for all } k \geq k_0+1, \end{aligned} \tag{E.16}$$

where

$$0 \leq M_7 \triangleq M_1 \| X(k_0) \| < \infty,$$
$$0 < M_8 \triangleq M_0 + \frac{M_0 M_1 K_{\tilde{w}}}{1-\mu} < \infty.$$

Surely, M_7 and M_8 are independent of k.

From (E.15) and (E.16), it follows that $\{y(k)\}$ is bounded stable. The proof of the second equation of (E.5) is the same, which leads to the conclusion that $\{u^*(k)\}$ is bounded stable.

Theorem 4.3.1 is then established.

Q.E.D.

Remark E.1.1 *The boundedness of* $\{g(k)\}$ *and* $\{w(k)\}$ *is guaranteed by Lemmas 4.3.3 and 4.2.2, respectively.*

E.2 Proof of Theorem 4.4.2.

(1) According to (4.112), $\beta_0(k)$ is bounded for all k. From (4.132),

$$\begin{aligned} \| \Theta_{\tilde{w}}(k) \| &= \left\{ 1 + \frac{\lambda^2 (a_1^2 + a_2^2)}{[\beta_0(k)^2 + \lambda]^2} \right\}^{\frac{1}{2}} \\ &\leq K_{\tilde{w}}, \qquad \text{for all } k, \end{aligned}$$

where

$$K_{\tilde{w}} \triangleq \left(1 + a_1^2 + a_2^2\right)^{\frac{1}{2}}.$$

Hence, $\tilde{w}(z^{-1}, k)$ in (4.133) is bounded for all k.

(2) Ignoring the error between $z_4(k)$ and $\bar{z}_4(k)$ in (4.66), from (4.132), (4.111), and (4.25) one has

$$\begin{aligned} \| \Theta_{\tilde{w}}(k+1) - \Theta_{\tilde{w}}(k) \| &= \frac{\lambda \left(a_1^2 + a_2^2\right)^{\frac{1}{2}}}{[\beta_0(k+1)^2 + \lambda]\,[\beta_0(k)^2 + \lambda]} \left|\beta_0(k+1)^2 - \beta_0(k)^2\right| \\ &\leq \frac{\left(a_1^2 + a_2^2\right)^{\frac{1}{2}}}{\lambda} e_1^2 \left|\sin^2 \delta(k+1) - \sin^2 \delta(k)\right| \\ &\leq \frac{\left(a_1^2 + a_2^2\right)^{\frac{1}{2}}}{\lambda} e_1^2 \bar{\epsilon}_{\tilde{w}} \end{aligned}$$

where

$$\bar{\epsilon}_{\tilde{w}} \triangleq \max_{0 \leq k < \infty} \left|\sin^2 \delta(k+1) - \sin^2 \delta(k)\right|.$$

Due to (4.40), $\bar{\epsilon}_{\tilde{w}}$ satisfies

$$\lim_{h \to 0} \bar{\epsilon}_{\tilde{w}} = \lim_{h \to 0} \left[\max_{0 \leq k < \infty} \left|h\omega_0 \omega_s(k) \sin 2\delta(k) + o(h)\right|\right] = 0.$$

Define

$$\epsilon_{\tilde{w}} \triangleq \frac{\left(a_1^2 + a_2^2\right)^{\frac{1}{2}}}{\lambda} e_1^2 \bar{\epsilon}_{\tilde{w}}.$$

Clearly, $\epsilon_{\tilde{w}}$ satisfies

$$\lim_{h \to 0} \epsilon_{\tilde{w}} = 0. \tag{E.17}$$

Therefore,

$$\sup_{0 \leq k < \infty} \| \Theta_{\tilde{w}}(k+1) - \Theta_{\tilde{w}}(k) \| \leq \epsilon_{\tilde{w}}$$

where $\epsilon_{\tilde{w}}$ is sufficiently small as indicated in (E.17).

(3) From (4.133), $\tilde{w}(z, k)$ can be written as

$$\tilde{w}(z, k) = \left[\beta_0(k)^2 + \lambda\right] z^2 + \lambda a_1 z + \lambda a_2. \tag{E.18}$$

The roots of (E.18) are solved by setting

$$z^2 + \bar{\lambda} a_1 z + \bar{\lambda} a_2 = 0$$

where

$$0 < \bar{\lambda} \triangleq \frac{\lambda}{\beta_0(k)^2 + \lambda} \leq 1 \tag{E.19}$$

due to $\lambda > 0$. Define

$$D(\bar{\lambda}) \triangleq \bar{\lambda}^2 a_1^2 - 4\bar{\lambda} a_2.$$

The solution of the roots of (E.18) is given by

$$z_{1,2} = \frac{-\bar{\lambda} a_1 \pm D(\bar{\lambda})^{\frac{1}{2}}}{2}.$$

For stability it is required that

$$|z_{1,2}| = \left| \frac{-\bar{\lambda} a_1 \pm D(\bar{\lambda})^{\frac{1}{2}}}{2} \right| < 1. \tag{E.20}$$

There are three cases, each resulting in a choice of $\bar{\lambda}$ satisfying (E.20):

Case 1: $D(\bar{\lambda}) = 0$. From the condition (E.20),

$$\left| \frac{-\bar{\lambda} a_1}{2} \right| < 1$$

which gives

$$0 < \bar{\lambda} < \frac{2}{|a_1|}. \tag{E.21}$$

Case 2: $D(\bar{\lambda}) < 0$. The condition (E.20) becomes

$$\left| \frac{-\bar{\lambda} a_1 \pm j \left(4\bar{\lambda} a_2 - \bar{\lambda}^2 a_1^2\right)^{\frac{1}{2}}}{2} \right| < 1$$

which results in

$$0 < \bar{\lambda} < \frac{1}{|a_2|}. \tag{E.22}$$

Case 3: $D(\bar{\lambda}) > 0$. The condition (E.20) is written as

$$\left| \frac{-\bar{\lambda} a_1 \pm \left(\bar{\lambda}^2 a_1^2 - 4\bar{\lambda} a_2\right)^{\frac{1}{2}}}{2} \right| < 1 \tag{E.23}$$

which is equivalent to requiring that

$$\left| -\bar{\lambda} a_1 \right| + \left(\bar{\lambda}^2 a_1^2 - 4\bar{\lambda} a_2\right)^{\frac{1}{2}} < 2 \tag{E.24}$$

or

$$\left|\bar{\lambda}a_2\right| \leq 1 - \left|\bar{\lambda}a_1\right|, \tag{E.25}$$

resulting in

$$0 < \bar{\lambda} < \frac{1}{|a_1| + |a_2|}. \tag{E.26}$$

Summarising (E.21), (E.22), and (E.26) with the consideration of (E.19), one concludes that: with the selection of $\bar{\lambda}$ within the range of

$$\left\{0 < \bar{\lambda} < \min\left\{\frac{2}{|a_1|}, \frac{1}{|a_1| + |a_2|}, 1\right\}\right\} \triangleq \bar{\lambda}_0, \tag{E.27}$$

the roots of (E.18) satisfy that

$$|z_{1,2}| < 1, \qquad \text{for all } k.$$

From (E.19) and (E.27), for stability it is required that

$$0 < \frac{\lambda}{\beta_0(k)^2 + \lambda} \leq \bar{\lambda}_0 < 1$$

which gives

$$\begin{aligned} 0 < \lambda &\leq \frac{\bar{\lambda}_0}{1 - \bar{\lambda}_0}\beta_0(k)^2 \\ &\leq \frac{\bar{\lambda}_0}{1 - \bar{\lambda}_0}\beta_{0max}^2, \qquad \text{due to (4.112)} \\ &\triangleq \lambda_0. \end{aligned} \tag{E.28}$$

There exists, therefore, a choice of λ satisfying (E.28) such that

$$\tilde{w}(z^{-1}, k) \neq 0, \qquad \text{for all } |z^{-1}| \leq 1 \text{ and all } k.$$

In view of Theorem 4.4.1(d), Theorem 4.4.2 is then established.

Q.E.D.

Remark E.2.1 *In the derivation of the inequalities involved in the selection of* $\bar{\lambda}$ *in* **Case 3** $(D(\bar{\lambda}) > 0)$*, the conditions (E.24) and (E.25) are used to replace the condition (E.23). The region of* $\bar{\lambda}$ *given by (E.26) may therefore be narrower than that satisfying (E.23). Consequently, a value of* λ *which is out of the range of (E.28) may still lead to a stable closed-loop system.*

Appendix F

Derivation of Algorithm 5.1.

Consider the discrete-time system having the form

$$y(k) = \phi(k-1)^T\Theta + w(k),$$

where $\phi(k-1)$ and Θ are $(1 \times r)$ vectors, and $w(k)$ is a bounded noise.

Lemma F.0.1 *The algorithm (5.4)-(5.5) minimises the following quadratic cost function*

$$\bar{S}_N(\Theta) = \mu(N-1)\bar{S}_{N-1}(\Theta) + \sigma(N-1)\left[y(N) - \phi(N-1)^T\Theta\right]^2, \qquad \text{(F.1)}$$

where $N \geq 1$.

Proof of Lemma F.0.1.

Let

$$\bar{\Phi}_{N-1}^T\bar{\Phi}_{N-1} \triangleq \mu(N-1)\bar{\Phi}_{N-2}^T\bar{\Phi}_{N-2} + \sigma(N-1)\phi(N-1)\phi(N-1)^T \qquad \text{(F.2)}$$

be an $(r \times r)$ matrix with $\bar{\Phi}_0^T\bar{\Phi}_0 \triangleq \sigma(0)\phi(0)\phi(0)^T$,

$$\bar{\Psi}_{N-1} \triangleq \left[\begin{array}{cc} \mu(N-1)\bar{\Psi}_{N-2} & \sigma(N-1)\phi(N-1) \end{array}\right]$$

be an $(r \times N)$ matrix with $\bar{\Psi}_0 \triangleq \sigma(0)\phi(0)$, and

$$Y_N^T \triangleq \left[\begin{array}{cccc} y(1) & y(2) & \cdots & y(N) \end{array}\right]$$

be a $(1 \times N)$ vector. Differentiating (F.1) with respect to Θ and setting the result equal to zero gives

$$\bar{\Phi}_{N-1}^T \bar{\Phi}_{N-1} \Theta - \bar{\Psi}_{N-1} Y_N = 0. \tag{F.3}$$

Define

$$P(N-1)^{-1} \triangleq \bar{\Phi}_{N-1}^T \bar{\Phi}_{N-1} \tag{F.4}$$

where $\left(\bar{\Phi}_{N-1}^T \bar{\Phi}_{N-1}\right)^{-1}$ is assumed to exist. Using the form of (F.2), one writes

$$P(N-1)^{-1} = \mu(N-1)P(N-2)^{-1} + \sigma(N-1)\phi(N-1)\phi(N-1)^T. \tag{F.5}$$

Note that

$$\bar{\Psi}_{N-1} Y_N = \mu(N-1)\bar{\Psi}_{N-2} Y_{N-1} + \sigma(N-1)\phi(N-1)y(N). \tag{F.6}$$

Let $\hat{\Theta}(N)$ denote the value of Θ satisfying (F.3). From (F.3)-(F.6), it is readily obtained that

$$\hat{\Theta}(N) = \hat{\Theta}(N-1) + \sigma(N-1)P(N-1)\phi(N-1)\left[y(N) - \phi(N-1)^T \hat{\Theta}(N-1)\right].$$

The above equation establishes (5.4). Equation (5.5) follows by applying Lemma 3.1 of [170] to (F.5).

Q.E.D.

Appendix G

Proofs of Theorems in Chapter 5.

G.1 Proof of Theorem 5.2.1.

Step 1: From the definition of $\mu(k)$ in (5.9)-(5.11),

$$0 < \mu_{min} \leq \mu(k) \leq 1, \qquad \text{for all } k. \tag{G.1}$$

It follows from (F.5) and (G.1) that, if $P(-1)$ is positive definite ($K_0 > 0$), so is $P(k)$ for $k \geq 0$, and that

$$\sup_{0 \leq k < \infty} \| P(k) \| \leq C. \tag{G.2}$$

Step 2: Define

$$V(k) \triangleq \tilde{\Theta}(k)^T P(k-1)^{-1} \tilde{\Theta}(k) \geq 0, \qquad \text{for all } k, \tag{G.3}$$

where

$$\tilde{\Theta}(k) \triangleq \hat{\Theta}(k) - \Theta_0.$$

The following expression is then readily derived from (5.4), (5.6), (5.7), (5.1), and (F.5):

$$\begin{aligned} V(k) - \mu(k-1)V(k-1) \;=\; & \sigma(k-1)\Big[w(k)^2 \\ & - \frac{\mu(k-1)e(k)^2}{\mu(k-1) + \sigma(k-1)\phi(k-1)^T P(k-2)\phi(k-1)}\Big]. \end{aligned} \tag{G.4}$$

From Lemma 4.2.2 and the definition of $\sigma(k-1)$ in (5.8), equation (G.4) becomes

$$\begin{aligned} V(k) - \mu(k-1)V(k-1) &\leq \sigma(k-1)\left[\Delta_w^2 \right. \\ &\qquad \left. - \frac{\mu(k-1)e(k)^2}{\mu(k-1) + \sigma(k-1)\phi(k-1)^T P(k-2)\phi(k-1)}\right] \\ &\leq 0 \end{aligned}$$

which, according to (G.1), results in

$$V(k) \leq V(k-1), \qquad \text{for all } k. \tag{G.5}$$

From (G.3) and (G.5), $V(k)$ is a nonincreasing function, bounded below by zero, and

$$\lim_{k\to\infty} \sigma(k-1)\left[w(k)^2 - \frac{\mu(k-1)e(k)^2}{\mu(k-1) + \sigma(k-1)\phi(k-1)^T P(k-2)\phi(k-1)}\right] = 0.$$

Hence,

$$\lim_{k\to\infty} \sup \left|\frac{e(k)^2}{D(k)}\right| \leq \Delta_w^2 \tag{G.6}$$

where

$$D(k) \triangleq 1 + \frac{1}{\mu_{min}}\phi(k-1)^T P(k-2)\phi(k-1). \tag{G.7}$$

In view of Lemma 4.2.3(i)-(iii),

$$\phi(k-1)^T\phi(k-1) \leq 2\tilde{K}_3^2 + 6\tilde{K}_2^2 + \tilde{K}_1^2\tilde{K}_2^2 + 2\tilde{K}_1\tilde{K}_2, \qquad \text{for all } k, \tag{G.8}$$

where

$$\tilde{K}_1 \triangleq \sup_{0\leq k<\infty} |u(k)|, \tag{G.9}$$

$$\tilde{K}_2 \triangleq \max_{0\leq\tau\leq k} \{|z_1(\tau)|, |z_2(\tau)|, |z_3(\tau)|, |z_4(\tau)|, |z_4(\tau)[d(\tau) - y_F(\tau)]|\}, \tag{G.10}$$

$$\tilde{K}_3 \triangleq \sup_{0\leq k<\infty} |y(k)|; \tag{G.11}$$

$\tilde{K}_1$, $\tilde{K}_2$, and $\tilde{K}_3$ are independent of Δ_w. Therefore, from (G.2), (G.8), and (G.7),

$$1 \leq D(k) \leq \tilde{K}_4^2, \qquad \text{for all } k, \tag{G.12}$$

where

$$\tilde{K}_4 \triangleq \left[1 + \frac{C}{\mu_{min}}\left(2\tilde{K}_3^2 + 6\tilde{K}_2^2 + \tilde{K}_1^2\tilde{K}_2^2 + 2\tilde{K}_1\tilde{K}_2\right)\right]^{\frac{1}{2}}. \tag{G.13}$$

Clearly, $\tilde{K}_4$ is independent of Δ_w.

Step 3: Substituting (G.12) into (G.6) gives

$$\lim_{k\to\infty} \sup |e(k)| < \tilde{K}_4 \Delta_w \tag{G.14}$$

which, with the use of (5.7), establishes conclusion (b). Conclusion (a) then follows by substituting (G.11) into conclusion (b). Using (5.4) and (5.7),

$$\| \hat{\Theta}(k) - \hat{\Theta}(k-1) \|^2 = \sigma(k-1)^2 \phi(k-1)^T P(k-1)^2 \phi(k-1) e(k)^2. \tag{G.15}$$

Conclusion (c) is readily derived from (G.15) by using (G.2), (G.8), and (G.14) and noting that

$$\tilde{K}_5 \triangleq C\tilde{K}_4 \left(2\tilde{K}_3^2 + 6\tilde{K}_2^2 + \tilde{K}_1^2\tilde{K}_2^2 + 2\tilde{K}_1\tilde{K}_2\right)^{\frac{1}{2}} \tag{G.16}$$

from which $\tilde{K}_5$ is independent of Δ_w. Finally, from (G.5) and (G.3),

$$\tilde{\lambda}_{min}\left[P(k-1)^{-1}\right] \tilde{\Theta}(k)^T \tilde{\Theta}(k) \leq \tilde{\lambda}_{max}\left[P(-1)^{-1}\right] \tilde{\Theta}(0)^T \tilde{\Theta}(0) \tag{G.17}$$

where $\tilde{\lambda}\left[P(k)^{-1}\right]$ represents the eigenvalue(s) of $P(k)^{-1}$. Due to (G.2), it follows from (G.17) that

$$\| \tilde{\Theta}(k) \|^2 \leq \tilde{K}_6^2 \| \tilde{\Theta}(0) \|^2, \qquad \text{for } k \geq 1, \tag{G.18}$$

where $\tilde{K}_6$ is defined as

$$\tilde{K}_6 \triangleq \left\{C\tilde{\lambda}_{max}\left[P(-1)^{-1}\right]\right\}^{\frac{1}{2}}, \tag{G.19}$$

independent of Δ_w. Conclusion (d) is established from (G.18). Theorem 5.2.1 is thus proved.

Q.E.D.

G.2 Proof of Theorem 5.2.2.

Following the steps shown in the proof of Theorem 5.2.1, one immediately has

$$\lim_{k\to\infty} \sup |\tilde{e}(k)| < \tilde{K}_4' \Delta_w \tag{G.20}$$

where $\tilde{K}_4'$ is independent of Δ_w, and is defined as

$$\tilde{K}_4' \triangleq \left[1 + \frac{C}{\mu_{min}}\left(2\tilde{K}_3^2 + 6\tilde{K}_2^2\right)\right]^{\frac{1}{2}}; \tag{G.21}$$

$\tilde{K}_2$ and $\tilde{K}_3$ are given by (G.10) and (G.11), respectively. Using (5.21), the condition (G.20) establishes conclusion (b). Due to (5.15),

$$|\tilde{y}(k)| \leq |y(k)| + |\beta_0(k-1)u(k-1)|, \qquad \text{for all } k.$$

Using (G.9), (G.11), and (4.112), the above condition becomes

$$\sup_{0\leq k<\infty} |\tilde{y}(k)| \leq \tilde{K}_3' \tag{G.22}$$

where

$$\tilde{K}_3' \triangleq \tilde{K}_3 + \beta_{0max}\tilde{K}_1. \tag{G.23}$$

Clearly, $\tilde{K}_3'$ is independent of Δ_w. Conclusion (a) then follows by substituting (G.22) into conclusion (b). Conclusions (c) and (d) follow from the same procedure as the proof of Theorem 5.2.1(c)-(d), by noting that

$$\tilde{K}_5' \triangleq C\tilde{K}_4'\left(2\tilde{K}_3^2 + 6\tilde{K}_2^2\right)^{\frac{1}{2}}. \tag{G.24}$$

$\tilde{K}_6'$ has the same definition as given by (G.19).

Q.E.D.

G.3 Proof of Theorem 5.3.1.

(1) Suppose that $k > k_0$ so that Assumption 5.3.2 holds. From (5.1) and (5.2) it readily follows that

$$y(k) - \hat{y}(k) = \tilde{\phi}(k-1)^T\left[\Theta_0 - \hat{\Theta}(k-1)\right] + w(k), \quad \text{for } k > k_0, \tag{G.25}$$

where $\tilde{\phi}(k-1)$ is defined by (5.13) and $\hat{\Theta}(k)$ is obtained from Algorithm 5.1. An alternative expression for $\hat{y}(k+1)$ in (5.2) can be written as

$$\hat{y}(k+1) = \hat{G}(q^{-1})y(k) + \hat{g}(k) + \beta_0(k)u(k), \quad \text{for } k > k_0, \tag{G.26}$$

where $\hat{G}(q^{-1})$ and $\hat{g}(k)$ are given by (5.31) and (5.32), respectively. Substituting (G.26) and Assumption 5.3.2(i) into (5.33) yields

$$\rho(k)u^0(k) = y^*(k+1) - \hat{y}(k+1) + \beta_0(k)u(k)$$

where

$$\rho(k) \triangleq \frac{\beta_0(k)^2 + \lambda}{\beta_0(k)} > 0$$

due to Assumption 5.3.2(ii). Hence,

$$\hat{y}(k+1) = \tilde{y}^*(k+1) - \rho(k)\left[u^0(k) - u(k)\right] \tag{G.27}$$

where

$$\tilde{y}^*(k+1) \triangleq y^*(k+1) - [\rho(k) - \beta_0(k)]\, u(k). \tag{G.28}$$

(2) The control input $\{u(k)\}$ is bounded by (5.34). The output $\{y(k)\}$ and the additional signals, $\{z_i(k)\}$ $(i = 1, 2, 3, 4)$, $\{y_F(k)\}$, and $\{d(k)\}$, are bounded by Lemma 4.2.3(i)-(ii), respectively. Then, from Theorem 5.2.1(b), for each ϵ>0, there exists $k_1 > k_0$ such that

$$|y(k) - \hat{y}(k)| \leq \tilde{K}_4\Delta_w + \epsilon, \qquad \text{for } k \geq k_1, \tag{G.29}$$

or

$$\hat{y}(k) - \tilde{K}_4\Delta_w - \epsilon \leq y(k) \leq \hat{y}(k) + \tilde{K}_4\Delta_w + \epsilon, \qquad \text{for } k \geq k_1. \tag{G.30}$$

Define the interval

$$\begin{aligned} \mathbf{L} &= \left[\begin{array}{cc} l_1 & l_2 \end{array}\right] \\ &= \left[\begin{array}{cc} \tilde{y}^*(k) - \tilde{K}_4\Delta_w - \epsilon & \tilde{y}^*(k) + \tilde{K}_4\Delta_w + \epsilon \end{array}\right]. \end{aligned} \tag{G.31}$$

From here on, it is assumed that $k \geq k_1$, so that the condition (G.30) holds.

(3) In the following, the proof of the convergence of Algorithm 5.3 is given for four cases (numbered **(a)**-**(d)**) arising from the control algorithm (5.33)-(5.34). The basic idea behind the proof is to show that there exists some $k_2 > k_1$ such that $y(k) \in \mathbf{L}$ for all $k \geq k_2$.

(a) If the control algorithm (5.33)-(5.34) gives $u(k) = u^0(k)$, then $y(k+1) \in \mathbf{L}$.

(b) If the control algorithm (5.33)-(5.34) gives $u(k) = u_{max}$, then $y(k+1) \in \mathbf{L}$.

(c) If the control algorithm (5.33)-(5.34) gives $u(k) = u_{min}$, then $y(k+1) \in \mathbf{L}$.

(d) If $y(k) \in \mathbf{L}$, then $y(k+1) \in \mathbf{L}$.

Proof of (a):

If $u(k) = u^0(k)$, then from (G.27) it readily follows that $\hat{y}(k+1) = \tilde{y}^*(k+1)$. From (G.30) and (G.31) one immediately has that $y(k+1) \in \mathbf{L}$, which establishes **(a)**.

Proof of (b) and (c):

Step 1: If $u(k) = u_{max}$, then from (5.34) one has that $u^0(k) \geq u_{max}$. Using (G.27), it follows that $\hat{y}(k+1) \leq \tilde{y}^*(k+1)$. From (G.30) and (G.31), one has

$$y(k+1) \leq \tilde{y}^*(k+1) + \tilde{K}_4\Delta_w + \epsilon \triangleq l_2$$

which, according to Lemma 5.3.1(i), yields

$$y(k) < y(k+1) \leq l_2. \tag{G.32}$$

Step 2: If $u(k) = u_{min}$, then $u^0(k) \leq u_{min}$ due to (5.34). As in *Step 1*, $\hat{y}(k+1) \geq \tilde{y}^*(k+1)$ follows from (G.27), and the condition

$$y(k) > y(k+1) \geq \tilde{y}^*(k+1) - \tilde{K}_4\Delta_w - \epsilon \triangleq l_1 \tag{G.33}$$

results from using (G.30), (G.31), and Lemma 5.3.1(ii).

Step 3: There are two possibilities for the existence of (G.32) when $u(k) = u_{max}$:

(i) $y(k) \in \mathbf{L}$: then from (G.32) $y(k+1) \in \mathbf{L}$;

(ii) $y(k) \ni \mathbf{L}$ and $y(k) < l_1$: then, according to (G.32) and Lemma 5.3.1(i), at each sampling step $y(k)$ increases by an amount $\geq r_2 > 0$. There then exists $k' > k$ such that $y(k') \geq l_1$ is satisfied, while (G.32) holds. Hence, $y(k') \in \mathbf{L}$.

If $y(k)$ stops increasing before $y(k) \geq l_1$, say, $y(k'') < l_1$, then $u(k'') \neq u_{max}$, and $u(k'') = u^0(k'')$ is the only possibility (since $u(k'') = u_{min}$ will result in $y(k'') > l_1$, as indicated in (G.33)). Therefore, as in **(a)** above, $y(k''+1) \in \mathbf{L}$.

Step 4: There are two possibilities for the existence of (G.33) when $u(k) = u_{min}$:

(i) $y(k) \in \mathbf{L}$: then from (G.33) $y(k+1) \in \mathbf{L}$;

(ii) $y(k) \ni \mathbf{L}$ and $y(k) > l_2$: then, from (G.33) and Lemma 5.3.1(ii), $y(k)$ decreases by an amount $\leq r_1 < 0$ at each sampling step. Similar to *Step 3*, there must exist $k' > k$ such that $y(k') \leq l_2$ while (G.33) holds. Hence, $y(k') \in \mathbf{L}$.

If $y(k)$ stops decreasing before $y(k) \leq l_2$, say, $y(k'') > l_2$, then $u(k'') \neq u_{min}$, and $u(k'') = u^0(k'')$ is the only possibility (since $u(k'') = u_{max}$ will result in $y(k'') < l_2$, as indicated in (G.32)). Hence, as in **(a)** above, $y(k''+1) \in \mathbf{L}$.

Step 1 combined with *Step 3* establishes **(b)**, while *Step 2* with *Step 4* establishes **(c)**.

Proof of (d):

If $y(k) \in \mathbf{L}$, then there are three possibilities for the control input $u(k)$:

(i) $u(k) = u^0(k)$: then by **(a)**, $y(k+1) \in \mathbf{L}$.

(ii) $u(k) = u_{max}$: then by using *Step 3*(i), $y(k+1) \in \mathbf{L}$.

(iii) $u(k) = u_{min}$: then by using *Step 4*(i), $y(k+1) \in \mathbf{L}$.

The above (i)-(iii) establish **(d)**.

In conclusion of **(a)**-**(d)**, it follows that there exists some $k_2 > k_1$ such that

$$y(k) \in \mathbf{L}, \qquad \text{for } k \geq k_2.$$

It follows from the definition of $\mathbf{L}$ in (G.31) that

$$|y(k) - \tilde{y}^*(k)| \leq \tilde{K}_4 \Delta_w + \epsilon, \qquad \text{for } k \geq k_2. \tag{G.34}$$

(4) From (G.29) and (G.27),

$$\left|y(k) - \tilde{y}^*(k) + \rho(k-1)\left[u^0(k-1) - u(k-1)\right]\right| \leq \tilde{K}_4 \Delta_w + \epsilon, \quad \text{for } k \geq k_1.$$

Due to (G.34), the above condition can be written as

$$|\rho(k-1)u(k-1)| \leq \left|\rho(k-1)u^0(k-1)\right| + 2\tilde{K}_4 \Delta_w + 2\epsilon, \quad \text{for } k \geq k_2. \tag{G.35}$$

On the other hand, from (5.33) and (4.128), for $k > k_0$, one has

$$\rho(k-1)u^0(k-1) = y^*(k) - \tilde{\phi}(k-1)^T\hat{\Theta}(k-1), \tag{G.36}$$

$$\rho(k-1)u^*(k-1) = y^*(k) - \tilde{\phi}(k-1)^T\Theta_0. \tag{G.37}$$

From (G.36), (G.37), and (G.25), one writes

$$\rho(k-1)\left[u^0(k-1) - u^*(k-1)\right] = y(k) - \hat{y}(k) - w(k), \quad \text{for } k > k_0.$$

Due to (G.29) and Lemma 4.2.2, the above equation becomes

$$\left|\rho(k-1)u^0(k-1)\right| \leq |\rho(k-1)u^*(k-1)| + \left(\tilde{K}_4 + 1\right)\Delta_w + \epsilon, \quad \text{for } k \geq k_1. \tag{G.38}$$

From (G.35) and (G.38), one immediately has

$$|u(k-1)| \leq |u^*(k-1)| + \frac{1}{\rho(k-1)}\left[\left(3\tilde{K}_4 + 1\right)\Delta_w + 3\epsilon\right], \quad \text{for } k \geq k_2. \tag{G.39}$$

(5) From (G.34) and (G.28),

$$|y(k) - y^*(k) + [\rho(k-1) - \beta_0(k-1)]\,u(k-1)| \leq \tilde{K}_4\Delta_w + \epsilon, \quad \text{for } k \geq k_2,$$

which, according to (G.39), leads to

$$\begin{aligned} |y(k) - y^*(k)| \leq\ & [\rho(k-1) - \beta_0(k-1)]\,|u^*(k-1)| \\ & + \frac{[\rho(k-1) - \beta_0(k-1)]}{\rho(k-1)}\left[\left(3\tilde{K}_4 + 1\right)\Delta_w + 3\epsilon\right] \\ & + \tilde{K}_4\Delta_w + \epsilon, \qquad \text{for } k \geq k_2. \end{aligned} \tag{G.40}$$

Due to

$$0 < \frac{[\rho(k-1) - \beta_0(k-1)]}{\rho(k-1)} = \frac{\lambda}{\beta_0(k-1)^2 + \lambda} < 1$$

and

$$\rho(k-1) - \beta_0(k-1) \leq \frac{\lambda}{\beta_{0min}},$$

the condition (G.40) becomes

$$|y(k) - y^*(k)| \leq \frac{\lambda}{\beta_{0min}}|u^*(k-1)| + \left(4\tilde{K}_4 + 1\right)\Delta_w + 4\epsilon, \quad \text{for } k \geq k_2. \tag{G.41}$$

From (4.139),

$$\lim_{k\to\infty} \sup |u^*(k)| \leq \epsilon_{u^*}. \tag{G.42}$$

Since $\epsilon > 0$ may be chosen arbitrarily small, the condition (5.47) is readily established from (G.41) and (G.42) by noting the definition of $\tilde{K}_u$ in (5.48).

Theorem 5.3.1 is thus proved.

Q.E.D.

Bibliography

[1] AIEE subcommittee in interconnections and stability factors, "First report of power system stability", *Electrical Engineering*, 56(2):261-282, February 1937.

[2] Byerly, R. T., and Kimbark, E. W., (eds.), *Stability of large electrical power systems*, IEEE Press, New York, 1974.

[3] Anderson, P. M., and Fouad, A. A., *Power system control and stability*, Iowa State University Press, Ames, Iowa, U.S.A., 1977.

[4] Kimbark, E. W., *Power system stability*, Vol. III, John Wiley and Sons Inc., New York, 1956.

[5] Hore, R. A., *Advanced studies in electrical power system design*, Chapman and Hall, London, 1966.

[6] Yu, Y. N., *Electrical power system dynamics*, Academic Press, London, 1983.

[7] Concordia, C., "Steady-state stability of synchronous machines as affected by voltage regulator characteristics", *AIEE Trans. Power Apparatus and Systems*, PAS-63(5):215-220, May 1944.

[8] Heffron, W. G., and Phillips, R. A., "Effect of a modern amplidyne voltage regulator on underexcited operation of large turbine generators", *AIEE Trans. Power Apparatus and Systems*, PAS-71(1):692-697, August 1952.

[9] Messerle, H. K., and Bruck, R. W., "Steady-state stability of synchronous generators as affected by regulators and governors", *IEE Proc.*, 103, Pt. C:24-34, March 1956.

[10] Aldred, A. S., and Shackshaft, G., "The effect of the voltage regulator on the steady-state and transient stability of a synchronous generator", *IEE Proc.*, 105, Pt. A:420-427, August 1958.

[11] Aldred, A. S., and Shackshaft, G., "A frequency-response method for the predetermination of synchronous-machine stability", *IEE Proc.*, 107, Pt. C:2-10, March 1960.

[12] Stapleton, C. A., "Root-locus study of synchronous-machine regulation", *IEE Proc.*, 111(4):761-768, April 1964.

[13] Battisson, M. J., and Mullineux, N., "Stability criteria for linear control systems", *IEE Proc.*, 112(3):549-556, March 1965.

[14] Gove, R. M., "Geometric construction of the stability limits of synchronous machines", *IEE Proc.*, 112(5):977-985, May 1965.

[15] Jacovides, L. J., and Adkins, B., "Effect of excitation regulation on synchronous-machine stability", *IEE Proc.*, 113(6):1021-1034, June 1966.

[16] Undril, J. M., "Power system stability studies by the method of Liapunov: I — state space approach to synchronous machine modeling", *IEEE Trans. Power Apparatus and Systems*, PAS-86(7):791-801, July 1967.

[17] Ewart, D. N., and DeMello, F. P., "A digital computer program for the automatic determination of dynamic stability limits", *IEEE Trans. Power Apparatus and Systems*, PAS-86(7):867-875, July 1967.

[18] Yu, Y. N., and Vongsuriya, K., "Nonlinear power system stability study by Liapunov function and Zubov's method", *IEEE Trans. Power Apparatus and Systems*, PAS-86(12):1480-1485, December 1967.

[19] DeMello, F. P., and Concordia, C., "Concepts of synchronous machine stability as affected by excitation control", *IEEE Trans. Power Apparatus and Systems*, PAS-88(4):316-329, April 1969.

[20] Ellis, H. M., Hardy, J. E., Blythe, A. L., and Skooglund, J. W., "Dynamic stability of the Peace River transmission system", *IEEE Trans. Power Apparatus and Systems*, PAS-85(6):586-600, June 1966.

[21] Schleif, F. R., and White, J. H., "Damping for the northwest-southwest tieline oscillations — an analog study", *IEEE Trans. Power Apparatus and Systems*, PAS-85(12):1239-1247, December 1966.

[22] Schleif, F. R., Martin, G. E., and Angell, R. R., "Damping of system oscillations with a hydrogenerating unit", *IEEE Trans. Power Apparatus and Systems*, PAS-86(4):438-442, April 1967.

[23] Dandeno, P. L., Karas, A. N., McClymont, K. R., and Watson, W., "Effect of high-speed rectifier excitation systems on generator stability limits", *IEEE Trans. Power Apparatus and Systems*, PAS-87(1):190-201, January 1968.

[24] Shier, R. M., and Blythe, A. L., "Field tests of dynamic stability using a stabilizing signal and computer program verification", *IEEE Trans. Power Apparatus and Systems*, PAS-87(2):315-322, February 1968.

[25] Hanson, O. W., Goodwin, C. J., and Dandeno, P. L., "Influence of excitation and speed control parameters in stabilizing intersystem oscillations", *IEEE Trans. Power Apparatus and Systems*, PAS-87(5):1306-1313, May 1968.

[26] Schleif, F. R., Hunkins, H. D., Martin, G. E., and Hattan, E. E., "Excitation control to improve powerline stability", *IEEE Trans. Power Apparatus and Systems*, PAS-87(6):1426-1434, June 1968.

[27] Schleif, F. R., Hunkins, H. D., Hattan, E. E., and Gish, W. B., "Control of rotating exciters for power system damping: pilot applications and experience", *IEEE Trans. Power Apparatus and Systems*, PAS-88(8):1259-1266, August 1969.

[28] Klopfenstein, A., "Experience with system stabilizing excitation controls on the generation of the Southern California Edison Company", *IEEE Trans. Power Apparatus and Systems*, PAS-90(2):698-706, March/April 1971.

[29] Larsen, E. V., and Swann, D. A., "Applying power system stabilizers, Part I, II, III", *IEEE Trans. Power Apparatus and Systems*, PAS-100(6):3017-3046, June 1981.

[30] IEEE Tutorial Course, *Power system stabilization via excitation control*, 81 EHO 175-0 PWR, IEEE Publishing Services, New York, 1980.

[31] Bayne, J. P., Lee, D. C., and Watson, W., "A power system stabilizer for thermal units based on derivation of accelerating power", *IEEE Trans. Power Apparatus and Systems*, PAS-96(6):1777-1783, November/December 1977.

[32] DeMello, F. P., Hannett, L. N., and Undrill, J. M., "Practical approaches to supplementary stabilizing from accelerating power", *IEEE Trans. Power Apparatus and Systems*, PAS-97(5):1515-1522, September/October 1978.

[33] Lee, D. C., Beaulieu, R. E., and Service, J. R. R., "A power system stabilizer using speed and electrical power inputs — design and field experience", *IEEE Trans. Power Apparatus and Systems*, PAS-100(9):4151-4157, September 1981.

[34] Gibbard, M. J., "Robust design of fixed-parameter power system stabilisers over a wide range of operating conditions", *IEEE/PES 1990 Summer Metting*, 90 SM 318-6 PWRS, June 1990.

[35] Jay, F., (ed.), *IEEE standard dictionary of electrical and electronics terms*, (3rd edition), IEEE Inc., New York, 1984.

[36] Wittenmark, B., "Stochastic adaptive control methods: a survey", *Int. J. Control*, 21(5):705-730, May 1975.

[37] Jacobs, O. L. R., "Introduction to adaptive control" in *Self-tuning and adaptive control: theory and applications*, by Harris, C. J., and Billings, S. A., (eds.), Peter Peregrinus, London, 1985.

[38] Gupta, M. M., (ed.), *Adaptive methods for control system design*, IEEE Press, New York, 1986.

[39] Åström, K. J., "Adaptive feedback control", *IEEE Proc.*, 75(2):185-217, February 1987.

[40] Elliott, H., Cristi, R., and Das, M., "Global stability of adaptive pole placement algorithms", *IEEE Trans. Automatic Control*, AC-30(4):348-356, April 1985.

[41] Lozano-Leal, R., and Goodwin, G. C., "A globally convergent adaptive pole placement algorithm without a persistency of excitation requirement", *IEEE Trans. Automatic Control*, AC-30(8):795-798, August 1985.

[42] Goodwin, G. C., Hill, D. J., and Palaniswami, M., "A perspective on convergence of adaptive control algorithms", *Automatica*, 20(5):519-531, September 1984.

[43] Pierre, D. A., "A perspective on adaptive control of power systems", *IEEE Trans. Power Systems*, PWRS-2(2):387-396, May 1987.

[44] Chalam, V. V., *Adaptive control systems — techniques and applications*, Marcel Dekker Inc., New York and Basel, 1987.

[45] Ledwich, G., "Adaptive excitation control", *IEE Proc.*, 126(3):249-253, March 1979.

[46] Sheirah, M. A. H., Malik, O. P., and Hope, G. S., "A self-tuning automatic voltage regulator", *Electric Power Systems Research*, 2(3):199-213, November 1979.

[47] Xia, D., and Heydt, G. T., "Self-tuning controller for generator excitation control", *IEEE Trans. Power Apparatus and Systems*, PAS-102(6):1877-1885, June 1983.

[48] Kanniah, J., Malik, O. P., and Hope, G. S., "Excitation control of synchronous generators using adaptive regulators, Part I, II", *IEEE Trans. Power Apparatus and Systems*, PAS-103(5):897-910, May 1984.

[49] Ghosh, A., Ledwich, G., Malik, O. P., and Hope, G. S., "Power system stabilizer based on adaptive control techniques", *IEEE Trans. Power Apparatus and Systems*, PAS-103(8):1983-1989, August 1984.

[50] Ghosh, A., Ledwich, G., Hope, G. S., and Malik, O. P., "Power system stabiliser for large disturbances", *IEE Proc.*, 132, Pt. C(1):14-19, January 1985.

[51] Sen Gupta, D. P., Narahari, N. G., Boyd, I., and Hogg, B. W., "An adaptive power-system stabiliser which cancels the negative damping torque of a synchronous generator", *IEE Proc.*, 132, Pt. C(3):109-117, May 1985.

[52] Romero, D. R., and Heydt, G. T., "An adaptive excitation system controller in a stochastic environment", *IEEE Trans. Power Systems*, PWRS-1(1):168-175, February 1986.

[53] Cheng, S. J., Malik, O. P., and Hope, G. S., "Self-tuning stabiliser for a multi-machine power system", *IEE Proc.*, 133, Pt. C(4):176-185, May 1986.

[54] Cheng, S. J., Chow, Y. S., Malik, O. P., and Hope, G. S., "An adaptive synchronous machine stabilizer", *IEEE Trans. Power Systems*, PWRS-1(3):101-109, August 1986.

[55] Chandra, A., Malik, O. P., and Hope, G. S., "A self-tuning controller for the control of multi-machine power systems", *IEEE/PES 1987 Summer Meeting*, 87 SM 452-6 PWRS, July 1987.

[56] Cheng, S. J., Malik, O. P., and Hope, G. S., "Damping of multi-modal oscillations in power systems using a dual-rate adaptive stabilizer", *IEEE Trans. Power Systems*, PWRS-3(1):101-108, February 1988.

[57] Wu, Q. H., and Hogg, B. W., "Robust self-tuning regulator for a synchronous generator", *IEE Proc.*, 135, Pt. D(6):463-473, November 1988.

[58] Gu, W., and Bollinger, K. E., "A self-tuning power system stabilizer for wide-range synchronous generator operation", *IEEE Trans. Power Systems*, PWRS-4(3):1191-1199, August 1989.

[59] Seifi, H., Hughes, F. M., and Shuttleworth, R., "Adaptive power system stabilizer using a bang-bang pole-placement strategy", *Int. J. Control*, 51(1):33-50, January 1990.

[60] Fan, J. Y., Ortmeyer, T. H., and Mukundan, R., "Power system stability improvement with multivariable self-tuning control", *IEEE Trans. Power Systems*, PWRS-5(1):227-234, February 1990.

[61] Wu, Q. H., and Hogg, B. W., "Self tuning control for turbogenerators in multimachine power systems", *IEE Proc.*, 137, Pt. C(2):146-158, March 1990.

[62] Mao, C., Malik, O. P., Hope, G. S., and Fan, J., "An adaptive generator excitation controller based on linear optimal control", *IEEE/PES 1990 Summer Meeting*, 90 SM 425-9 EC, July 1990.

[63] Mao, C., Prakash, K. S., Malik, O. P., Hope, G. S., and Fan, J., "Implementation and laboratory test results for an adaptive power system stabilizer based on linear optimal control", *IEEE/PES 1990 Summer Meeting*, 90 SM 427-5 EC, July 1990.

[64] Lim, C. M., and Hiyama, T., "Self-tuning control scheme for stability enhancement of multimachine power systems", *IEE Proc.*, 137, Pt. C(4):269-275, July 1990.

[65] Bollinger, K. E., and Gu, W., "A comparison of rotor damping from adaptive and conventional PSS in a multi-machine power system", *IEEE Trans. Energy Conversion*, EC-5(3):453-461, September 1990.

[66] Ostojic, D., and Kovacevic, B., "On the eigenvalue control of electromechanical oscillations by adaptive power system stabilizer", *IEEE Trans. Power Systems*, PWRS-5(4):1118-1126, November 1990.

[67] Wu, Q. H., and Hogg, B. W., "Laboratory evaluation of adaptive controllers for synchronous generators", *Automatica*, 27(5):845-852, September 1991.

[68] Sharaf, S. M. Z., Hogg, B. W., Abdalla, O. H., and El-Sayed, M. L., "Multivariable adaptive controller for a turbogenerator", *IEE Proc.*, 133, Pt. D(2):83-89, March 1986.

[69] Wu, Q. H., and Hogg, B. W., "Adaptive controller for a turbogenerator system", *IEE Proc.*, 135, Pt. D(1):35-42, January 1988.

[70] Pahalawaththa, N. C., Hope, G. S., Malik, O. P., "Multivariable self-tuning power system stabilizer simulation and implementation studies", *IEEE/PES 1989 Winter Meeting*, 89 WM 016-7 EC, January/February 1989.

[71] Ibrahim, A. S., Hogg, B. W., and Sharaf, M. M., "Self-tuning controllers for turbogenerator excitation and governing systems", *IEE Proc.*, 136, Pt. D(5):238-251, September 1989.

[72] Ibrahim, A. S., Hogg, B. W., and Sharaf, M. M., "Self-tuning automatic voltage regulators for a synchronous generator", *IEE Proc.*, 136, Pt. D(5):252-260, September 1989.

[73] Ghandakly, A., and Idowu, P., "Design of a model reference adaptive stabilizer for the exciter and governor loops of power generators", *IEEE Trans. Power Systems*, PWRS-5(3):887-893, August 1990.

[74] Pahalawaththa, N. C., Hope, G. S., and Malik, O. P., "MIMO self-tuning power system stabilizer", *Int. J. Control*, 54(4):815-829, October 1991.

[75] Haber, R., Keviczky, L., and Unbehauen, H., "Application of adaptive control on nonlinear dynamic processes - a survey on input-output approaches", *IFAC 10th Triennial World Congress*, Vol. III(1.4-1):1-14, Munich, FRG., 1987.

[76] Isidori, A., *Nonlinear control systems*, (2nd edition), Spring-Verlag, New York, 1989.

[77] Han, K., "The structure of linear systems and the calculation of feedback systems", *Proceedings of the Chinese Conference on Control Theory and Its Applications*, 43-55, Science Press, Beijing, China, 1981.

[78] Gao, L., Chen, L., and Fan, Y., "A new design method of nonlinear control systems with applications in power systems", *Technical Report*, Department of Automation, Tsinghua University, Beijing, China, 1988.

[79] Mielczarski, W., and Zajaczkowski, A., "Nonlinear controller for synchronous generator", *IFAC Symposium on Nonlinear Control System Design*, 14-16, Capri, Italy, June 1989.

[80] Gao, L., Chen, L, Fan, Y., and Ma, H., "A new nonlinear control design with application in power systems", *IFAC Symposium on Nonlinear Control System Design*, 286-290, Capri, Italy, June 1989.

[81] Lu, Q., and Sun, Y., "Nonlinear stabilizing control of multimachine systems", *IEEE Trans. Power Systems*, PWRS-4(1):236-241, February 1989.

[82] Gao, L., Chen, L., Fan, Y., and Ma, H., "The DFL-nonlinear control with application in power systems", *Technical Report No. EE9001*, Department of Electrical Enginnering and Computer Science, University of Newcastle, Australia, 1990.

[83] Wang, Y., Gao, L., and Hill, D. J., "On the design of new nonlinear excitation controllers of power systems", *Technical Report No. EE9067*, Department of Electrical Enginnering and Computer Science, University of Newcastle, Australia, 1990.

[84] Mielczarski, W., and Zajaczkowski, A., "Nonlinear stabilization of synchronous generator", *11th IFAC World Congress*, 13-17, Tallinn, USSR, August 1990.

[85] Gao, L., Chen, L., Fan, Y., and Ma, H., "A nonlinear control design for power systems", *Technical Report No. EE9083*, Department of Electrical Enginnering and Computer Science, University of Newcastle, Australia, 1990.

[86] Wang, Y., Hill, D. J., and Gao, L., "Transient stabilization of power systems with adaptive control laws", *Technical Report No. EE9094*, Department of Electrical Enginnering and Computer Science, University of Newcastle, Australia, 1990.

[87] Mielczarski, W., and Zajaczkowski, A., "Nonlinear controller of a synchronous generator", *Proceedings of Australasia Universities Power and Control Engineering Conference*, 254-259, Monash University, Australia, October 1991.

[88] Hogg, B. W., "Representation and control of turbogenerators in electric power systems" in *Modelling of dynamical systems — Vol. 2*, by Nicholson, H., (eds.), Peter Peregrinus, London, 1980.

[89] Bergan, A. R., *Power system analysis*, Prentice-Hall, New York, 1986.

[90] Yu, Y. N., Vongsuriya, K., and Wedman, L. N., "Application of an optimal control theory to a power system", *IEEE Trans. Power Apparatus and Systems*, PAS-89(1):55-62, January 1970.

[91] Anderson, J. H., "The control of a synchronous machine using optimal control theory", *IEEE Proc.*, 59(1):25-35, January 1971.

[92] Yu, Y. N., and Siggers, C., "Stabilization and optimal control signals for a power system", *IEEE Trans. Power Apparatus and Systems*, PAS-90(4):1469-1481, July/August 1971.

[93] Davison, E. J., and Rau, N. S., "The optimal output feedback control of a synchronous machine", *IEEE Trans. Power Apparatus and Systems*, PAS-90(5):2123-2134, September/October 1971.

[94] Moussa, H. A. M., and Yu, Y. N., "Optimal power system stabilization through excitation and/or governor control", *IEEE Trans. Power Apparatus and Systems*, PAS-91(3):1166-1174, May/June 1972.

[95] Yu, Y. N., and Moussa, H. A. M., "Optimal stabilization of a multi-machine system", *IEEE Trans. Power Apparatus and Systems*, PAS-91(3):1174-1182, May/June 1972.

[96] Humpage, W. D., Smith, J. R., and Rogers, G. J., "Application of dynamic optimisation to synchronous-generator excitation controllers", *IEE Proc.*, 120(1):87-93, January 1973.

[97] Anderson, J. H., and Raina, V. M., "Power system excitation and governor design using optimal control theory", *Int. J. Control*, 19(2):289-308, February 1974.

[98] Raina, V. M., Anderson, J. H., Wilson, W. J., and Quintana, V. H., "Optimal output feedback control of power systems with high-speed excitation systems", *IEEE Trans. Power Apparatus and Systems*, PAS-95(2):677-686, March/April 1976.

[99] Daniels, A. R., Lee, Y. B., and Pal, M. K., "Nonlinear power-system optimisation using dynamic sensitivity analysis", *IEE Proc.*, 123(4):365-370, April 1976.

[100] Quintana, V. H., Zohdy, M. A., and Anderson, J. H., "On the design of output feedback excitation controllers of synchronous machines", *IEEE Trans. Power Apparatus and Systems*, PAS-95(3):954-961, May/June 1976.

[101] Daniels, A. R., Lee, Y. B., and Pal, M. K., "Combined suboptimal excitation control and governing of a.c. turbogenerators using dynamic sensitivity analysis", *IEE Proc.*, 124(5):473-478, May 1977.

[102] Habibullah, B. S., "Optimal governor control of a synchronous machine", *IEEE Trans. Automatic Control*, AC-26(2):391-395, April 1981.

[103] Okongwv, E. H., Wilson, W. J., and Anderson, J. H., "Microalternator stabilization using a physically realizable optimal output feedback controller", *IEEE Trans. Power Apparatus and Systems*, PAS-101(10):3771-3779, October 1982.

[104] Chan, W. C., and Hsu, Y. Y., "An optimal variable structure stabilizer for power system stabilization", *IEEE Trans. Power Apparatus and Systems*, PAS-102(6):1738-1746, June 1983.

[105] Sahba, M., "Optimal control of power system generators incorporating nonlinear state feedback", *IEE Proc.*, 130, Pt. D(6):345-349, November 1983.

[106] Urdaneta, A. J., and Bacalao, N. J., "Tuning of power system stabilizers using optimization techniques", *IEEE Trans. Power Systems*, PWRS-6(1):127-134, February 1991.

[107] Pérez-Arriaga, I. J., *Selective modal analysis with applications to electric power systems*, Ph.D. thesis, Electrical Engineering, Massachusetts Institute of Technology, June 1981.

[108] Aldred, A. S., "Electronic analogue computer simulation of multi-machine power-system networks", *IEE Proc.*, 109, Pt. A(45):195-202, June 1962.

[109] Shackshaft, G., "General-purpose turbo-alternator model", *IEE Proc.*, 110(4):703-713, April 1963.

[110] Cooper, C. B., "The computation of a.c. machine problems", *Proceedings of the First International Power Systems Computation Conference*, Queen Mary College, University of London, England, August 1963.

[111] Kozlowski, A., "Improved programmes for power system stability studies", *Proceedings of the First International Power Systems Computation Conference*, Queen Mary College, University of London, England, August 1963.

[112] Lokay, H. E., and Bolger, R. L., "Effect of turbine-generator representation in system stability studies", *IEEE Trans. Power Apparatus and Systems*, PAS-84(10):933-942, October 1965.

[113] Nicholson, H., "Dynamic optimisation of a boiler-turboalternator model", *IEE Proc.*, 113(2):385-399, February 1966.

[114] Olive, D. W., "New techniques for the calculation of dynamic stability", *IEEE Trans. Power Apparatus and Systems*, PAS-85(7):767-777, July 1966.

[115] Malik, O. P., and Cory, B. J., "Study of asynchronous operation and resynchronisation of synchronous machines by mathematical models", *IEE Proc.*, 113(12):1977-1990, December 1966.

[116] Young, C. C., *Modern concepts of power system dynamics — the synchronous machine*, 70M62-PWR, IEEE Special Publication, 1970.

[117] Hammons, T. J., and Winning, D. J., "Comparisons of synchronous-machine models in the study of the transient behaviour of electrical power systems", *IEE Proc.*, 118(10):1442-1458, October 1971.

[118] Young, C. C., "Equipment and system modeling for large-scale stability studies", *IEEE Trans. Power Apparatus and Systems*, PAS-91(1):99-109, January/February 1972.

[119] Kundur, P., and Bayne, J. P., "A study of early valve actuation using detailed prime mover and power system simulation", *IEEE Trans. Power Apparatus and Systems*, PAS-94(4):1275-1287, July/August 1975.

[120] Rafian, M., "Real-time power system simulation", *IEE Proc.*, 134, Pt. C(3):206-223, May 1987.

[121] Glavitsch, J., "Theoretical investigations into the steady-state stability of synchronous machines", *The Brown Boveri Review*, 49(3/4):95-104, March/April 1962.

[122] Gibbard, M. J., "Co-ordinated design of multimachine power system stabilisers based on damping torque concepts", *IEE Proc.*, 135, Pt. C(4):276-284, July 1988.

[123] Discussion on "Comparisons of synchronous-machine models in the study of the transient behaviour of electrical power systems", *IEE Proc.*, 119(9):1329-1337, September 1972.

[124] D'Azzo, J. J., and Houpis, C. H., *Linear control system analysis and design*, McGraw-Hill, Singapore, 1981.

[125] Adkins, B., *The general theory of alternating current machines: application to practical problems*, Chapman and Hall, London, 1975.

[126] Pahalawaththa, N. C., *MIMO adaptive power system stabilizer*, Ph.D. thesis, University of Calgary, January 1988.

[127] Iyer, S. N., and Cory, B. J., "Optimum control of a turbo-generator including an exciter and governor", *IEEE Trans. Power Apparatus and Systems*, PAS-90(5):2142-2148, September/October 1971.

[128] Iyer, S. N., and Cory, B. J., "Optimisation of turbo-generator transient performance by differential dynamic programming", *IEEE Trans. Power Apparatus and Systems*, PAS-90(5):2149-2157, September/October 1971.

[129] Mukhopadhyay, B. K., and Malik, O. P., "Optimal control of synchronous-machine excitation by quasilinearisation techniques", *IEE Proc.*, 119(1):91-98, January 1972.

[130] Elmetwally, M. M., Rao, N. D., and Malik, O. P., "Experimental results on the implementation of an optimal control for synchronous machines", *IEEE Trans. Power Apparatus and Systems*, PAS-94(4):1192-1200, July/August 1975.

[131] Wilson, W. J., Raina, V. M., and Anderson, J. H., "Nonlinear output feedback excitation controller design based on nonlinear optimal control and identification methods", *IEEE/PES 1976 Summer Meeting*, A76 343-4, July 1976.

[132] Reddy, P. B., and Sannuti, P., "Asymptotic approximation method of optimal control applied to a power-system problem", *IEE Proc.*, 123(4):371-376, April 1976.

[133] Parker, A. M., "ADSTAB: A power system transient stability program for research use", *Technical Report 1/85*, Department of Electrical and Electronic Engineering, University of Adelaide, Australia, 1985.

[134] Elmqvist, H., "Simnon — user's guide", *Report LUTFD2/(TFRT-3091)*, Department of Automatic Control, Lund Institute of Technology, Sweden, 1975.

[135] Elmqvist, H., "SIMNON: An interactive simulation program for nonlinear systems", *Proceedings Simulation'77*, Montreux 1977.

[136] Åström, K. J., "A Simnon tutorial", *Report LUTFD2/(TFRT-3168)*, Department of Automatic Control, Lund Institute of Technology, Sweden, 1982.

[137] Shackshaft, G., and Neilson, R., "Results of stability tests on an underexcited 120MW generator", *IEE Proc.*, 119(2):175-188, February 1972.

[138] Billings, S. A., Gray, J. O., and Owens, D. H., (eds.), *Nonlinear system design*, Peter Peregrinus, London, 1984.

[139] Desoer, C. A., and Wong, K. K., "Small-signal behavior of nonlinear lumped networks", *IEEE Proc.*, 56(1):14-22, January 1968.

[140] Blaquière, A., *Nonlinear system analysis*, Academic Press, New York, 1966.

[141] Åström, K. J., and Wittenmark, B., *Computer controlled systems — theory and design*, Prentice-Hall, New Jersey, 1984.

[142] Hsu, Y., and Chen, C., "Design of SIMO excitation controllers for synchronous generators", *IEEE Trans. Aerospace and Electronic Systems*, AES-23(4):468-472, July 1987.

[143] Pérez-Arriaga, I. J., Schweppe, F. C., and Verghese, G. C., "Selective modal analysis: basic results", *Proceedings of IEEE International Conference on Circuits and Computers*, 649-656, Port Chester, N.Y., 1980.

[144] Pérez-Arriaga, I. J., Verghese, G. C., and Schweppe, F. C., "Determination of relevant state variables for selective modal analysis", *Proceedings of Joint Automatic Control Conference*, Charlottesville, Virginia, June 1981.

[145] Verghese, G. C., Pérez-Arriaga, I. J., and Schweppe, F. C., "Measuring state variable participation for selective modal analysis", *Proceedings of IFAC Symposium on Digital Control*, 29-33, New Delhi, India, January 1982.

[146] Pérez-Arriaga, I. J., Verghese, G. C., and Schweppe, F. C., "Selective modal analysis with applications to electric power systems, Part I: heuristic introduction", *IEEE Trans. Power Apparatus and Systems*, PAS-101(9):3117-3125, September 1982.

[147] Verghese, G. C., Pérez-Arriaga, I. J., and Schweppe, F. C., "Selective modal analysis with applications to electric power systems, Part II: the dynamic stability problem", *IEEE Trans. Power Apparatus and Systems*, PAS-101(9):3126-3134, September 1982.

[148] Verghese, G. C., Pérez-Arriaga, I. J., Schweppe, F. C., and Tsai, K. W. K., "Selective modal analysis in power systems", *Technical Report EL-2830*, EPRI, 1983.

[149] Pérez-Arriaga, I. J., Verghese, G. C., Pagola, F. L., and Schweppe, F. C., "Selective modal analysis in power systems", *American Control Conference*, Vol. 2:650-655, San Francisco, U.S.A., June 1983.

[150] Pagola, F. L., and Pérez-Arriaga, I. J., "Design of power system stabilizers using eigenvalue sensitivities and SMA techniques", *8th Power System Computation Conference*, Helsinki, Finland, August 1984.

[151] Sancha, J. L., and Pérez-Arriaga, I. J., "Selective modal analysis of power system oscillatory instability", *IEEE Trans. Power Systems*, PWRS-3(2):429-438, May 1988.

[152] Pérez-Arriaga, I. J., Verghese, G. C., Pagola, F. L., Sancha, J. L., and Schweppe, F. C., "Developments in selective modal analysis of small-signal stability in electric power systems", *Automatica*, 26(2):215-231, March 1990.

[153] Kailath, T., *Linear systems*, Prentice-Hall, New Jersey, 1980.

[154] Vidyasagar, M., "New directions of research in nonlinear system theory", *IEEE Proc.*, 74(8):1060-1091, August 1986.

[155] Hermann, R., and Krener, A. J., "Nonlinear controllability and observability", *IEEE Trans. Automatic Control*, AC-22(5):728-740, October 1977.

[156] DeCarlo, R. A., *Linear systems — a state variable approach with numerical implementation*, Prentice-Hall, New Jersey, 1989.

[157] Goodwin, G. C., and Sin, K. S., *Adaptive filtering prediction and control*, Prentice-Hall, New Jersey, 1984.

[158] Hope, G. S., Nichols, S. T., and Carr, J., "Measurement of transfer functions of power system components under operating conditions", *IEEE Trans. Power Apparatus and Systems*, PAS-96(6):1798-1808, November/December 1977.

[159] Abdalla, O. H., and Walker, P. A. W., "Optimal control of a laboratory power system model with output feedback", *IEEE/PES 1979 Summer Meeting*, A79 451-6, July 1979.

[160] Åström, K. J., and Bell, R. D., "A 10th-order linear drum boiler turbine model", *Report LUTFD2/(TFRT-3154)*, Department of Automatic Control, Lund Institute of Technology, Sweden, 1979.

[161] Bell, R. D., and Åström, K. J., "A low-order non-linear dynamic model for drum boiler-turbine-alternator units", *Report LUTFD2/(TFRT-7162)*, Department of Automatic Control, Lund Institute of Technology, Sweden, 1979.

[162] Sharaf, M. M., and Hogg, B. W., "Evaluation of online identification methods for optimal control of a laboratory model turbogenerator", *IEE Proc.*, 128, Pt. D(2):65-73, March 1981.

[163] Lang, R. D., Hutchison, M. A., and Yee, H., "Microprocessor-based identification system applied to synchronous generators with voltage regulators", *IEE Proc.*, 130, Pt. C(5):257-265, September 1983.

[164] Swidenbank, E., and Hogg, B. W., "Application of system identification techniques to modelling a turbogenerator", *IEE Proc.*, 136, Pt. D(3):113-121, May 1989.

[165] Morrell, D. J. G., and Hogg, B. W., "Identification and validation of turbogenerator models", *Automatica*, 26(1):135-156, January 1990.

[166] Clarke, D. W., and Gawthrop, P. J., "Self-tuning controller", *IEE Proc.*, 122(9):929-934, September 1975.

[167] Clarke, D. W., and Gawthrop, P. J., "Self-tuning control", *IEE Proc.*, 126(6):633-640, June 1979.

[168] Ljung, L., *Theory and practice of recursive identification*, MIT Press, Cambridge, Mass, 1983.

[169] Ljung, L., *System identification: theory for the user*, Prentice-Hall, New Jersey, 1987.

[170] Åström, K. J., and Wittenmark, B., *Adaptive control*, Addison-Wesley Publishing Company, 1989.

[171] Fortescue, T. R., Kershenbaum, L. S., and Ydstie, B. E., "Implementation of self-tuning regulators with variable forgetting factors", *Automatica*, 17(6):831-835, November 1981.

[172] Osorio Cordero, A., "Theoretical study of a self-tuning regulator with variable forgetting factor", *M.Sc. Report*, Department of Computing and Control, Imperial College, England, 1979.

[173] Osorio Cordero, A., and Mayne, D. Q., "Deterministic convergence of a self-tuning regulator with variable forgetting factor", *IEE Proc.*, 128, Pt. D(1):19-23, January 1981.

[174] Singh, S., "A modified algorithm for invertibility of nonlinear systems", *IEEE Trans. Automatic Control*, AC-26(2):595-598, April 1981.

[175] Descusse, J., and Moog, C. H., "Decoupling with dynamic compensation for strong invertible affine nonlinear systems", *Int. J. Control*, 42(6):1387-1398, December 1985.

[176] Isidori, A., *Nonlinear control systems: an introduction*, Spring-Verlag, New York, 1985.

[177] Isidori, A., Moog, C. H., and Deluca, A., "A sufficient condition for full linearization via dynamic state feedback", *Proceedings of the 25th IEEE Conference on Decision and Control*, Vol. 1:203-207, Athens, Greece, December 1986.

[178] Descusse, J., and Moog, C. H., "Dynamic decoupling for right invertible nonlinear systems", *Systems & Control Letters*, 8(4):345-349, March 1987.

[179] Cheng, D., *Geometric theory for nonlinear systems*, Science Press, Beijing, China, 1988.

[180] Charlet, B. J., Lévine, J., and Marino, R., "On dynamic feedback linearization", *Systems & Control Letters*, 13(2):143-151, February 1989.

[181] Gao, L., Hill, D. J., and Wang, Y., "Direct feedback linearization for SISO systems with non-smooth nonlinearities", *Technical Report No. EE9005*, Department of Electrical Enginnering and Computer Science, University of Newcastle, Australia, 1990.

[182] Singh, S. N., "Nonlinear state-variable-feedback excitation-and-governor-control design using decoupling theory", *IEE Proc.*, 127, Pt. D(3):131-141, May 1980.

[183] Haber, R., and Keviczky, L., "Identification of nonlinear dynamic systems - survey paper", *4th IFAC Symposium on Identification and System Parameter Estimation*, 62-112, Tbilisi, USSR., 1976.

[184] Anbumani, K., Patnaik, L. M., and Sarma, I. G., "Self-tuning minimum-variance control of nonlinear systems of the Hammerstein model", *IEEE Trans. Automatic Control*, AC-26(4):959-961, August 1981.

[185] Anbumani, K., Sarma, I. G., and Patnaik, L. M., "Self-tuning cascade control of linear and nonlinear systems", *Proceedings of IFAC Symposium on Digital control*, 53-56, New Delhi, India, January 1982.

[186] Kung, M., and Womack, B. F., "Stability analysis of a discrete-time adaptive control algorithm having a polynomial input", *IEEE Trans. Automatic Control*, AC-28(12):1110-1112, December 1983.

[187] Kung, M., and Womack, B. F., "Discrete-time adaptive control of linear systems with preload nonlinearity", *Automatica*, 20(4):477-479, July 1984.

[188] Haber, R., and Keviczky, L., "Adaptive dual extremum control by finite order Volterra model", *Problems of Control and Information Theory*, 3(4):247-260, 1974.

[189] Beghelli, S., and Guidorzi, A., "Bilinear system identification from input/output sequences", *4th IFAC Symposium on Identification and System Parameter Estimation*, 360-370, Tbilisi, USSR., 1976.

[190] Goodwin, G. C., Long, R. S., and McInnis, B., "Adaptive control of bilinear systems", *Technical Report No. 8017*, Department of Electrical Enginnering and Computer Science, University of Newcastle, Australia, 1980.

[191] Svoronos, S., Stephanopoulos, G., and Aris, R., "On bilinear estimation and control", *Int. J. Control*, 34(4):651-684, October 1981.

[192] Goodwin, G. C., McInnis, B., and Long, R. S., "Adaptive control algorithms for waste water treatment and pH neutralization", *Optimal Control Applications & Methods*, 3:443-459, July-September 1982.

[193] Elliott, H., Depkovich, T., and Draper, B., "Nonlinear adaptive control of mechanical linkage systems with application to robotics", *American Control Conference*, 1050-1055, San Francisco, U.S.A., June 1983.

[194] Yeo, Y. K., and Williams, D. C., "Adaptive bilinear model predictive control", *American Control Conference*, 1455-1461, San Francisco, U.S.A., June 1983.

[195] Ohkawa, F., and Yonezawa, Y., "A model reference adaptive control system for discrete bilinear systems", *Int. J. Control*, 37(5):1095-1101, May 1983.

[196] Dochain, D., and Bastin, G., "Adaptive identification and control algorithms for nonlinear bacterial growth systems", *Automatica*, 20(5):621-634, September 1984.

[197] Kotta, U., and Nurges, U., "Identification of input-output bilinear systems", *IFAC 9th Triennial World Congress*, 723-727, Budapest, Hungary, 1984.

[198] Leonaritis, I. J., and Billings, S. A., "Input-output parametric models for non-linear systems; Part I: deterministic non-linear systems, Part II: stochastic non-linear systems", *Int. J. Control*, 41(2):303-344, February 1985.

[199] Haber, R., Vajk, I., Keviczky, L., "Nonlinear system identification by 'linear' systems having signal-dependent parameters", *6th IFAC Symposium on Identification and System Parameter Estimation*, Washington, D.C., 1982.

[200] Vuchkov, I. N., Valev, K. D., and Tsochev, V. K., "Identification of parametrically dependent processes with applications to chemical technology", *7th IFAC Symposium on Identification and System Parameter Estimation*, York, U.K., 1985.

[201] Haber, R., and Keviczky, L., "Identification of 'linear' systems having signal-dependent parameters", *Int. J. Systems Science*, 16(7):869-884, July 1985.

[202] Diekmann, K., and Unbehauen, H., "On-line parameter estimation in a class of nonlinear systems via modified least-squares and instrumental variable algorithms", *7th IFAC Symposium on Identification and System Parameter Estimation*, York, U.K., 1985.

[203] Elliott, H., and Wolovich, W. A., "Parameterization issues in multivariable adaptive control", *Automatica*, 20(5):533-545, September 1984.

[204] IEEE Committee Report, "Computer representation of excitation systems", *IEEE Trans. Power Apparatus and Systems*, PAS-87(6):1460-1464, June 1968.

[205] IEEE Committee Report, "Excitation system models for power system stability studies", *IEEE Trans. Power Apparatus and Systems*, PAS-100(2):494-509, February 1981.

[206] Lu, H., Hazell, P. A., and Daniels, A. R., "Co-ordinated single-variable excitation control and governing of turboalternators" *IEE Proc.*, 129, Pt. C(6):278-284, November 1982.

[207] Watson, W., and Manchur, G., "Experience with supplementary damping signals for generator static excitation", *IEEE Trans. Power Apparatus and Systems*, PAS-92(1):199-203, January/February 1973.

[208] IEEE Committee Report, "Dynamic models for steam and hydro turbines in power system studies", *IEEE Trans. Power Apparatus and Systems*, PAS-92(6):1904-1915, November/December 1973.

[209] Desoer, C. A., "Slowly varying discrete system," *Electronics Letters*, 6(11):339-340, May 1970.

[210] Wen, C., and Wang, Y., *Solutions manual: Digital control and estimation — a unified approach* (by Middleton, R. H., and Goodwin, G. C., Prentice Hall, New Jersey, 1990), Department of Electrical Enginnering and Computer Science, University of Newcastle, Australia, 1991.

[211] Chen, C., *Linear system theory and design*, Holt, Rinehart, and Winston, New York, 1984.